STUDY OF CHLORIDE INDUCED CORROSION OF REINFORCEMENT STEEL IN CRACKED CONCRETE

A THESIS

submitted by

SANGOJU BHASKAR

for the award of the degree

of

DOCTOR OF PHILOSOPHY

BUILDING TECHNOLOGY AND CONSTRUCTION MANAGEMENT DIVISION
DEPARTMENT OF CIVIL ENGINEERING

INDIAN INSTITUTE OF TECHNOLOGY MADRAS

CHENNAI 600 036

MARCH 2013

THESIS CERTIFICATE

This is to certify that the thesis titled **STUDY OF CHLORIDE INDUCED CORROSION OF REINFORCEMENT STEEL IN CRACKED CONCRETE**, submitted by **Sangoju Bhaskar** to the Indian Institute of Technology Madras, Chennai, for the award of the degree of **Doctor of Philosophy**, is a bonafide record of the research work done by him under our supervision. The contents of this thesis, in full or in parts, have not been submitted to any other Institute or University for the award of any degree or diploma.

Prof. Ravindra Gettu
Research Guide
Professor, BTCM Division
Dept. of Civil Engineering
IIT Madras, Chennai-600 036

Dr. B. H. Bharatkumar
Research Guide
Senior Principal Scientist
CSIR-SERC
Taramani, Chennai-600 113

Place: Chennai

Date:

ACKNOWLEDGEMENTS

This thesis is the outcome of the work carried out at CSIR-Structural Engineering Research Centre (CSIR-SERC), Chennai, as a PhD scholar (External) at Indian Institute of Technology Madras, Chennai. Firstly, I wish to thank God, the Almighty for giving me wisdom and strength to complete this PhD. The writing of this thesis is a wonderful experience in which many people contributed in a unique way and are worth mentioning. I take this opportunity in expressing my gratitude to the following in particular.

I am grateful to the management, CSIR-SERC, Chennai for giving permission to do my PhD at IIT Madras, Chennai. I am grateful to the Director, Dr. Nagesh R. Iyer, CSIR-SERC and former Director, Dr. N. Lakshmanan, for their confidence on me in carrying out this work. First and foremost, I am deeply grateful to Professor Ravindra Gettu, BTCM Division, IITM, supervisor, for his kind co-operation, critical and thought provoking technical discussions, which inspired me in orienting my research inclinations in better ways. He always made me feel welcome in his office with a smiling face, no matter how busy he was. I really enriched my knowledge in understanding the importance of material science during these years. I would like to thank Dr. B.H. Bharatkumar, Principal Scientist, CSIR-SERC, for being my external supervisor and providing suggestions during the course of my research work. I am grateful to my Doctoral Committee members Professor K. Ramamurthy and Dr. Manu Santhanam, Associate Professor, BTCM Division, IITM, Dr. K. Ramanjaneyulu, Head ACTEL, CSIR-SERC and Professor K. Ganesh Babu, OED, IITM, for their constant suggestions during the course of my research work. I sincerely thank the reviewers for their feedback on my thesis.

I thank Dr. S. Arunachalam, Advisor (M), CSIR-SERC, Shri T. S. Krishnamurthy, Chief Scientist and Dr. K. Ravisankar, Chief Scientist, CSIR-SERC, for their encouragement during preparation of the thesis work. I once again sincerely thank Dr. K. Ramanjaneyulu, Head ACTEL, CSIR-SERC and Dr. Radhakrishna G. Pillai, Assistant Professor, IIT Madras for their critical review and advice during the write-up of my thesis. This dissertation would not have been possible without the significant support and encouragement from many people. I would like to thank Dr. J.K. Dattatreya, former Principal Scientist and Dr. K. Balaji Rao, Chief Scientist, CSIR-

ABSTRACT

The durability of reinforced concrete (RC) structures in chloride-rich environments depends mainly on the risk of the steel rebar being corroded due to chloride attack. For durability to be achieved in such environment, the corrosion process is to be delayed by reducing the chloride penetration. This can be achieved by proper selection of materials such as cement type, and the use of chemical and mineral admixtures. Chemical admixtures, like superplasticizers and corrosion inhibitors, once added to the mix could alter the microstructure and thereby improve the durability. Similarly, mineral admixtures like fly ash reduce the pore size of the concrete mix by means of secondary hydration. However, RC structures under service generally develop cracks and the influence of cracking on the durability depends on the concrete composition, quality, exposure conditions, crack width and its orientation, etc. Cracks in the cover concrete facilitate easy access to the penetration of dissolved Cl^- resulting in rapid corrosion initiation and propagation leading to substantial reduction in service life. From the durability point of view, most design codes specify maximum permissible crack widths, and caution that the limitation of crack width is not the means to avoid corrosion in the case of severe chloride attack.

This research programme focuses on the influence of cement type, polycarboxylic ether superplasticizer (PCE SP) and calcium nitrite inhibitor (CNI) on the corrosion resistance of cracked RC structural components in chloride-rich environment. Two types of cement [ordinary portland cement (OPC) and fly ash based portland pozzolana cement (PPC)] with three water to cement ratios (w/c) have been used in the study. A specially designed U-shaped RC specimen with a provision to create cracks has been used for evaluating the influence of different parameters on the corrosion resistance of reinforcement steel. The U-shaped specimen is reinforced with a deformed bar of 12 mm diameter having 20 mm clear cover. Flexural cracks of required width were created in the flange portion of U-shaped specimen by stressing the tie rods with nuts provided in the stubs. Guidelines given in IS 456 (2005) have been followed in choosing the w/c and surface crack widths [0.2 mm and 0.4 mm]. The corrosion process was accelerated by using an impressed anodic potential of 10 V for a specified duration while the flange of the U-shaped specimen was submerged in 3.5% NaCl solution.

The durability parameters, such as the rapid chloride penetration test (RCPT) value, water absorption and sorptivity on standard specimens (uncracked) and corrosion performance based on half-cell potential, resistivity, total charge passed and gravimetric weight loss of corroded rebars of U-shaped specimens have been evaluated. It is observed that the RCPT value of PPC concretes is found to be nearly one-third that of the corresponding OPC concretes. Also, the total charge passed and gravimetric weight loss indicate that PPC concretes performed better in terms of corrosion resistance, which would result in extended service life. RCPT values of concretes with PCE SP are nearly the same as that of control concretes (OPC or PPC alone) but the reduction in weight loss of the rebar in concrete with PCE SP is slightly lower than that of the corresponding control concrete. Though the water absorption and sorptivity values of concretes with CNI are comparable, the RCPT values increase substantially and are about 1.6 times that of respective control concrete. This may be attributed to the highly ionic nature of CNI, which seems to induce more charge to pass through the concrete. At the end, the service lives have been estimated based on the experimentally evaluated diffusion coefficient and the estimated corrosion current densities. The service life of PPC concrete is more than twice that of the service life of corresponding OPC concrete.

The main conclusions drawn from the studies are: (i) PPC concrete is superior in terms of corrosion resistance even in cracked concrete compared to the corresponding OPC concretes, (ii) concretes with low w/c (i.e., better quality indicated by lower permeability and higher strength) perform better against corrosion resistance of rebars even in cracked concrete, (iii) increase in weight loss is higher between the uncracked specimens and the specimens with 0.2 mm flexural crack widths than between specimens with the 0.2 mm and 0.4 mm flexural crack widths, which implies that the presence of the crack influences corrosion more than the (flexural) crack width itself, and (iv) visual observation during accelerated corrosion, the total charge passed and the gravimetric weight loss (% reduction in weight) results reveal that concretes with CNI did not show any corrosion inhibition effect.

Keywords: Concrete; durability; cracking; corrosion of rebar; PCE SP; CNI, impressed current, service life

TABLE OF CONTENTS

Table of Contents (Contd.,)   **Page No.**

LIST OF TABLES

LIST OF FIGURES

CHAPTER 1

INTRODUCTION

1.1. General

Concrete is the most popular and widely used construction material due to its relatively low cost, versatility and adaptability. The main limitation of concrete, even of good quality, is the presence of micro-cracks, voids and capillary pores through which chlorides, CO_2, moisture, etc., penetrate and initiate the corrosion of reinforcement bars (rebars). Experience in the recent past shows that structures made of reinforced concrete (RC) do not provide adequate resistance to aggressive environments. Rebar corrosion is a major concern that causes extensive damage to the RC structures which include the following (Palsson and Mirza, 2002; Broomfield, 2006):

- cracking and spalling of the cover concrete
- loss in load-carrying capacity due to a reduced cross sectional area of rebar
- loss in load-carrying capacity due to loss in bond at the concrete-rebar interface, and
- loss in ductility due to an uneven distribution of cross-sectional area along the length of the rebar

Hence, to build environmentally sustainable concrete structures, modern construction should be driven by considerations of concrete durability rather than strength. Durability is the ability of a material or structure to withstand its design service conditions for the design life for which it is designed without significant deterioration. American Concrete Institute (ACI 201.2R, 2010) defines concrete durability as its resistance to weathering action, chemical attack and other degradation processes while the British Standard (BS 8110, 1997) defines a durable concrete as one that is designed and constructed to protect embedded reinforcement from corrosion and should perform satisfactorily in the working environment for the life-time of the structure. Nevertheless, concrete durability is mainly related to the transport properties and its chemical composition. Transport properties are a function of concrete permeability/penetrability and cracking (Richardson, 2002). Penetrability is

affected by several parameters such as the water to cement ratio (w/c) and the degree of hydration of the cement paste, presence of cracks, etc. A reduction in penetrability and elimination of cracking or minimization of the crack width increases durability of concrete.

The influence of cracking on the durability of concrete structures is a complex function of the composition, concrete quality, exposure conditions, crack width, type, length, depth, frequency and orientation with respect to reinforcement, crack healing, etc. (ACI 222R, 2010; Scott and Alexander, 2007). Cracks in the cover concrete produce at least three specific effects: (i) they tend to facilitate the onset of corrosion by providing easy access for the penetration of dissolved Cl^- and CO_2 so as to induce depassivation; (ii) they accelerate the rate of corrosion, by reducing the barrier to diffusion of oxygen, at least near the cracks themselves; and (iii) they produce substantial non-uniformity in the physical and chemical environment around the steel, thus providing favourable conditions for corrosion to occur. Thus cracking can result in substantial reduction in service life owing to rapid initiation and propagation of rebar corrosion. The presence of cracks may not only shorten the time to corrosion initiation but also increase the corrosion rate in the corrosion propagation stage. Despite the research that was done on the influence of cracks on chloride-induced corrosion (Beeby, 1978; Suzuki et al., 1990; Arya and Ofori-Darko, 1996; Edvardsen, 1999; Scott and Alexander, 2007), corrosion mitigation in the marine environment continues to be an issue for many years and still engages considerable effort and resources. Also, there is a considerable difference in opinion in the published literature regarding the relationship between the presence of cracks and corrosion. Most codes of practice specify maximum permissible crack widths from the durability point of view. For appearance and corrosion, the maximum surface width of crack, in general, should not exceed 0.3 mm (BS 8110, 1997; IS 456, 2005). ACI 224 (2010) and ACI 318 (2010) limit crack widths up to 0.4 mm, however, it is recognised that corrosion is not clearly correlated with surface crack widths. The European design code, CEB (1989) also cautions that the limitation of crack widths is not the means to avoid corrosion in the case of severe chloride attack on horizontal concrete surfaces. Though considerable research has been carried out on the influence of cracking on rebar corrosion, aspects regarding the type of binder and admixtures used, and width of pre-crack need more detailed study.

The durability of RC structures built in chloride rich environments depends mainly on the risk of rebar corrosion due to chloride penetration. The durability in such environments can be achieved by proper selection of materials such as cement type, addition of chemical and mineral admixtures in improving the impermeability, resistance to chloride ion diffusion, increasing threshold chloride concentration, etc. (Holm and Geiker, 1992). In the recent years, chemical admixtures are being widely used to improve fresh state properties such as workability, flowability, reducing shrinkage, etc. Considerable amount of research was carried out on the fresh state properties of concrete, when superplasticizer are added, however, very little research is available on the long term durability studies such as corrosion resistance, pertinently in the presence of cracks. Similarly, there is a disagreement in the published literature regarding the performance of corrosion inhibitors, especially nitrite based inhibitors in cracked concrete.

1.2. Objectives and Scope

The proposed research program envisages systematic experimental investigations on the effect of commercially available polycarboxylic ether superplasticizer (PCE SP) and calcium nitrite inhibitor (CNI) on long term durability of RC under chloride-rich environments. In the study, the mechanisms of admixtures are not directly studied; rather the action of the admixture in improving the durability/controlling corrosion or delaying the onset of corrosion is assessed. This study is expected to improve the understanding of the process and governing factors in the presence of cracks of pre-defined widths on the corrosion resistance performance of RC specimens exposed to laboratory based chloride-rich environment. The main objectives are as follows:

- To investigate the corrosion resistance of cracked and uncracked concretes in chloride-rich laboratory environment
- To evaluate the corrosion resistance of ordinary portland cement (OPC) and fly ash based portland pozzolana cement (PPC) concretes
- To investigate the effect of water/cement (w/c) ratio on the corrosion resistance of cracked concrete
- To evaluate the influence of addition of polycarboxylic ether superplasticizer (PCE SP) and calcium nitrite inhibitor (CNI) on corrosion resistance

- To estimate the probable service life of RC structural elements of selected concretes

The scope of this study is limited to the following aspects:
- Study is limited to three w/c (0.57, 0.47 and 0.37) that are considered based on the durability parameters suggested by IS 456 (2005)
- Study is limited by considering two surface crack widths, 0.2 and 0.4 mm (i.e., below and above, respectively, of the value of 0.3 mm specified by BS 8110 (1997) and IS 456 (2005).

1.3. Structure of the Thesis

The research strategy that is followed in order to achieve the objectives specified in the previous section and the results obtained are described one after the other in the thesis.

A detailed description of corrosion mechanisms, the influence of cracking on corrosion behaviour of reinforcement steel, corrosion monitoring and corrosion control measures is given in Chapter 2. The factors affecting the corrosion of rebars, mainly the chloride induced corrosion are reviewed; the need and motivation for conducting this study are emphasized.

Chapter 3 discusses the experimental programme including mix proportions selected, materials used, test variables, their combinations, etc. Details of U-shaped test specimen with emphasis on the crack initiation are presented in this chapter. Details of the evaluation of basic mechanical and durability parameters, accelerated corrosion tests and other corrosion assessment techniques used to evaluate the relative performance of chosen materials are also presented.

Chapter 4 deals with the experimental results on the corrosion resistance performance of OPC and PPC concretes. The basic mechanical and durability test results such as compressive strength, split tensile strength, rapid chloride permeability test (RCPT) value, sorptivity, etc., of OPC and PPC concretes are evaluated and discussed. The influence of crack width and the type of cement, i.e., OPC or PPC on the corrosion resistance performance has been discussed.

The study of the effect of the PCE SP and CNI on the corrosion resistance of RC is presented in Chapter 5. It is intended to provide an overall picture of the influence of PCE SP and CNI on basic strength and durability through tests such as compressive strength, split tensile strength, RCPT and corrosion resistance performance through accelerated corrosion tests. The corrosion resistance performance is finally evaluated through visual observation and gravimetric weight loss measurement of rebars after exposing the U-shaped specimens for a specified period in a chloride-rich environment in the laboratory.

Chapter 6 discusses the estimation of service life of RC structural components under chloride attack based on the assumption that the total service life is the sum of corrosion initiation period and stable propagation period.

The conclusions drawn from the research work are summarized and are presented in Chapter 7. Also, the scope for further research is highlighted.

This page is intentionally left blank

CHAPTER 2

STATE-OF-THE-ART-REVIEW OF CORROSION OF REBARS IN CONCRETE

2.1. General

Rebars embedded in concrete are normally protected against corrosion by the alkalinity of the pore water in the concrete. However, due to the ingress of aggressive agents such as chlorides, CO_2, etc., through the cover concrete, the passivity is lost, which results in corrosion of rebar. Moreover, concrete structures in service generally develop cracks in cover concrete, which could provide easy access to the aggressive agents. The cracks formed prior to initiation of rebar corrosion have an important impact on the corrosion of rebar. In an aggressive environment, depassivation of the rebar near the crack will take place faster compared to that in uncracked areas. Corrosion then begins, with the depassivated rebar in the cracked zone being the anode and the remaining being cathode. Whereas in the case of uncracked concrete, the corrosion will initiate only when sufficient amount of chloride ions reach the rebar location. The influence of cracking on rebar corrosion is a complex function of the concrete composition, quality, exposure conditions, crack widths, etc. Therefore, understanding of the effects of different parameters on the corrosion resistance performance of RC and on service life is essential for making durable structure.

The objective of this chapter is to summarize the dominant mechanisms responsible for rebar corrosion and also the effects of cracks in concrete on rebar corrosion. More emphasis is given to chloride-induced corrosion, which is the focus of this study. Also, different corrosion assessment techniques and measures used to control the corrosion are briefly described. A detailed review of the current understanding on the influence of cracking on rebar corrosion and the corrosion resistance performance of concrete with chemical admixtures such as superplasticizers and corrosion inhibitors is also given. Finally, a brief discussion on the estimation of the effect of chloride induced corrosion on the service life also presented.

2.2. Mechanisms of Rebar Corrosion in Concrete

Rebars embedded in fresh concrete are passivated by the highly alkaline environment present within the concrete. Such passivation is caused by a dense ferrous (Fe^{2+}) or ferric (Fe^{3+}) oxide layer that prevents further oxidization of the rebar (Broomfield, 2006). Due to diffusion of chloride ions (Cl^-) or carbon dioxide (CO_2), the passive layer may, however, be disrupted by a reduction in alkalinity. The rebar corrosion is an electrochemical process in which both chemical reactions and flow of electrical current are involved (Broomfield, 2006; Bentur et al., 1998). It involves two separate, though coupled, chemical reactions that take place simultaneously on the steel surface. They are known as 'anodic' and 'cathodic' reactions:

Anodic reaction: $\qquad Fe \rightarrow Fe^{2+} + 2e^-$ (2.1)

Cathodic reaction: $\qquad \dfrac{1}{2}O_2 + H_2O + 2e^- \rightarrow 2(OH)^-$ (2.2)
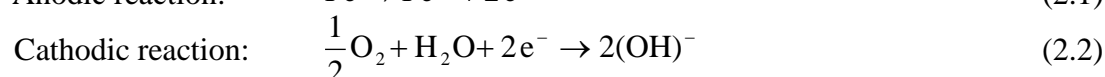
The actual loss of metal involved in the corrosion processes takes place near the anodic sites, as indicated by the following equations and also shown in Figure 2.1.

$$Fe^{2+} + 2(OH)^- \rightarrow Fe(OH)_2 \qquad \text{(ferrous hydroxide)} \qquad (2.3)$$

$$4\,Fe(OH)_2 + O_2 + 2\,H_2O \rightarrow 4\,Fe(OH)_3 \qquad \text{(ferric hydroxide)} \qquad (2.4)$$

$$2\,Fe(OH)_3 \rightarrow Fe_2O_3 . H_2O + 2\,H_2O \qquad \text{(hydrated ferric oxide or rust)} \ (2.5)$$
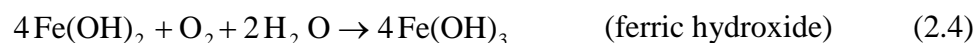
The form of the corrosion products may vary and depend on the available reagents and the relative potentials. The actual metal removal process (described in Equations 2.3 - 2.5) continues only if there is a cathodic reaction, which will act as a sink for the electrons produced at the anodic site. Therefore, if oxygen and water are not available at the cathodic sites, the corrosion process will not occur.

In Figure 2.1, the direction of current is represented by the accepted sign convention: i.e., positive direction is the direction of flow of positive charge and hence, the flow of positive charge is presented.
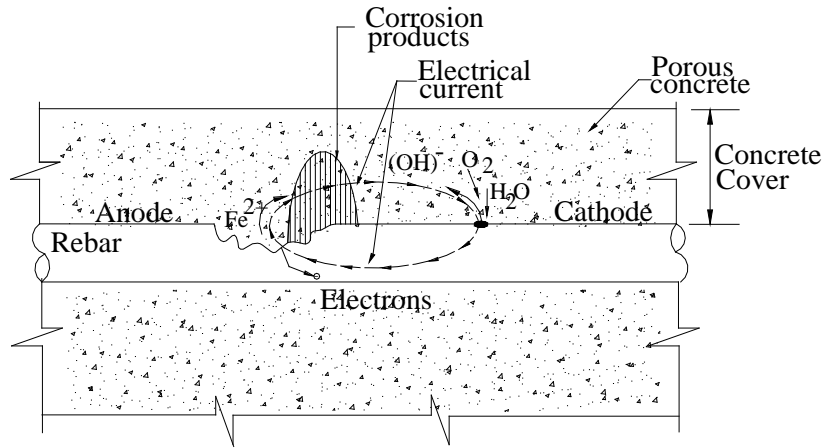
Figure 2.1: Corrosion process on the surface of steel (adapted from Bentur et al., 1998)

The electrochemical process is demonstrated by the flow of current in the closed loop shown in Figure 2.2. An external current flow through the pore solution of the concrete surrounding the rebar, which consists of hydroxyl ions (OH^-) moving from the cathode to the anode, and also ferrous ions (Fe^{2+}) moving from the anode to the cathode. The hydroxyl ions combine with the ferrous ions to form ferrous hydroxide, $Fe(OH)_2$. In the presence of water and oxygen, the ferrous hydroxide is further oxidized to form ferric oxide, Fe_2O_3 (USDT, 2000). Typical products include FeO, Fe_2O_3, Fe_3O_4, $Fe(OH)_2$, $Fe(OH)_3$ and $Fe(OH)_3.3H_2O$; their relative volumes are shown in Figure 2.3 (Taylor et al., 1999; Broomfield, 2006; Yu and Bull, 2006).
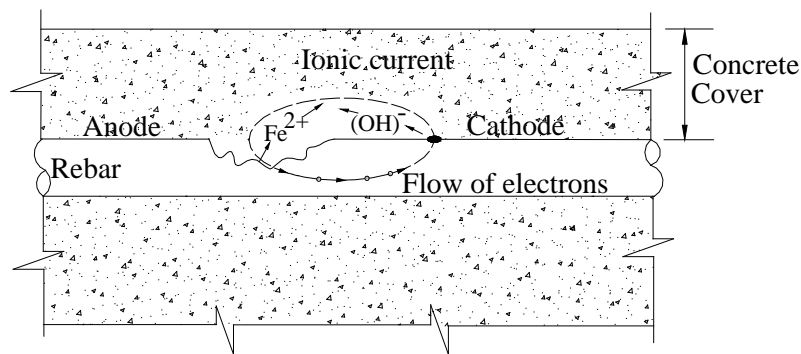
Figure 2.2: Reaction at anodic and cathodic sites (adapted from Bentur et al., 1998)

9
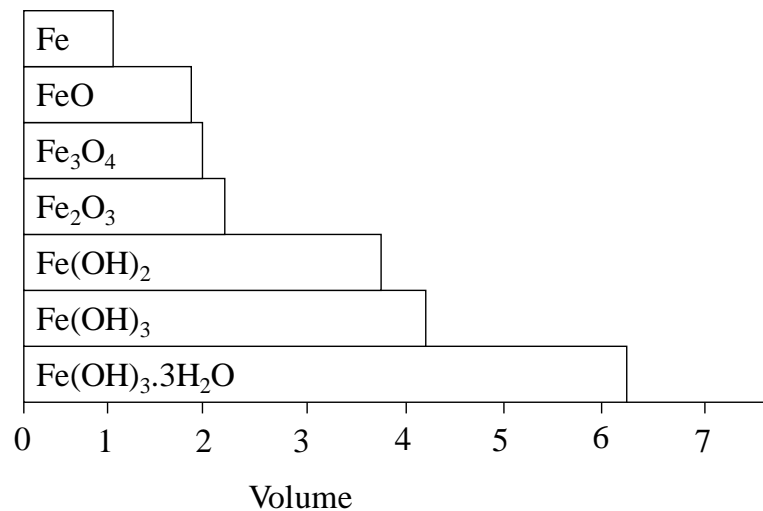
Figure 2.3: Relative volumes of the different types of rust products (Yu and Bull, 2006)

In summary, for corrosion to occur five specific conditions are required (Kurtis and Mehta, 1997):

(i)   The presence of an anode to produce electrons

(ii) The presence of a cathode to accept electrons

(iii) The availability of oxygen at the cathode site

(iv) The availability of moisture/water at the cathode site, and

(v)   The electron connection between the anode and cathode sites to transfer electrons

If any of the above listed conditions is absent, corrosion will not occur. In other words, the factors influencing the corrosion rate of rebar embedded in concrete include (Thompson and Lankard, 1997):

- Availability of oxygen and moisture at the cathode
- Resistivity of the concrete
- Cathode to anode ratio
- Relative humidity

The schematic description of the factors that affect the corrosion rate is shown in Figure 2.4. The most important of these are the availability of oxygen at the cathodic areas, and the presence of aqueous solution in the concrete pores adjacent to the steel. This is necessary to provide a medium through which the ionic current from the

10

cathode to the anode can flow. The water in the concrete pores (i.e., a dilute solution of alkali and calcium hydroxides) serves as a vehicle for ionic flow. If the pores dry out or if the structure of the concrete is so dense, then the pores are not well interconnected, the electrical resistance in the concrete is high and the flow of ions through the pores is difficult (Bentur et al., 1998). Under such circumstances, the corrosion process will slow down or stop.
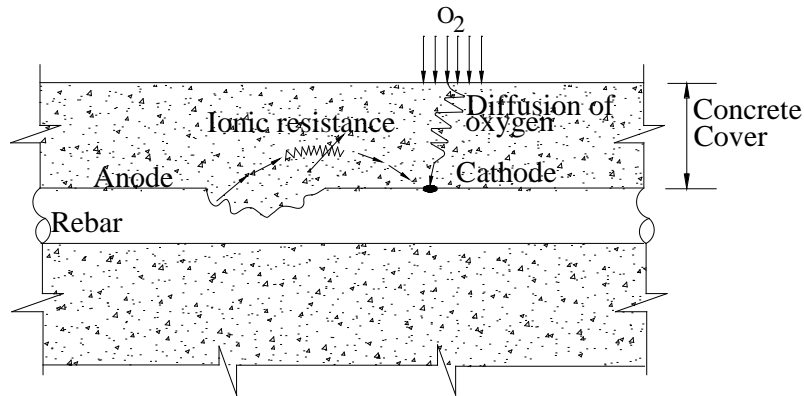
Figure 2.4: Schematic description of most important factors that affect the corrosion rate (adapted from Bentur et al., 1998)

2.2.1. Chloride induced corrosion (ClC)

The rebar corrosion induced by chloride ions is the most frequent cause with highest costs and effects on structural safety (USDT, 2000). However, the actual mechanism of corrosion initiation by chloride ions in the concrete is not yet completely known (ACI 222R, 2010). The possible sources of chlorides in concrete are aggregates, mixing water, admixtures, marine environment, salts used for de-icing, etc. As mentioned earlier, in sound concrete, due to high alkalinity of concrete pore solution, rebar is protected from corrosion by a thin passive layer or oxide layer. The oxide films that normally develop on rebar are either ferrous (Fe^{2+}) or ferric (Fe^{3+}) in nature. Both are chemically stable in the absence of carbonation or chloride. However, ferric oxide is the most stable, especially in the presence of chlorides. Over time, the ferrous oxide is converted to the more stable iron oxyhydroxide ($\cdot FeOOH$). However, the conversion process is never totally completed (Bentur et al., 1998). Chloride ions react with the ferrous oxide to form a soluble complex that dissolves in the

11

surrounding solution causing local failure of the passive layer. This passivation breakdown occurs when chloride levels exceed a certain threshold level at the rebar surface, typically 0.4 to 1% chloride concentration by mass of binder (Montemor et al., 2003; Page, 1992; Mackechnie et al., 2004). The possible reactions that occur are given in Table 2.1.

Table 2.1: Possible reactions that occur in chloride induced corrosion (Bentur et al., 1998; Callister, 2000)

Depassivation of protective layer	$Fe^{2+} + 2\,Cl^- \rightarrow FeCl_2$ (soluble in pore solution)
Corrosion of steel	$Fe \rightarrow Fe^{2+} + 2\,e^-$ (oxidation) $\dfrac{1}{2}O_2 + H_2O + 2\,e^- \rightarrow 2(OH)^-$ (reduction)
Formation of rust	$Fe^{2+} + 2(OH)^- \rightarrow Fe(OH)_2$ $2\,Fe(OH)_2 + \dfrac{1}{2}O_2 + H_2O \rightarrow 2\,Fe(OH)_3$ $\rightarrow Fe_2O_3 . 3H_2O$ (Rust)

As in the case of oxide corrosion of steel, ferrous hydroxide is oxidized to rust in the presence of oxygen and water. The resulting corrosion products and accompanying processes of cracking, spalling and delamination of concrete occurring in both oxide induced and chloride induced corrosion are similar but the rate and the mode of occurrence of various aspects of corrosion are different. The rate of chloride induced corrosion is much faster than oxide corrosion and its distinguishing feature is pitting leading to local cross sectional loss of material (Dillard et al., 1993).

2.2.2. Carbonation induced corrosion (CaC)

Carbonation is a process in which carbon dioxide from the atmosphere diffuses through the porous concrete. The carbonation process can reduce the pH to 8 or 9, at which the passivating/oxide film is no longer stable (Broomfield, 2006). The alkalinity of concrete may also be lowered by acidifying gases such as sulphur dioxide. With adequate supply of oxygen and moisture, corrosion can start. The carbonation of concrete is a slow process, the rate of which is determined by the rate of penetration of carbon dioxide into the concrete that primarily depends on the

porosity and permeability of the concrete. The carbonation process involves the following stages. First, the atmospheric carbon dioxide (CO_2) reacts with water in the concrete pores to form carbonic acid (H_2CO_3).

$$H_2O + CO_2 \rightarrow H_2CO_3 \tag{2.6}$$

This is followed by reaction of the carbonic acid with calcium hydroxide ($Ca(OH)_2$) to form calcium carbonate ($CaCO_3$).

$$H_2CO_3 + Ca(OH)_2 \rightarrow CaCO_3 + 2H_2O \tag{2.7}$$
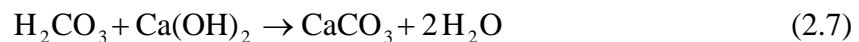
The above process leads to the depassivation of the rebar in contact with the carbonated zones. The water released during the chemical reactions can sustain both the formation of carbonic acid and the carbonation process. The carbonates formed are larger molecules than the hydroxides, thereby increasing the density of the cement paste and locally, the strength (Neville, 1996). The formation of carbonic acid lowers the pH of the concrete pore solution. As soon as the carbonation front reaches the rebar, in the presence of water and oxygen, the corrosion process begins. Carbonation induced corrosion occurs most rapidly when there is very little concrete cover over rebar and also in highly permeable concretes. Factors influencing the rate of carbonation of concrete (Parrott, 1990) are:

- amount of CO_2 in air
- relative humidity of concrete
- amount of precipitation of $CaCO_3$
- concrete carbonation resistance (concrete permeability, amount of $Ca(OH)_2$ in concrete)

The most common method to measure carbonation is spraying with 0.5% - 2% phenolphthalein solution on freshly broken concrete surfaces. The surface where the pH is greater than 9 turns purple with gradually lightening shades of pink for pH of 8-9. The location where the surface is colourless represents the depth to which carbonation has been occurred and the pH of the cement is at or below approximately 8.

2.3. Influence of Cracking on Rebar Corrosion

Generally, all concrete structures are cracked and the influence of cracking on long term durability is a complex function governed by many parameters such as composition of materials, exposure condition, crack width, etc (Alonso et al., 1998; ACI 222R, 2010). At least, two different corrosion mechanisms are theoretically possible for rebar corrosion in cracked concrete (Schießl and Raupach, 1997). In Mechanism 1, the anodic and cathodic reactions take place side by side (i.e., microcell corrosion). In Mechanism 2, the anodic and cathodic reactions occur some distance apart (i.e., macrocell corrosion). In an aggressive environment, depassivation of the rebar near the crack will take place before it occurs in uncracked areas (Bentur et al., 1998; François and Maso, 1998). Corrosion then begins, with the depassivated rebar in the cracked zone being the anode and the remaining being cathodic, as shown in Figure 2.5. Subsequently the rate of corrosion will be controlled either by the diffusion of oxygen through the cover concrete to the cathodic areas or by the electrical resistance of concrete around the rebar. Thus, the subsequent corrosion rates are limited by the same factors as they are for uncracked concrete.
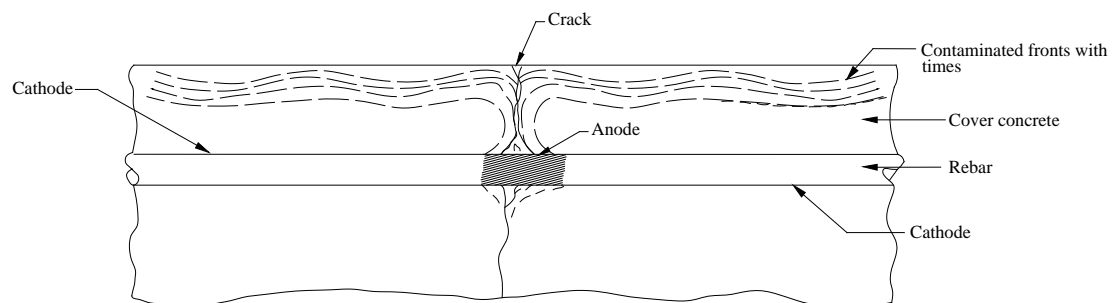
Figure 2.5: Depassivation of the rebar near the crack (adapted from Bentur et al., 1998)

Considerable amount of research was carried out describing the influence of cracking in concrete on reinforcement corrosion. Beeby (1978) concluded that corrosion was likely to start first where the rebar intersects a crack and that in the short term (say, 1 to 2 years), there would be considerable influence of the crack width on the amount of corrosion and in the longer term, the influence of the width would be very small or negligible. This implies that after corrosion initiates, the influence of the crack on the corrosion rate is very small, which is supported by other studies also (Arya and Ofori-Darko, 1996; Schießl and Raupach, 1997). Nevertheless, several researchers have

suggested a relationship between crack width and corrosion rates on the basis that cracks permit air, salt and other impurities to penetrate to rebar and also make reinforced concrete so heterogeneous as to cause macrocell corrosion of reinforcing steel (Okada and Miyagawa, 1980; François and Maso, 1988; Ohno et al., 1996; Arya and Ofori-Darko, 1996). Suzuki et al. (1990) showed that for specimens with a single crack, the steel at the crack intersection was depassivated earlier than that at uncracked sections, and in specimens with multiple cracks, corrosion initiated earlier at the major (wider) cracks, which was attributed to macrocell corrosion. Nevertheless, it was observed that the macrocell action was not strong enough to prevent subsequent corrosion at the minor cracks completely. Arya and Ofori-Darko (1996) found that the crack frequency was a governing factor in the rate of corrosion and suggested that the cover be increased to reduce the crack frequency. Mohammed et al. (2001) observed that the crack frequency depends on the type of rebars, i.e. plain or deformed. A cracked beam with plain bars has fewer surface cracks as well as internal cracks compared to a cracked beam with deformed bars. Pettersson et al. (1996) conducted both laboratory and field experiments (in marine atmosphere) with crack widths of 0.4 mm and 0.8 mm. They found that the corrosion rate decreased as a function of exposure time, which was attributed to the healing effect in the cracks and increase of concrete resistivity. Crack healing is the deposition of a solid material containing ettringite, magnesium hydroxide (brucite) and calcium carbonate which is beneficial for smaller crack widths (Mohammed et al., 2003). Water to cement ratio also appears to be the principal factor affecting macrocell corrosion in cracked concrete (Ohno et al., 1996). François and Arliguie (1998) had alternatively suggested that, rather than the crack width or crack presence, the load applied played an important role in the penetration of aggressive agents and in the corrosion of rebar. Poursaee and Hansson (2008) carried out studies on the influence of longitudinal cracks (cracks parallel to the rebar) on the corrosion protection of rebar in high performance concrete (HPC). It was observed by them that HPC did not provide any beneficial influence on the corrosion. However, in the case of transverse cracks, HPC was found to provide better protection to the steel than normal concrete. In a very recent study by François et al. (2011), it was reported that cracks whatever their width allows the corrosion onset at cracks and along the steel-concrete interface damaged zone caused by the creation of cracks. This process leads to corrosion cracks

formation, which modify the environmental conditions at the level of steel leading to the generalization of corrosion all along the rebars.

Most codes of practice specify maximum permissible crack widths from the durability point of view. For appearance and corrosion, the maximum surface width of crack, in general should not exceed 0.3 mm (BS 8110, 1997; IS 456, 2005). ACI 224 (2010) and ACI 318 (2010) limit crack widths to 0.4 mm, however, it is recognised that corrosion is not clearly correlated with surface crack widths. The European design code, CEB (1989) also cautions that the limitation of crack widths is not the means to avoid corrosion in the case of severe chloride attack on horizontal concrete surfaces.

From the above studies, it is understood that reinforcement corrosion can be solved only by a combination of good concrete quality, adequate cover and crack width limitation. Though considerable research has been carried out on the influence of cracking on reinforcement corrosion, aspects regarding the type of binder and admixtures used, and width of pre-crack need more detailed study.

2.4. Corrosion Assessment Techniques

There are number of factors that influence the corrosion process, it is very difficult to assess or monitor corrosion deterioration in a structure with one equipment or technique. A combination of various tests can lead to a correct and reliable evaluation of the condition of a structure. To assess the corrosion activity or the condition of the rebar in the concrete, techniques such as visual inspection, electrochemical techniques such as half-cell potential, concrete resistivity, linear polarization resistance, tafel plot, electrochemical impedance spectroscopy (or AC impedance), etc., can be used (Gu and Beaudoin, 1998; Hover, 1998; Silverman and Carrico, 1988; Limaye et al., 2000; Broomfield et al., 2002; Montemor et al., 2003; Andrade and Martinez, 2005; Song and Saraswathy, 2007; Pradhan and Bhattacharjee, 2009). An understanding of the underlying principles of these electrochemical methods is needed to obtain meaningful results. Also, accelerated laboratory techniques such as artificial environments like alternate wetting and drying and impressed current/voltage are normally used to evaluate the corrosion resistance of different materials (Saraswathy and Song, 2007a; 2008; Rajamane et al., 2008). The following are some of the commonly used techniques in assessing the chloride induced corrosion of rebar in concrete.

2.4.1. Visual inspection

Visual inspection is usually the first step in any condition assessment of the structure. The aim is to get first hand information about the corrosion damage in a deteriorated structure (ACI 201.1R, 2010; ACI 364.1R, 2010; Frank et al., 2002). However, visual inspection can only provide useful information when done in a rational and systematic manner. Generally, visual inspection shall be done in the form of recording appearance of brown stains, mapping of corrosion cracks, surface damage, etc. Based on the visual inspection, the quantity of area to be covered, the type of tests that are to be carried out, the time required for the detailed investigation can be decided.

2.4.2. Chloride content and pH

As mentioned previously, corrosion of rebar in concrete takes place either due to ingress of chlorides or carbon dioxide or both from the environment. The chlorides available in the atmosphere ingress into the concrete through voids, pores, cracks, etc., and reach the rebar. Once the chloride concentration exceeds the threshold level, the protective layer over the rebar is depassivated and corrosion starts (Broomfield, 2006).

Chloride content and pH in hardened concrete can be measured through the chemical analysis of powdered concrete samples. It is to be noted that hydrated cement has certain chemical and physical binding capacity of chloride ions. This is important as only the free chlorides are relevant to the corrosion of reinforcement. However, it is worthy to note at this point that due to carbonation of concrete, bound chlorides may be released, and consequently the risk of corrosion due to chlorides would increase. Free chloride content in the concrete powder sample can be obtained by doing Mohr's titration method with (0.1 N) $AgNO_3$ solution (Mangat and Gurusamy, 1987a; 1987b) or by specific ion probe method (Cady and Gannon, 1992). The chloride induced corrosion of rebar initiates only after the chloride concentration near the rebar surface reaches a minimum concentration, known as critical chloride threshold level. Mohammed and Hamada (2001) defined the critical chloride threshold level as the "chloride ion concentration of steel bars in concrete, provided that there are no voids/damages at the rebar-concrete interface". Critical threshold values for different steel reinforcement types have been reported in the literature (Alonso et al., 2000; Trejo and Pillai, 2003; 2004). The critical or threshold chloride concentration, at the

rebar level, at which corrosion will occur depends upon various factors and cannot generally be fixed (Richardson, 2002). These include microstructure and metallurgical parameters of the rebar, the complex microstructure of the surrounding concrete and transition zone, the pH of the concrete pore solution, the local environmental characteristics, and the test procedures used to evaluate this parameter (Alonso et al., 2000; Pillai and Trejo, 2005). Corrosion risk classification (an indication of the threshold value) is presented in Table 2.2 (Yu and Bull, 2006).

Table 2.2: Corrosion risk classification at different chloride levels (Yu and Bull, 2006)

Chloride content (% wt. of cement)	Chloride content (% wt. of concrete for 400 kg cement/m^3)	Risk of corrosion
< 0.4	< 0.07	Negligible
0.4 - 1.0	0.07 - 0.17	Possible
1.0 - 2.0	0.17 - 0.35	Probable
> 2.0	> 0.35	Certain

2.4.3. Half-cell potential (HCP) measurement

As explained earlier, corrosion of reinforcement is associated with the anodic and cathodic areas along the reinforcement with consequent changes in electro-potential of the steel. Half-cell potential is an electrochemical method (also referred to as open circuit or corrosion potential) and is one of the most widely used methods for the detection of the probability of corrosion of steel reinforcement in concrete. The technique is based on the measurement of the potential difference between the reinforcement and a reference electrode in the form of a half-cell (Broomfield, 2006; Rodriguez et al., 1994).

The half-cell is a simple device consisting of an electrode and an electrolyte. The electrolyte is normally made from a soluble salt of the electrode metal, i.e., the reference electrode is a piece of metal in a solution of its own ions, such as copper/copper sulphate ($Cu/CuSO_4$), mercury/mercury chloride (Calomel; Hg/Hg_2Cl_2) and silver/silver chloride (Ag/AgCl). Half-cell potential measurement is

based on the electrical and electrolytic continuity between the embedded steel, reference electrode on the concrete surface and the voltmeter. Electrical conduction between the reference electrode and the concrete is established by the transport of ions. This can be ensured by placing a wet sponge between the reference electrode and the concrete surface. Figure 2.6 shows the schematic view of half-cell measurement using $Cu/CuSO_4$ electrode (ASTM C 876, 2009).

The numerical value of the measured potential between the embedded rebar and the reference electrode depends on the type of reference electrode used and the corrosion condition of the steel in the concrete. It is, therefore, important to indicate the reference electrode being used for the half-cell potential measurements. The criteria for the probability of corrosion are given in Table 2.3. The technique is particularly useful because it can be utilized to evaluate the probability of corrosion before damage is evident at the surface of a RC structure; i.e., the half-cell potential measurements give an indication of the corrosion risk of rebar and are linked empirically to the probability of corrosion.
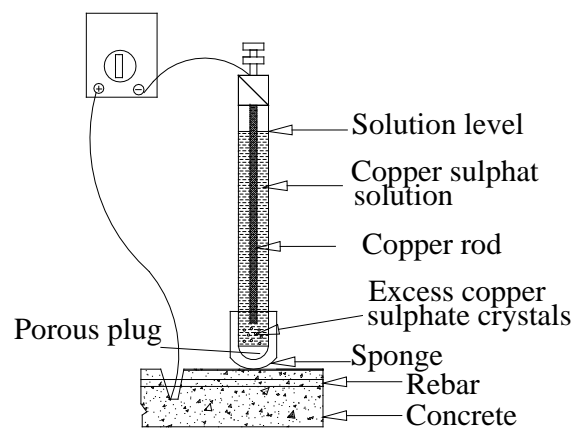
Figure 2.6: Schematic of half-cell potential measurement

Table 2.3: Criteria for corrosion of rebar in concrete for different half-cells
(Broomfield, 2006; Mackechnie et al., 2004; ASTM C 876, 2009)

Cu/CuSO$_4$ electrode	Hg/Hg$_2$Cl$_2$ electrode	Ag/AgCl electrode	Likely corrosion condition
> -200 mV	> -126 mV	> -106 mV	Low (10% risk of corrosion)
-200 to -350 mV	-126 to -276 mV	-106 to -256 mV	Intermediate corrosion risk
< -350 mV	< -276 mV	< -256 mV	High (>90% risk of corrosion)
< - 500 mV	< - 426 mV	< - 406 mV	Severe corrosion

2.4.4. Concrete resistivity measurement

Corrosion of rebar in concrete is an electrochemical process that can be electrolytically minimised by a dry or impermeable material. Concrete resistivity, therefore, influences the corrosion rate of embedded steel once corrosive conditions exist. Resistivity depends on the moisture condition of the concrete, permeability and diffusivity of concrete and on the concentration of ionic species in the pore water. The Wenner four-probe system (see Figure 2.7) is a commonly used device to measure resistivity and consists of four equally spaced probes, which make contact with the concrete surface. In this method, a low frequency alternating current is passed between the two outermost probes and the resulting potential difference between the inner two probes is measured (Frank et al., 2002).

The resistivity ($\bullet$) in $\bullet$ -cm may be expressed as:

$$\rho = \frac{2\pi aV}{I} \qquad (2.8)$$

where: V = voltage difference (Volts)

I = applied current (Amperes)

a = electrode spacing (centimtres)
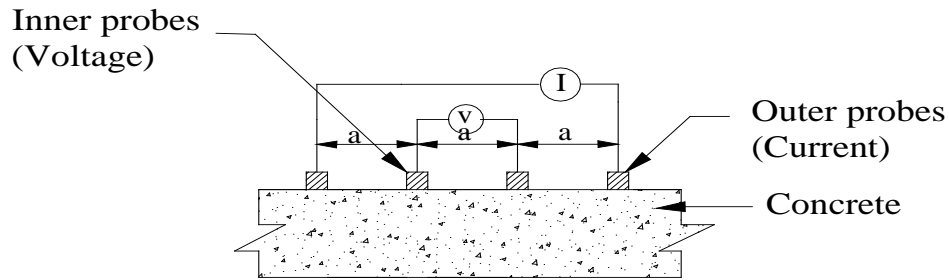
Figure 2.7: Schematic of Wenner four probe resistivity measurement

Table 2.4 provides an empirical interpretation of resistivity measurements with reference to corrosion rate of depassivated steel (Langford and Broomfield, 1987). Resistivity values are dependent on the moisture content of the concrete and therefore may vary from time to time. Resistivity measurements should not be seen as definitive measures of corrosion activity but rather be used to complement with other techniques.

Table 2.4: Likely corrosion rate based on concrete resistivity (Langford and
        Broomfield, 1987)

Resistivity of concrete (k.• .cm)	Likely corrosion rate
< 5	Very high
5 - 10	High
10 - 20	Low to moderate
> 20	Low

2.4.5. Linear polarisation resistance (LPR) technique

In RC structures, determination of the actual rate of corrosion of reinforcement has prominent importance. A commonly adopted method is known as the "Linear Polarisation Resistance" (LPR) technique for the on-site study of corrosion rate of steel in concrete (Frank et al., 2002; Malhotra and Carino, 2004). The term polarization refers to the forced change in the potential as a result of the passage of current. In the polarization resistance test, the current to cause a small change in the value of the potential of the corroding bar is measured.

Three electrodes are used, viz. counter/auxiliary, working, and reference electrodes. The counter electrode applies current or potential to the embedded steel reinforcement, which is the working electrode. The reference electrode (e.g. Ag/AgCl) measures the change in potential due to applied current or potential. Measurements are performed by applying a potential either as a constant pulse (potentiostatic), or a potential sweep (potentiodynamic), and measuring the current response. Alternatively, a current pulse (galvanostatic) or a current sweep (galvanodynamic) can be applied, and the potential response is measured. In each case, the conditions are selected such that the shift in potential, • E falls within the linear range of ±10 to 20 mV (Stern and Geary, 1957). The change in potential is related to the corrosion current, i_{corr}, by the equation:

$$i_{corr} = \frac{B}{R_p} \qquad (2.9)$$

where, B = a constant parameter (in concrete varying from 26 to 52 mV depending on the passive (52 mV) or active (26 mV) condition of the steel; 26 mV is commonly used for corrosion of steel in concrete) and R_p = change in potential•(E)/applied current (• I); R_p is also known as polarization resistance.

The corrosion rate (in terms of current density per given steel surface area) can be deduced as follows:

$$\text{Corrosion rate} = \frac{i_{corr}}{A} \ (\mu A/cm^2) \qquad (2.10)$$

where, A is the polarized steel surface area.

The major limitation of this technique is the difficulty in knowing the actual surface area of steel that is polarized by the applied potential, or the area which is actively corroding. Therefore, corrosion is generally considered to be uniform over the polarized area and the measured corrosion current is divided by the estimated polarized area to give an average corrosion rate. Other limitations are (a) it is an instantaneous corrosion rate (b) it gives no indication of how long corrosion has been going on and (c) it gives no indication on how the corrosion rate varies with time and ambient conditions. Also, it should be noted that these measurements are affected by temperature and relative humidity (RH).

Despite this, the LPR technique is popular for measuring corrosion rate because: (a) it is a non-destructive technique; (b) it is simple to apply and (c) it usually needs only a few minutes for corrosion rate determination. To overcome the problem of accurate determination of the actual polarised area of steel (especially for on-site application), commercial galvanostatic devices, such as GECOR-6 and GECOR-8, make use of guard-ring around the counter/auxiliary electrode to constrain the applied electric field from the counter electrode (NDT, 2006). The guard-ring ensures that a measurement is taken from a defined area of steel and prevents gross errors in the estimation of the area of steel. The schematic diagram of corrosion rate measurement with a guard-ring is shown in Figures 2.8 and 2.9 (Luping, 2002). Table 2.5 gives the classification of measured corrosion rates as proposed by Frank et al. (2002) and Rodriguez et al. (1994).
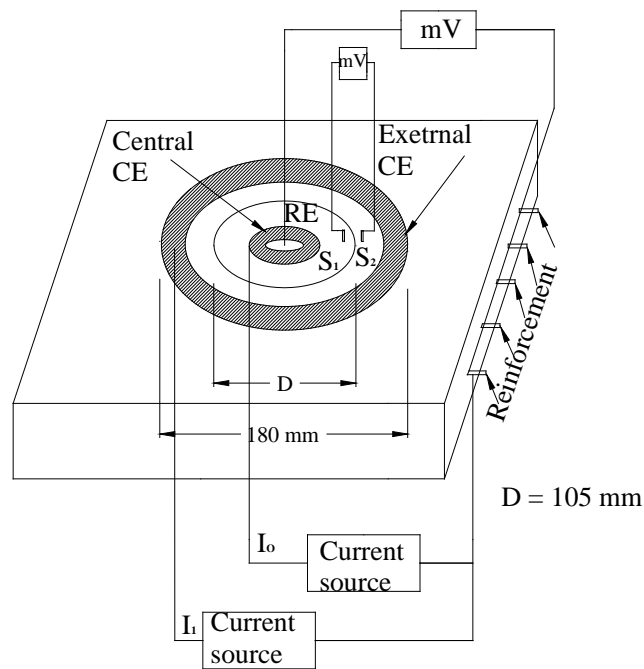
Figure: 2.8: Schematic of the electrodes arrangement on the GECOR-6 disc (adapted from Luping, 2002)
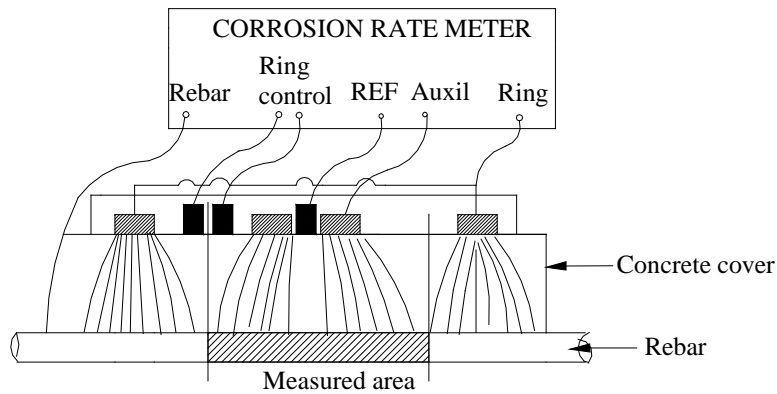
Figure: 2.9: Schematic of linear polarisation with guard electrode for confinement
(adapted from Luping, 2002)

Table 2.5: Qualitative guideline for the assessment of corrosion rate

Corrosion rate or corrosion current density ($\mu A/cm^2$)	Qualitative assessment of corrosion state
< 0.1 - 0.2	Negligible
0.2 - 0.5	Low to moderate
0.5 - 1.0	Moderate to high
> 1.0	High

2.4.6. Accelerated corrosion technique

Accelerated corrosion studies are more commonly used for quick assessment of corrosion behaviour of different materials in RC. Accelerated corrosion environment in RC can be simulated generally by exposing the specimens in the following two ways (Palumbo et al., 1994; Yuan et al., 2007):

(i) Using impressed current (or voltage)
(ii) Exposure studies in alternate wetting and drying conditions (laboratory and field)

Impressed voltage technique is a conventional way of accelerating the corrosion process and adopted by many researchers (Okaba et al., 1997; FDOT, 2000; Austin et

24

al., 2004; Güneyisi et al., 2006; Bhaskar et al., 2006; Sahmaran et al., 2008; Srinivasan et al., 2008; Saraswathy and Song, 2008; Prabakar et al., 2010a). The advantages of this method are: achieving a high degree of corrosion within a short period of time and the easy control of the corrosion degree desired. The impressed current technique consists of applying a constant positive potential (impressed voltage) or constant current from a DC source to the steel bar embedded in concrete to induce significant corrosion in a short period of time (Sakr, 2005). After applying the constant voltage for a given duration, corrosion current/charge passed can be plotted and the degree of induced corrosion can be evaluated theoretically using Faraday's law, or the percentage of actual amount of steel lost due to corrosion can be evaluated with the help of a gravimetric test conducted on the extracted bars after subjecting them to accelerated corrosion. Using the actual amount of steel lost in corrosion, an equivalent corrosion current density can be determined. Maaddawy and Soudki (2003) reported that the impressed current technique is reliable for simulating the corrosion of steel reinforcement in concrete. However, they stated that the use of low current density levels (up to 200 $\mu A/cm^2$) to induce corrosion is more realistic than using higher current density levels since a low current density allows the gradual dissipation of corrosion products, which is closer to the real situation. The test results of impressed current/voltage technique are very useful for relative laboratory assessment of durability characteristics of concretes and protective coatings. However, they may not directly yield any useful estimate of the service life of RC members (Yuan et al., 2007; Poursaee and Hansson, 2009).

Field exposure studies in actual environment and alternative wetting and drying conditions in the laboratory can be used for the assessment of relative performance of various types of concretes and rebars. In fact, the test methodology described in ASTM G 109 (2010) covers alternative wetting and drying (ponding cycles) procedure for determining the effects of chemical admixtures on the corrosion of metals in concrete. However, these methods necessitate long durations of exposures.

2.4.7. Gravimetric weight loss method

To evaluate the corrosion damage, the gravimetric weight loss method is generally used. The amount of corrosion loss of the rebar can be estimated as the loss in weight over the initial weight. The initial weight can be taken as the measured weight of rebar per running length, W_1. The final weight of corroded rebar can be measured as W_2 after cleaning the corroded rebar (ASTM G 1, 2009). From the initial and final weights, percent loss in weight due to corrosion can be determined as follows:

$$C_R = \frac{W_1 - W_2}{W_1} \times 100$$
(2.11)

2.4.8. Summary of corrosion assessment techniques

Corrosion assessment/evaluation methods described above are summarised in Table 2.6 for a quick review. All these techniques can be effectively used for long term corrosion monitoring, in that the progress of changes in the condition can be monitored. Among these, half-cell potential and chloride content techniques are very effective for assessing the probability of chloride induced corrosion. Resistivity measurements can tell us the capacity of the concrete to allow corrosion and is used alongside the half-cell potential and LPR measurements but cannot indicate if corrosion has started or not. Identifying the areas (anodic sites) of probable corrosion, growth of anodic sites over a period of time using half-cell potential, changes in corrosion rates using LPR and changes in concrete resistivity with time are more helpful in predicting long term durability than that of single time measurement. The only reliable method of assessing carbonated concrete is the determination of carbonation depth (Broomfield, 2006). In such circumstances linear polarization is very useful in assessing carbonated structures, particularly as half cell potentials are difficult to interpret for carbonation induced corrosion. It should be noted that a combination of test methods is often needed to provide a proper assessment of corrosion activity. Soleymani and Ismail (2004) showed that different corrosion testing methods predicted the same corrosion activity level for only 24% of specimens that they studied. They reported that the chloride content method usually give a lower corrosion activity level compared to other techniques such as LPR method which predicts higher corrosion activity levels.

Table 2.6: Summary of corrosion assessment/evaluation methods

Test Method	Main Application	Advantages	Limitation
Visual inspection	Identification of surface defects such as rust stains, cracks (width/length) and cover concrete spalling	Provides useful information if done in a rational and systematic manner; physical comparison of one over the other	Visual survey should be followed up by testing to confirm the cause of corrosion, in most cases
Half-cell potential	Monitoring technique. Identifying the areas of probability of corrosion of rebar before damage is evident at surface. Qualitative judgment can be made over a period of time and deterioration can be noted	It is portable and almost non-destructive. Field measurements can be readily made and results can be plotted in the form of equipotential contour diagrams, which can indicate likely/probable areas of corrosion	Requires access to the rebar to make electrical contact. Does not provide information on rate of corrosion
Resistivity	Measuring the ability of the concrete to resist the corrosion current. The higher the resistance the slower the corrosion process	Non-destructive. Simple to operate and many measurements can be rapidly made. Very useful when used in conjunction with other methods of testing, e.g. half-cell potential	It is not reliable at high moisture contents. The electrodes require good contact and nearby bars can affect test readings
Chloride content	Chloride levels at rebar position and chloride profile can be known. Corrosion initiation time can be estimated	Field measurements can be readily made using portable equipment and results can be interpreted for corrosion initiation along with other methods such as half cell potential etc.	Concrete powder samples need to be collected at different cover depths and also from near the steel-concrete interface
Linear polarization resistance (LPR)	Instantaneous corrosion rate measurement of rebar in concrete	The test is almost non-destructive. Field measurements can be readily made and results can be interpreted for corrosion severity	Requires access to the rebar to make electrical contact. Information on exposed surface area of rebar is needed
Gravimetric weight loss	Corrosion damage in terms of weight loss	Loss of damage (in terms of weight loss in material) will be known physically. Easy in interpreting the results	Destructive
Impressed current	Accelerating the corrosion of rebar in concrete. Achieving a high degree of corrosion within a short period of time	Helpful tool for comparing various types of materials against corrosion performance. Laboratory test. Corrosion degree can be controlled by varying the current/voltage or the time interval	Qualitative measurement. The corrosion process under impressed technique is different when compared to the corrosion process under a natural environment

This page is intentionally left blank

2.5. Corrosion Control Measures

It can be said that corrosion of the rebar in concrete is a general phenomenon and needs to be controlled. Corrosion control is usually handled in design codes in the form of minimum concrete cover, minimum grade of concrete, maximum allowable crack width, etc. (Crane, 1983; BS 8110, 1997; IS 456, 2005; Yu and Bull, 2006; ACI 224.1R, 2010). When exposure conditions are particularly harsh, there is a need to apply special measures beyond the minimum provided in the design codes. These include both passive and active measures. Passive measures refer to the improvement of durability of concrete that includes the use of high quality concretes produced by the incorporation of various chemical admixtures (e.g., superplasticizers, shrinkage reducing admixtures, corrosion inhibitors) and mineral admixtures. Active corrosion systems, on the other hand, directly reduce the corrosion rate, which include cathodic protection and galvanization. Some of the commonly used corrosion control measures are summarized as follows (Sakumoto et al., 1996; Andrade and Alonso, 1996; USDT, 2000; Chung, 2000; Mani and Srinivasan, 2001):

- Good quality concrete with low water-to-cement ratio (w/c) and use of superplasticizers
- Provision of adequate concrete cover
- Use of epoxy coated and galvanized steel
- Concrete coatings
- Use of pozzolans (fly ash, silica fume, slag)
- Use of corrosion inhibitors
- Use of electrochemical techniques such as cathodic protection, chloride extraction
- Use of stainless steel (very high Cr) that produces a stable passivating film

For better understanding of some of the above measures and also for the present study, a brief review of the use of superplasticizers, mineral admixtures and corrosion inhibitors are provided below.

2.5.1. Mineral admixtures

Admixtures such as fly ash, blast furnace slag, silica fume, rice husk ash, etc., can be used as partial replacement with ordinary portland cement (OPC) to improve the concrete durability and further reduce the use of raw materials (Saricimen et al., 1995;

Bijen, 1996; Coutinho, 2003; Dinakar et al., 2007; Basheer and Barbhuiya, 2010). Scott et al. (2005) conducted a long term corrosion study to determine the effectiveness of combinations of mineral and chemical admixtures, such as calcium nitrite, silica fume, fly ash, ground granulated blast furnace slag, and disodium tetrapropenyl succinate. They recommended a triple combination of calcium nitrite, silica fume and fly ash (or a double combination of calcium nitrite and blast furnace slag) for optimal protection against corrosion. Scott and Alexander (2007) later reported that blended cements increase the concrete resistivity, which could result in lower cover depths when compared with those for ordinary portland cement (OPC) concrete considering oxygen availability to be a governing factor. Similarly, Pradhan and Bhattacharjee (2007) concluded that portland pozzolana cement (PPC) and portland slag cement (PSC) performed better than OPC against chloride induced corrosion in normal uncracked concrete.

Limited work has been reported on the corrosion resistance of different concretes exposed to severe chloride environments under cracked conditions. Pettersson et al. (1996) conducted both laboratory and field experiments (in marine atmosphere) with crack widths of 0.4 mm and 0.8 mm. They found that the corrosion rate decreased as a function of exposure time, which was attributed to the healing effect in the cracks due to the deposition of ettringite, magnesium hydroxide (brucite) and calcium carbonate (Mohammed et al., 2003). Otieno et al. (2010b) studied the influence of crack widths and types of binders (OPC and OPC with Corex slag) on the corrosion initiation and propagation of reinforcement. The results (corrosion rate) show that for a given crack width, the corrosion is sensitive to the binder type, and for a given binder type and w/c, the corrosion rate increases with increase in crack width. Results further shows that the use of blended cement was found to not only lengthen the passive corrosion state of the uncracked RC but also had a significant influence on the corrosion rates of cracked RC.

2.5.2. Chemical admixtures

2.5.2.1. Superplasticizers

In general, superplasticizers (SPs) have been looked upon as workability agents. Though, plasticizers or superplasticizers (also known as dispersants) do not chemically react with the hydrated cement paste, they affect the microstructure of

cement gel and concrete mainly due to the reduction of water (Ramachandran, 1995). Thus beyond the improvements in fluid properties, there is a considerable improvement in the durability of concrete. The dispersion mechanism in sulphonated melamine formaldehyde (SMF) and sulphonated naphthalene formaldehyde (SNF) based SPs are mainly due to electrostatic repulsion and the dispersion mechanism in Polycarboxylic ether (PCE) based superplasticizers are based on electrostatic repulsion and steric hindrance (Rixom and Mailvaganam, 1999). Considerable research is reported on the influence of superplasticizers on fresh and durability parameters of concrete (Dhir et al., 1987; Rixom and Mailvaganam, 1999; Jayasree and Gettu, 2008). The importance of superplasticizer and the properties of concretes in terms of strength and durability parameters were summarized by many researchers (Dhir et al., 1987; Swamy, 1989; Collepardi et al., 1990a). Based on a number of studies, it can be concluded that superplasticizer reduce the porosity and sorptivity of concrete through reduction in water content and therefore superplasticizer should be seen as agents of concrete durability rather than simply as agents of concrete workability. It can be said that superplasticizers reduce the porosity and permeability of concrete; hence, can reduce the ingress of corrosive elements. However, not much research has been reported on the effect of superplasticizers on the long term durability of reinforced concrete. Gomà et al. (1990) evaluated the effects of different plasticizers on electrochemical behaviour of rebars subjected to accelerated carbonation and reported that some performed well over the others. It was observed that many researchers studied the influence of superplasticizers on a particular mix by adding the SP and reducing the water content (Dhir et al., 1987; Swamy, 1989; Hover, 1998). Nevertheless, by doing so, the dispersing action of SP is not fully evaluated. Roy and Northwood (1997), on the other hand, evaluated the performance of concrete with and without superplasticizer and without changing the water content. It was reported that concrete with SP had lower water penetrability than the one without SP. The improved performance was attributed to better dispersion of cement particles resulting in a greater degree of hydration. Khatib and Mangat (1999) further studied the influence of SP addition on porosity and pore structure of cement paste at constant w/c. They reported that the inclusion of SP in cement paste led to a reduction in the total pore volume and to a refinement of the pore structures. On the corrosion behaviour of rebar in cement paste, Selim (1998) studied exclusively in the presence of water reducing admixture and found that the selected admixtures provided better

protection for rebar corrosion. Among all dispersants, it was observed that PCE superplasticizers provide better durability parameters (Papayianni et al., 2005).

2.5.2.2. Corrosion inhibiting admixtures

One can improve the impermeability of concrete by adding mineral admixtures and superplasticizers (by reducing the w/c). Nevertheless, the rebars embedded even in good quality concretes with covers up to 40 – 60 mm can exhibit corrosion in 25 to 30 years under aggressive environments (Tuutti, 1980; 1982). This means that additional corrosion protection is often needed to protect rebars subjected to severe chloride exposures. This can be achieved by adding corrosion inhibiting admixtures to the concrete (Dhir et al., 1987; Berke and Weil, 1992). A corrosion inhibitor may be defined as a 'chemical compound that decreases the corrosion rate when present in the corrosion system at a suitable concentration' (ISO 8044, 1999). Corrosion inhibitors are either organic (e.g., mixtures of alkanolamines, amines or amino acids, fatty acid esters, etc.) or inorganic (e.g., nitrites, nitrates, etc.), and can be divided into three types: anodic, cathodic and mixed, depending on the interference at the anodic or cathodic sites or whether both are involved (Hansson et al., 1998; Ormellese et al., 2006). They can be either mixed into the fresh concrete (admixed corrosion inhibitors, ACI), or applied to hardened concrete and then allowed to penetrate (penetrating corrosion inhibitors, PCI) through the concrete to the rebar. Both anodic and cathodic reactions are necessary for corrosion to occur. By preventing one of these, corrosion can be inhibited. The mechanism of action of anodic inhibitors is that they usually react with the corrosion products to form a more stable protective layer on the metal surface (i.e., anodic locations). Cathodic inhibitors adsorb on the steel surface and act as a barrier to the reduction of oxygen, which is one of the primary sources for cathodic reaction. The effectiveness of the cathodic inhibitor is related to its molecular structure. Mixed inhibitors influence both the anodic and the cathodic processes. Many of them form a monomolecular layer on the rebar that strongly adsorbs onto the metal surface, and interferes with the anodic and cathodic reactions in the area of adsorption. Therefore, a mixed inhibitor is usually more desirable for the synergistic effect/action (Berke and Weil, 1992). However, in India, the most widely used inhibitor is calcium nitrite inhibitor (CNI).

Admixed Inhibitors

<u>Inorganic inhibitors:</u> Inorganic inhibitor is the one (for example, nitrite inhibitor) that reacts with ferrous ions to form a protective ferric oxide film. It was observed that for concrete exposed to the chloride environment, chlorides (Cl^-), nitrites (NO_2^-), and hydroxyl (OH^-) anions will compete to combine with ferrous cations. Thus, the Cl^-/OH^- and Cl^-/NO_2^- ion ratios are important parameters that affect corrosion protection. As these ratios increase, the probability of chloride ions forming complexes with iron ions also increases and, as a result, the initiation of localized corrosion may be expected (Bentur et al., 1998; Berke and Hicks, 2004; Gaidis, 2004). The calcium nitrite inhibitor is more effective in higher grades of concrete and where chloride concentrations are not more than about 1% by mass of cement. Also, the Cl^-/NO_2^- ratio should be below 1.5 (Berke and Rosenberg, 1990; Berke and Hicks, 2004).

Hope and Ip (1990) concluded that the combination of calcium nitrite and sodium molybdate is more effective than calcium nitrite alone in corrosion protection. Berke et al. (2002) tried various combinations of admixtures to improve the corrosion resistance of rebars in concrete. They reported that as silica fume content increases, there is a substantial decrease in chloride ion penetration (coulombs); however, there was an increase in coulombs due to the presence of calcium nitrite. They further reported that the increase in coulombs is not indicative of increased chloride ion penetration but rather due to the increased negatively charged ionic concentration in the pore water. Montes et al. (2005) and Ann et al. (2006) reported that compressive strength can increase with the presence of CNI. Some other researchers reported that the addition of calcium nitrite influences the hydration process of cement paste (Ma et al., 1998) by accelerating and stabilising the formation of the crystal phase of calcium hydroxide, which leads to an increase in the micropore diameter in the hardened cement paste, and thus an increase in chloride permeability compared to concrete without inhibitor. Many others also observed the increase in chloride permeability due to the presence of CNI (Berke, 1987). To understand more, Amara et al. (2000) performed rapid chloride ion permeability studies on four different concretes with and without nitrite based inhibitor, and observed higher permeability at early ages in concretes with nitrite based inhibitor.

Proper dosage of calcium nitrite inhibitor is very important in the corrosion performance. Mackechnie and Alexander (2001) and Elsener (2001) observed that the level of corrosion protection depends on the dosage of inhibitor used and the chloride level during service. Al-Amoudi et al. (2003) studied the effectiveness of corrosion inhibitors in contaminated concretes and concluded that inhibitors delay the corrosion and the type and dosage of corrosion inhibitor varies with the nature and level of contamination. Berke and Hicks (2004) recommended calcium nitrite inhibitor dosages for different ingress chloride concentrations based on the physical examination of rebar and measurement of the average chloride content at the rebar level.

From the chemical reaction point of view, the inhibitive action of calcium nitrite depends on its reaction with ferrous ions (Fe^{2+}) leading to the formation of a stable passivating layer. The possible chemical reactions are as follows (González et al., 1998):

$$2\,Fe^{2+} + 2(OH)^- + 2(NO_2)^- \rightarrow 2\,NO + Fe_2O_3 + H_2O \qquad (2.12)$$

$$Fe^{2+} + (OH)^- + (NO_2)^- \rightarrow NO + \bullet \cdot FeOOH \qquad (2.13)$$
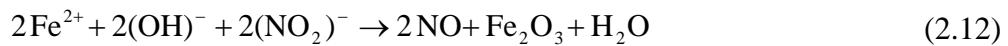
It is reported that both nitrite and chloride ions (anions) tend to react with ferrous ions (cations), therefore, the amount of nitrite ions present can be a key factor affecting the performance of corrosion inhibitor (Ann et al., 2006). In determining the minimal dosage of calcium nitrite to prevent corrosion, the concentration ratio of NO_2^- to Cl^- ions has been generally preferred, which is often regarded as 0.5 to 1.0 (El-Jazairi and Berke, 1990; Berke, 1991) or 0.7 to 1.0 (Gaidis and Rosenberg 1987). Another concept is that the NO_2^- / Cl^- ratio should be above 1.0, and then the reaction will be between nitrite and iron that reinforces the passive layer. If it is less than 1.0, then the chloride ions will react with the iron to begin the corrosion process (www.concreteconstruction.net; 2010). Also, it is reported that the Cl^- / NO_2^- ratio should be below 0.9 (Husain et al., 2004). Short et al., (as reported by González et al., 1998) observed that inadequate dosage of CNI can lead to pitting and counterproductive. From the above, it can be understood that the protective action of CNI depends on many factors. Again, the duration of the protective action of nitrites remains a controversial issue. The nitrites may be diminished by consumption of the inhibitor, or its diffusion to the surrounding environment under immersion conditions.

According to Resenberg and Gaidis (as reported by González et al., 1998), in zones where the passivating oxide layer has been destroyed due to chloride ions, the nitrites does not take part in the passivation, rather, they react at an earlier stage with the anodic corrosion products and is consumed. Because passivating layers are only a few nanometers thick (Gancedo et al., 1989), the inhibitor uptake is so small that the inhibition mechanism as presented in Eq. (2.12) and (2.13) does not preclude the preservation of the protective effect of nitrites for long periods, as experimentally checked by several authors (Andrade et al., 1986, Berke, 1987; Berke and Sundberg 1990).

However, El-Jazairi and Berke (1990) carried out field studies and observed no adverse effects of nitrites on corrosion over a 10 year period of use. They also said that the duration of the protective effect of nitrites remains a controversial subject and is related to concrete quality. Thus, low quality concrete exposed to aggressive conditions such as those of the marine environments are unlikely to benefit from the addition of nitrites (Jin et al., 1991). Possibility of leaching of inhibitor is also a concern. González et al. (1998) concluded that the use of inhibitors for preventing corrosion in reinforced concrete structures is a reasonable choice; however research is still needed in relation to (i) the search of alternate inhibitors for nitrites, (ii) the duration of the protective effect of nitrites and (iii) their ability to protect previously rusted surfaces. It was further concluded that nitrite inhibitor does not function to improve low quality concrete but to raise the quality of high quality concrete, why because, the inhibitor spreads throughout the concrete to protect the rebar and the low permeability concrete prevents the inhibitor leaching. Further, the leaching is more in immersed structures when compared to aerial structures. Another aspect to be noted from environmental point of view is its toxicity. Elsener (2001), stated that calcium nitrite when dissolved in water forms NO_2^- that are considered quite toxic, because they can oxidize the haemoglobins (in the blood) to methemoglobine (containing Fe^{3+} ions) that are not able to transport oxygen. Therefore, it was not allowed as inhibitor for reinforced concrete (RC) structures in ground water or water reservoirs because of a significant leaching out of nitrite ions (Schiessl and Mörsch, 2000).

Other researchers have also reported the ineffective results of calcium nitrite on the properties of concrete and its poor performance in preventing corrosion of rebars. For example, Ma et al. (1998) suggested that the addition of CNI into high performance

concrete in combination with fly ash weakened the concrete resistance to chloride diffusion, and the compressive strength of mixtures containing CNI was reduced in comparison with that of control concrete. Li et al. (1999; 2000) reported an increase in micropore volume in the high performance concrete mixture with CNI and observed that CNI lowers the resistance to chloride diffusion and also the sulphate attack. The reason explained was that the addition of CNI accelerates the formation of calcium hydroxide and ettringite crystals. High content of calcium hydroxide and ettringite crystals fastens the eroding process of sulphate ions, and weakens the mixture's resistance to sulphate attack. Kondratova et al. (2003) reported that the information on the performance of calcium nitrite inhibitor (CNI) in cracked concrete is contradictory. Montes et al. (2004) reported that CNI alone did not improve the corrosion protection, however, observed that the combination of good quality concrete (w/c = 0.37 and lower) and the use of CNI plus fly ash improved the corrosion protection.

In the recent past, different inhibitors such as anodic (calcium nitrite, $Ca(NO_2)_2$; sodium nitrite, $NaNO_2$; zinc oxide, ZnO), cathodic (monoethanolamine, diethanolamine, and triethanolamine), mixed and bipolar inhibition mechanism (BIM) inhibitors were studied by many researchers (Fadayomi, 1997; Saraswathy and Song, 2007b; Tamizhselvi and Knight, 2007; Srinivasan et al., 2008; Mohammed and Knight, 2008; Prabakar et al., 2010a). They stated that corrosion performance improved with the presence of inhibitor and some of them also stated that the properties such as compressive strength, bond strength, permeability, etc., vary depending on the type and dosage of inhibitor.

Similarly, in the case of cracked concretes, different conclusions were made on the corrosion performance of inorganic inhibitors. Berke and Rosenberg (1990) reported that calcium nitrite inhibitor performed well for crack widths up to 0.25 mm. On the other hand, Collepardi et al. (1990b) observed the effect of sodium nitrite ($NaNO_2$) (4% by weight of cement) on the chloride induced corrosion of rebar in cracked concrete and found that it aggravates the local corrosion process when a large amount of chloride ions reach (through crack) the steel reinforcement. Scott et al. (2005) stated that calcium nitrite inhibitor provided good protection against corrosion in uncracked concrete but was not particularly effective in the presence of cracking.

36

Organic inhibitors: Organic based corrosion inhibitors are also known as adsorption corrosion inhibitors because they adsorb on to the surface of the steel and suppress both the cathodic and anodic reactions on the metal surface; thus, providing better corrosion protection. Maeder (1996) studied the influence of organic and mixed inhibitors that are based on amino alcohols (AMA). The results on cracked beams indicate that the corrosion inhibitor specimens performed better than that of control. Kondratova et al. (2003) studied the effectiveness of a calcium nitrite based inhibitor and an organic corrosion inhibitor in uncracked and precracked reinforced concrete slabs exposed in a natural marine environment. They reported that the organic corrosion inhibitor was more efficient than the CNI in terms of corrosion rate reduction in uncracked concrete whereas in cracked concrete both corrosion inhibitors were relatively inefficient. Bolzoni et al. (2004) studied the effectiveness of amino alcohols, alkanolamines and amine esters in addition to calcium nitrite based inhibotor. Their studies revealed that the addition of inhibitors enhanced the critical chloride levels up to 0.8 to 1.2 %. Addition of amino alcohols and nitrite based inhibitors reduced the chloride and corrosion rate appreciably. Similarly, Ormellese et al. (2006) carried out long term studies on amine-esters, aminoalcohols and alkanolamines, and reported that the organic corrosion inhibitors delay the onset of corrosion due to the reduction in the penetration rate of chlorides by filling the concrete pores and blocking the porosity of concrete by the formation of complex compounds.

Penetrating Corrosion Inhibitors (PCIs) or Migrating Corrosion Inhibitors (MCIs)

Penetrating corrosion inhibitors (PCIs) can be organic or inorganic compounds; however, organic compounds seem to be more effective (for neutralizing and film forming). PCIs are based on amino carboxylate chemistry and are effectively "mixed" inhibitors that work on both anodes and cathodes. The PCI migrates first by diffusion through the moisture that is normally available in concrete, then by its high vapour pressure and finally by following the microcracks. The PCI requires time to migrate through the concrete pores to reach the rebar surface and form a protective layer. Once the PCIs reach the metal, they form a monomolecular film, which is physically adsorbed on the metal surface (www.corrosionsource.com, 2010; www.cortecvci.com, 2012). Limaye et al. (2000) presented experimental studies on PCI that is based on bipolar inhibition mechanism (BIM). It was observed that the PCI reduced the

corrosion rate; however, it was less effective than the admixed inhibitor. Also, indicated that the inhibitor's performance is dependent on the severity of corrosion and the conditions at the steel surface. Mackechnie et al. (2004) reported that the inhibitor transportation rate declines as the depth of penetration increases and effective inhibition may not be possible if the chloride levels by mass of cement are above 1.0% at the reinforcement. Heiyantuduwa and Alexander (2006) and Heiyantuduwa et al. (2006) studied both carbonating and chloride contaminated conditions, and their results indicate that both admixed and penetrating organic corrosion inhibitors extended the life of RC structures. For chloride induced corrosion, it was reported that the inhibitor was more effective in higher grades of concrete and where chloride concentrations are not more than about 1% by mass of cement. They further indicated that reinforcement embedded in concrete contaminated with high levels of chloride ions (> 2% by mass of cement) was subjected to severe corrosion, and treatment with organic corrosion inhibitors is almost totally ineffective. It was finally concluded that the use of corrosion inhibitors to treat chloride induced corrosion needs to be carefully considered as their performance is dependent on the severity of corrosion and the conditions at the steel surface.

2.6. Service Life of RC Structures Affected by Chloride Induced Corrosion

This section discusses various stages of deterioration of chloride induced corrosion and the available procedures/models, for providing a simple and reasonable evaluation of the service life of RC structures exposed to chloride environments. Generally, service life refers to the period of time during which a structure meets or exceeds the minimum requirements set for it. The requirements limiting the service life can be technical, functional or economical (Sommerville, 1986; ACI 365.1R, 2010). Technical service life is the time in service until a defined unacceptable state is reached, such as spalling of concrete, loss to the rebar cross section, safety level below acceptable, etc. Functional service life is the time in service until the structure no longer fulfills the functional requirements, such as the needs for increased clearance, higher axle and wheel loads, etc. Economic service life is the time in service until replacement of structure (or part of it) is economically more advantageous than keeping it in service. In this subsection, the technical service life or

also referred as the 'service life' of the RC structures subjected to chloride-rich environments.

The factors that cause the deterioration and limit the service life of RC structures include the presence of chlorides, carbonation, aggressive chemicals, such as acids and sulphates, freeze-thaw and mechanical loads, such as fatigue, vibration and local occasional overloads (ACI 365.1R, 2010). There is very limited information on the synergistic effects of various deterioration mechanisms. Also, many service life prediction models focus on the effect of one or two degradation processes (ACI 365.1R, 2010). As discussed earlier, there are two major processes that lead to the corrosion of reinforcement in concrete. They are: (i) carbonation of cover concrete, and (ii) chloride ingress through cover concrete. Carbonation induced corrosion occurs more commonly in relatively dry environments with sufficient carbon dioxide to diffuse into the cover concrete. However, in chloride rich environments, the ingress of chlorides is usually faster than that of carbonation process and is more likely to cause the premature end of service life (Austroads, 2000). The critical chloride threshold concentration (C_{tc}) is defined as the chloride concentration at the rebar at which depassivation starts (i.e., the breakdown of the passive layer surrounding the rebar occurs; Page and Treadaway, 1982). The knowledge of C_{tc} is important for service life estimations, which depend on various factors and cannot generally be fixed (Richardson, 2002). Once rebar corrosion is initiated, it progresses continuously and shortens the service life by causing surface cracking and subsequent spalling of the cover concrete due to the expansion of the corroding steel. Besides the major deteriorating processes, the quality of concrete, mainly the permeability, length, width and density of cracks, and the thickness of cover concrete also have a great bearing upon the corrosion deterioration (Ahmad, 2003).

Many investigators have expressed corrosion in RC into two stages: (i) initiation stage and (ii) propagation stage (Tuutti, 1982; Cady et al., 1984; Schiessl, 1987; Broomfield et al., 1993; Amey et al., 1998). In the initiation stage, the main processes would be the ingress of chloride ions towards the rebar. In this stage, the corrosion rate of rebar is very low, as long as the content of chloride is below the C_{tc} and the passivity of the reinforcement is maintained. The duration of the initiation stage could vary widely, depending on the aggressiveness of the temperature, humidity and chloride conditions of the environment, the quality of the cover concrete and the critical chloride

threshold of the system. At the beginning of the propagation stage, the corrosion of rebar is activated and from then on, more corrosion products will be formed with time that can finally lead to cracking and spalling of the cover concrete. In the propagation stage, the most important parameter influencing the service life is the corrosion rate of the rebar. This can change with time, particularly when cracking or spalling of the cover concrete occurs, and will be governed by certain corrosion mechanisms, such as transportation of Fe^{2+} ions across the rust layer or the availability of oxygen and moisture at the steel-cementitious interface.

However, as the corrosion damage of the RC becomes more severe with time, the cover concrete will crack and spall. As a result, the rate of ingress of moisture, chlorides and oxygen and/or the rate of removal of the rust layer, which is protective in nature, increases. The corrosion process/progress at this stage has a different mechanism from that before the cover concrete is cracked or spalled. After severe cracking or spalling of the cover concrete, the rebar becomes directly exposed to the environmental agents, so that unpredictable changes of environmental parameters, such as wetting/drying, heating/cooling, etc. would immediately influence the corrosion rate of rebar. It was reported that the rate of corrosion will be uniform or constant (stable) at the initial stages of propagation period and will vary (unstable) at the later stages (Austroads, 2000).

Therefore, the deterioration stages of RC structures due to rebar corrosion can be classified into three, namely (Austroads, 2000):

- corrosion initiation,
- stable corrosion propagation and
- unstable/unpredictable corrosion propagation

Figure 2.10 shows the deterioration stages of rebar corrosion in RC structures. These stages are dominated by different processes, viz., the ingress of chlorides into the cover concrete, the corrosion of reinforcement under stable conditions, and the corrosion of reinforcement under unstable conditions, respectively.
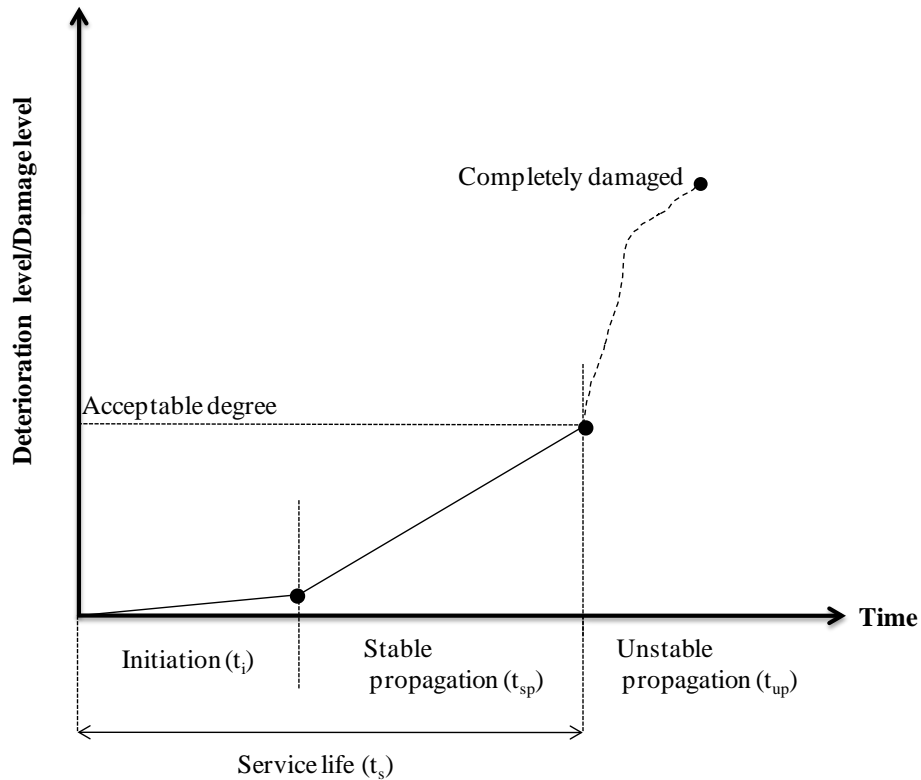
Figure 2.10: Deterioration stages of rebar corrosion in RC (adapted from Austroads, 2000)

The successful evaluation of the initiation, stable propagation and unstable propagation periods is the basis for service life prediction. If all these periods are known, then the service life could be reasonably predicted. It is seen that different researchers have different opinions of what should be defined as the service life. Methodologies/models developed/used for different applications have been discussed by many researchers (Bazant, 1979; Andrade et al., 1990; Ahmad et al., 1997; Weyers, 1998; Austroads, 2000; Anoop et al., 2003; Ahmad, 2003; Baroghel-Bouny et al., 2009; ACI 365.1R, 2010; Life-365, 2010; Otieno et al., 2011; Anoop et al., 2012). In the present case, it is focused mainly on the experimental prediction of service life. According to Geiker et al. (1993), the service life can be defined as the period until repair becomes necessary. Visible large cracks, spalled and delaminated areas are usually considered as severe damage. When a certain percentage of structural elements exhibit these types of damage, the repair or rehabilitation work can become necessary (Andrade et al.,1990; Purvis et al., 1992; Purvis et al., 1994; Chamberlin et al., 1993; Weyers et al., 1994). The service life can also be defined as the duration before certain critical values of measurable properties are reached (Andrade et al., 1990). In general, the service life is dependent on the time for the

initiation of rebar by the ingress of chlorides through cover concrete (Tuutti, 1982; Polder et al., 2006; Visser and Polder, 2006). In practice, there may be a risk to continue keeping the structure in service during its unpredictable propagation stage when damages such as spalling and cracking already exist. To ensure high safety level, the service or use of structures should be stopped as soon as the structure exhibits or experiences unstable corrosion propagation. On the other hand, it may also be too conservative to end the service life at the onset of the stable corrosion propagation stage because corrosion damage at this time is very minimal or negligible.

2.7. Summary

The current level of information available on different corrosion mechanisms in RC, the influence of cracking, the accelerated corrosion, corrosion assessment techniques and different corrosion control measures has been described in this chapter. From the corrosion protection point of view, the measures used essentially should have one or more of the basic three effects: i) reduce the ingress of aggressive agents, such as chlorides, CO_2, etc., into the concrete (low permeability concrete); ii) increase the threshold chloride level at which corrosion initiates (corrosion inhibitors); and iii) reduce the corrosion rate of the active corrosion (improvement in crack resistance of concrete, cathodic protection, etc.).

Aggressive agents, such as chlorides and CO_2, penetrate rapidly through cracks and depassivate the protective oxide layer over rebar in cracked portions early than that of in uncracked portions. Some researchers reported that the corrosion rates increases with an increase in crack width and also that blended cements improve corrosion inhibition. Most codes of practice specify maximum permissible crack width from the durability point of view. For appearance and corrosion, many codes of practice limit the maximum surface width to 0.3 mm or 0.4 mm but recognise that corrosion is not clearly correlated with surface crack width. The European design code, CEB (1989), also cautions that the limitation of crack width is not the means to avoid corrosion in the case of severe chloride attack.

Corrosion assessment techniques such as half-cell potential and chloride content determination are very effective for assessing the probability of chloride induced corrosion. Identifying the areas (anodic sites) of probability of corrosion, growth of

anodic sites over a period of time using half-cell potential, changes in corrosion rates using LPR and changes in concrete resistivity with time are more helpful in predicting long term durability than that of single time measurement. Researchers have used accelerated corrosion procedures such as impressed current technique in order to achieve the desired degree of corrosion within a short period.

In the case of nitrite inhibited concrete exposed to the chloride environment, the Cl^-, NO_2^- and OH^- anions will compete to combine with ferrous cations; thus, the ratio of Cl^-/OH^- and Cl^-/NO_2^- ions are important. As these ratios increase, the probability of chloride ions forming complexes with iron ions also increases and, as a result, the influence of a corrosion inhibitor may not be significant. Therefore, the use of corrosion inhibitors in chloride induced corrosion needs to be carefully considered as their performance is dependent on the severity of corrosion and the conditions at the rebar surface. The review shows that the calcium nitrite inhibitor is more effective in higher grades of concrete and where chloride concentrations are not more than about 1% by mass of cement. Some researchers reported that the addition of calcium nitrite to a good quality concrete provided good corrosion resistance in the presence of cracks of 0.2 mm in width but others reported that corrosion inhibitors (calcium nitrite) does not perform well in cracked concrete.

2.8. Need for the Present Study

Though considerable research has been carried out on the influence of cracking on chloride induced corrosion of steel reinforcement in embedded concrete, the influence of the type of binder and admixtures, and the width of the existing (pre-)crack need more detailed study. The synergistic effect of mineral and chemical admixtures, like fly ash, superplasticizers and corrosion inhibitors, may lead to significant improvement in delaying the onset of rebar corrosion in RC structures. Scanty research is available on the effect of superplasticizers on the long term durability, such as corrosion behaviour of RC. Also, there is a disagreement in the published literature regarding the performance of corrosion inhibitors, especially nitrite based inhibitors in cracked concrete. Finally, there is a need to analyse the effect of the type of concrete used on the corrosion propagation period in addition to corrosion initiation period, so that the total service life of concretes subjected to chloride-rich

43

environment is reasonably estimated. Hence, the present work aims at studying the corrosion resistance of cracked concretes in chloride-rich laboratory environment when used with combinations of cements and chemical admixtures such as PCE SP and CNI.

CHAPTER 3

EXPERIMENTAL PROGRAMME

3.1. General

Concrete of good quality can be developed by proper selection of materials, suitable mix proportions, amount of water added to the mix, workmanship, compaction, curing, admixtures, etc. Durability parameters such as resistance to chloride ion ingress, water absorption, etc. can be improved by adding mineral and chemical admixtures. Good quality concrete will have better strength and durability parameters that enhance the service life of RC structures. Different tests are needed to evaluate the strength and durability parameters of RC.

The objective of the study is to evaluate the mechanical and durability parameters of concretes made using chemical and mineral admixtures. The objective is also to study in detail about the corrosion resistance of different concretes with and without cracks. Appropriate tests are needed to evaluate mechanical, durability and long term effects such as corrosion resistance performance of concrete. For evaluating this, the specimens need to expose for longer durations in the case of natural environment or shorter durations in the case of accelerated corrosion environments. This chapter highlights the materials and mix proportions used in the research work; test specimens and methods used for evaluating different mechanical, durability and corrosion assessment parameters. These include compressive strength, flexural and splitting tensile strengths, water absorption, chloride-ion penetration, accelerated corrosion of embedded rebar, weight loss of rebar, etc. For most of these tests, standard test specimens are available. However, to study corrosion resistance performance of concrete in the presence of cracks, appropriate test specimen and also accelerated corrosion methodology is needed.

This chapter discusses about the experimental programme of the study including mix proportions selected, materials used, test variables and their combinations, etc. U-shaped test specimen developed at CSIR-SERC is proposed to be used for studying the corrosion resistance of different concretes with and without cracks. Details of U-shaped test specimen with emphasis on the crack initiation due to mechanical loading

are presented. Experimental programme planned for the evaluation of basic mechanical and durability parameters and the accelerated corrosion used to evaluate the relative performance of chosen materials is also presented.

3.2. Materials Used

Two cements, ordinary portland cement (OPC) and fly ash based portland pozzolana cement (PPC) that are commonly used in reinforced concrete (RC) construction, potable water, fine aggregate, coarse aggregate, thermo-mechanically treated (TMT) deformed bars, polycarboxylic ether superplasticizer (PCE SP) and calcium nitrite inhibitor (CNI) were employed in this study. The details about the materials used are presented in the following sections.

3.2.1. Cement

Commercially available OPC and PPC of the same manufacturing source are taken. As per the manufacturer's specifications, the PPC is fly ash based factory ground conforming to IS 1489 (2005); the fly ash constituent is around 20 - 25% by mass of the PPC. The chemical composition of the cements is given in Table 3.1 and the values are in agreement with the approximate oxide limits reported in the literature (Shetty, 2005; Saraswathy and Song, 2007a). The loss on ignition of OPC is 3.6% where as the loss of ignition of PPC is 4.3%. The physical and engineering properties are presented in Table 3.2.

Table 3.1: Chemical composition of cements (%)

Compound	OPC	PPC
CaO	63.0 – 64.0	40.0 – 43.0
SiO_2	18.8 – 19.1	28.0 – 32.0
Al_2O_3	4.6 – 6.4	8.3 – 10.0
Fe_2O_3	3.7 – 5.2	3.8 – 6.0
MgO	0.7 - 3.0	1.0 – 2.0
SO_3	1.2 - 1.7	1.9 – 2.8

Table 3.2: Physical and engineering properties of cements

Physical Properties	OPC	PPC
Specific gravity	3.15	2.98
Initial setting time	140 minutes	160 minutes
Final setting time	220 minutes	360 minutes
Compressive strength of mortar cubes at 28 days (N/mm^2)	48.9	48.0

3.2.2. Coarse and fine aggregates

Two fractions of graded coarse aggregate (CA) of crushed granite with maximum size aggregates (MSA) 20 mm and 12 mm were used in the ratio of 1.5:1 (60 % of 20 mm MSA & 40 % of 12 mm MSA). The combined aggregate grading for the above proportions is presented in Table 3.3. The specific gravity, bulk density and fineness modulus of the combined aggregate are 2.68, 1600 kg/m^3 and 6.81, respectively.

Table 3.3: Gradation of coarse aggregate (CA)

Sieve size (mm)	% Wt. retained	Cum. % wt. retained	Cum. % passing
40	0	0	100
20	0.3	6	94
10	2.86	63.2	36.8
4.75	1.70	97.2	2.8
2.36	0.14	100	0

River sand satisfying IS 383 (2007) was used as the fine aggregates; the grading is presented in Table 3.4. The specific gravity and fineness modulus were found to be 2.67 and 2.78, respectively.

Table 3.4: Gradation of fine aggregate (FA)

Sieve size (mm)	% Wt. retained	Cum. % wt. retained	Cum. % passing
10	0	0	100
4.75	2.5	2.5	97.5
2.36	4.0	6.5	93.5
1.18	22.0	28.5	71.5
0.6	34.5	63.0	37.0
0.3	24.5	87.5	12.5
0.15	12.0	99.5	0.5

3.2.3. Steel

Thermo-mechanically treated (TMT) deformed bars with diameters of 12 mm and 16 mm are used. The chemical composition of rebar computed as per ASTM E 415 (2005) is presented in Table 3.5.

Table 3.5: Chemical composition of the rebar (Chennai Mettex Lab Pvt. Ltd.)

Composition	%	Composition	%
Carbon (C)	0.234 (0.30)[*]	Aluminium (Al)	0.011
Manganese (Mn)	0.658	Copper (Cu)	0.000
Silicon (Si)	0.121	Tin (Sn)	0.000
Sulphur (S)	0.025 (0.060)[*]	Tungsten (W)	0.000
Phosphorous (P)	0.025 (0.060)[*]	Boron (B)	0.00082
Chromium (Cr)	0.064	Cobalt (Co)	0.007
Nickel (Ni)	0.049	Niobium (Nb)	0.000
Molybdenum (Mo)	0.020	Lead (Pb)	0.000
Titanium (Ti)	0.002	Nitrogen (N)	0.007
Vanadium (V)	0.000		

Note: * the values in parentheses denote the maximum values as per IS 1786 (2008)

3.2.4. Chemical admixtures

Commercially available Polycarboxylic ether superplasticizer (PCE SP) and calcium nitrite inhibitor (CNI) is chosen for the study. As per the manufacturer's specification, the superplasticizer has a specific gravity of 1.09 and solid content of about 30% by weight, and complies with IS 9103 (2004). The corrosion inhibitor contains about 30% calcium nitrite by mass and meets the ASTM C 494 (2010) requirements for Type C (accelerating admixtures).

3.3. Concrete Mixes

In the present study, ACI 211 (2010) guidelines for the mix design and IS 456 (2005) guidelines for durability requirements are followed. A slump of 25 mm to 50 mm is chosen for the concrete mix and water content of 170 kg/m^3 is considered. As per IS 456 (2005), for reinforced concrete, the maximum free water to cement ratio (w/c) is 0.55. Keeping this in mind, trials have been made and the upper limit of w/c was adopted as 0.57. In order to have different grades of concrete, water to cement ratios (w/c) 0.47 and 0.37 are also considered. The mix composition per cubic metre of concrete is presented in Table 3.6. The aggregates are considered to be in the saturated surface dry condition.

Table 3.6: Quantities per cubic metre (kg/m^3) of concrete

w/c	Cement	Sand	CA	Water
0.57	300	870	1056	170
0.47	362	815	1056	170
0.37	460	732	1056	170

The dosage of the PCE SP is decided by trial and error for obtaining a slump in the range of 125 mm to 150 mm. Accordingly, the SP dosages in liquid form are 0.3%, 0.25% and 0.2%, by mass of cement, for the concretes with w/c = 0.57, 0.47 and 0.37, respectively.

The dosage of the CNI is fixed at 10 l/m^3; which is within the dosage range recommended by the manufacturer of 5 l/m^3 to 30 l/m^3. As stated earlier, the main aim of the present work was to understand the corrosion resistance performance of

different concretes in chloride induced environment under cracked conditions. Hence, in the present study, as described earlier, specimens with pre-cracks of surface widths 0.2 and 0.4 mm, along with specimens without any pre-crack are proposed to be studied. Accordingly, the variables considered in the experimental study are as listed below:

Cement Type: OPC and PPC

Water to cement ratio: 0.57, 0.47 and 0.37

Crack Width: 0, 0.2 and 0.4 mm.

The different cement-chemical admixture combinations employed and studied are listed below:

1. OPC (Control concrete)
2. PPC
3. OPC with PCE SP
4. PPC with PCE SP
5. OPC with CNI
6. PPC with CNI
7. OPC with CNI and SP
8. PPC with CNI and SP

3.4. Test Specimens

3.4.1. Standard specimens for mechanical and durability studies

Standard specimens used are cubes of 150 mm, cylinders of 150 mm diameter and 300 mm height and prisms of 100 mm×100 mm×500 mm were cast and tested for mechanical properties such as compressive, split tensile and flexural strengths, respectively. Cylinder specimens of 75 mm diameter by 150 mm height and 100 mm diameter by 200 mm height cylinders are used for durability parameters such as water absorption, sorptivity, rapid chloride permeability test (RCPT) value and diffusion coefficient.

3.4.2. U-shaped specimen for corrosion studies in cracked concrete

A simple U-shaped specimen, developed at CSIR-SERC, is used for initiating flexural cracks of a required width (Rajamane et al., 2008). The specimen has a horizontal portion (flange) of 100 mm×100 mm×600 mm and two integral vertical stubs of size 100 mm×150 mm cross section and 200 mm height at the ends. A deformed TMT steel rod of 12 mm diameter is placed with 20 mm clear cover at the bottom.

During casting, provisions are made to have holes at the top of the stub to insert two tie rods for inducing a compressive force producing bending in the horizontal portion. Figure 3.1 shows the cross section of the U-shaped specimen with tie rods and photographs of the U-shaped mould and the cast specimen are shown in Figure 3.2 and 3.3. After 28 days of water curing followed by 30 days air curing, flexural cracks of the prescribed width (i.e., 0.2 or 0.4 mm) are created by stressing the tie rods with nuts. Sometimes, this leads to multiple cracks on the surface of the horizontal portion (flange/beam), some of which are observed on the surface to reach the reinforcement bar. However, the maximum surface crack width is considered.
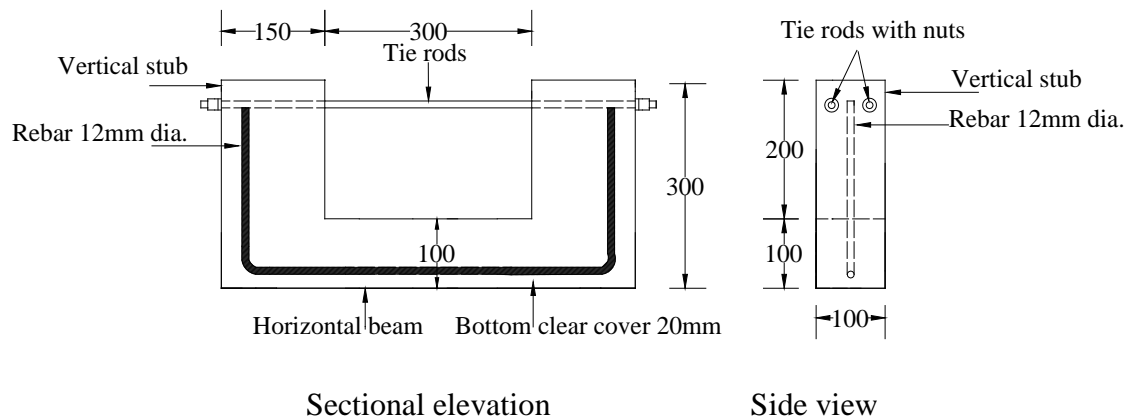
Figure 3.1: U–shaped specimen
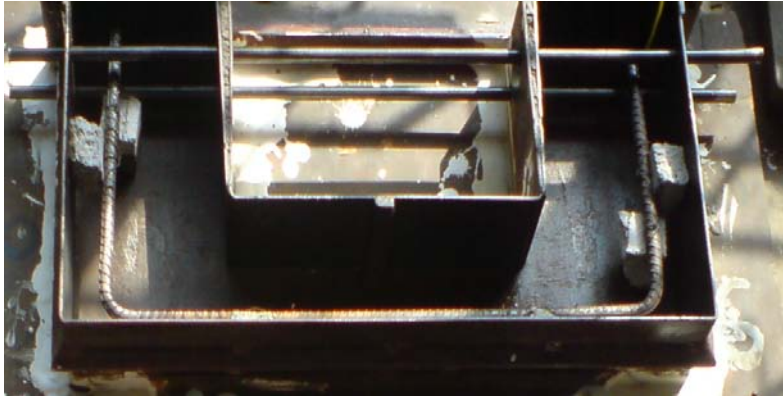
Figure 3.2: Mould with rebar

Figure 3.3: Cast specimen with tie rods

3.4.3. Number of specimens

The number of specimens considered for each parameter is three; i.e., 9 U-shaped specimens are cast for each w/c (crack width = 0 (i.e., uncracked), 0.2 and 0.4 mm). Cubes, prisms, cylinders, U-shaped specimens cast for a typical concrete mix (for example, OPC concrete alone) are presented in Table 3.7 and same numbers of specimens are cast for other mixes also. The total numbers of U-shaped specimens cast were 216.

Table 3.7: Number of specimens for a typical mix

Description	w/c			Total
	0.57	0.47	0.37	
Cubes (150 mm)	3	3	3	9
Prisms (100×100×500 mm)	3	3	3	9
Cylinders (150×300 mm)	3	3	3	9
Cylinders (100×200 mm)	3	3	3	9
Cylinders (75×150 mm)	3	3	3	9
U-shaped specimens (100×100×600 mm)	9	9	9	27

A tilting type mixer is used for mixing the ingredients. In all cases, the specimens were placed in three layers and compacted using a table vibrator. For the U-shaped specimens, the reinforcement bars are cleaned before casting and wires soldered to them for applying the electrical connection, as described in the later sections. All the specimens are kept in the moulds for 24 hours, then demoulded and cured in water for 28 days.

3.5. Tests on Mechanical and Durability Parameters

Mechanical as well as durability parameters, such as compressive strength, splitting tensile strength, flexural strength, water absorption, sorptivity, RCPT value, etc., are evaluated after 28 days. The procedures adopted are described below.

3.5.1. Mechanical properties

Compressive and flexural strengths are evaluated as per IS 516 (2002) with 150 mm concrete cubes and 100×100×500 mm prisms under third-point loading, respectively. In each case, three specimens are tested and their average values are reported.

For the split tensile strength, concrete cylinders of 150 mm diameter and 300 mm length are used. The test is carried out by placing the cylindrical specimen horizontally between the loading surfaces of a compression testing machine and the load is applied until failure of the cylinder, along the vertical diameter. To reduce the magnitude of the high compression stresses near the points of application of the load, narrow packing strips of plywood are placed between the specimen and loading platens of the testing machine. The tests are carried out on three specimens and the average values are recorded.

3.5.2. Durability parameters

Different durability tests related to the transport mechanisms and penetrability are described in the following.

3.5.2.1. Sorptivity

The performance of concrete subjected to aggressive environments is a function, to a large extent, of the penetrability of the pore system. In unsaturated concrete, the rate of ingress of water or other liquids is largely controlled by absorption due to capillary rise. The water absorption of a concrete surface depends on many factors (Rathishkumar et al., 2002; Dias, 2004) including (a) concrete mixture proportions, (b) the presence of chemical admixtures and supplementary cementitious materials, (c) the composition and physical characteristics of the cementitious component and the aggregates, (d) the type and duration of curing, (e) the degree of hydration or age, (f) the presence of surface treatments such as sealers or form oil, and placement method including consolidation and finishing. For the present study, 50 mm thick slices are cut from cylinders of 100 mm diameter and 200 mm height. The slices are kept in an oven for 48 hours at 100±5ºC, taken out, allowed to cool for 24 hours and weighed. Then, the slices are put on a weld mesh allowing free access of water at the bottom surface. The water level is kept not more than 5 mm above the base of the specimen. Figure 3.4 gives the details of sorptivity test. Weights of the specimens are

noted, after 30 and 60 minutes, after wiping off any excess water with a damp tissue. The quantity of absorbed water during the time period from 30 to 60 minutes is determined from the difference in weights. The sorptivity is calculated as

$$s = \frac{\Delta W}{(A.d)t^{1/2}}$$ (3.1)

where: s =   sorptivity (mm/$\sqrt{}$(min.))

t =   elapsed time (min.)

ΔW =   Weight of specimen after 60 min. (g.) - weight of specimen after 30 min (g.)

A =   Surface area of specimen through which water penetrates (mm^2)

d =   density of water (g/mm^3)
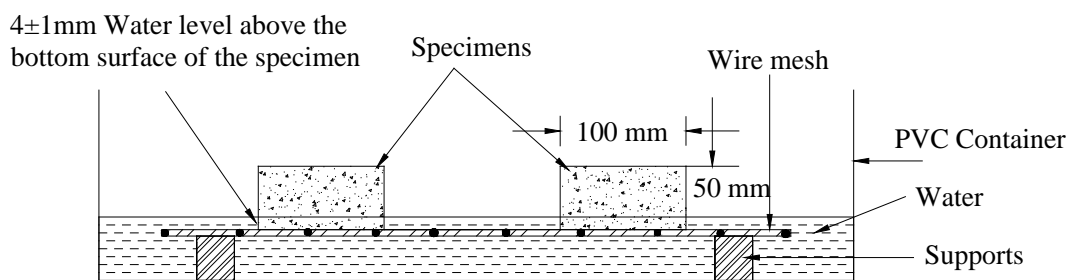
Figure 3.4: Details of the sorptivity test

3.5.2.2. Water absorption

Water absorption test is used to estimate the maximum amount of water absorbed by a dry specimen and, therefore, provides a measure of the total, water permeable pore space. Cylinders of 75 mm diameter and 150 mm height are kept in oven at 105±5°C for 48 hours, and the dry weights are recorded (W_1). Later, the specimens are allowed to cool at room temperature and then the specimens are immersed completely in water for 24 hours. The weight of the final surface-dry specimen after immersion is recorded (W_2). Water absorption (w), in percent is calculated as

$$w = \frac{W_1 - W_2}{W_1} \times 100$$ (3.2)

55

3.5.2.3. Rapid chloride permeability test (RCPT)

The rapid chloride permeability test (RCPT) is conducted on concrete discs as per ASTM C 1202 (2009). Cylinders of 100 mm diameter and 200 mm height are cut into discs of 50 mm thickness. The specimens are submerged in water for 24 hours. Then, the specimens are subjected to the RCPT by impressing a 60 V current. Figure 3.5 shows the details of the RCPT setup. The two cells consist of Plexiglas reservoirs as shown in Figure 3.6. The capacity of each reservoir is such that when the solution level is at the brim, the volume is equal to 250 ml. One side of the reservoir is filled with 3% NaCl solution (i.e., cell is connected to the negative terminal of the power supply) and the other side is filled with 0.3N NaOH solution (i.e., connected to the positive terminal of the power supply). Current is measured every 30 minutes up to 6 hours. From the results using current and time, charge passed is calculated in terms of coulombs at the end of 6 hours. Table 3.8 shows the guidelines provided by ASTM C 1202.
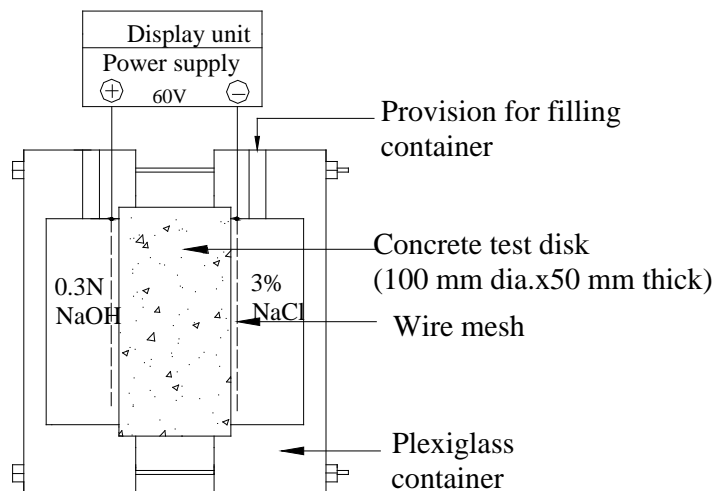
Figure 3.5: Details of the RCPT test setup

Table 3.8 Chloride permeability based on charge passed

Charge Passed (coulombs)	Chloride Permeability
> 4,000	High
2,000 – 4,000	Moderate
1,000 – 2,000	Low
100 – 1,000	Very Low
< 100	Negligible

3.6. Accelerated Corrosion

In the present study, it is proposed that the corrosion process is accelerated by impressing an anodic potential between the rebar anode and steel plate cathode. As discussed earlier, impressed current is a conventional way of accelerating the corrosion process and adopted by many researchers (Okaba et al., 1997; FDOT 2000; Güneyisi et al., 2006; Austin et al., 2004; Saraswathy and Song 2008; Sahmaran et al., 2008). However, Maaddawy and Soudki (2003) stated that the use of low current density levels to induce corrosion was more realistic than using higher current density levels since a low current density allows the gradual dissipation of corrosion products, which is close to the real situation. Nevertheless, in the present study, the technique is used to achieve the desired theoretical degree of corrosion of steel within a certain time frame and finally the relative corrosion resistance performance of different concretes in terms of the chosen variables.

Initially, the flange (or beam) portion of U-shaped specimens is immersed in a 3.5% NaCl solution for 24 hours to ensure full saturation of the test specimen. The NaCl solution level in the plastic tray is maintained well above the rebar position of the flange portion. Later, a constant 10 V anodic potential is applied for the specified durations. Figure 3.7 shows a schematic of the accelerated corrosion test setup and Figure 3.8 shows the photograph of the U-shaped specimen ready for accelerated corrosion.
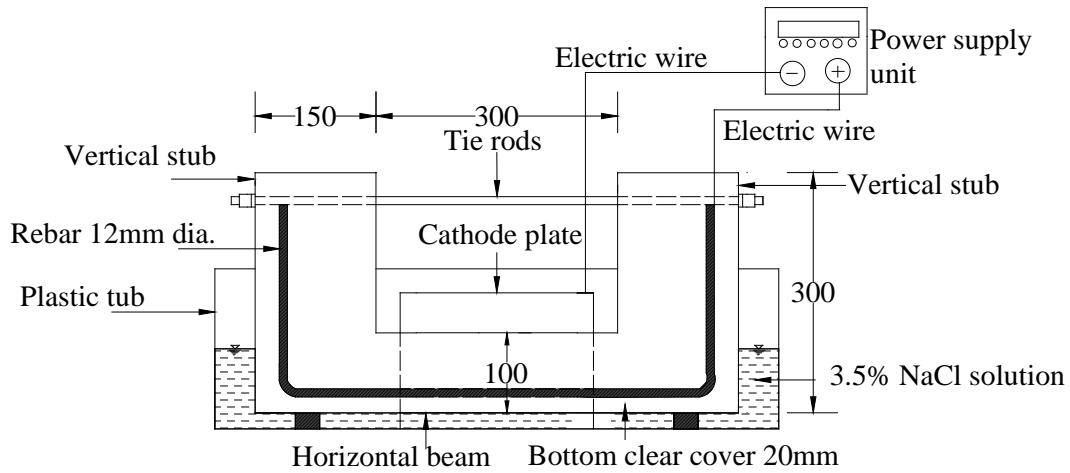
Figure 3.6: Accelerated corrosion test setup

Figure 3.7: Photograph of U-shaped uncracked specimen ready for accelerated corrosion

3.7. Weight Loss

The actual amount of corrosion of the rebar (C_R) can be estimated by determining the gravimetric weight loss of the reinforcement, which is measured as the relative loss in weight over the initial weight, and represents the average weight loss over the length considered:

$$C_R = \frac{W_1 - W_2}{W_1} \times 100 \qquad (3.3)$$

where,　W_1　=　initial weight of the rebar

　　　　W_2　=　weight of the rebar after removal of corrosion products

In the present experimental program, techniques such as visual observation, half-cell potential and resistivity are used, and the test results are noted at regular intervals. Half-cell potential measurements with copper/copper sulphate (Cu/CuSO$_4$) electrode and resistivity measurements with the Wenner four probe resistivity meter will be taken. Gravimetric weight loss measurements are to be taken at the end of the stipulated duration of accelerated impressed voltage test.

3.8. Summary

In this chapter, the details of materials selected, test variables and their combinations, experiments to be performed during the study have been presented. Different test methods used for evaluating mechanical, durability and corrosion assessment properties and the procedure for testing have been described. The experiments carried out for different concretes, discussion of test results and their interpretation are presented in the following chapters.

This page is intentionally left blank

CHAPTER 4

INFLUENCE OF PORTLAND POZZOLANA CEMENT ON CORROSION RESISTANCE

4.1. General

Long term durability parameters of concrete such as corrosion resistance performance depend on many factors such as type of binder, compaction, curing, quality of concrete, type of exposure to the environment, etc. It is known that the durability will be enhanced by adding mineral admixtures, like fly ash (added to the concrete mix by replacing the OPC or by using the fly ash based PPC), silica fume, etc., to the concrete. The corrosion resistance performance of such concretes, however, in the presence of cracks needs to be investigated.

Hence, studies are proposed on the influence of type of binder, viz., ordinary portland cement (OPC) and fly ash based portland pozzolana cement (PPC) on the corrosion resistance performance. The main objective of the chapter is to study the corrosion behaviour of concretes with the flexural cracks in chloride-rich accelerated corrosion environment. Another objective is to evaluate the effect of w/c on mechanical, durability and the corrosion resistance performance.

Corrosion resistance of OPC and fly ash based PPC concretes, when exposed to chloride-rich accelerated laboratory environment is assessed in this chapter. The variables include three w/c and two crack widths 0.2 mm and 0.4 mm. Reinforced concrete U-shaped specimens with cracks under flexural conditions (which is more realistic) is used in the chloride-rich accelerated corrosion. A deformed TMT steel bar of 12 mm diameter is placed at the bottom with 20 mm clear cover (refer Figure 3.1). Results of mechanical and durability properties on cubes and cylinders of standard specimens, half-cell potential, resistivity, total charge passed and gravimetric weight loss of corroded rebars of U-shaped specimens are presented.

4.2. Mechanical and Durability Parameters of the Concretes

The mechanical properties, such as compressive, split tensile and flexural strengths, and durability parameters, such as water absorption, sorptivity, RCPT etc., are evaluated by following the procedures given in Chapter 3 on the concrete cubes and cylinders after 28 days of water curing. Figures 4.1 - 4.3 show the tests in progress for water absorption, sorptivity and RCPT. Tables 4.1 and 4.2 present the mechanical and durability parameters obtained for both OPC and PPC concretes for the three w/c 0.57, 0.47 and 0.37. In each case, three specimens are tested and the average values are reported. The individual specimen results are presented in Table A.1 of Appendix A.

Figure 4.1: Photograph of immersion of cylinders for the water absorption test

Figure 4.2: Photograph of the sorptivity test

Figure 4.3: Photograph of RCPT setup

Table 4.1: Average mechanical properties (at 28 days) of OPC & PPC concretes

Property	Concrete type	w/c		
		0.57	0.47	0.37
Compressive strength (MPa)	OPC	33.2	44.7	53.7
	PPC	30.7	41.4	51.2
Split tensile strength (MPa)	OPC	2.4	3.8	4.0
	PPC	2.7	3.7	4.6
Flexural strength (MPa)	OPC	4.1	5.6	6.4
	PPC	5.0	5.6	6.9

Table 4.2: Average durability parameters (at 28 days) of OPC & PPC concretes

Property	Concrete type	w/c		
		0.57	0.47	0.37
RCPT (Coulombs or Amp-sec)	OPC	2600	2100	1900
	PPC	861	720	520
Sorptivity (mm/min.$^{0.5}$)	OPC	0.097	0.092	0.087
	PPC	0.060	0.049	0.043
Water absorption (%)	OPC	5.8	5.1	4.7
	PPC	6.5	6.0	5.0

63

It can be observed from Tables 4.1 and 4.2 that, as w/c decreases, the mechanical as well as durability (water absorption, sorptivity and the charge passed in the RCPT) parameters improve, as expected. It can also be observed that the compressive strengths of PPC concrete are nearly same as those of OPC concretes and the difference is about 5% to 8%. The overall variation in compressive strength values of OPC and PPC concretes from their mean of the respective concretes is in the range of +6.2 to -7%. The individual specimen results are presented in Table A.1 of Appendix A. The flexural and split tensile strengths of PPC concrete are slightly above that of the corresponding OPC concretes. Though the compressive strengths are almost same, it is observed that the RCPT value of PPC concrete is nearly one-third that of OPC concrete, which means that the PPC concrete is much less permeable in terms of chloride ingress (Rajamane et al., 2008; Prabakar et al., 2011). Similar observations were also reported by Sivasundaram et al. (1989), Bilodeau et al. (1994), and Malhotra and Mehta (2002) in the case of high volume fly ash concretes. Based on ASTM C 1202, the chloride permeability or penetrability can be classified as 'moderate' for the OPC concretes and 'very low' for PPC concretes. The overall variation in RCPT values and water absorption of OPC and PPC concretes from their mean is in the range of ±7 and +6 to -9, respectively. The individual specimen results are presented in Tables A.2 and A.3 of Appendix A. Also, from Table 4.2, it can be seen that the sorptivity (rate of water absorption) values of PPC concrete are lower than that of OPC concrete. The difference in resistance to chloride ion penetration and sorptivity are probably due to the combination of mechanisms, such as a more compact microstructure, lower conductivity, etc., as also observed by earlier researchers (e.g., Mangat and Molloy, 1991; Mangat et al., 1994; Mackechnie and Alexander, 1996).

4.3. Accelerated Corrosion with U-shaped RC Specimens

As already described in Chapter 3, U-shaped specimens are used here for performing accelerated corrosion tests. An anodic potential 10 V is impressed between the rebar anode and steel plate cathode. The specimens are subjected to the impressed voltage after 28 days of water curing followed by 30 days of air curing. Initially, the specimens are immersed in a 3.5 % NaCl solution for 24 hours to ensure full saturation of the specimen. The NaCl solution level in the plastic tray is maintained

well above the rebar depth (refer to Figure 3.7). Then, the impressed voltage is maintained for about 22 days.

The test duration of 22 days corresponds to the theoretical time needed to attain a weight loss of about 20% in the rebar embedded in an uncracked specimen of concrete with w/c = 0.57. The theoretical time was estimated based on Faraday's law given by Equation 4.1, by which the loss of iron over time can be obtained from the area under the curve of corrosion current versus time (Holm, 1987; Liu and Weyers, 1996). In other words, the amount of corrosion is related to the electrical energy consumed and is a function of voltage, amperage and time interval (Cabrera, 1996; Congqi et al., 2006).

$$\Delta\omega = \frac{AIt}{ZF} \tag{4.1}$$

where: $\Delta\omega$ =   metal weight loss due to corrosion

         A =   atomic weight of iron (56g)

         I =   corrosion current (amp)

         t =   time elapsed (sec)

         Z =   valency of the reacting electrode (iron) taken as 2

         F =   Faraday's constant (96500 amp sec)

Figures 4.4 (a & b) and 4.5 show details of the accelerated corrosion test in progress. Since corrosion is basically an electrochemical phenomenon, measurements of electrochemical parameters are helpful to identify the presence and severity of corrosion. Half-cell potential measurements with reference to copper-copper sulphate electrode and resistivity measurements with a Wenner four probe resistivity meter have been recorded. GECOR-6 is used to monitor corrosion rates for some selected cases only (NDT, 2006).

Figure 4.4a: Typical view of accelerated corrosion test set-up: Uncracked specimens without tie rods

Figure 4.4b: Typical view of accelerated corrosion test set-up with data-logger: Uncracked specimens without tie rods (closer view)

Figure 4.5: Typical view of accelerated corrosion test set-up: Cracked specimens with tie rods

4.3.1. Half-cell potential and resistivity measurements

During the period of accelerated corrosion, half-cell potential and resistivity measurements are taken at regular intervals after disconnecting the power supply and taking the specimen out of the NaCl solution. The half-cell potentials measured with the saturated copper/copper sulphate electrode are shown in Figures 4.6 - 4.8 for w/c equal to 0.57, 0.47 and 0.37, respectively. Each series is designated by the notation 'cement type-w/c-flexural crack width' (i.e. OPC-0.57-0, denote OPC binder, w/c of 0.57 and uncracked specimen). Comparing all three, it can be easily observed that the half-cell potentials of PPC concrete are initially less negative compared to those of OPC concretes. There is some improvement in the PPC concrete, since the initial half-cell potentials decrease as the w/c decreases. For OPC concrete, it is observed that the uncracked specimens show more negative potentials than -350 mV within 2 days of exposure whereas the cracked specimens show more negative potentials than -350 mV right from the beginning, and later both maintain the same trend throughout the test period. In the case of PPC concrete, it is observed that the uncracked specimens showed potentials more negative than -350 mV after nearly about 7 - 10 days of exposure. Also, 0.2 mm cracked specimens showed less negative potentials than that

of corresponding OPC concretes. These trends are in agreement with those observed in the resistivity results that are measured with the Wenner four probe resistivity meter, where it can be seen, from Figures 4.9 - 4.11, that the initial resistivity values of PPC concrete are higher than those of the corresponding OPC concretes. Similar observations were also made by Scott and Alexander (2007) and Prabakar et al. (2011), where it is reported that the concretes with 30-35% fly ash as replacement exhibited substantially higher resistivity compared to that of OPC concrete. In general, the resistivity values of uncracked specimens are higher than those of the cracked ones, as expected. The initial resistivity values of cracked specimens of PPC concretes for w/c equal to 0.47 and 0.37 are still more than that of corresponding uncracked specimens of OPC concretes.

From these tests, it can be stated that the PPC concrete offers higher resistance to corrosion current compared to OPC concrete. Also, initially the half cell potentials of PPC concrete are less negative compared to OPC concrete indicating that the probability of corrosion initiation in the PPC concretes is lower compared to that of OPC concretes. Later on, the potentials of OPC concrete are more or less stable, probably due to practical conditions such as loss of contact of the electrode with the concrete surface due to the formation of rust and wider corrosion cracks on the bottom surface of U-shaped specimen. Although, the half cell potential is a good indicator of corrosion initiation, it may not be effective in reflecting the corrosion progression (Gadve et al., 2009; Sharp et al., 1988).
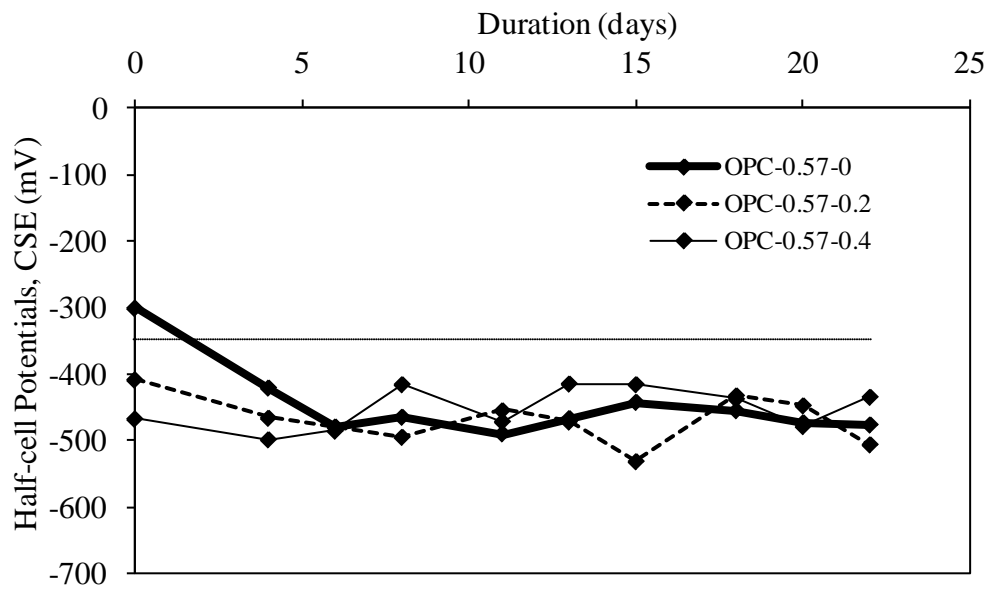
(a) OPC concrete
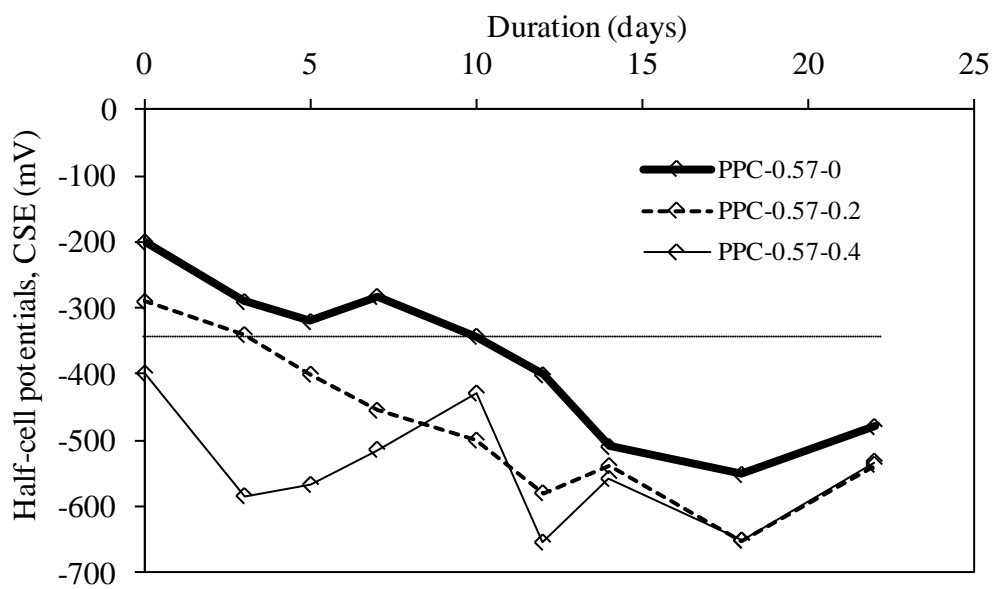
(b) PPC concrete

Figure 4.6: Half-cell potentials of OPC and PPC concretes for w/c = 0.57
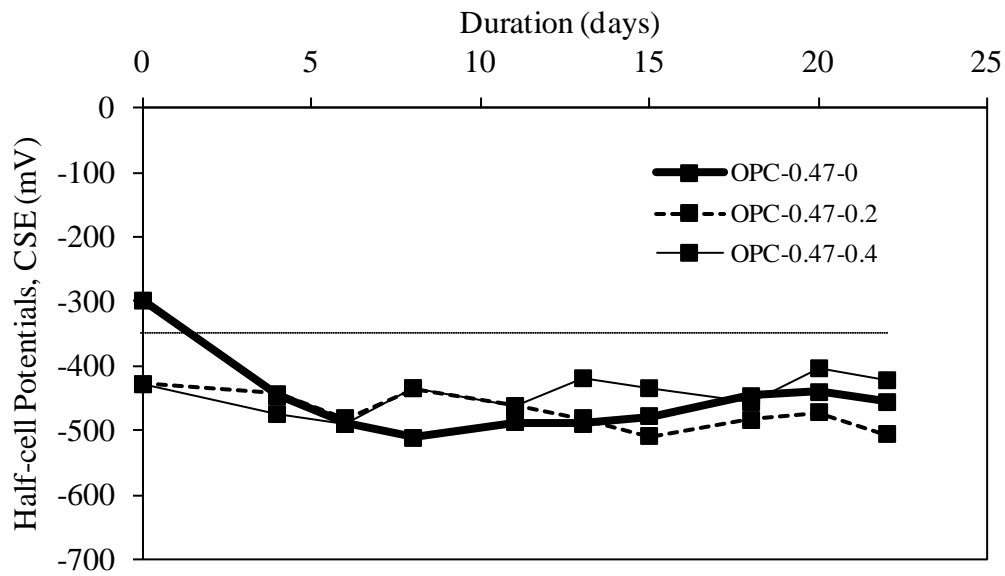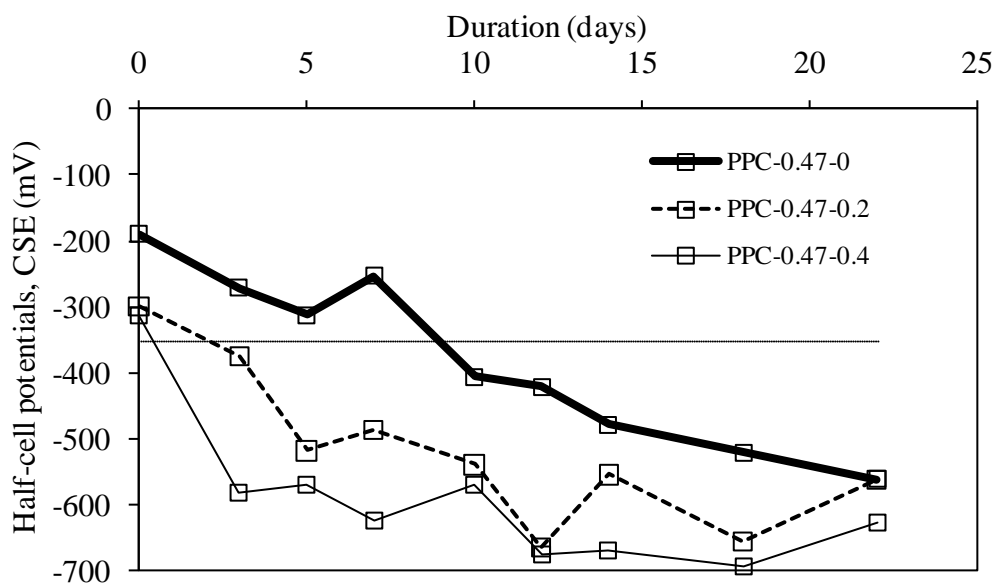
(a) OPC concrete

(b) PPC concrete

Figure 4.7: Half-cell potentials of OPC and PPC concretes for w/c = 0.47
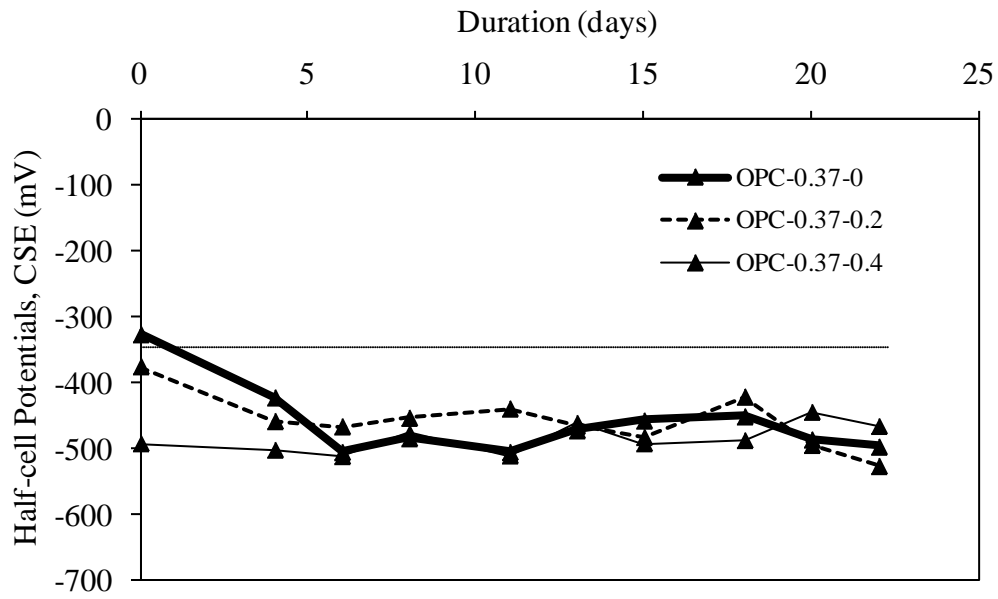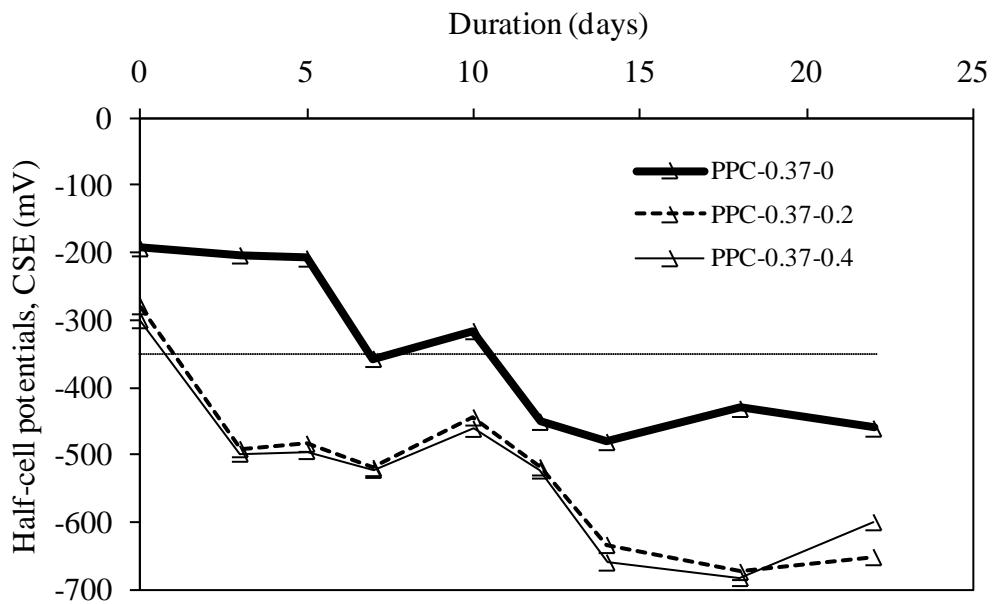
(a) OPC concrete

(b) PPC concrete

Figure 4.8: Half-cell potentials of OPC and PPC concretes for w/c = 0.37
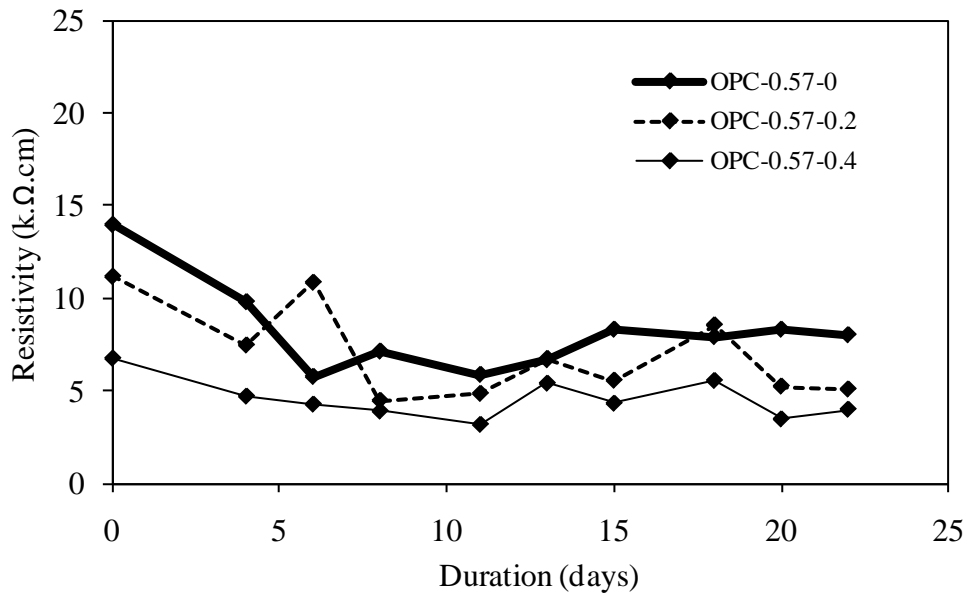
(a) OPC concrete
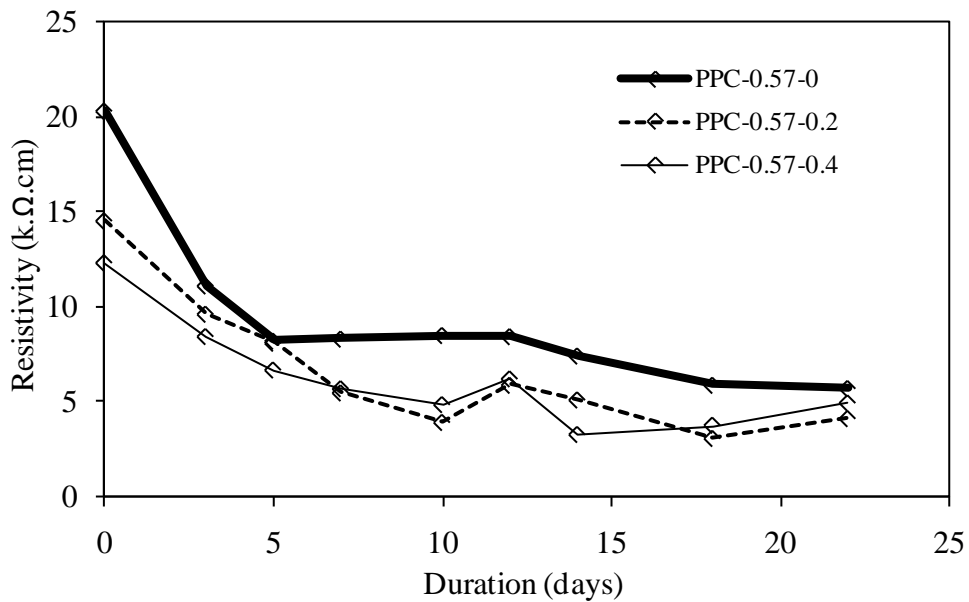
(b) PPC concrete

Figure 4.9: Resistivity measurements, OPC and PPC concretes for w/c = 0.57
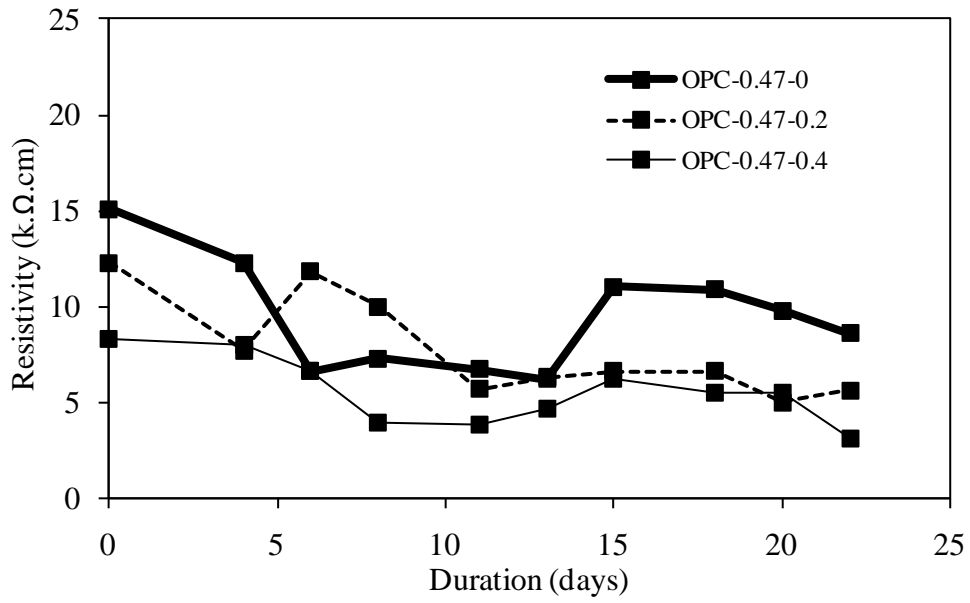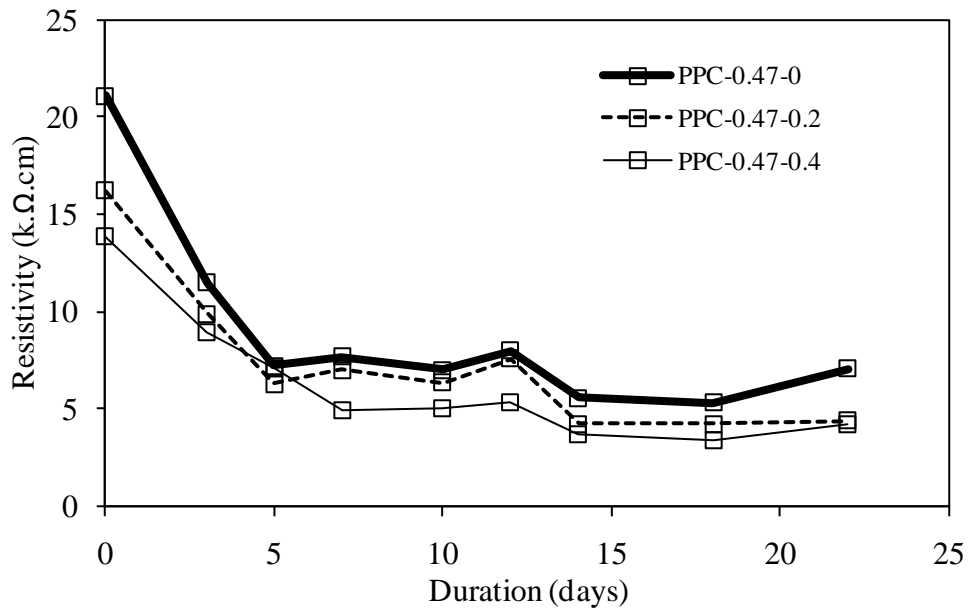
(a) OPC concrete

(b) PPC concrete

Figure 4.10: Resistivity measurements, OPC and PPC concretes for w/c = 0.47
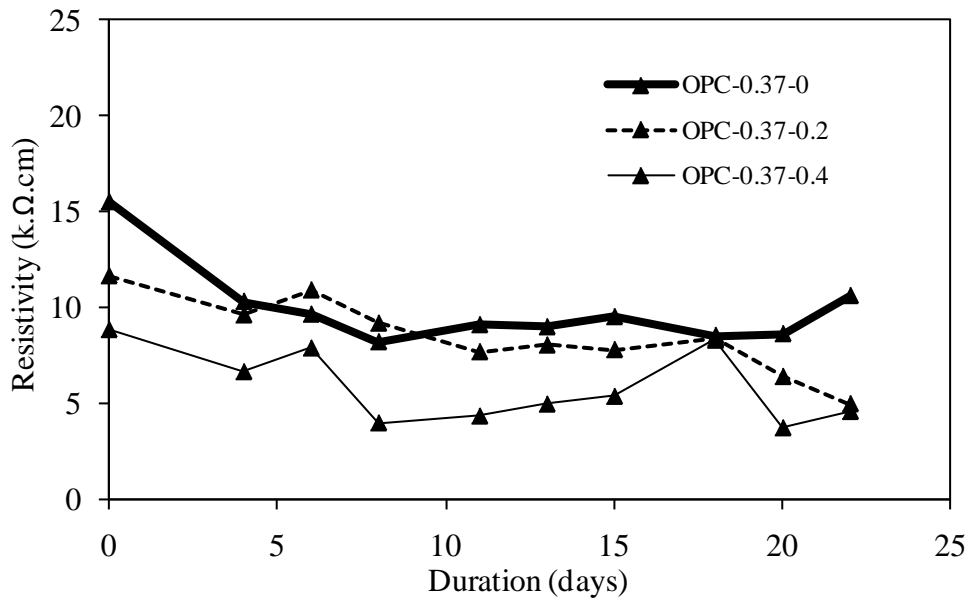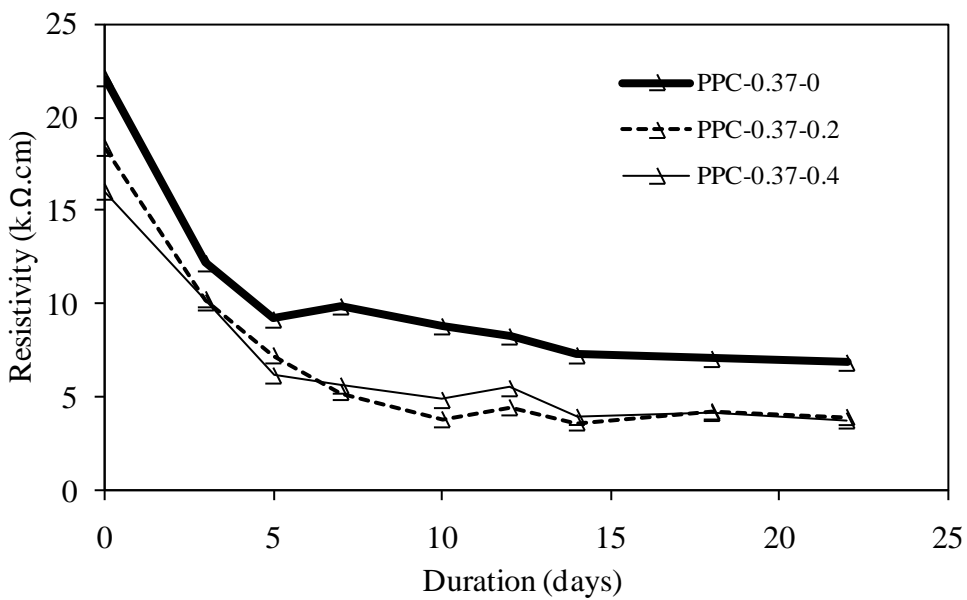
(a) OPC concrete

(b) PPC concrete

Figure 4.11: Resistivity measurements, OPC and PPC concretes for w/c = 0.37

4.3.2. Corrosion current

The corrosion current is monitored and recorded every hour using an automatic data logger. The data for corrosion current/charge passed in all the series for 22 days (i.e., 528 hours) are presented in Figures 4.12 - 4.14 for OPC and PPC concretes, for w/c equal to 0.57, 0.47 and 0.37, respectively. In each series, three specimens are used and the average values are reported. It can be seen from these figures that the reduction in w/c from 0.57 to 0.37, resulted in a reduction of the total charge passed in both cracked and uncracked specimens. The charge passed in concrete specimens with w/c equal to 0.57 is higher than that of specimens with w/c equal to 0.47, and the charge passed for w/c equal to 0.47 is more than that of concrete with w/c equal to 0.37. Also, the charge passed is more in the cracked specimens compared to their corresponding uncracked specimens, which can be attributed to macrocell corrosion.

The change in charge passed can be divided into three stages (Sakr, 2005). The first stage is characterized by an initial decrease in current values with time, which may be attributed to the formation of an iron oxide layer that protects the steel temporarily. The second stage is characterized by an increase in current due to the formation of micro-cracks that result from steel corrosion and facilitate the penetration of ions into the steel. The third stage is characterized by relatively small current variations. It is confirmed that the concrete with a lower w/c delays corrosion or depassivation (completion of first stage). It can be seen that the total charge passed decreases with a decrease in the w/c, and is higher for the cracked specimens due to macrocell corrosion, as reported by Okada and Miyagawa (1980). Moreover, as the crack width increases, the total charge passed also increases. The decrease in charge passed for a lower w/c is due to higher impermeability and lower electrical conductivity of concrete as indicated by the lower water absorption and chloride ion penetration. The higher charge passed in cracked specimens is due to the fact that the time to depassivation is lowered by the cracking.

The work reported by Tuutti (1982) demonstrated very little effect of crack on corrosion of rebar, in the long run, although initially cracked section exhibited higher corrosion rates. However, in the present study, the specimen is exposed to accelerated corrosive environment and is under load throughout the test duration. Thus, the presence of flexural crack and its development due to the loading makes the environment surrounding the rebar more heterogeneous (i.e., discontinuities due to the

formation of microcracks and debonding around the rebar) so as to cause macrocell corrosion of the rebar. Therefore, the corrosion current observed is more than that of the uncracked concrete. Also, the specimen is in an electrolyte solution, and the rust products developed during the corrosion process leach out through the crack(s), resulting in more corrosion current and also local/pitting corrosion.
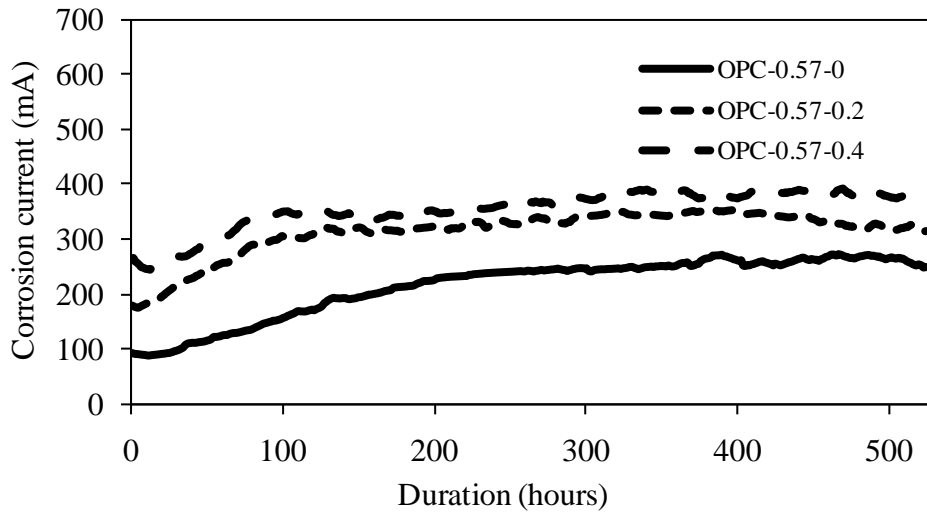
(a) OPC concrete
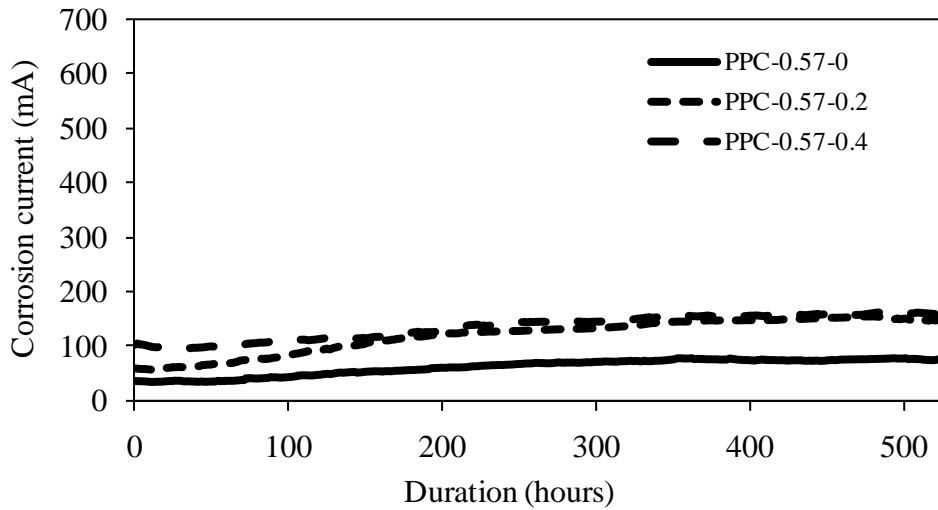
(b) PPC concrete

Figure 4.12: Corrosion current as a function of exposure duration, OPC and PPC concretes for w/c = 0.57
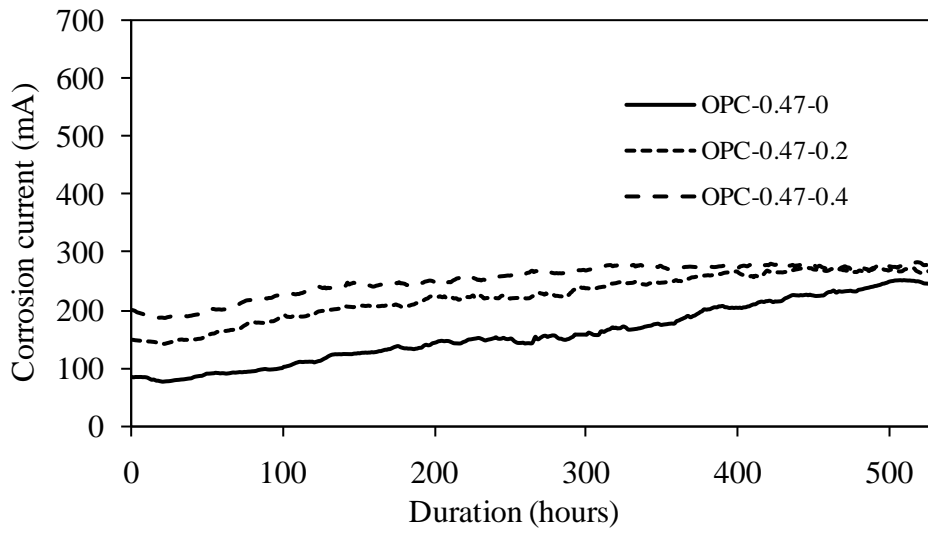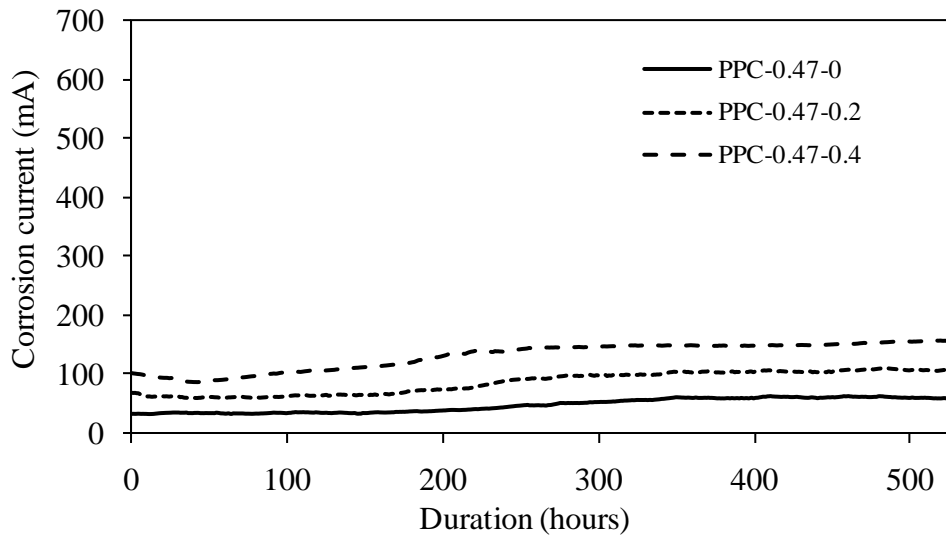
(a) OPC concrete

(b) PPC concrete

Figure 4.13: Corrosion current as a function of exposure duration, OPC and PPC concretes for w/c = 0.47
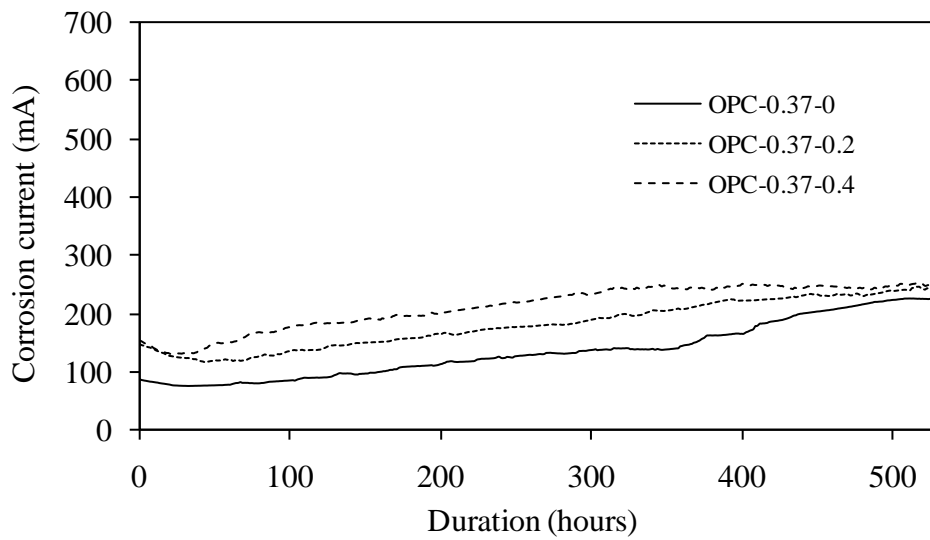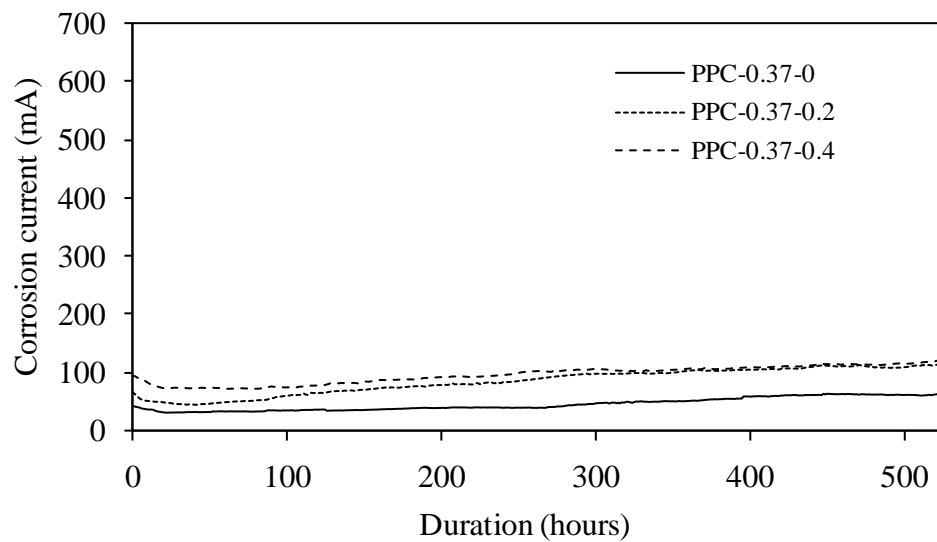
(a) OPC concrete

(b) PPC concrete

Figure 4.14: Corrosion current as a function of exposure duration, OPC and PPC
concretes for w/c = 0.37

78

The areas under the curve or the total charge passed in all series are presented for both OPC and PPC concretes in Table 4.3. Comparing OPC and PPC concretes in Figures 4.12 to 4.14 and the data in Table 4.3, it is clear that that the total charge passed in PPC concretes is 2.6 to 2.8 times less than that of the corresponding OPC concretes. This could be due to lower permeability, increased resistivity and increased chloride binding capacity (Arya and Xu, 1995; Mangat et al., 1994; Scott and Alexander, 2007). Thangavel et al. (2009) reported that chloride ions are adsorbed on the surface of the pozzolanic material and chemically react with its aluminate phase forming the insoluble chloroaluminate complexes $3CaO.Al_2O_3.CaCl_2.10H_2O$. Therefore, the use of fly ash blended cement is beneficial in restricting the mobility of chloride ions within the hydrated cement paste. Also, due to the secondary hydration process and pore filling effect, the interfacial transition zone (ITZ) in PPC concrete is stronger (Vedalakshmi et al., 2008).

Table 4.3: Charge passed in OPC & PPC concretes, Amp-days (constant 10 V for 528 hours)

Description	Concrete type	w/c		
		0.57	0.47	0.37
Uncracked	OPC	4.7	3.5	3.0
	PPC	1.4	1.04	0.99
0.2 mm-crack	OPC	6.9	4.9	4.0
	PPC	2.6	1.87	1.83
0.4 mm-crack	OPC	7.8	5.5	4.7
	PPC	3.0	2.85	2.12

4.3.3. Corrosion rate measurements

As already discussed in Chapter 2, the corrosion rate measurements of embedded rebars in concrete can be measured by using the linear polarization resistance (LPR) technique. In the field, measurements are commonly done using galvanostatic LPR techniques (application of a small current) with a guard ring sensor to confine the area of steel under the test. The LPR instrument used in the present study was a commercial device called the GECOR-6 (NDT, 2006). Measurements were taken by placing the sensor on the concrete surface directly over the rebar and making an

electrical connection to the rebar. Before placing the sensor, the concrete surface has to be wetted. Polarised surface area of the rebar in cm^2 has to be given as input to the GECOR instrument. (i.e., the area corresponds to the 105 mm diameter circle concentric to the sensor). For a single rebar of diameter '*D*' (cm), with the sensor centered over it, the area (*A*) in square centimeters will be:

$$A = 3.142 \times D \times 10.5 \tag{4.3}$$

After the specified polarisation period (default value = 100 seconds), the instrument displays the corrosion rate in µA/cm^2. Note that Mackechnie et al. (2004) indicated that corrosion rates fluctuate significantly in response to environmental and material influences, and single readings are generally inadequate. Several readings over different days have been, therefore, recommended to obtain a reliable indication of corrosion rate.

However, during the measurement, the apparatus gave the warning 'confinement not achieved' for many specimens. Also, sometimes, a 'measuring error' was noticed. The message 'confinement not achieved' appears due to the following: (a) confinement of the signal not achieved due to size of the specimen (b) poor contact between concrete and sensor or between the rate meter and the reinforcement, and (c) high concrete resistivity. In the present study, the 'confinement not achieved' could be either due to small size (the lateral dimension of the specimen is only 100 mm) of the specimen or due to poor contact between the sensor and concrete surface due to rust coming out through the corrosion induced cracks. It was also confirmed by NDT James Instruments customer support that the minimum dimension of the specimen needs to be 200 mm in order to eliminate the confinement problem. Hence, the corrosion rate measurements recorded for some cases using GECOR-6 were discarded and not reported here.

4.3.4. Corrosion induced cracks

During the accelerated corrosion test, the specimens were monitored visually for corrosion induced cracks at regular intervals. In the initial stages of accelerated corrosion, the corrosion follows Mechanism 1 (microcell) in uncracked specimens and follows Mechanism 2 (macrocell) in cracked specimens. That is, in cracked specimens, rust stains are observed first at the pre-crack (flexural cracks) and later

corrosion induced longitudinal cracks develop. In the uncracked specimens, more uniform corrosion is observed and the corrosion induced cracks develop along the rebar at later periods. After sometime, more uniform corrosion is observed in both uncracked and cracked specimens because the corrosion cracks interconnect and a single longitudinal corrosion crack developed along the rebar. After the test, the specimens are taken out from NaCl solution to measure the corrosion induced crack widths after flushing the surface with water. Subsequently, the corrosion induced crack length (crack trajectory) and average crack widths in the middle 300 mm portion covered by the cathode plate are measured.

The corrosion crack width has been measured at 30 mm intervals using a crack measuring microscope with an accuracy of 0.02 mm; the results are presented in Table 4.4. It can be observed that, for cracked specimens of OPC, the average corrosion induced crack width is lower than that of uncracked specimens. Similarly, it is observed that the corrosion induced crack width decreases as the flexural crack width increases. Nevertheless, the corrosion induced crack length increases as the flexural crack width increases. The decrease in corrosion induced crack width with an increase in flexural crack width may be due to the free outflow of corrosion products through crack openings that reduces the expansive force of the corroding rebar and consequently the tensile stress induced in the cover concrete. The increase in the crack width with a decrease in w/c may be due to the higher tensile strength resulting in increased build-up of corrosion products before the corrosion crack develops.

Table 4.4: Corrosion induced crack dimensions of OPC & PPC concretes

Description	Concrete type	w/c = 0.57		w/c = 0.47		w/c = 0.37	
		Length (cm)	Width (mm)	Length (cm)	Width (mm)	Length (cm)	Width (mm)
Uncracked	OPC	31.80	0.83	31.28	0.95	32.64	1.21
	PPC	32.36	0.15	32.64	0.22	32.28	0.43
0.2 mm-crack	OPC	32.55	0.73	34.20	0.81	33.60	1.14
	PPC	34.32	0.56	32.16	0.38	33.07	0.55
0.4 mm-crack	OPC	32.91	0.58	33.07	0.68	33.96	1.03
	PPC	34.30	0.44	33.48	0.54	33.12	0.48

In the case of PPC concrete, similar trends are observed for cracked specimens with 0.2 and 0.4 mm crack widths. The average corrosion induced crack width is more for

the specimens with 0.2 mm crack width compared to specimens with 0.4 mm crack width. However, the average corrosion induced crack width for the uncracked specimens is lower than that of specimens with both 0.2 mm and 0.4 mm crack widths. This may be because, in the PPC concretes, the amount of corrosion (i.e., the weight loss of rebar) is nearly one-third that of OPC concrete. Therefore, the rust would exert less pressure on the cover concrete, lowering the corrosion crack width. Also, for a given weight loss, the corrosion induced crack width is smaller in the case of PPC concrete. These observations reveal that assessing corrosion damage by measuring the corrosion induced crack width may not give reliable results because the corrosion induced crack width is influenced by many factors such as composition of materials, initial condition of the component or structure, i.e., pre-cracking due to mechanical loading, etc.

After measuring the crack induced crack width and length along the crack trajectory, the middle 300 mm length of each specimen is split open and the rebar is examined visually for corrosion. It is observed that more uniform/generalized corrosion occurred in the rebars of the uncracked specimens, and both uniform and macrocell corrosion are observed in the rebars of cracked specimens.

4.3.5. Weight loss measurements

The gravimetric weight loss of the rebar is measured as the relative loss in weight over the middle 300 mm length, and represents the average weight loss over the length considered. After breaking open the specimen, the rebar is cleaned as per ASTM G 1 (2009) to remove the rust; Figures 4.15 and 4.16 shows the corroded rebars of OPC and PPC concretes for w/c equal to 0.37 after cleaning. The initial weight is taken from the measured weight of rebar per running length. The weight loss due to corrosion is lower in concrete with lower water to cement ratios (also observed earlier by means of total charge passed) could be due to increased impermeability and lower electrical conductivity. The gravimetric weight loss results are presented in Table 4.5 and in Figure 4.17. The individual results for uncracked, 0.2 mm and 0.4 mm are presented in Tables B.1 - B.3 of Appendix B.

Uncracked specimens
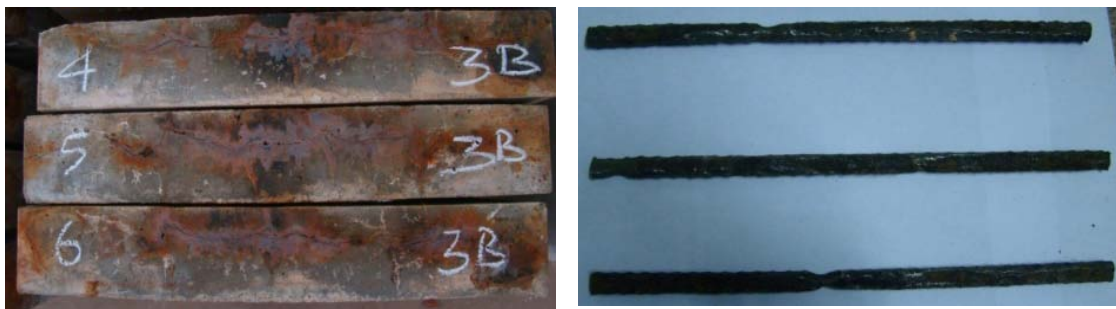
0.2 mm crack width specimens

0.4 mm crack width specimens

Figure 4.15: Corroded specimens and rebars after split open and cleaning, OPC
concrete, w/c = 0.37

(a) Uncracked specimens
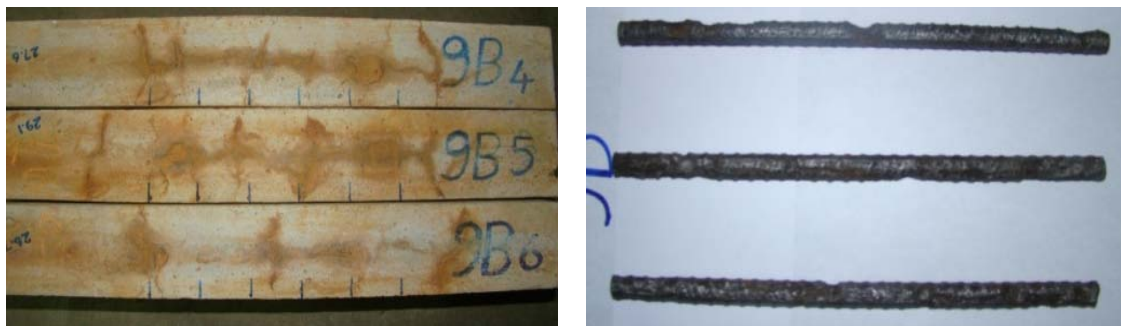
(b) 0.2 mm crack width specimens

(c) 0.4 mm crack width specimens

Figure 4.16: Corroded specimens and rebars after split open and cleaning, PPC
concrete, w/c = 0.37

Table 4.5: Gravimetric weight loss measurements (% reduction) of OPC & PPC concretes for different w/c

Description	Concrete type	w/c		
		0.57	0.47	0.37
Uncracked	OPC	18.6	13.95	11.90
	PPC	6.71	5.10	4.55
0.2 mm-crack	OPC	30.20	23.12	18.20
	PPC	15.14	13.11	11.57
0.4 mm-crack	OPC	33.40	25.21	22.43
	PPC	17.63	16.33	12.30
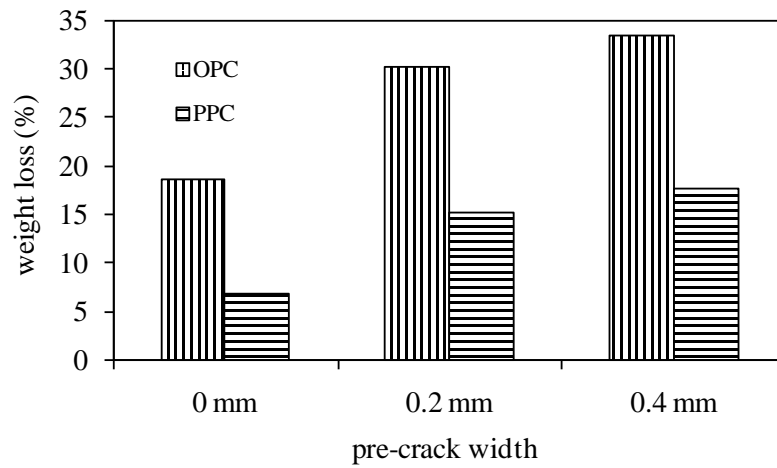
(a) w/c = 0.57
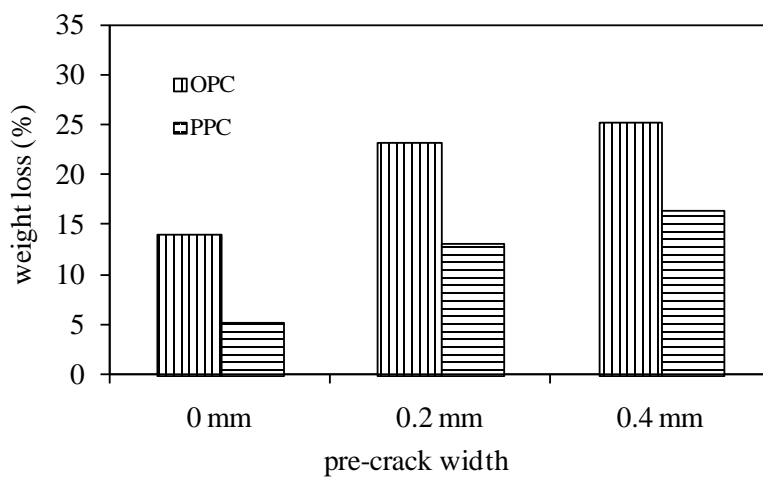
(b) w/c = 0.47

Figure 4.17: Comparison of gravimetric weight loss measurements of OPC and PPC concretes
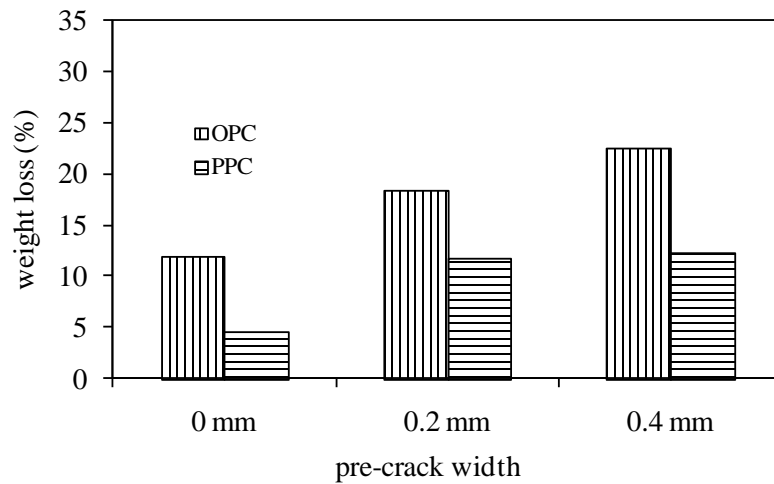
(c) w/c = 0.37

Figure 4.17: Comparison of gravimetric weight loss measurements of OPC and PPC
concretes

The increase in weight loss between the uncracked to 0.2 mm crack width specimens
is observed to be higher than between the 0.2 mm and 0.4 mm crack width specimens.
Hence, it implies that the presence of the crack influences corrosion more than the
crack width itself. This may be due to the effect of macrocell corrosion and can also
indicate a nonlinear relationship between the flexural crack width and degree of
corrosion. The weight loss for both uncracked and cracked specimens of OPC
concrete is in the range of 11.9 % to 22.4 %, 13.9 % to 25.2 % and 18.5 % to 33.4 %,
respectively for w/c of 0.37, 0.47 and 0.57. Similarly, the weight loss for both
uncracked and cracked specimens of PPC concrete is in the range of 4.5 % to 12.3 %,
5.1 % to 16.3 % and 6.7 % to 17.6 %, respectively, for w/c of 0.37, 0.47 and 0.57. The
overall improvement factor in gravimetric weight loss of PPC concrete over OPC
concrete is in the range of 2.6 to 2.7 in the case of uncracked concretes and 1.5 to 2.0,
in the case of cracked concretes.

The net diameters of corroded rebars, after cleaning, have been determined with
vernier calipers; 8 readings were taken on each rod. The statistical parameters such as
the average, maximum (max.), minimum (min.), standard deviation (SD), and
coefficient of variation (COV) for the net rebar diameters in OPC and PPC concretes
are shown in Table 4.6. The results show that the diameter reduced more for the OPC
concretes compared to PPC concretes. Further, it was observed that the reduction (i.e.,
pitting) was higher in the case of cracked concretes. Typical pit formations in the

86

rebars of the 0.4 mm crack width (flexural crack) specimens of OPC and PPC concretes with w/c equal to 0.37 are shown in Figure 4.18.

Table 4.6: Net diameters of corroded rebars in OPC and PPC concretes

Description	Concrete type	w/c = 0.57				
		Average (mm)	Max. (mm)	Min. (mm)	SD (mm)	COV (%)
Uncracked	OPC	9.11	10.24	7.40	0.86	9.44
	PPC	10.97	11.60	8.66	0.57	5.21
0.2 mm-crack	OPC	8.12	10.44	6.03	1.13	13.93
	PPC	10.01	11.40	7.74	1.12	11.21
0.4 mm-crack	OPC	7.91	10.64	5.88	1.23	15.56
	PPC	9.59	11.08	6.78	1.31	13.69
		w/c = 0.47				
Uncracked	OPC	10.42	11.20	8.92	0.49	4.69
	PPC	11.14	11.90	10.12	0.52	4.69
0.2 mm-crack	OPC	9.00	11.10	6.65	1.16	12.93
	PPC	10.38	11.68	8.76	0.74	7.13
0.4 mm-crack	OPC	8.89	10.84	6.50	1.19	13.38
	PPC	10.28	11.38	7.10	1.19	11.56
		w/c = 0.37				
Uncracked	OPC	10.63	11.34	8.85	0.50	4.74
	PPC	11.25	11.66	10.32	0.29	2.60
0.2 mm-crack	OPC	8.80	10.90	6.48	1.01	11.50
	PPC	10.50	11.78	8.94	0.99	9.44
0.4 mm-crack	OPC	8.85	10.76	6.00	1.28	14.44
	PPC	10.47	11.78	8.20	1.04	9.92

| (a) OPC concrete | (b) PPC concrete |

Figure 4.18: Pit formation in rebars of 0.4 mm crack width specimens, w/c = 0.37

4.4. Summary

Based on the experimental results obtained, it is evident that concretes with PPC perform significantly better than concretes with OPC not only in uncracked conditions but also in cracked conditions, when subjected to a chloride-rich environment. Furthermore, the following conclusions can be drawn from this study:

- The 28 day compressive strengths of PPC concretes are almost the same, the split tensile and the flexural strengths are higher than those of the corresponding OPC concretes. The 28 day sorptivity values of PPC concretes are marginally lower than that of OPC concretes possibly due to pore refinement.

- The chloride ion permeability (through the RCPT test) of PPC concrete is nearly one-third that of the corresponding OPC concrete.

- Electrochemical measurements such as half-cell potential and resistivity indicate a delay in the onset of corrosion in PPC concretes even under cracked conditions compared to that of the corresponding OPC concretes. This can be attributed to higher resistance to the corrosion current and lower penetrability due to pore refinement.

- It is evident from the studies that flexural/bending cracks can cause macrocell corrosion of rebars within the concrete, resulting in higher charge passed with an increase in the crack width.

- In the cracked specimens, rust stains are first observed at the cracks due to macroscopic corrosion whereas in the case of uncracked specimens, more uniform corrosion is observed. This shows that rebar corrosion initiates more rapidly in cracked concrete confirming that cracking influences the corrosion process significantly.

- It is observed that the corrosion induced crack width is generally more in case of uncracked specimens compared to cracked specimens. This is attributed due to more egress of corrosion products through crack openings. For the given exposure conditions, the corrosion induced crack widths of PPC concretes are much lower than those of the corresponding OPC concretes. Also, for the given rebar weight loss, the corrosion induced crack width is lower in the case of PPC concrete.

- Rebar corrosion is lower in concrete with lower water to cement ratios, as indicated by a reduction in the weight loss of rebars. This is due to increased impermeability and lower electrical conductivity.

- The overall improvement in gravimetric weight loss in the rebars within PPC concrete with respect to OPC concrete is in the range of about 2.6 to 2.7 in the case of uncracked concretes and about 1.5 to 2.0, in the case of cracked concretes. The results show that the reduction in diameter (i.e. due to pitting) of the rebars was more in OPC concretes compared to PPC concretes.

This page is intentionally left blank

CHAPTER 5

INFLUENCE OF PCE SUPERPLASTICIZER AND CNI ON CORROSION RESISTANCE

5.1. General

The corrosion resistance of concrete depends on many factors, such as the type of materials used, which include the type of binder, admixtures and quality of concrete, exposure conditions, etc., as already discussed in Chapter 4. It is well reported that chemical admixtures, such as superplasticizers and corrosion inhibiting admixtures enhance the durability of RC. However, little information is available on the durability, such as corrosion resistance, in the presence of cracks.

This chapter presents the influence of commercially available polycarboxylic ether superplasticizer (PCE SP), as well as calcium nitrite inhibitor (CNI), on the corrosion resistance of concrete/rebar system. The main objective of the chapter is to study corrosion in concretes made with the above chemical admixtures in the presence of cracks. The effect of w/c on mechanical, durability and the corrosion resistance is also studied.

The variables considered here include three w/c and two crack widths: 0.2 mm and 0.4 mm. As reported earlier, a slump in the range of 25 mm to 50 mm is considered for concretes without PCE SP, and a slump in the range of 125 mm to 150 mm is considered for concretes with PCE SP. The U-shaped RC specimen (refer Figure 3.1) with flexural cracks is exposed to the chloride-rich accelerated corrosion in the study. Results of mechanical and durability parameters on cubes and cylinders of standard specimens, half-cell potential, resistivity, total charge passed and gravimetric weight loss of corroded rebar of U-shaped specimens are presented.

5.2. Mechanical and Durability Parameters of the Concretes

The results of mechanical and durability parameters for the concretes, viz., OPC-SP, PPC-SP; OPC-CNI, PPC-CNI; and OPC-CNI-SP, PPC-CNI-SP for three w/c are given in Tables 5.1 and 5.2 (results of OPC and PPC concrete were already presented in Table 4.1 of Chapter 4 and have been repeated here, as needed, for comparison purposes). In each case, three specimens are tested and the average values are

reported. It can be seen from Tables 5.1 and 5.2 that as w/c decreases, the mechanical properties as well as the durability parameters improved, as expected. The individual results of compressive strength, RCPT value and water absorption of OPC-SP, PPC-SP; OPC-CNI, PPC-CNI; and OPC-SP-CNI, PPC-SP-CNI concretes are presented in Tables A.4 to A.12 of Appendix A. It was observed that the data for the concretes with CNI have significantly more scatter than the others, to confirm which, as a general trend more studies may be needed.

Table 5.1: Average mechanical properties (at 28 days) of different concretes

Property	Concrete	w/c		
		0.57	0.47	0.37
Compressive strength (MPa)	OPC	33.2	44.7	53.7
	PPC	30.7	41.4	51.2
	OPC-SP	32.9	44.3	54.0
	PPC-SP	32.5	44.8	54.0
	OPC-CNI	25.6	36.6	49.9
	PPC-CNI	27.7	37.0	51.6
	OPC-SP-CNI	25.6	38.1	50.6
	PPC-SP-CNI	27.2	38.6	49.9
Split tensile strength (MPa)	OPC	2.4	3.8	4.0
	PPC	2.7	3.7	4.6
	OPC-SP	2.3	3.8	4.1
	PPC-SP	3.1	3.4	3.7
	OPC-CNI	2.6	3.3	3.9
	PPC-CNI	2.8	3.4	3.9
	OPC-SP-CNI	2.4	3.1	3.2
	PPC-SP-CNI	2.6	3.2	3.5
Flexural strength (MPa)	OPC	4.1	5.6	6.4
	PPC	5.0	5.6	6.9
	OPC-SP	4.0	5.8	6.3
	PPC-SP	5.6	5.9	6.5
	OPC-CNI	3.2	3.4	5.7
	PPC-CNI	3.5	4.7	5.1
	OPC-SP-CNI	3.0	4.2	5.3
	PPC-SP-CNI	4.1	4.6	5.4

Table 5.2: Average durability parameters (at 28 days) of different concretes

Property	Concrete	w/c		
		0.57	0.47	0.37
Charge passed in the RCPT (Coulombs)	OPC	2600	2100	1900
	PPC	861	720	520
	OPC-SP	2550	2100	1950
	PPC-SP	860	760	525
	OPC-CNI	4500	3800	3000
	PPC-CNI	2600	2100	1300
	OPC-SP-CNI	4700	3400	3000
	PPC-SP-CNI	3000	2500	2000
Sorptivity (mm/min$^{0.5}$)	OPC	0.097	0.092	0.087
	PPC	0.060	0.049	0.043
	OPC-SP	0.062	0.053	0.051
	PPC-SP	0.055	0.044	0.041
	OPC-CNI	0.093	0.069	0.058
	PPC-CNI	0.054	0.048	0.038
	OPC-SP-CNI	0.070	0.062	0.047
	PPC-SP-CNI	0.053	0.044	0.033
Water absorption (%)	OPC	5.8	5.1	4.7
	PPC	6.5	6.0	5.0
	OPC-SP	4.9	3.9	3.2
	PPC-SP	5.9	5.5	4.9
	OPC-CNI	5.9	4.7	3.9
	PPC-CNI	5.0	3.9	3.5
	OPC-SP-CNI	5.1	4.8	3.7
	PPC-SP-CNI	4.4	3.8	3.0

Figures 5.1 and 5.2 again show the compressive strength results of different concretes with OPC and PPC with SP and/or CNI, along with OPC concrete alone (i.e., control concrete). The compressive strengths of the OPC concrete (control concrete) and the OPC-SP concrete are nearly the same at all w/c. Winnefeld et al. (2007) who studied the effect of molecular architecture (i.e., length of side chains, density of side chains

and molecular weight of polymer) of PCE superplasticizers and observed that there was no clear trend about the enhancement of 28 day strengths. They also reported that longer side chain lengths and lower side chain densities tend to decrease 28-day strengths. Nevertheless, for the PPC-SP concrete, there is a marginal improvement in compressive strength of about 5% to 8% compared to that of PPC concrete alone.

For compressive strength of concrete with CNI (at the adopted dosage of 10 l/m^3), it has been observed that there is a reduction when compared to that of the respective control concretes (refer to Table 5.1, and Figures 5.1 and 5.2). The reduction in compressive strength of concretes with CNI is about 20% and 10% respectively, compared to that of their respective OPC and PPC concretes. The results obtained agree with previous work, where the reduction in compressive strength has been attributed to the change in pore ratio and diameter (Li et al., 2000).
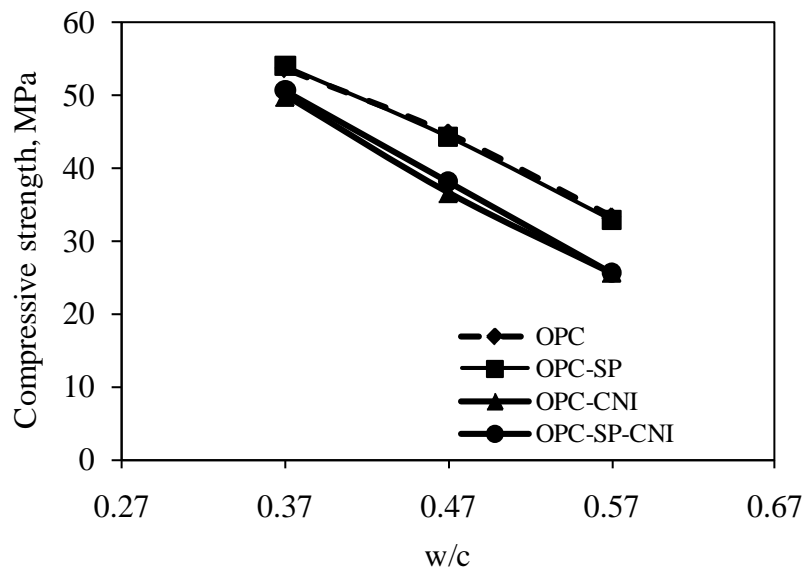
Figure 5.1: Compressive strengths of different OPC concretes
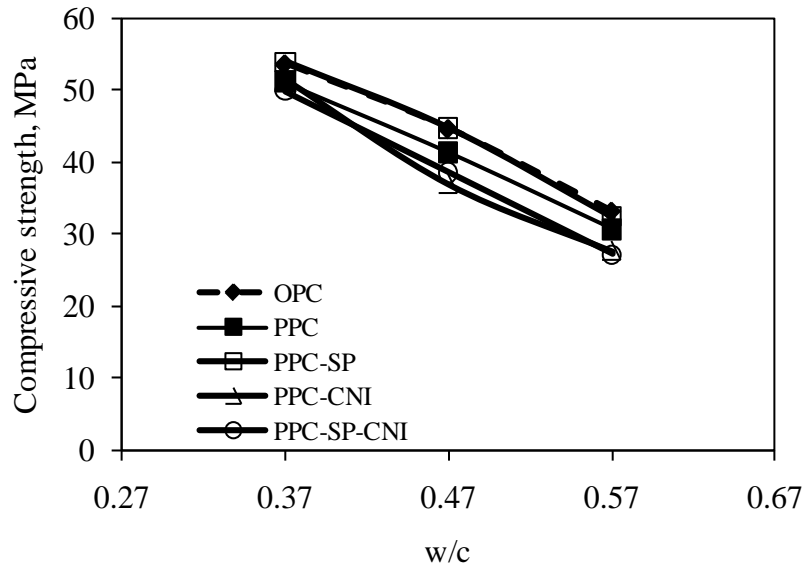
Figure 5.2: Compressive strengths of different PPC concretes in comparison to OPC concretes

Figures 5.3 and 5.4 show the water absorption values of different concretes with OPC and PPC with SP and/or CNI, along with those of the reference concrete (OPC alone). The corresponding sorptivity plots are shown in Figures 5.5 and 5.6. It can be seen that water absorption and sorptivity increase with an increase in w/c. The water absorption of OPC-SP and OPC-CNI are less compared to that of control concrete. However, the water absorption of PPC and PPC-SP is more compared to that of control concrete. Nevertheless, in both OPC and PPC concretes, it is observed that the concrete with PCE SP performed well from the durability point of view; i.e., there is a reduction in water absorption and also in sorptivity, compared to the corresponding control concretes. This may be attributed due to better dispersion of cement particles and refinement of pore structure (Khatib and Mangat, 1999).
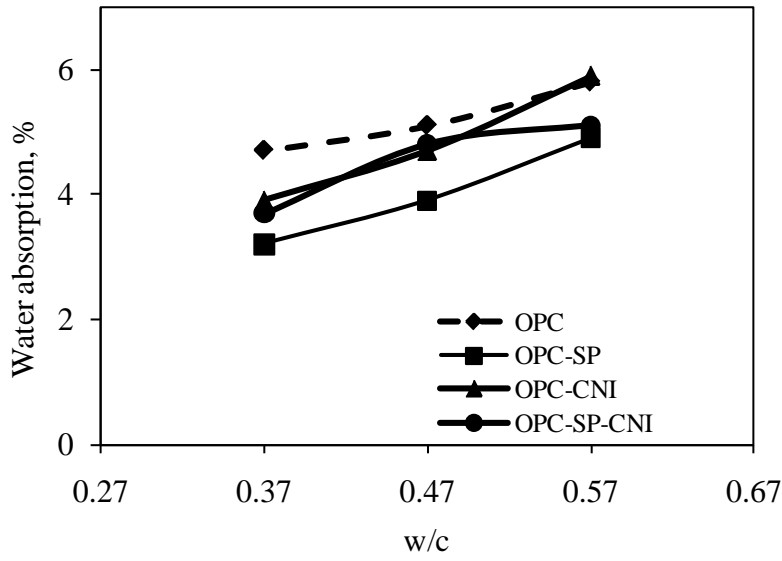
Figure 5.3: Water absorption plots of different OPC concretes
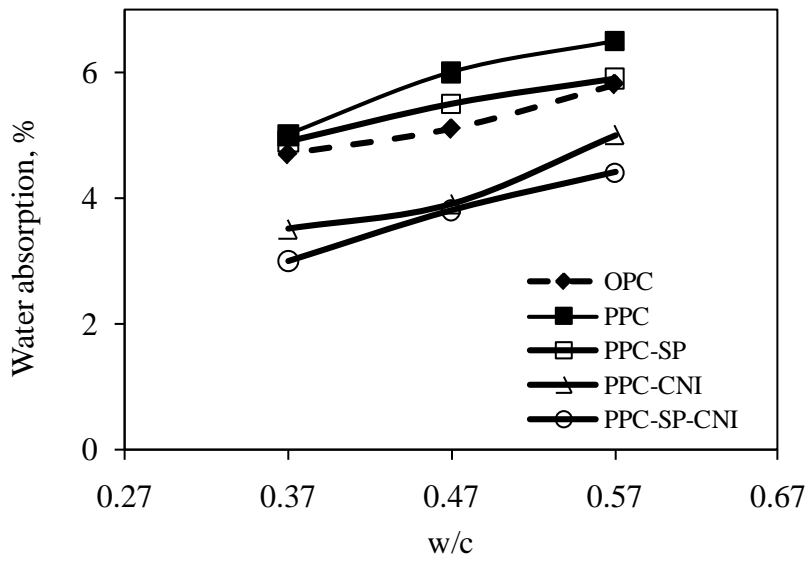
Figure 5.4: Water absorption of different PPC concretes in comparison to OPC
concretes
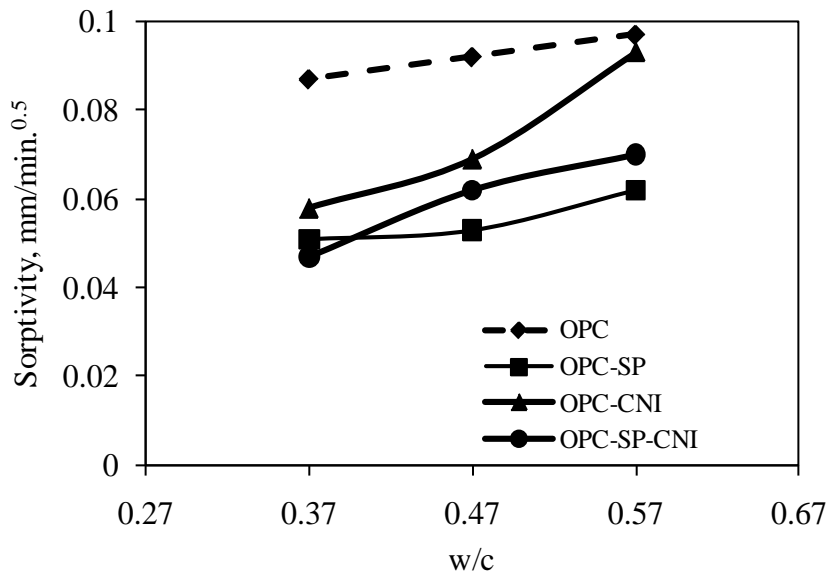
Figure 5.5: Sorptivity plots of different OPC concretes
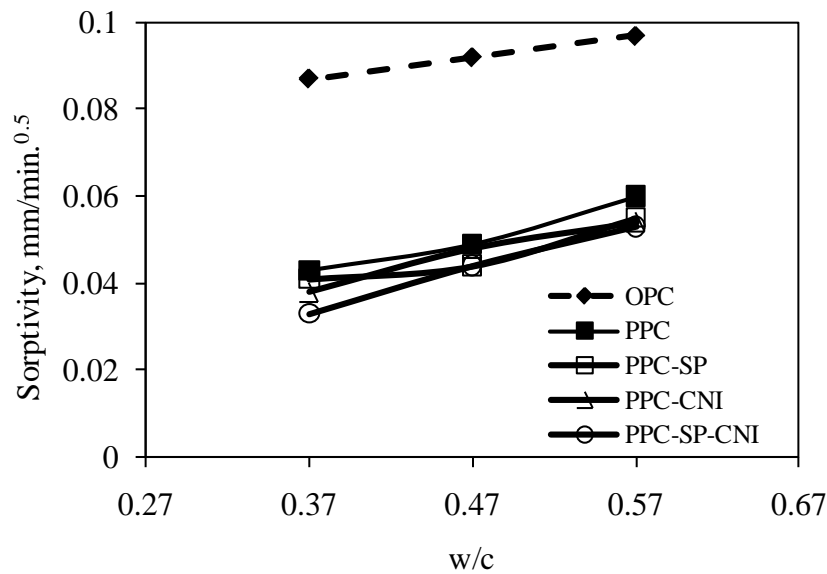
Figure 5.6: Sorptivity plots of different PPC concretes in comparison to OPC concretes

From Figures 5.3 to 5.6 and Table 5.2, it can be seen that the water absorption and sorptivity values of concrete with CNI are lower by about 30% and up to 15%, respectively, for the OPC concretes; and by about 17% and up to 35%, respectively, for the PPC concretes. The concrete with CNI performed better at lower water to cement ratio (w/c = 0.37), both in terms of water absorption and sorptivity.

Figures 5.7 and 5.8 show the plots of RCPT values of OPC and PPC concretes with reference to control concrete. There is not much difference between the RCPT values of concrete with SP and the corresponding reference concretes, both for OPC and PPC. That means the rapid chloride permeability is not significantly affected by the presence of SP and also the change in slump (slump for control concrete is in the range of 25 to 50 mm; slump for concretes with PCE SP is in the range of 125 to 150 mm), as also observed previously by Gagné et al. (1996).
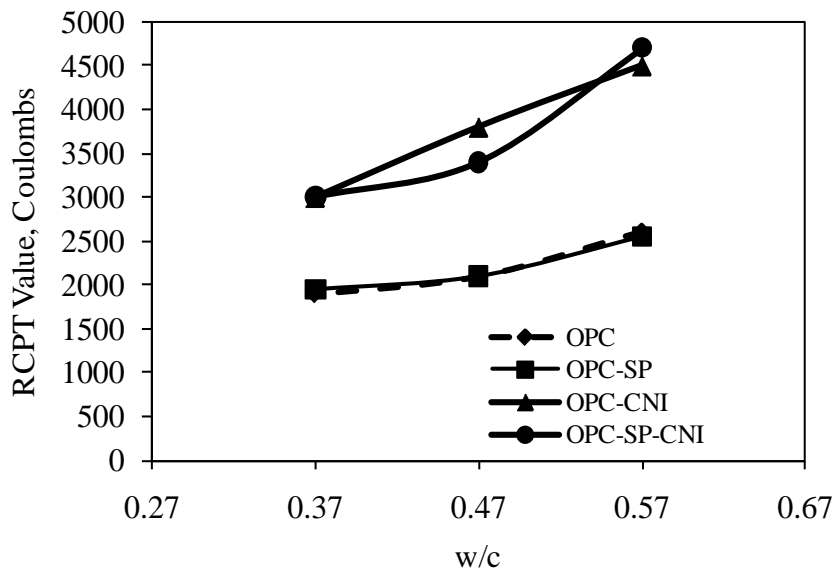
Figure 5.7: RCPT values of different OPC concretes
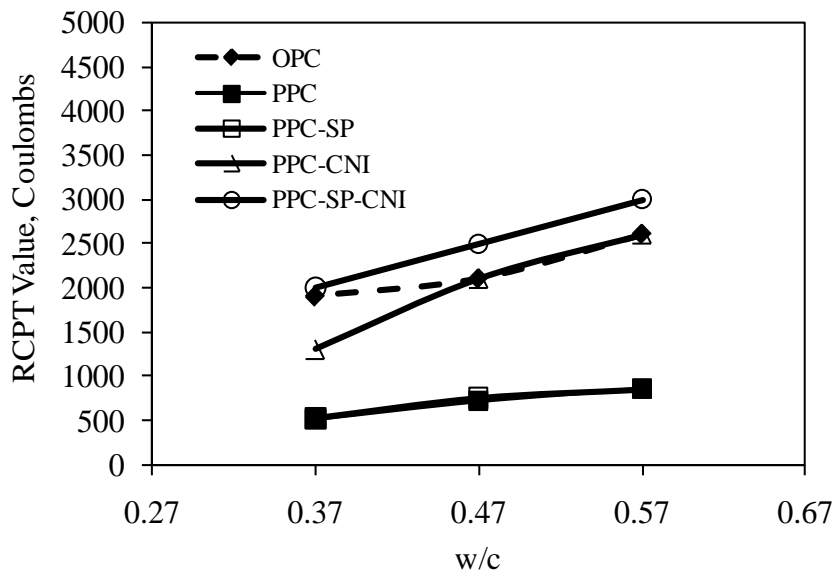
Figure 5.8: RCPT values of different PPC concretes in comparison to OPC concrete

However, the RCPT values of both OPC and PPC concretes with CNI are substantially higher; i.e., 1.6 to 1.8 times that of OPC concrete and about 2.5 to 3 times that of PPC concrete (refer to Figures 5.7 and 5.8). The higher value of RCPT in concrete with CNI can be attributed to the high ionic nature of CNI, which causes more negative charge to pass through the concrete. Similar results have also been obtained by other researchers, such as Berke (1987), Berke and Hicks (1996), Ann et al. (2006), and Issa et al. (2008).

Berke et al. (2002) studied the effect of various combinations of admixtures and reported that there was an increase in charge passed due to the presence of calcium nitrite. They further reported that such an increase is not indicative of higher chloride ion penetration but rather of the increased anion concentration in the pore water. Some researchers have reported that the addition of calcium nitrite influences the hydration process of cement paste by accelerating and stabilising the formation of the crystal phase of calcium hydroxide, which leads to an increase in the micropore diameter in the hardened cement paste (Ma et al., 1998). The larger pores could lead to an increase in chloride permeability when compared to the concrete without inhibitor (Li et al., 1999). Loulizi et al. (2000) performed RCPT studies on four different concretes with and without nitrite based inhibitor and observed higher RCPT values at early ages (• twice at 33 days) in concretes with nitrite based inhibitor.

5.3. Accelerated Corrosion Studies with U-Shaped RC Specimens

The U-shaped RC specimens of OPC-SP, OPC-CNI, OPC-SP-CNI, PPC-SP, PPC-CNI and PPC-SP-CNI have been subjected to 10 V constant impressed voltage for 22 days (528 hours). The corrosion current, half-cell potential and resistivity have been monitored periodically, and the results are reported in the following sections.

5.3.1. OPC and PPC concretes with PCE superplasticizer

5.3.1.1. Half-cell potential and resistivity measurements

During the period of accelerated corrosion, half-cell potential and resistivity measurements are taken at regular intervals after disconnecting the power supply and taking the specimen out of the NaCl solution. The half-cell potentials measured for OPC-SP and PPC-SP concretes with the saturated copper/copper sulphate electrode are shown in Figures 5.9, 5.10 and 5.11 for w/c equal to 0.57, 0.47 and 0.37,

respectively. Each series is designated by the notation 'mix type-w/c ratio-flexural crack width'. The half-cell potential values of concrete with SP are similar to that of the control concretes. It can be observed that the half-cell potentials of PPC-SP concrete are initially less negative compared to that of the half-cell potentials of OPC-SP concrete; similar to the observations made in the case of OPC and PPC concretes. As expected, the uncracked specimens have shown less negative potentials than that of cracked specimens. The uncracked specimens of concrete with w/c equal to 0.57 showed potentials more negative than -350 mV right from the beginning. It can be seen from Figures 5.12 - 5.14 that the initial resistivity values of PPC-SP concrete is higher compared to that of the corresponding OPC-SP concrete confirming that PPC concretes will have higher resistivity (Scott and Alexander, 2007). In general, the resistivity values of uncracked specimens are higher than those of the cracked ones, as expected.

5.3.1.2. Corrosion current

The corrosion current for OPC-SP and PPC-SP concretes for the three w/c, viz. 0.57, 0.47 and 0.37, are presented in Figures 5.15, 5.16 and 5.17, respectively. In each series, three specimens are used and their average is reported. In general, it is observed that a reduction of w/c from 0.57 to 0.37 reduced the total charge passed in both cracked and uncracked specimens. The charge passed in concrete specimens with w/c equal to 0.57 is higher than that of specimens with a w/c equal to 0.47, and the charge passed for w/c equal to 0.47 is more than that of concrete with a w/c equal to 0.37. As expected, the charge passed is more in the cracked specimens compared to their corresponding uncracked specimens.

It can also be observed from Figures 5.15 - 5.17 that the total charge passed decreases with a decrease in the w/c, as expected, and is higher for the cracked specimens due to the damage induced around the rebar (Okada and Miyagawa, 1980). The total charge passed is computed based on the areas under the individual corrosion current versus duration curves as computed in the Section 4.3.2 of Chapter 4 (results of OPC and PPC concrete were already presented in Table 4.3 of Chapter 4 and have been repeated here, as needed, for comparison purposes). Table 5.3 presents the total charge (Ampere-days) passed for specimens of concretes with SP. The total charge

passed is less in concretes with SP when compared to that of the respective concretes without SP. This is observed both in OPC-SP and PPC-SP concretes.
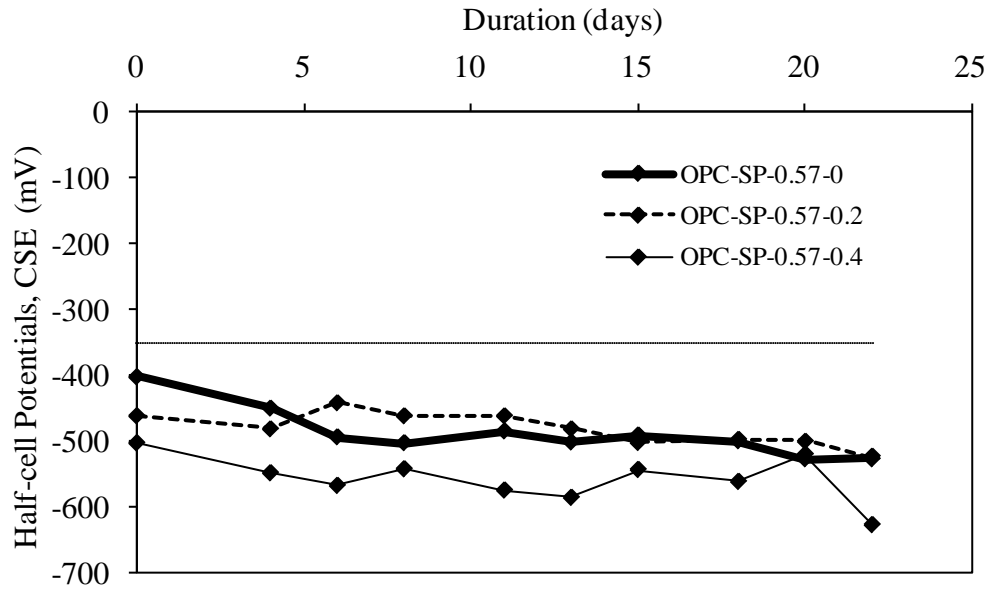
(a) OPC-SP concrete
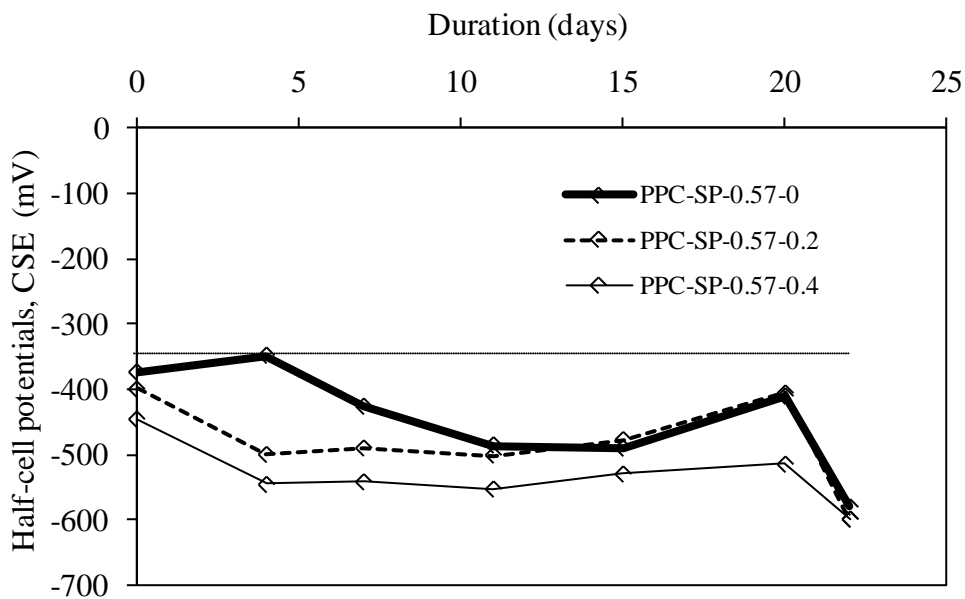
(b) PPC-SP concrete

Figure 5.9: Half-cell potentials of OPC-SP and PPC-SP concretes for w/c = 0.57
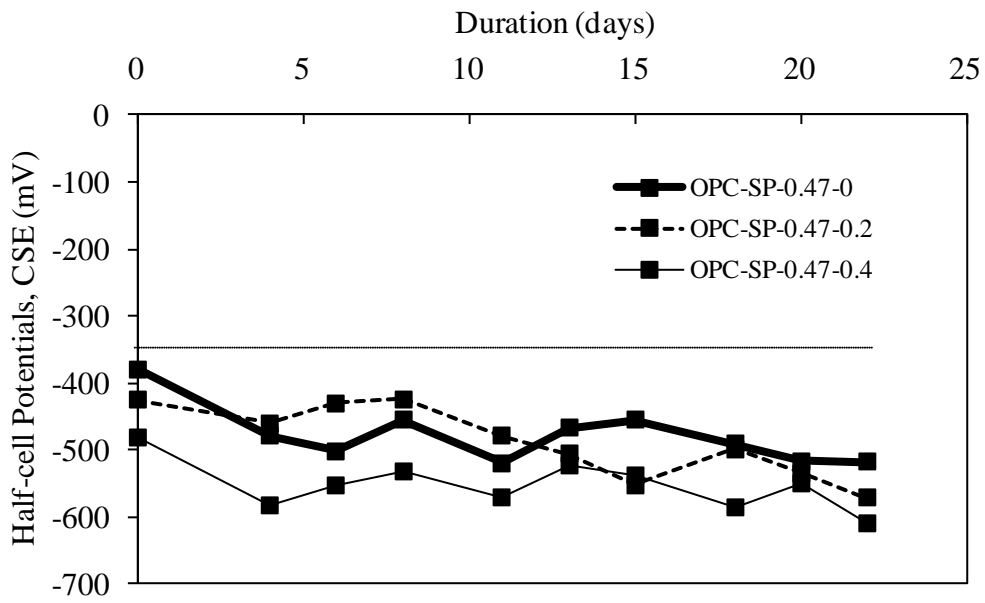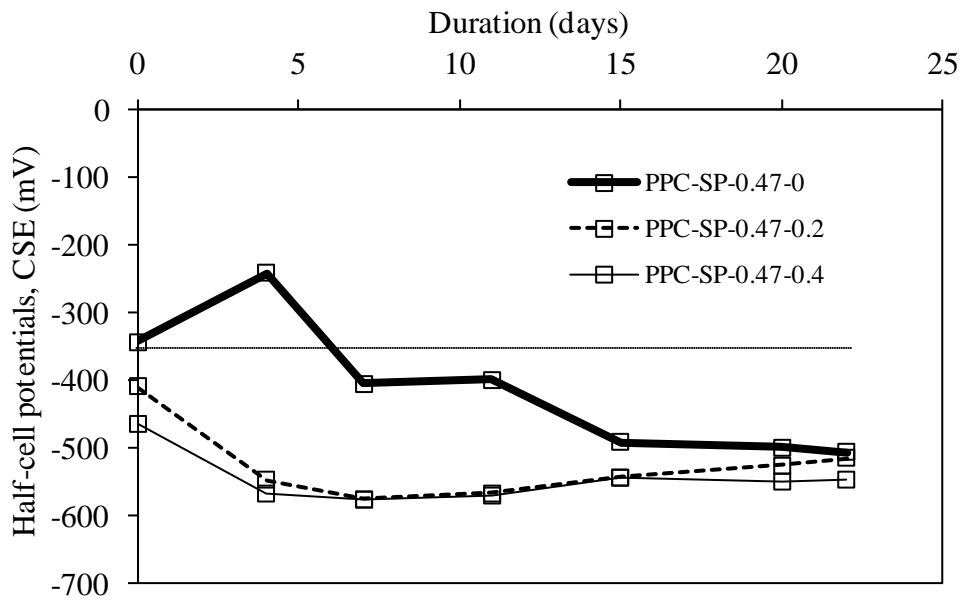
(a) OPC-SP concrete

(b) PPC-SP concrete

Figure 5.10: Half-cell potentials of OPC-SP and PPC-SP concretes for w/c = 0.47
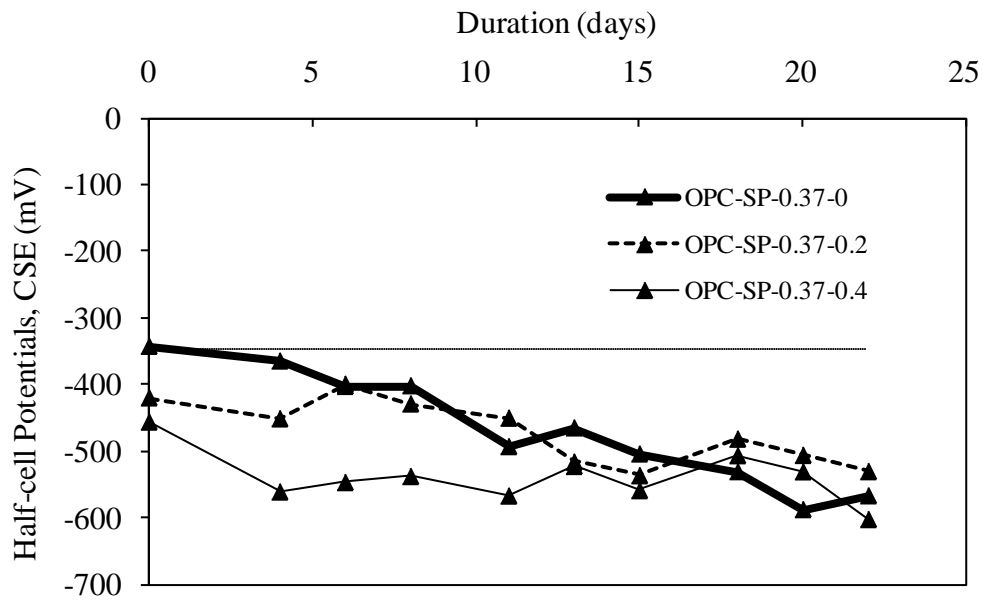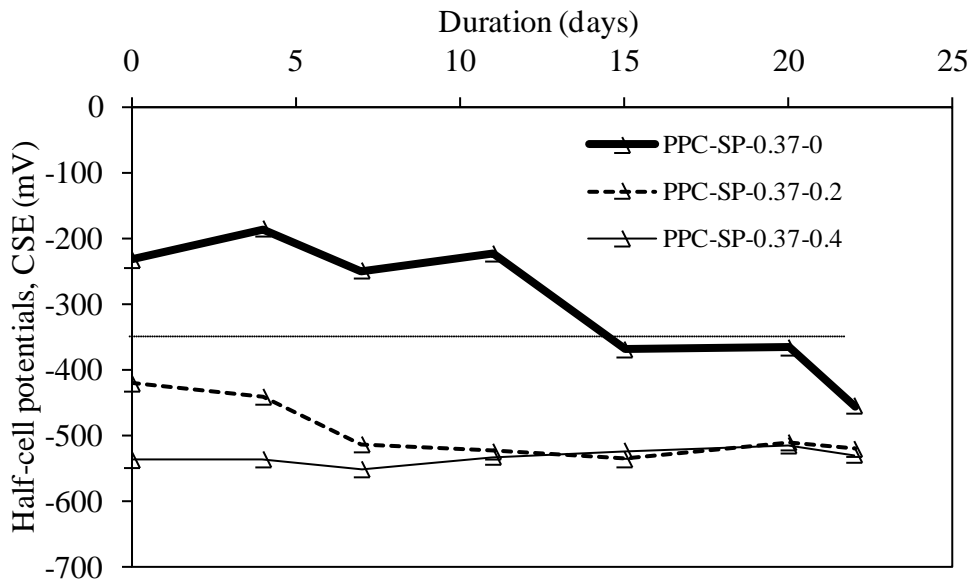
(a) OPC-SP concrete

(b) PPC-SP concrete

Figure 5.11: Half-cell potentials of OPC-SP and PPC-SP concretes for w/c = 0.37

(a) OPC-SP concrete
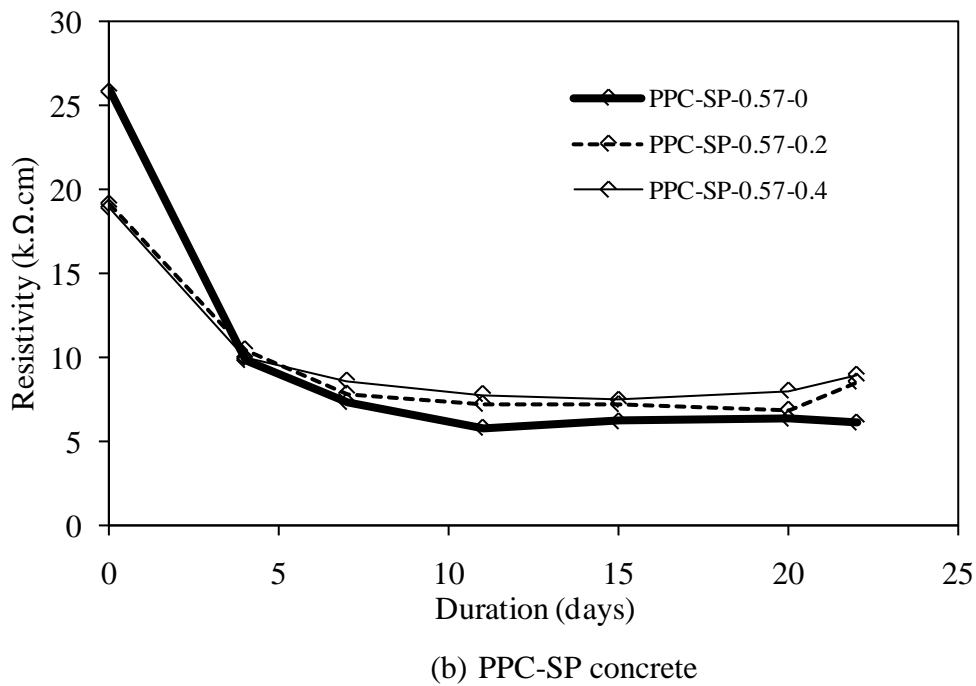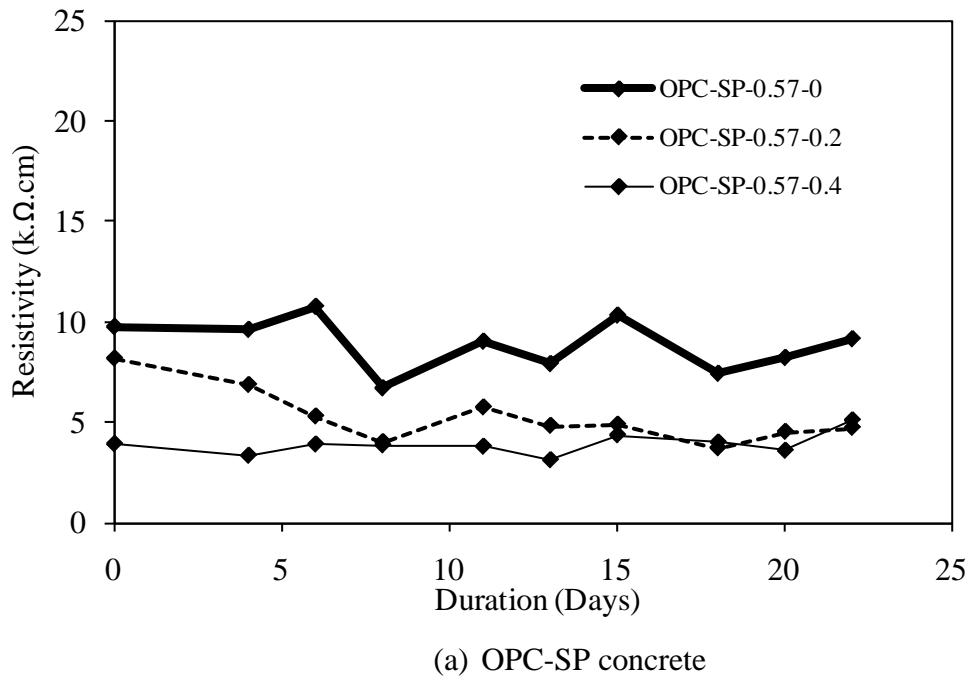
(b) PPC-SP concrete

Figure 5.12: Resistivity measurements of OPC-SP and PPC-SP concretes for
w/c = 0.57
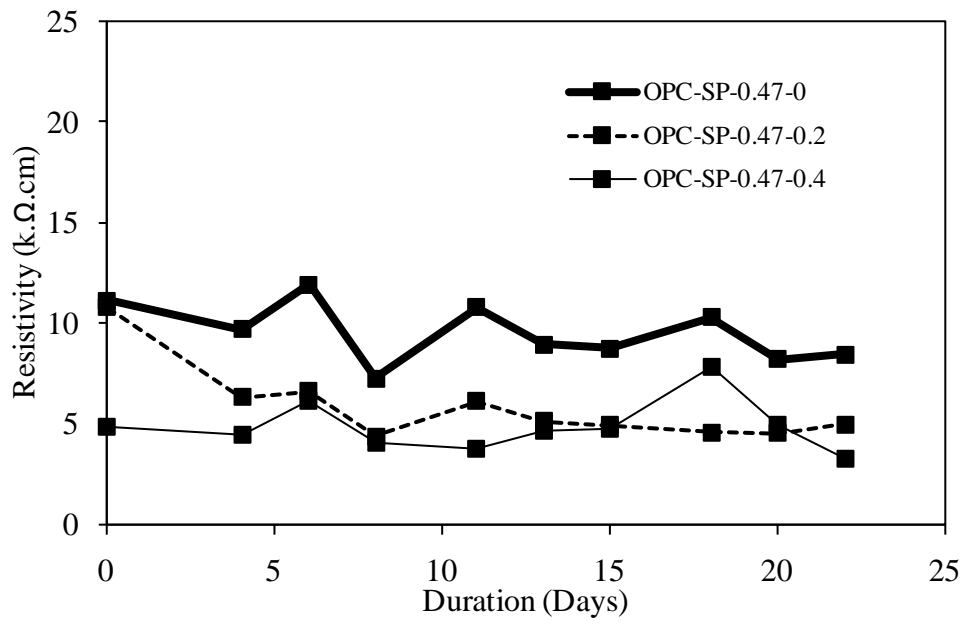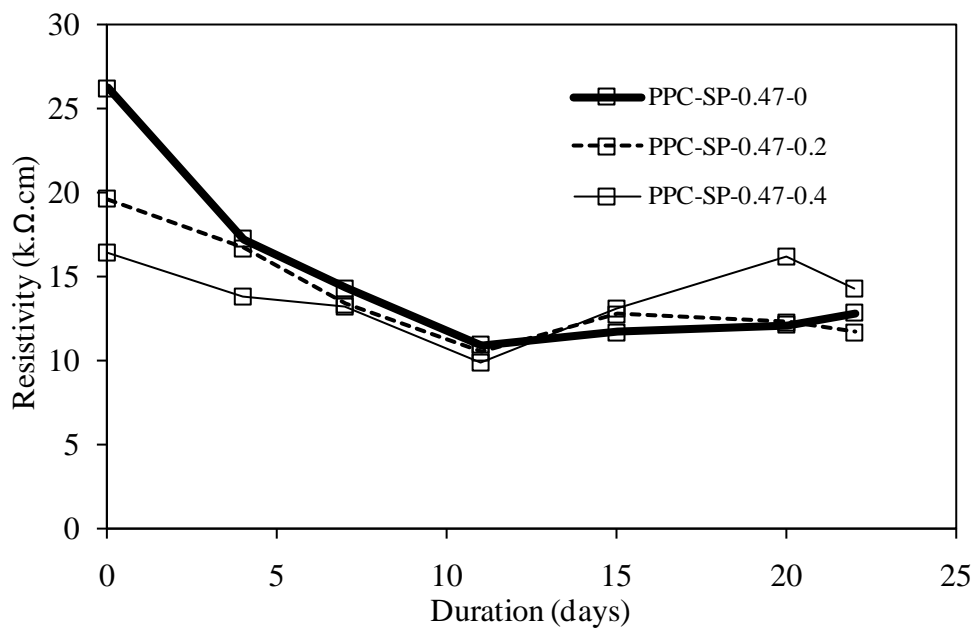
(a) OPC-SP concrete

(b) PPC-SP concrete

Figure 5.13: Resistivity measurements of OPC-SP and PPC-SP concretes for
w/c = 0.47
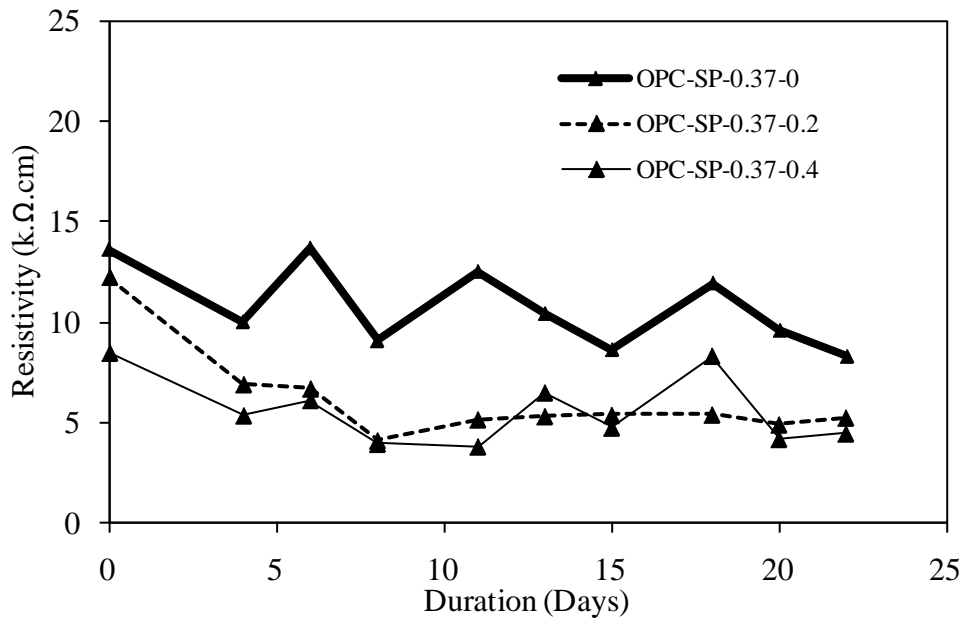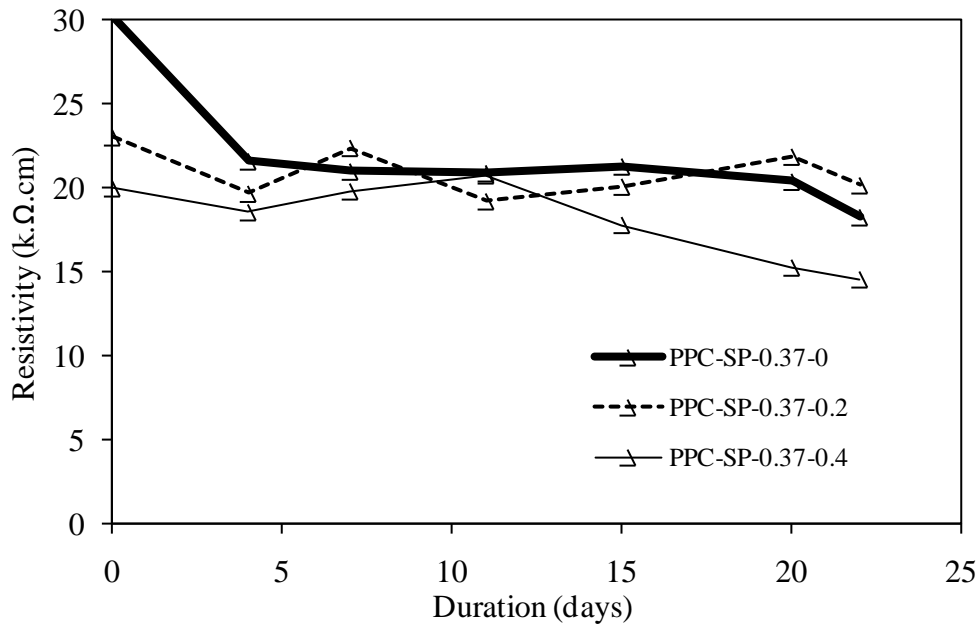
(a) OPC-SP concrete

(b) PPC-SP concrete

Figure 5.14: Resistivity measurements of OPC-SP and PPC-SP concretes for
w/c = 0.37
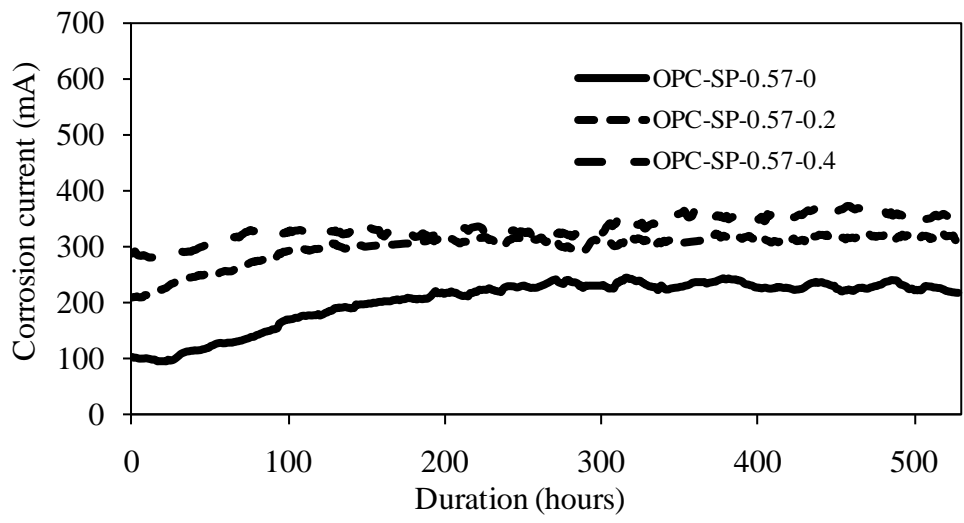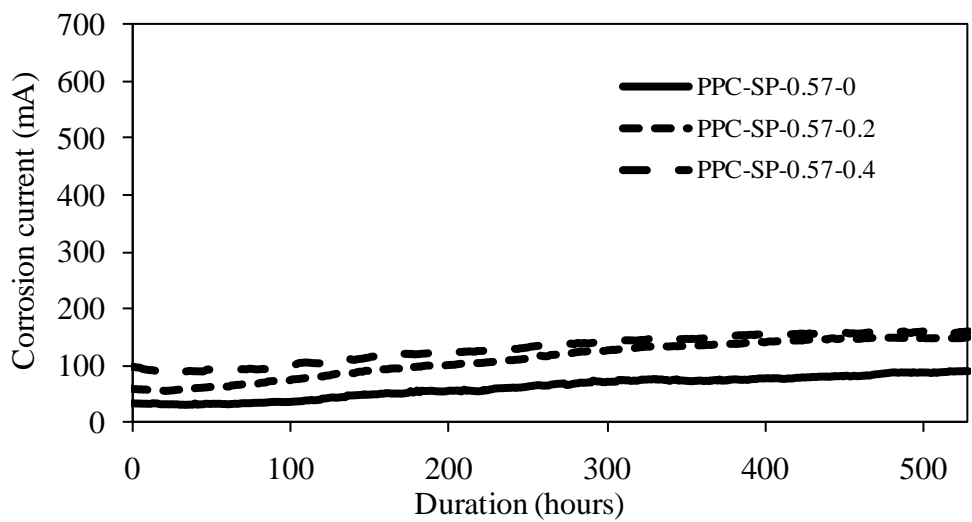
(a) OPC-SP concrete

(b) PPC-SP concrete

Figure 5.15: Corrosion current as a function of exposure duration, OPC-SP and
PPC-SP concretes for w/c = 0.57
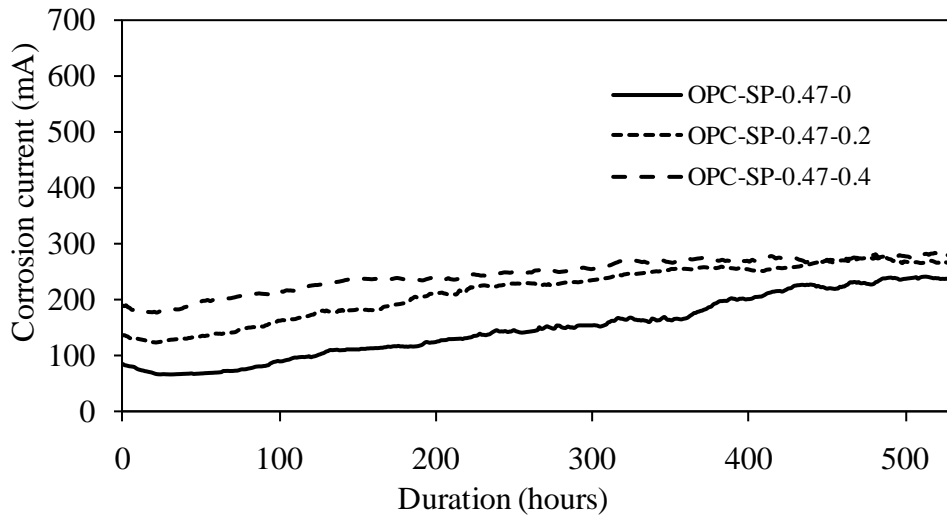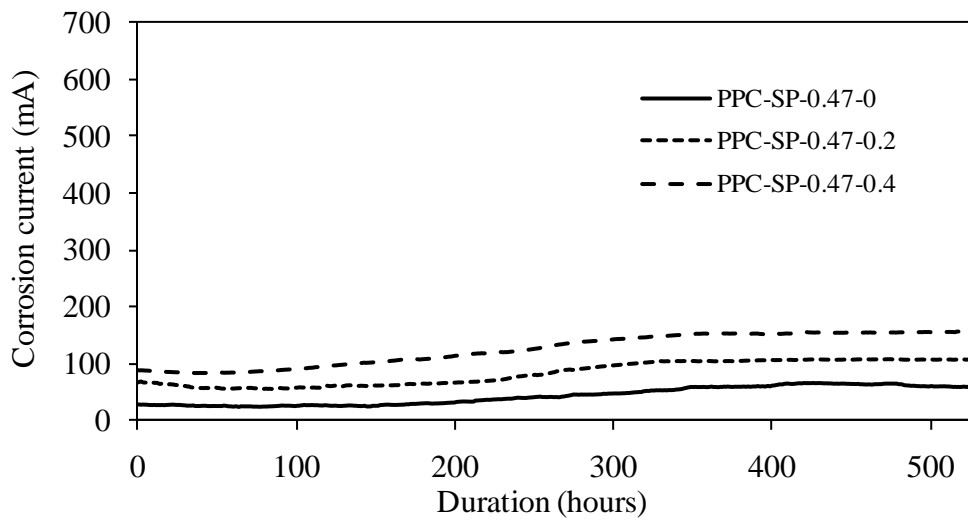
(a) OPC-SP concrete

(b) PPC-SP concrete

Figure 5.16: Corrosion current as a function of exposure duration, OPC-SP and PPC-SP concretes for w/c = 0.47
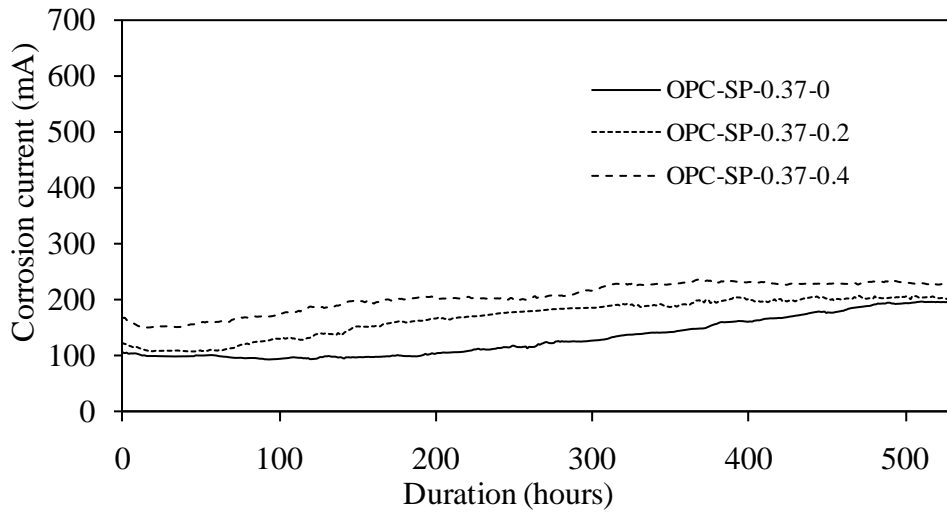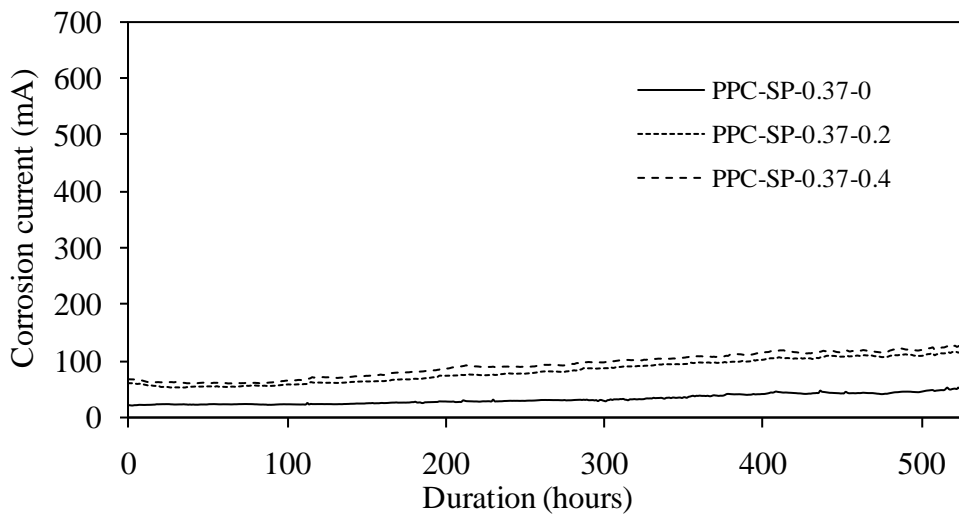
(a) OPC-SP concrete

(b) PPC-SP concrete

Figure 5.17: Corrosion current as a function of exposure duration, OPC-SP and PPC-SP concretes for w/c = 0.37

Table 5.3: Charge passed in OPC-SP & PPC-SP concretes, Amp-days (constant 10V for 528 hours)

Description	Concrete type	w/c		
		0.57	0.47	0.37
Uncracked	OPC	4.7	3.5	3.0
	PPC	1.4	1.04	0.99
	OPC-SP	4.5	3.3	2.9
	PPC-SP	1.4	0.98	0.72
0.2 mm-crack	OPC	6.9	4.9	4.0
	PPC	2.6	1.87	1.83
	OPC-SP	6.6	4.7	3.7
	PPC-SP	2.5	1.82	1.79
0.4 mm-crack	OPC	7.8	5.5	4.7
	PPC	3.0	2.85	2.12
	OPC-SP	7.3	5.4	4.5
	PPC-SP	2.8	2.75	2.04

5.3.1.3. Weight loss measurements

The corrosion-induced crack widths observed for OPC-SP and PPC-SP concretes are similar to that of OPC and PPC concretes. The gravimetric weight loss (C_R) results are presented in Table 5.4 (results of OPC and PPC concrete were already presented in Table 4.5 of Chapter 4 and have been repeated here, as needed, for comparison purposes). As can be expected, the weight loss is less for the concretes of lower w/c. Comparing the gravimetric weight loss results with those of OPC and PPC concretes, it can be seen that the weight loss of rebars in concrete with PCE SP is lower than that of the corresponding OPC (control concrete). The percent reduction in weight loss of rebars in concrete with PCE SP was marginally lower than that of the corresponding control concrete (OPC alone), and is about 7% to 17% in case of uncracked and 5% to 12% in case of cracked concrete. The percent reduction in weight loss of rebars in concrete with PCE SP was also lower than that of the corresponding PPC concrete alone and is about 4% to 17% in case of uncracked and 1% to 5% in case of cracked concrete. The individual results for uncracked, 0.2 mm and 0.4 mm are presented in Tables B.4, B.5 and B.6 of Appendix B, respectively.

Table 5.4: Gravimetric weight loss measurements (% reduction) of OPC-SP & PPC-SP concretes for different w/c

Description	Concrete type	w/c		
		0.57	0.47	0.37
Uncracked	OPC	18.6	13.95	11.90
	PPC	6.71	5.10	4.55
	OPC-SP	17.3	11.96	9.90
	PPC-SP	5.53	4.9	4.05
0.2 mm-crack	OPC	30.20	23.12	18.20
	PPC	15.14	13.11	11.57
	OPC-SP	28.8	20.30	17.15
	PPC-SP	13.68	12.2	11.1
0.4 mm-crack	OPC	33.40	25.21	22.43
	PPC	17.63	16.33	12.3
	OPC-SP	31.6	23.00	20.1
	PPC-SP	16.80	15.71	12.2

5.3.2. OPC-CNI and PPC-CNI concretes

5.3.2.1. Half-cell potential and resistivity measurements

Figures 5.18 - 5.20 show the half-cell potential measurements for OPC-CNI and PPC-CNI concretes. It can be observed that the potentials of concrete with CNI are initially less negative compared to that of respective control concretes without CNI and SP (i.e., OPC and PPC concretes). However, the potentials became more negative in a very short duration. Saraswathy and Song (2007b) and Trépanier et al. (2001) also observed less negative values for concretes with inhibitors compared to that of control concretes. Moreover, the resistivity values of OPC concretes with CNI shown in Fig. 5.21 are lower when compared to that of their respective control concretes without CNI. It can be recalled that the results of RCPT showed that chloride ion penetration is more in concretes with CNI.

(a) OPC-CNI concrete
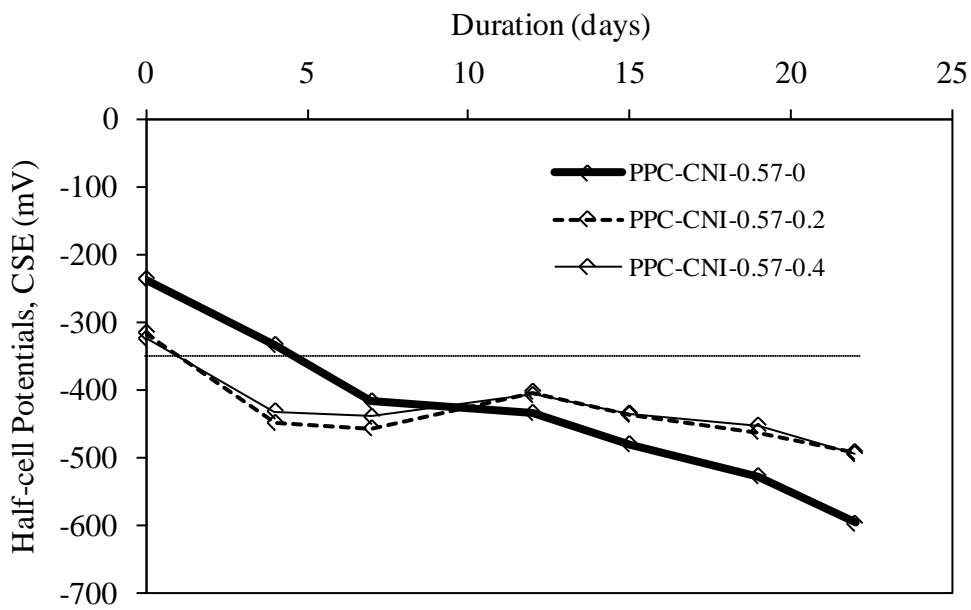
(b) PPC-CNI concrete

Figure 5.18: Half-cell potentials of OPC-CNI and PPC-CNI concretes for w/c = 0.57
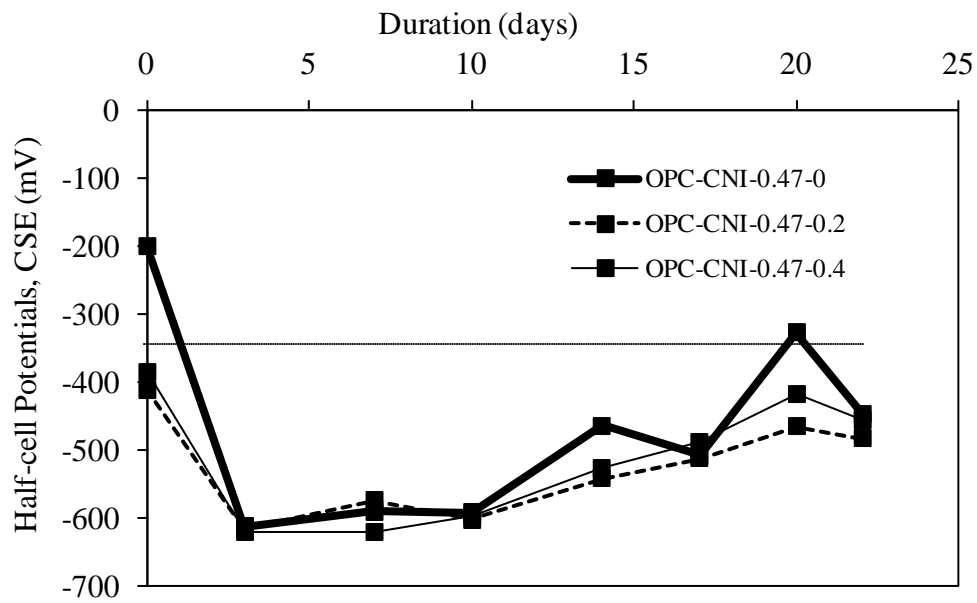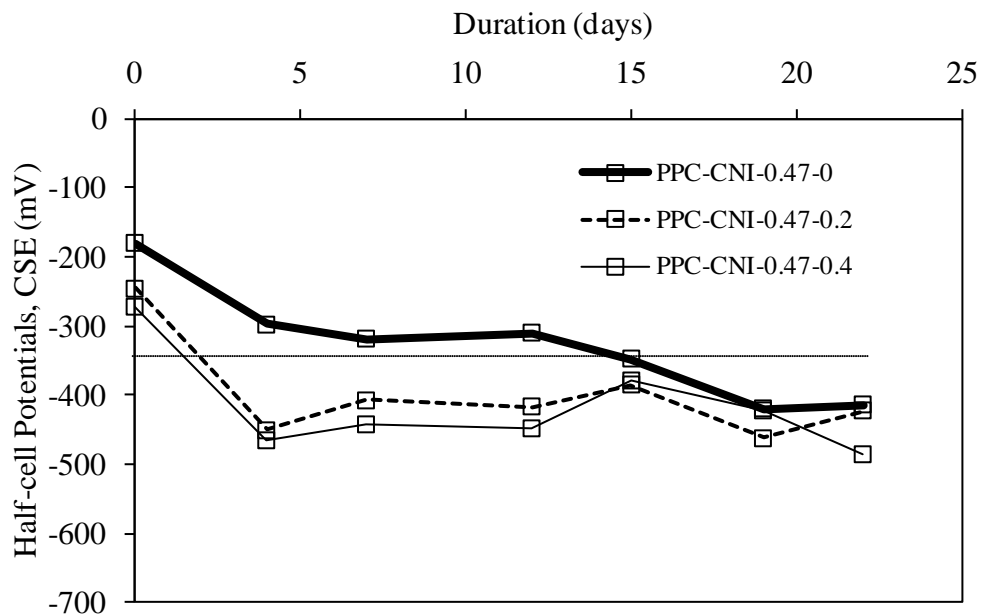
(a) OPC-CNI concrete

(b) PPC-CNI concrete

Figure 5.19: Half-cell potentials of OPC-CNI and PPC-CNI concretes for w/c = 0.47
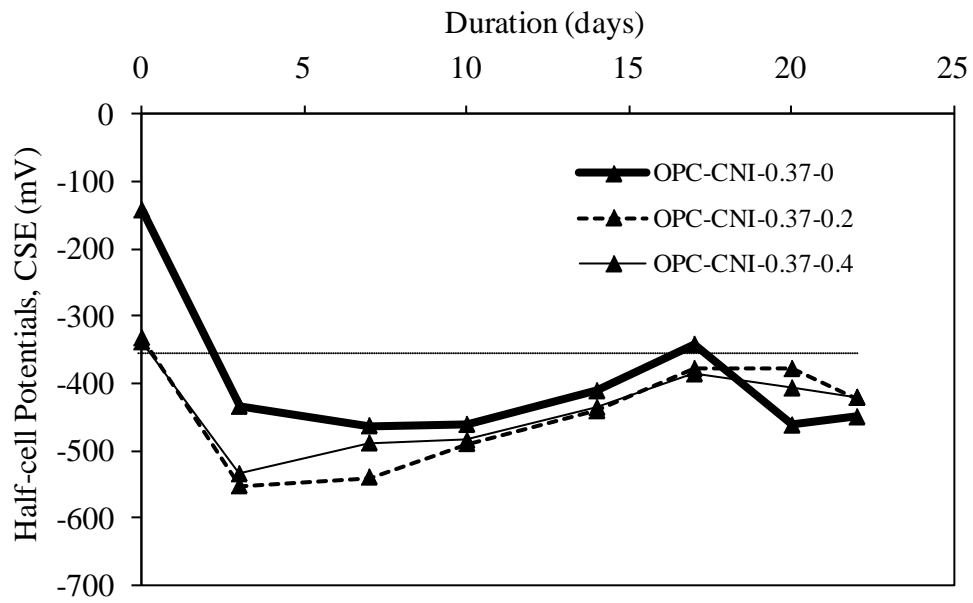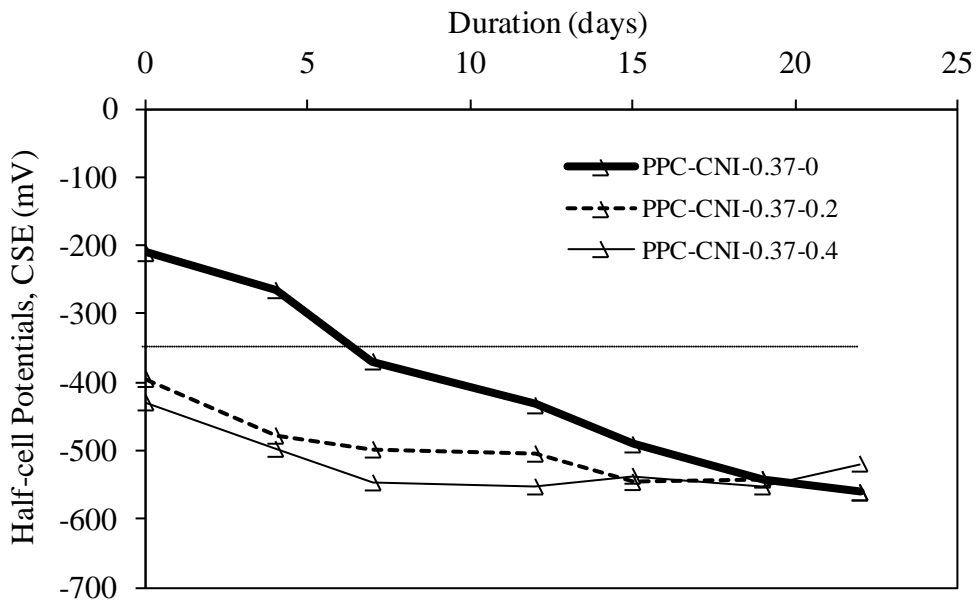
(a) OPC-CNI concrete

(b) PPC-CNI concrete

Figure 5.20: Half-cell potentials of OPC-CNI and PPC-CNI concretes for w/c = 0.37
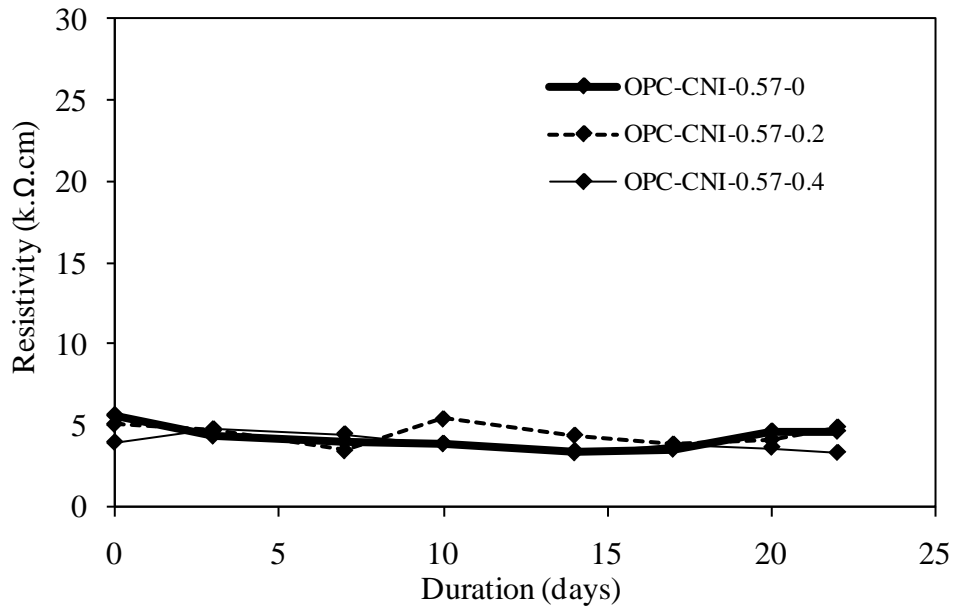
(a) w/c = 0.57
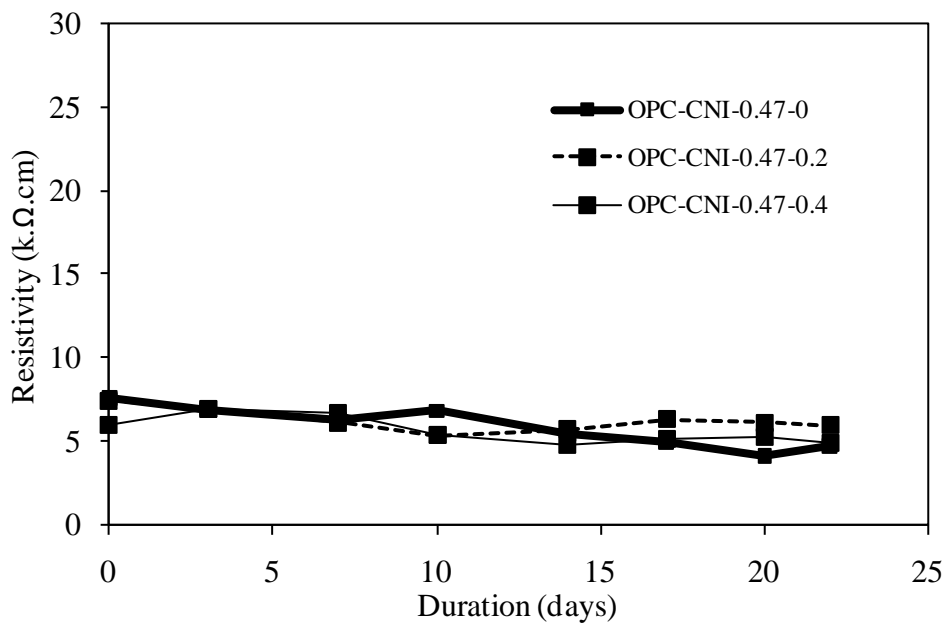
(b) w/c = 0.47

Figure 5.21: Resistivity values for different OPC-CNI concretes
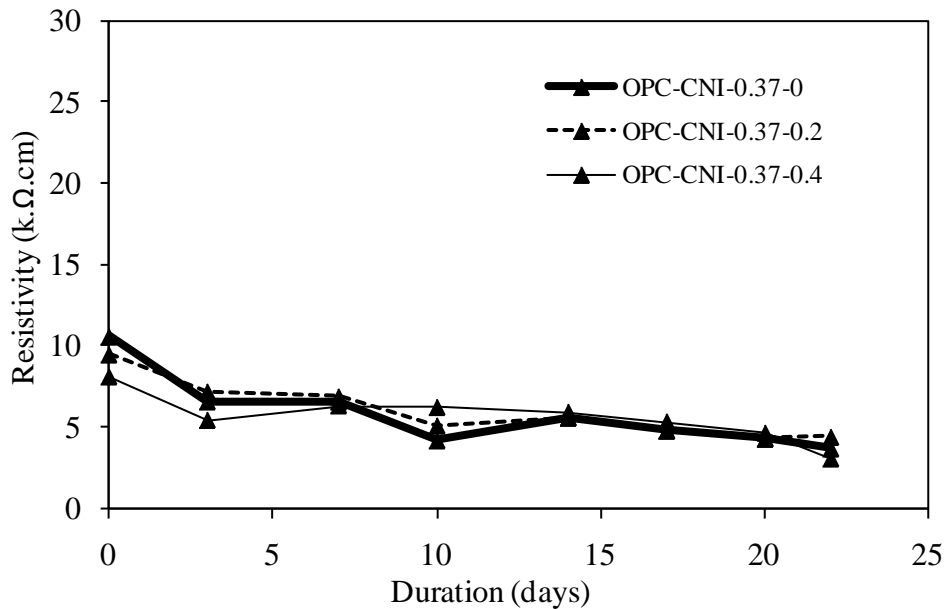
(c) w/c = 0.37

Figure 5.21: Resistivity values for different OPC-CNI concretes

5.3.2.2. Corrosion current and gravimetric weight loss results

The corrosion current for OPC-CNI and PPC-CNI concretes are presented in Figures 5.22, 5.23 and 5.24, for w/c equal to 0.57, 0.47 and 0.37, respectively. It is observed that for concretes with CNI, the corrosion current is more compared to that of other concretes (OPC, PPC, OPC-SP and PPC-SP), which could be due to higher conductivity and lower concrete resistivity. Table 5.5 presents the total charge (Ampere-days) passed for specimens of concretes with CNI (results of OPC, PPC, OPC-SP and PPC-SP concretes were already presented in Table 5.4). For the gravimetric weight losses of the rebars, the specimens have been broken and the middle 300 mm length of rebar is cleaned as per ASTM G 1 (2009) to remove the rust. It is measured as the relative loss in weight over the middle 300 mm length, and represents the average weight loss over the length considered. The initial weight is taken from the measured weight of rebar per running length. The percent reduction in gravimetric weight loss is presented in Table 5.6. As expected, the gravimetric weight losses are more compared to that of the respective control concretes (OPC and PPC) since the total charge passed is more. Also, during visual inspection, higher rate of corrosion in the form of high evolution of rust products from corrosion induced cracks is observed. The individual results for uncracked, 0.2 mm and 0.4 mm are presented

116

in Tables B.7, B.8 and B.9 of Appendix B, respectively. The dimensions of corrosion induced crack widths are presented in the next section.
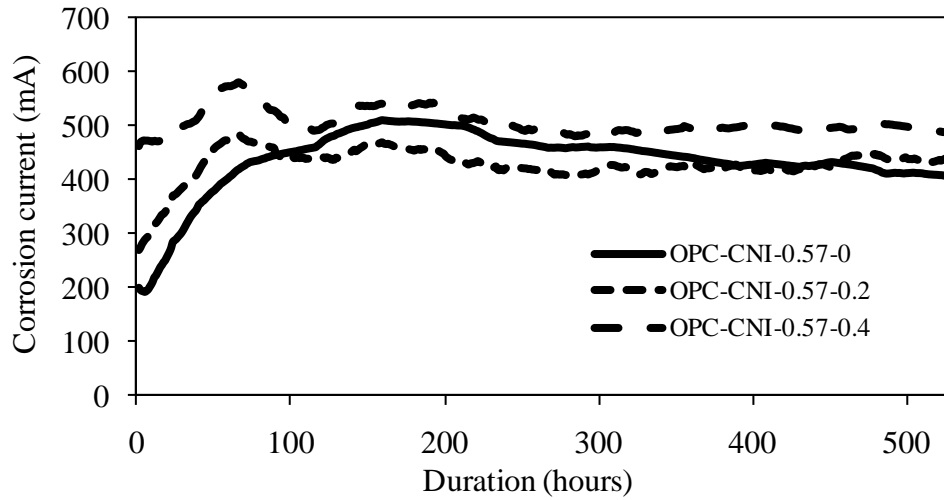
(a) OPC-CNI concrete
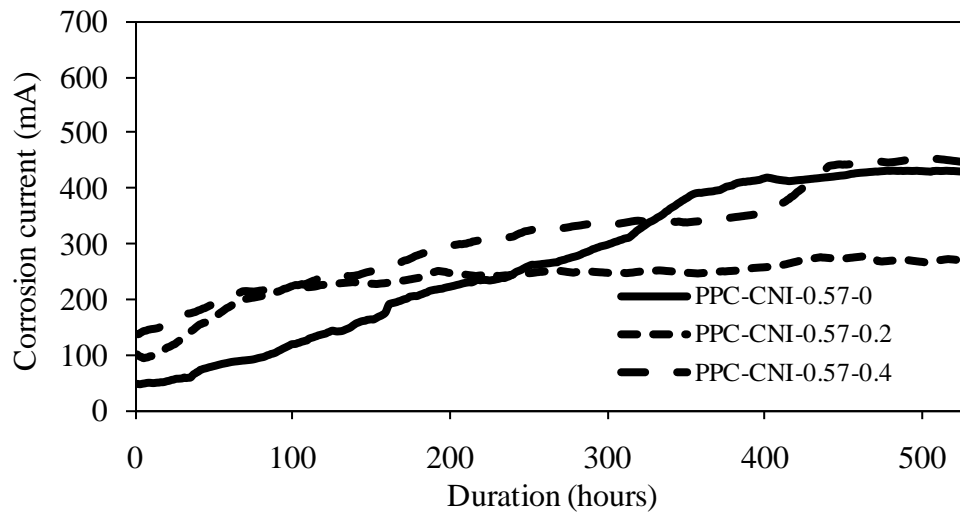
(b) PPC-CNI concrete

Figure 5.22: Corrosion current as a function of exposure duration, OPC-CNI and PPC-CNI concretes for w/c = 0.57
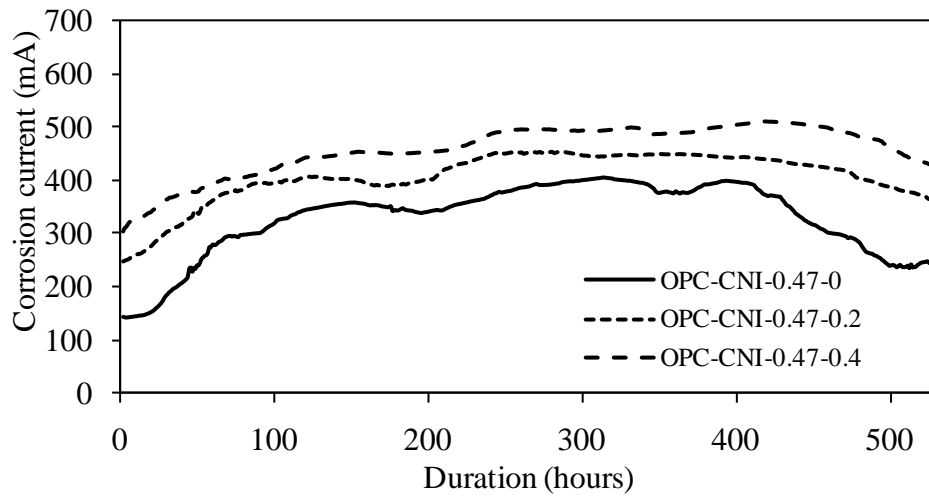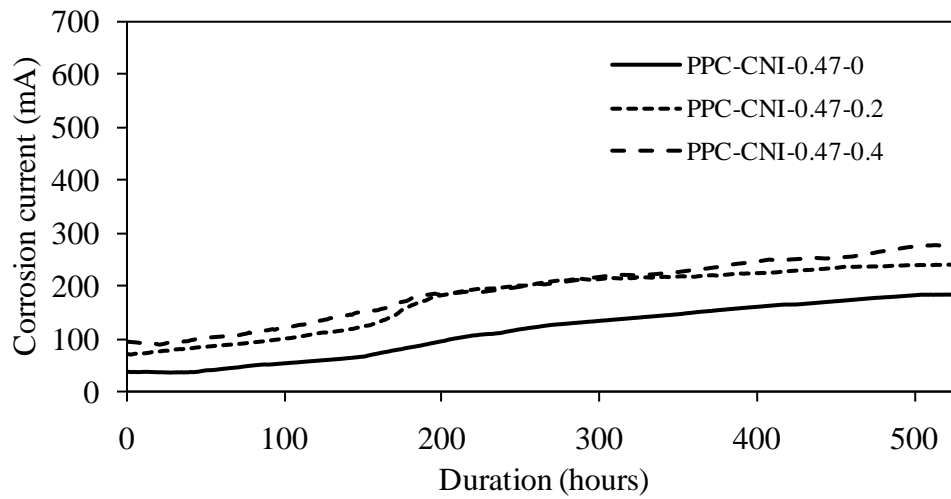
(a) OPC-CNI concrete

(b) PPC-CNI concrete

Figure 5.23: Corrosion current as a function of exposure duration, OPC-CNI and PPC-CNI concretes for w/c = 0.47
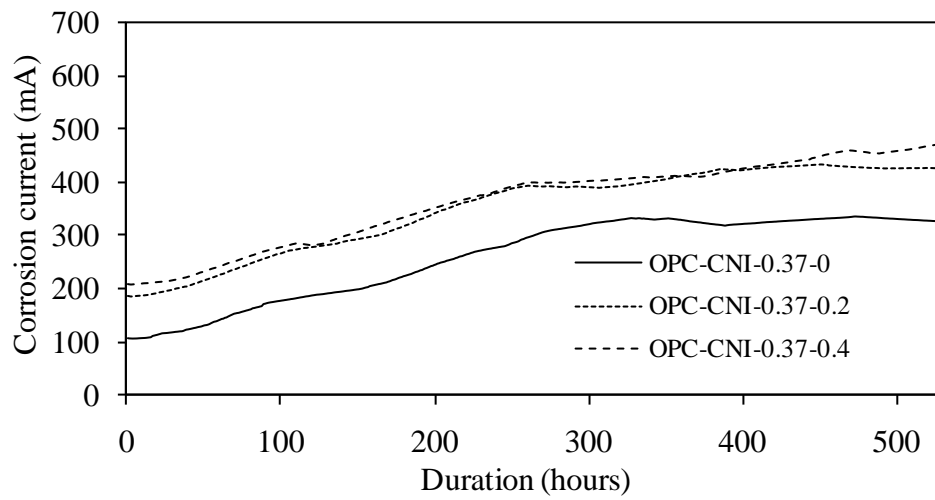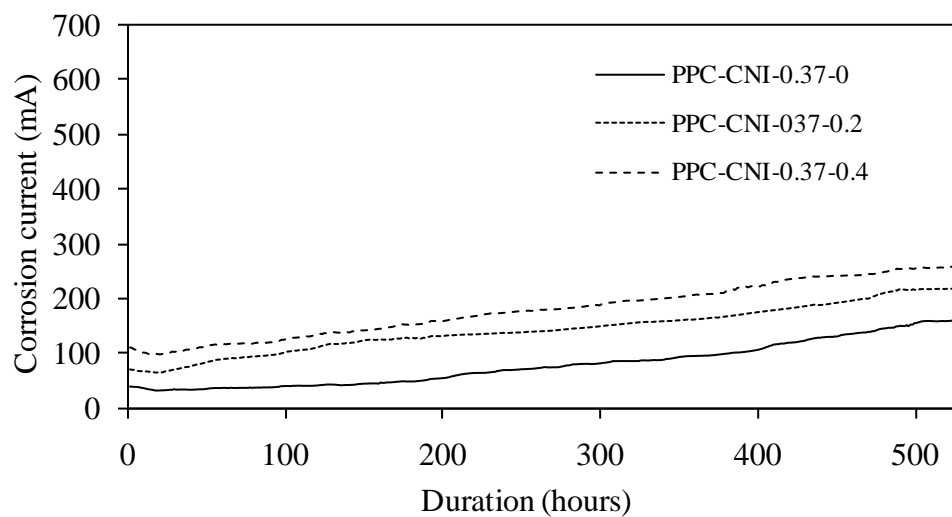
(a) OPC-CNI concrete

(b) PPC-CNI concrete

Figure 5.24: Corrosion current as a function of exposure duration, OPC-CNI and
PPC-CNI concretes for w/c = 0.37

Table 5.5: Charge passed in OPC-CNI & PPC-CNI concretes, Amp-days (constant 10V for 528 hours)

Description	Concrete type	w/c		
		0.57	0.47	0.37
Uncracked	OPC-CNI	9.6	7.2	5.7
	PPC- CNI	5.9	2.5	1.7
0.2 mm-crack	OPC-CNI	9.4	8.9	7.7
	PPC- CNI	5.2	3.9	3.2
0.4 mm-crack	OPC-CNI	11.1	10.1	8.0
	PPC- CNI	6.9	4.2	3.9

Table 5.6: Gravimetric weight loss measurements (% reduction) OPC-CNI & PPC-CNI concretes for different w/c

Description	Concrete type	w/c		
		0.57	0.47	0.37
Uncracked	OPC-CNI	39.0	30.0	24.0
	PPC-CNI	24.5	15.5	10.5
0.2 mm-crack	OPC-CNI	41.0	36.5	31.5
	PPC-CNI	27.5	18.5	15.5
0.4 mm-crack	OPC-CNI	45.0	41.0	33.5
	PPC-CNI	30.1	20.0	19.0

Visual observations, the total charge passed and the final gravimetric weight losses revealed that the concrete with CNI studied here did not exhibit any corrosion inhibition effect but rather aggravated the corrosion process and subsequent corrosion damage in terms of higher corrosion induced crack width and rebar weight loss. This has been observed both in OPC and PPC concretes with CNI. More tests are needed to clarify this seemingly anomalous response. Nevertheless, several previous researchers have observed similar results (Ma et al. 1998; Li et al. 1999, 2000; Kondratova et al. 2003; Montes et al. 2004).

In fact it is worth reiterating here that, in the present study, severe corrosion has been induced in a short period of exposure by means of constant impressed voltage. It is not known whether the inhibition mechanism is active or not during the corrosion

initiation process. Rosenberg and Gaidis (as reported by González et al., 1998) observed that in zones where the passivating oxide layer has been destroyed due to chloride ions, the nitrites does not take part in the passivation and rather react at an earlier stage with the anodic corrosion products and are consumed. Therefore, during the accelerated corrosion process, it is not known whether the nitrite ions actively participate in the inhibition mechanism or not, since the ingress of chloride ions is high compared to the availability of nitrite ions. Nevertheless, Song et al. (2009) reported good inhibition of nitrites in accelerated impressed voltage tests. Due to conflicting results, it can be said that CNI should be used cautiously and further elaborative research on the evaluation procedures is needed.

From the studies performed on concretes of OPC and PPC with CNI-SP (or SP-CNI), the results of half-cell potentials and resistivity values for concretes with CNI-SP for w/c equal to 0.57, 0.47 and 0.37 are presented in Figures 5.25, 5.26 5.27 and 5.28, respectively. The trend of half-cell potential and resistivity measurements are similar to those of concretes with CNI.

The corrosion current (as a function of exposure duration) measurements for OPC-CNI-SP and PPC-CNI-SP concretes are presented in Figures 5.29 - 5.31 for different w/c, and the total charge passed is presented in Table 5.7. The corrosion currents are similar to that of concretes with CNI. It can be seen from the Table 5.7 that the total charge passed in concretes with CNI-SP is higher compared to that of control concretes. However, the total charge passed is less compared with the concretes having CNI. That is, the presence of the PCE SP in concrete with CNI tends to improve the corrosion resistance, which concurs with the observations made in previous sections. The corrosion induced crack widths in the OPC-CNI, PPC-CNI, OPC-CNI-SP and PPC-CNI-SP concretes are presented in Tables 5.9 and 5.10. (Note that the results of OPC and PPC concrete were already presented in Table 4.4 of Chapter 4 and have been repeated here, as needed, for comparison purposes.) The crack width has been measured at 30 mm intervals using a crack measuring microscope with an accuracy of 0.02 mm. It can be observed that the corrosion induced crack widths are more for concretes with the CNI compared to those of the control concrete. The higher corrosion induced crack widths in the case of concretes with CNI could be due to the higher rate of corrosion. Also, it has been observed that for cracked specimens, the average corrosion crack width is lower than that of

121

uncracked specimens. The percent reduction in gravimetric weight loss results are presented in Table 5.8. The individual results for uncracked, 0.2 mm and 0.4 mm are presented in Tables B.7, B.8 and B.9 of Appendix B, respectively.
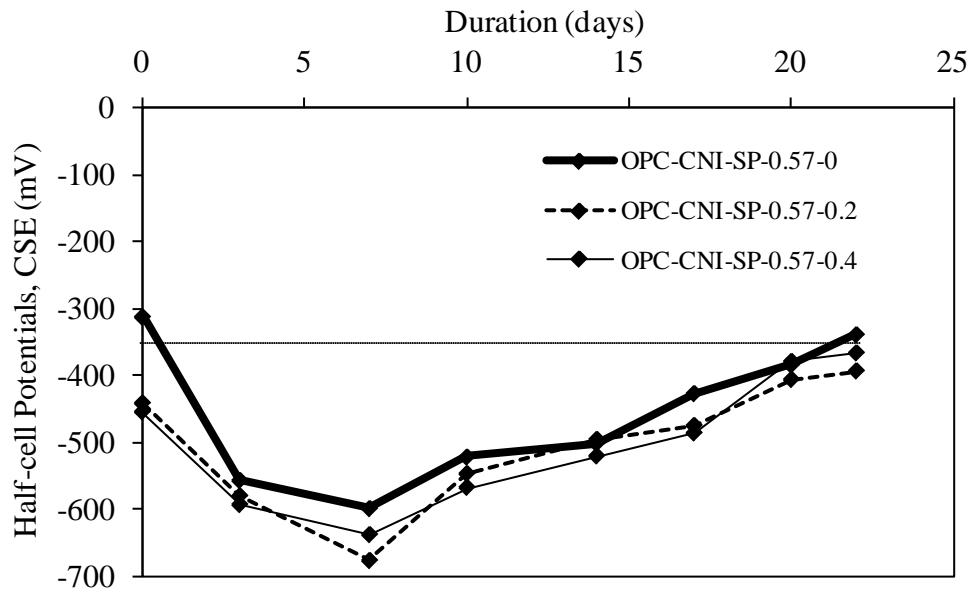
(a) OPC-CNI-SP concrete
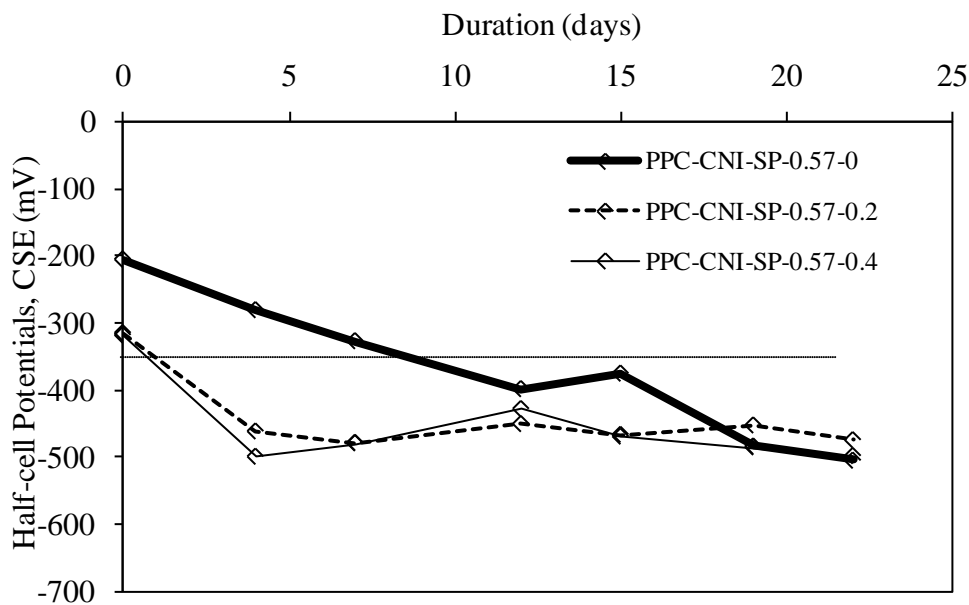
(b) PPC-CNI-SP concrete

Figure 5.25: Half-cell potentials of OPC-CNI-SP and PPC-CNI-SP concretes for w/c = 0.57
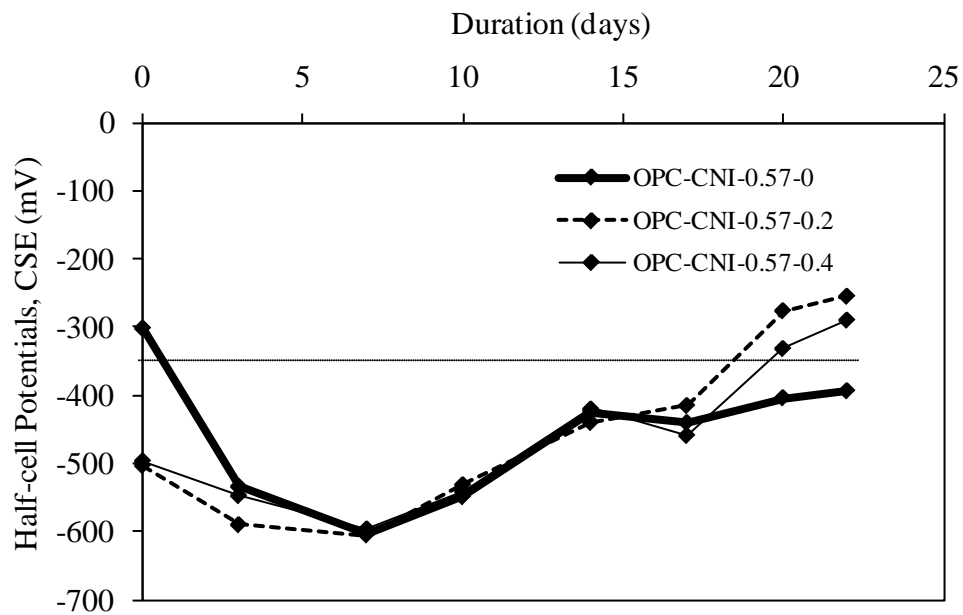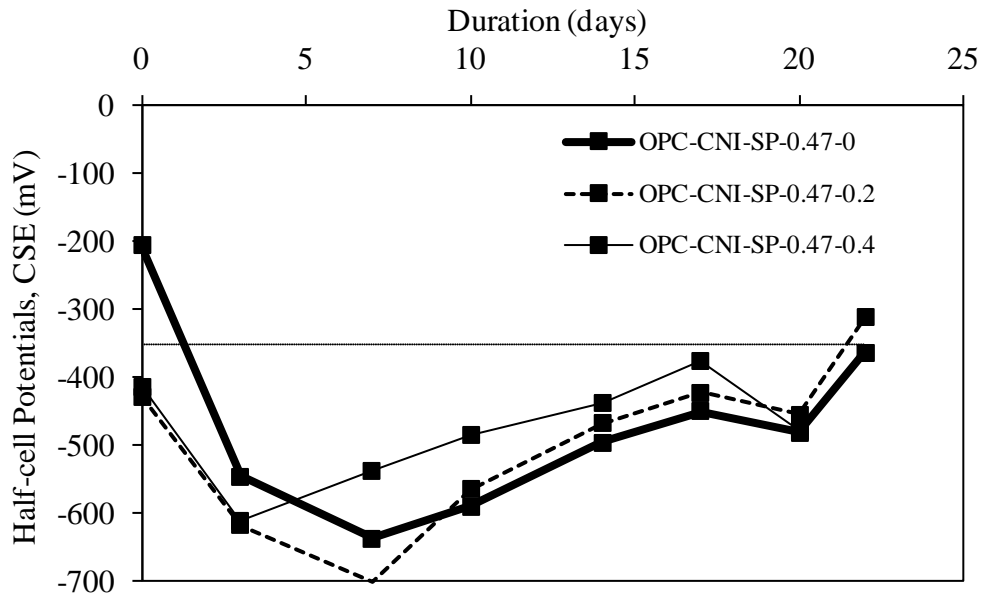
(a) OPC-CNI-SP concrete
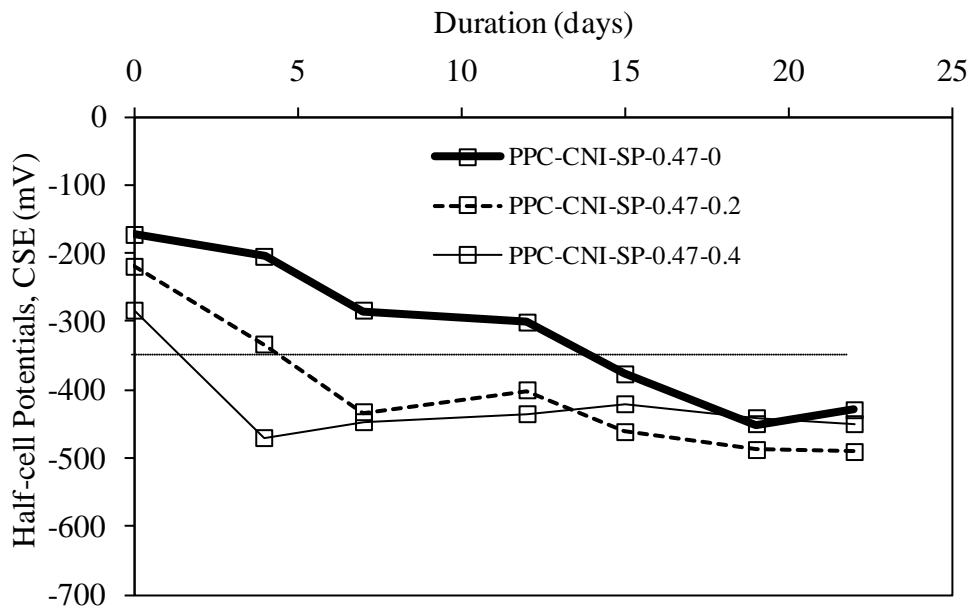
(b) PPC-CNI-SP concrete

Figure 5.26: Half-cell potentials of OPC-CNI-SP and PPC-CNI-SP concretes for w/c = 0.47
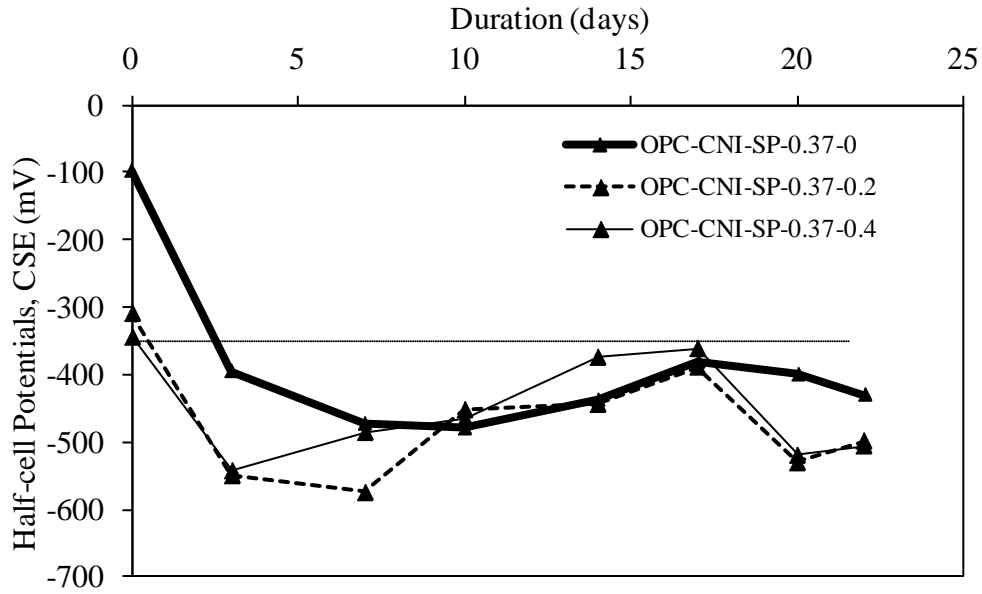
(a) OPC-CNI-SP concrete
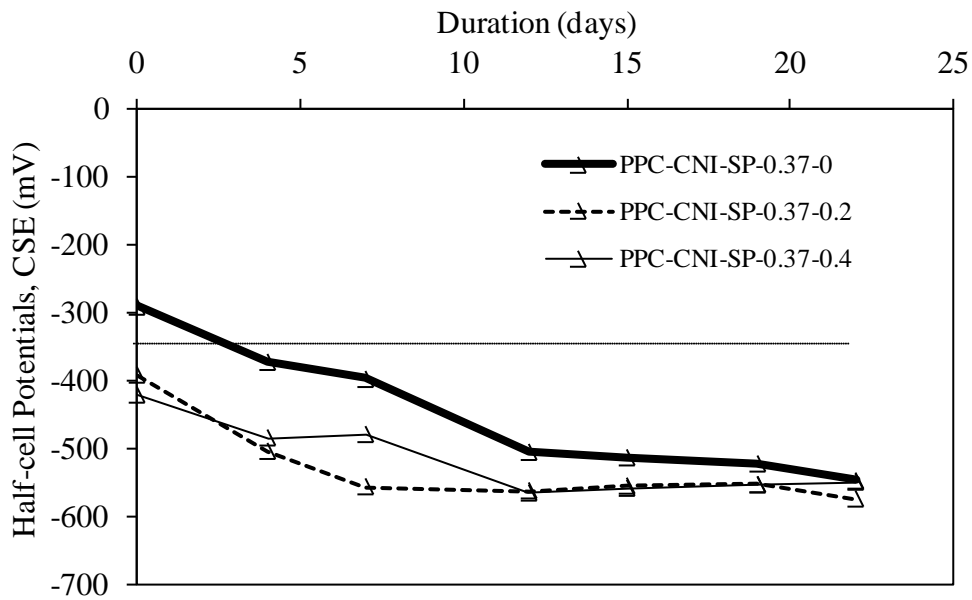
(b) PPC-CNI-SP concrete

Figure 5.27: Half-cell potentials of OPC-CNI-SP and PPC-CNI-SP concretes for
w/c = 0.37
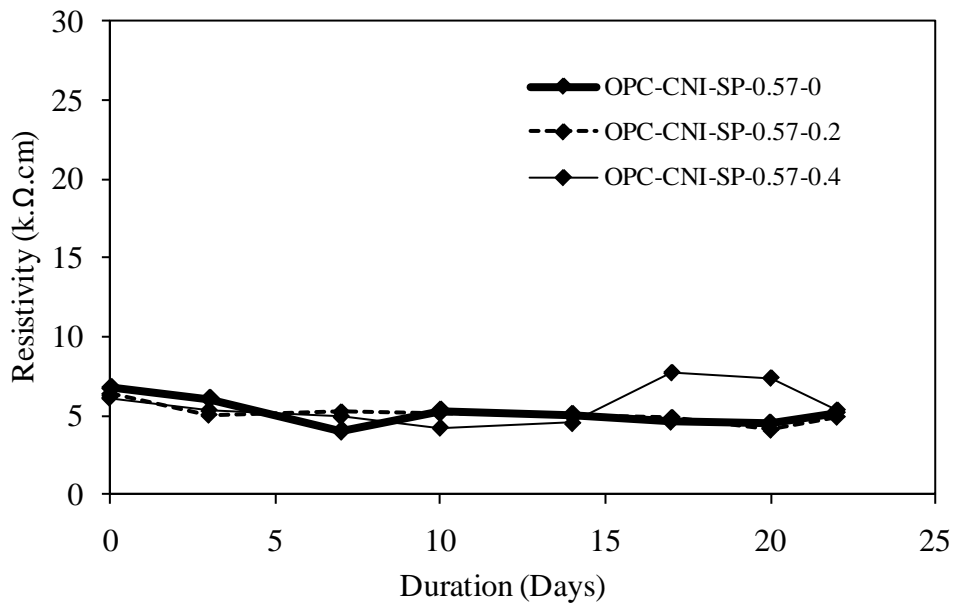
(a) w/c = 0.57
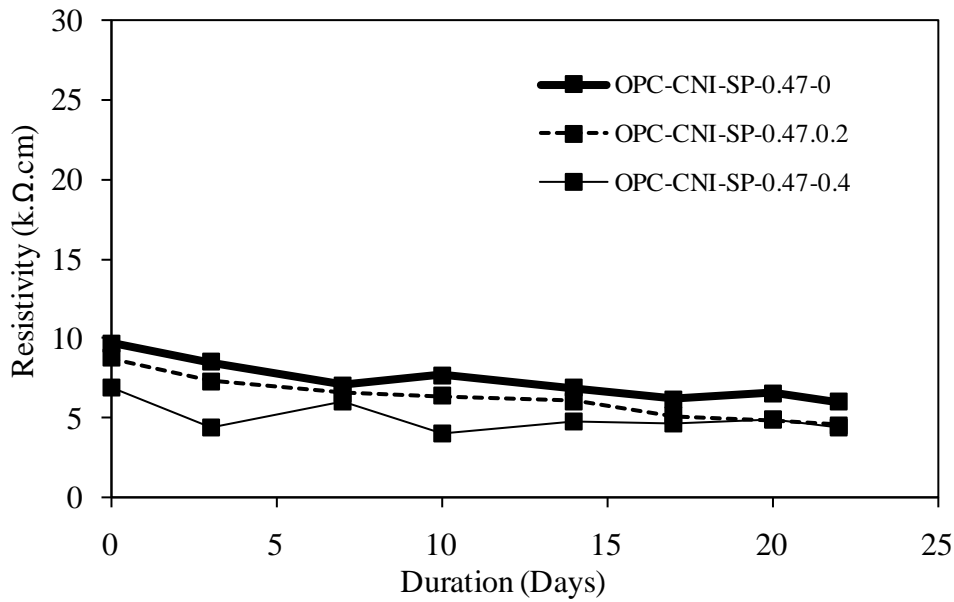
(b) w/c = 0.47

Figure 5.28: Resistivity values for different OPC-CNI-SP concretes
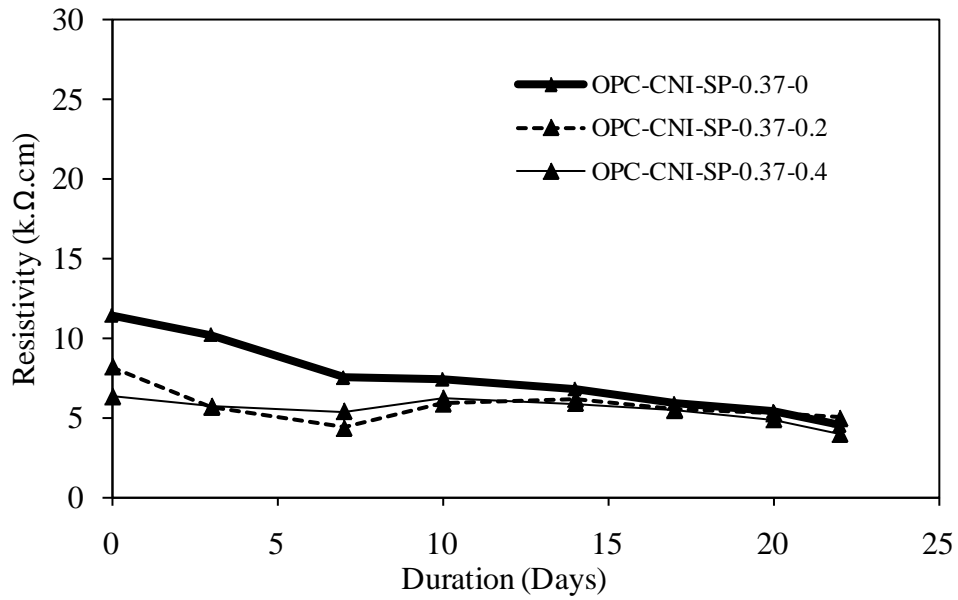
(c) w/c = 0.37

Figure 5.28: Resistivity values for different OPC-CNI-SP concretes
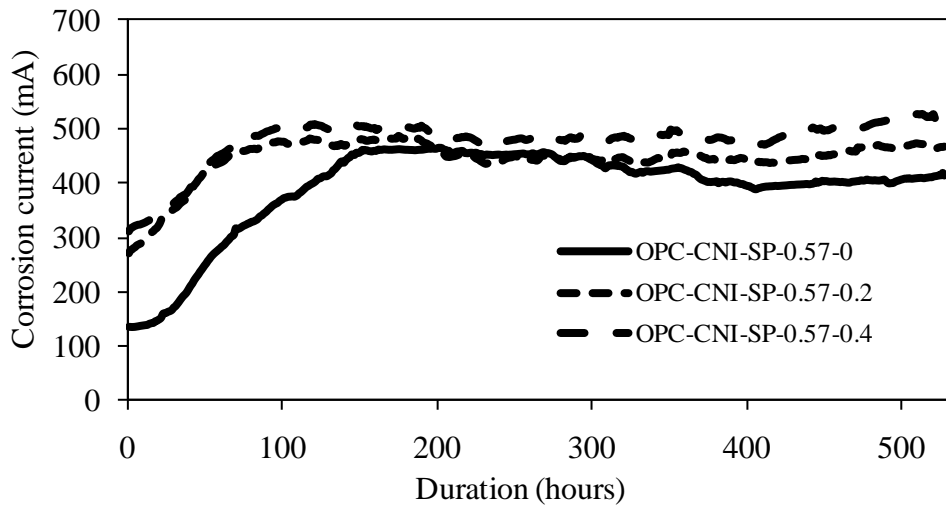
(a) OPC-CNI-SP concrete
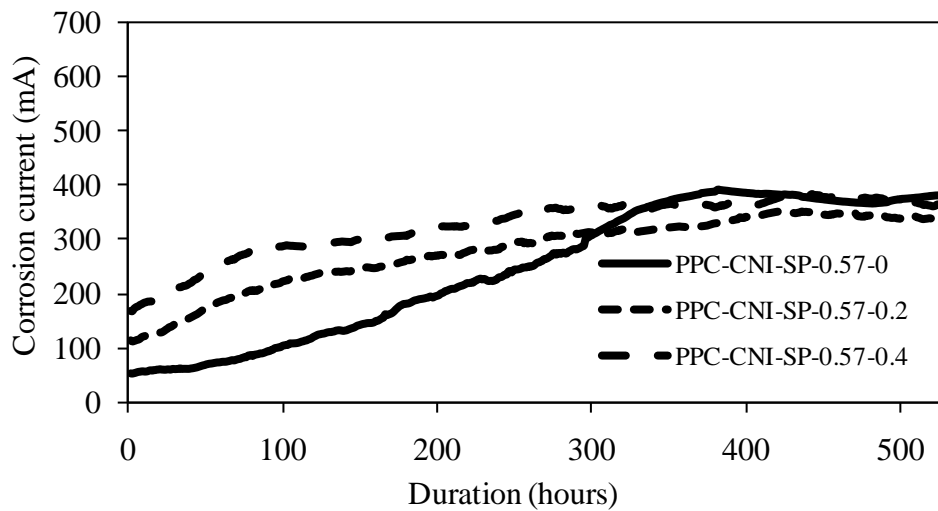
(b) PPC-CNI-SP concrete

Figure 5.29: Corrosion current as a function of exposure duration, OPC-CNI-SP and PPC-CNI-SP concretes for w/c = 0.57
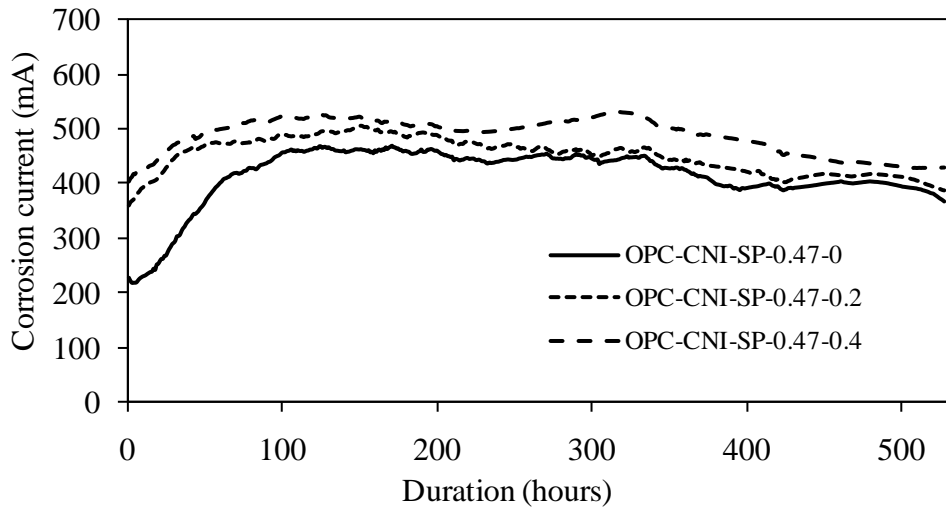
(a) OPC-CNI-SP concrete
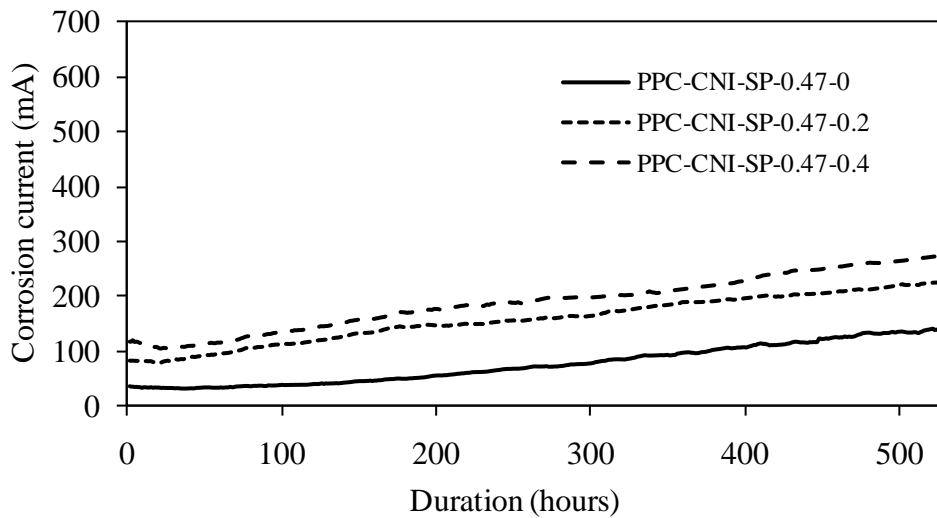
(b) PPC-CNI-SP concrete

Figure 5.30: Corrosion current as a function of exposure duration, OPC-CNI-SP and PPC-CNI-SP concretes for w/c = 0.47
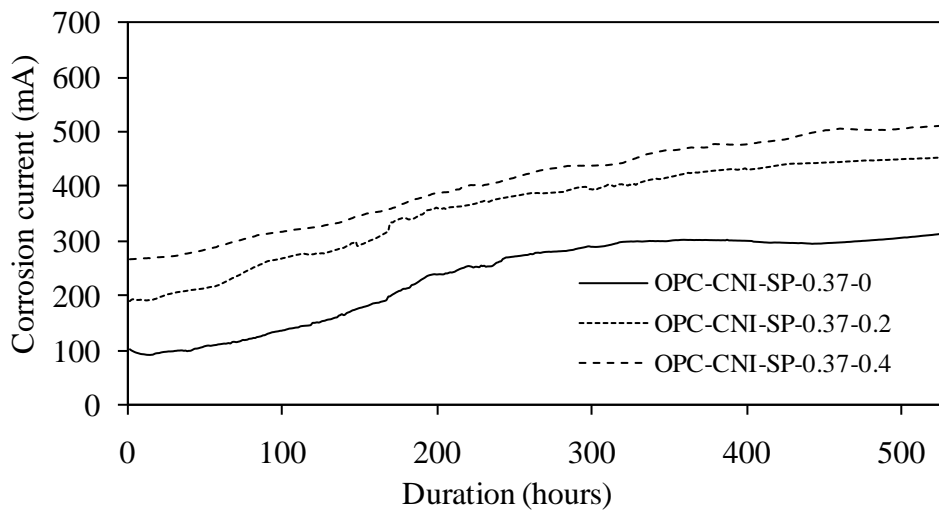
(a) OPC-CNI-SP concrete
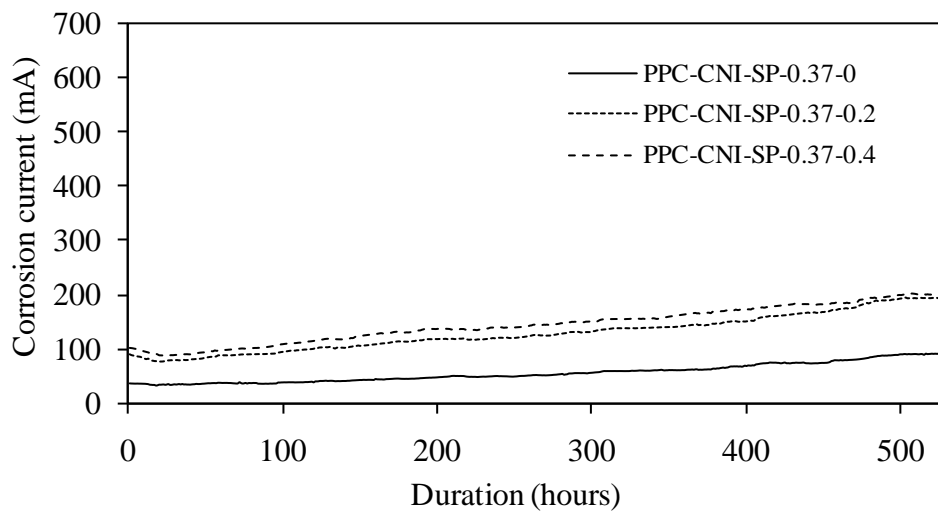
(b) PPC-CNI-SP concrete

Figure 5.31: Corrosion current as a function of exposure duration, OPC-CNI-SP and PPC-CNI-SP concretes for w/c = 0.37

Table 5.7: Charge passed in OPC-CNI-SP & PPC-CNI SP concretes, Amp-days (constant 10 V for 528 hours)

Description	Concrete type	w/c		
		0.57	0.47	0.37
Uncracked	OPC-CNI-SP	8.6	9.1	5.2
	PPC-CNI-SP	5.4	1.7	1.2
0.2 mm-crack	OPC-CNI-SP	9.8	9.9	7.9
	PPC-CNI-SP	6.1	3.5	2.8
0.4 mm-crack	OPC-CNI-SP	10.5	10.7	9.0
	PPC-CNI-SP	7.1	4.1	3.2

Table 5.8: Gravimetric weight loss measurements (% reduction) OPC-CNI-SP & PPC-CNI-SP concretes for different w/c

Description	Concrete type	w/c		
		0.57	0.47	0.37
Uncracked	OPC-CNI-SP	38.1	29.8	22.3
	PPC-CNI-SP	24.1	15.0	9.7
0.2 mm-crack	OPC-CNI-SP	41.2	34.9	30.3
	PPC-CNI-SP	26.2	17.9	14.6
0.4 mm-crack	OPC-CNI-SP	44.2	41.2	33.1
	PPC-CNI-SP	29.8	20.2	19.1

Table 5.9: Corrosion induced crack lengths and widths, OPC-CNI and PPC-CNI concretes

		w/c = 0.57		w/c = 0.47		w/c = 0.37	
		Length (cm)	Width (mm)	Length (cm)	Width (mm)	Length (cm)	Width (mm)
Uncracked	OPC	31.80	0.83	31.28	0.95	32.64	1.21
	PPC	32.36	0.15	32.64	0.22	32.28	0.43
	OPC-CNI	30.60	1.20	31.40	1.45	31.70	1.60
	PPC- CNI	32.00	1.60	32.00	1.40	32.20	0.75
0.2 mm-crack	OPC	32.55	0.73	34.20	0.81	33.60	1.14
	PPC	34.32	0.56	32.16	0.38	33.07	0.55
	OPC-CNI	32.40	0.90	32.06	0.99	32.10	1.30
	PPC- CNI	32.60	1.30	32.90	1.10	32.60	0.71
0.4 mm-crack	OPC	32.91	0.58	33.07	0.68	33.96	1.03
	PPC	34.30	0.44	33.48	0.54	33.12	0.48
	OPC-CNI	33.20	0.71	32.26	0.96	32.70	1.20
	PPC- CNI	32.80	1.11	33.10	1.00	33.00	0.69

Table 5.10: Corrosion induced crack lengths and widths, OPC-CNI-SP and PPC-CNI-SP concretes

		w/c = 0.57		w/c = 0.47		w/c = 0.37	
		Length (cm)	Width (mm)	Length (cm)	Width (mm)	Length (cm)	Width (mm)
Uncracked	OPC-CNI-SP	32.10	1.40	32.70	1.50	31.70	1.70
	PPC-CNI-SP	31.60	1.60	31.00	0.85	30.80	0.44
0.2 mm-crack	OPC-CNI-SP	32.80	1.10	33.00	1.10	32.20	1.50
	PPC-CNI-SP	32.50	1.50	31.70	0.75	32.20	0.54
0.4 mm-crack	OPC-CNI-SP	33.10	0.90	33.50	1.00	32.80	1.30
	PPC-CNI-SP	32.70	1.40	32.30	0.61	32.80	0.50

5.3.2.3. Trials with higher dosages of CNI

As discussed earlier, tests with a CNI dosage of 10 l/m^3 did not reveal any improvement of the corrosion resistance of the concrete due to the incorporation of

131

the CNI and rather gave results indicating an increase in corrosion and crack widths due to chloride ingress. Since researchers such as Nmai and McDonald (1999) have reported that high dosages of CNI are needed when the chloride exposure is severe, limited trials were done here after increasing the CNI dosage to 20 l/m^3 (PPC-CNI20) and 30 l/m^3 (PPC-CNI30) for the PPC concrete with w/c equal to 0.47. The mechanical and durability parameters for the increased dosages are presented in Table 5.11 (results of PPC alone (without CNI) and PPC-CNI (10 l/m^3 of CNI) concrete were already presented in Tables 5.1 and 5.2 and have been repeated here, as needed, for comparison purposes). It is observed that the mechanical properties of concretes are similar to that of the concretes with CNI dosage of 10 l/m^3, however, as the dosage increases, there is an increase in the RCPT values. The trends of the corrosion current evolution of PPC concretes with CNI in uncracked and cracked concretes are compared with PPC concrete without CNI for w/c equal to 0.47 in Figure 5.32. Also, the total charge passed is presented in Table 5.12. It can be seen that the total charge passed in concretes with CNI is very high compared to that of concrete without CNI, though the charge passed in PPC-CNI30 is slightly lower than that of PPC-CNI20.

Table 5.13 provides the percent gravimetric weight losses for increased dosages of CNI for w/c equal to 0.47. It can be observed that even with increased dosages of CNI, no improvement in corrosion resistance is observed. In concretes with CNI, large amount of rust products were oozing out from the corrosion induced cracks compared to that of concrete without CNI as can be seen in photographs in Figure 5.33. However, at higher CNI dosage (of 30 l/m^3) the weight loss is less than with the dosage of 20 l/m^3 but still more than that of concrete without CNI.

It is worthwhile to mention here again that with the addition of CNI in concrete, the resistivity of concrete has been reduced, which could be due to the presence of additional dissociated nitrite ions. It may be obvious that the corrosion current would be higher under applied voltage with CNI addition. However, in the case of corrosion under ambient exposures the result may not be the same. The reason for which has to be investigated with further specific studies.

132

Table 5.11: Mechanical and durability parameters for PPC-CNI20 and PPC-CNI30 (at 28 days)

CNI dosage	0 l/m³	10 l/m³	20 l/m³	30 l/m³
Cube compressive strength (MPa)	41.4	37.0	37.1	38.1
Split tensile strength (MPa)	3.7	3.4	2.5	2.5
Flexural strength (MPa)	5.6	4.7	4.9	5.3
RCPT (Coulombs)	720	2100	2250	2300
Water absorption (%)	6.0	3.9	2.7	2.6
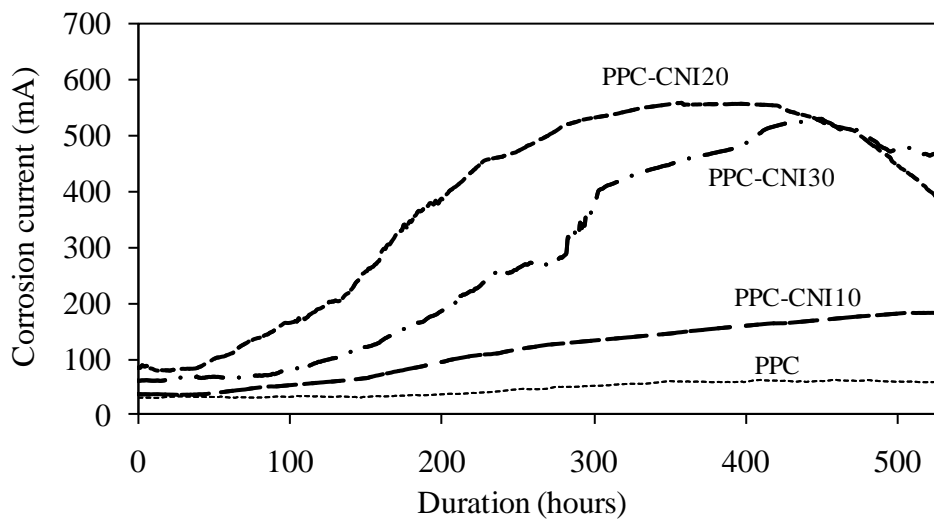
(a) uncracked
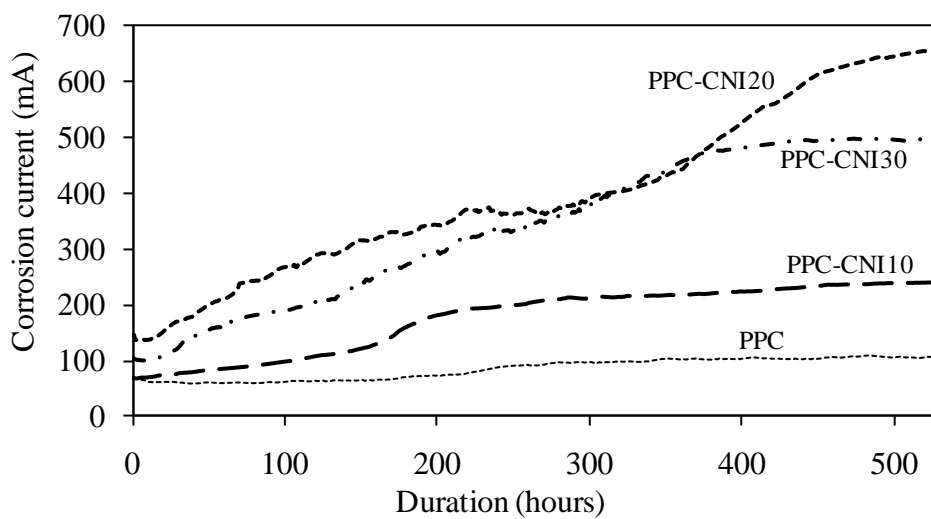
(b) 0.2 mm cracked

Figure 5.32: Corrosion current as a function of exposure duration for different dosages of CNI, PPC-0.47 concrete
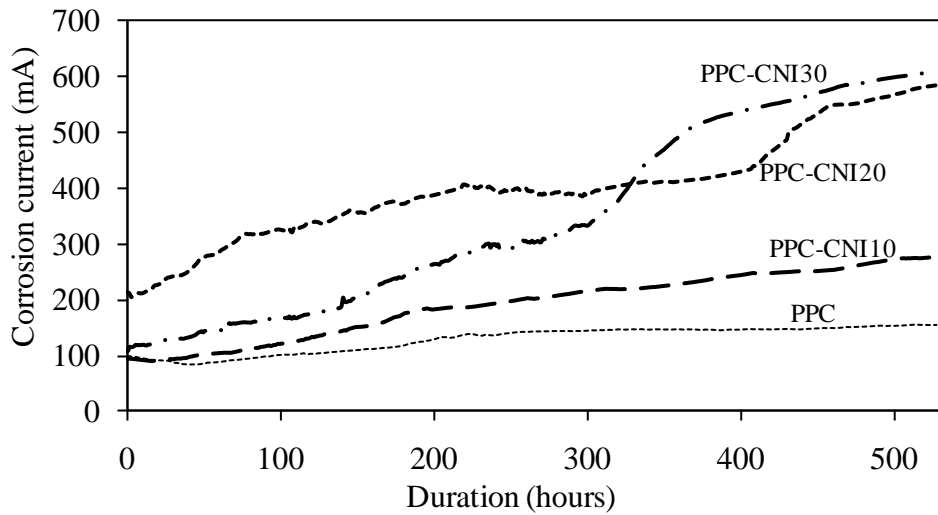
(c) 0.4 mm cracked

Figure 5.32: Corrosion current as a function of exposure duration for different dosages
of CNI, PPC-0.47 concrete

(a) PPC-0.47-0   (b) PPC-CNI-0.47-0

Figure 5.33: Oozing of rust products from PPC concrete with and without CNI

Table 5.12: Charge passed (Amp-days), PPC-CNI20 and PPC-CNI30 concretes

CNI dosage	0 l/m^3	10 l/m^3	20 l/m^3	30 l/m^3
Uncracked	1.04	2.5	9.0	6.9
0.2 mm-crack	1.87	3.9	8.7	7.5
0.4 mm-crack	2.85	4.2	9.2	8.0

Table 5.13: Gravimetric weight loss (% reduction), PPC-CNI20 and PPC-CNI30 concretes

CNI dosage	0 l/m^3	10 l/m^3	20 l/m^3	30 l/m^3
Uncracked	5.1	15.5	24.6	20.0
0.2 mm-crack	13.11	18.5	31.0	28.8
0.4 mm-crack	16.33	20.0	34.5	32.1

5.4. Summary

Based on the experimental results obtained from this study, following conclusions can be drawn:

- The durability-related parameters such as water absorption and sorptivity improve with the incorporation of PCE SP, as well as CNI, when compared with that of control concrete.

- The 28-day compressive strengths and RCPT values of concretes with PCE SP are similar to that of the respective OPC and PPC concretes. Nevertheless, there is an improvement in durability parameters such as water absorption and sorptivity.

- The 28-day compressive strengths of concretes with CNI are considerably lower, about 20% and 10% compared to that of respective OPC and PPC concretes.

- The chloride ion penetrability (through the RCPT test) of concretes with CNI is higher; 1.6 to 1.8 and 2.5 to 3 times that of the corresponding OPC and PPC concretes. This is attributed to the high ionic nature of CNI, which causes more negative charge to pass through the concrete.

- The resistivity values of concrete with CNI are significantly lower when compared to that of the respective OPC and PPC concretes. The half-cell potentials of concrete with CNI are initially less negative compared to that of respective concretes without CNI but become more negative in a very short time.

- The gravimetric weight loss results show that concrete with PCE SP performed better than the control concrete (OPC concrete) even under cracked condition. This is in addition to improving fresh state properties such as workability and slump. This may be due to better dispersion of cement particles and refinement of pore structure.

- The corrosion current is higher in concretes with CNI for both OPC and PPC concretes. The gravimetric weight loss of rebars in concrete with CNI is higher than that of the concretes without CNI. Visual observation, total charge passed and gravimetric weight loss (% reduction in weight) reveal that concrete with CNI did not show any corrosion inhibition effect. The possible reasons could be due to inadequate/inappropriate dosage, higher conductivity of the pore solution and low concrete resistivity. It could also be that the accelerated test parameters used here may not be the most appropriate for evaluating the performance of the CNI in concrete.

CHAPTER 6

SERVICE LIFE ESTIMATION

6.1. General

The deterioration of reinforced concrete (RC) structures due to chloride ingress (i.e., rebar corrosion) is a growing problem all over the world. A reliable prediction of the service life of RC structures is necessary for ensuring long term safety and also for making engineering judgements for the inspection/maintenance activities. However, such service life predictions are always complicated and difficult due to the fact that it is influenced by many factors that are mostly probabilistic or uncertain in nature (viz., the quality of cover concrete, thickness of cover concrete, mechanical loading conditions, exposure conditions, etc.). Generally, in chloride-rich environments, service life can be defined as the time for the initiation of rebar corrosion due to the ingress of chlorides through the cover concrete (Tuutti, 1982; Bentur et al., 1998; Life-365, 2010). However, it may be conservative to assume the end of service life to be at the onset of the rebar corrosion because corrosion damage to the reinforcement may be still insignificant.

The service life, in the present study, is assumed to be the sum of the initiation and propagation periods. Diffusion coefficient (D_c) and corrosion current density (i_{corr}) values are used in the estimation of the initiation and propagation periods. The sensitivity of different parameters on corrosion initiation period is also described. Finally, the service lives of selected concretes when exposed to chloride-rich accelerated laboratory environment are compared.

6.2. Estimation of Service Life

As in Austroads (2000), the present study assumes the service life as the sum of the corrosion initiation period (t_i) and stable propagation period (t_{sp}) (see Figure 6.1).

The service life (t_s) can be written as:

$$t_s = t_i + t_{sp} \qquad (6.1)$$

where: t_i =   the initiation period

          t_{sp} =   the stable propagation period
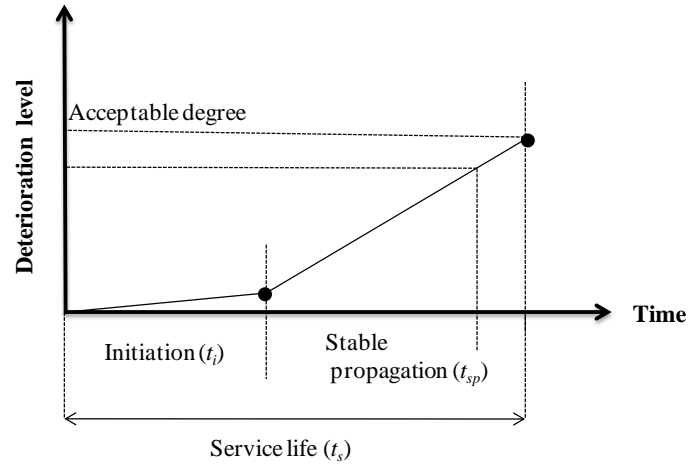
Figure 6.1: Service life estimation

6.2.1. Initiation period (t_i)

The initiation period (t_i) is the time from the construction to the time of initiation of corrosion. In other words, in the case of chloride induced corrosion, t_i defines the time it takes for chlorides to penetrate the concrete cover and accumulate in sufficient quantity (i.e., critical chloride content, C_{tc}) at the depth of the embedded rebar to initiate corrosion (Austroads, 2000; Ahmad, 2003; Ann and Song, 2007; Angst et al., 2009; Life-365, 2010). Many researchers use a diffusion based model (Fick's 2nd law of diffusion) for predicting t_i when exposed to chloride ions (Browne, 1980; Prezzi et al., 1996; ACI 365.1R, 2010; Life-365, 2010; Prabakar et al., 2010b). After applying the specific boundary conditions of $C_x = 0$ at $t = 0$, $0 < x < \bullet$; and $C_x = C_0$ at $x = 0$, $0 < t < \bullet$, the model can be described as (Andrade, 1993; Gjørv, 1994):

$$C(x,t) = C_0 \left[1 - erf \left(\frac{x}{2\sqrt{(D_c t_i)}} \right) \right] \tag{6.2}$$

where

$C(x,t)$	=	Chloride concentration at depth x (or C_{tc} in this case) after time t_i, as a % weight of concrete
C_0	=	Surface chloride concentration, % weight of concrete
D_c	=	Apparent chloride ion diffusion coefficient, mm^2/year
erf	=	Gaussian error function, and
x	=	Distance from exposed surface, mm

138

Once the values of C_{tc}, C_0 and D_c are available, the time for $C(x,t)$ at the depth of the rebar to reach C_{tc} gives t_i. In practice, the values C_{tc}, C_0 and D_c are dynamic in nature. However, reasonable values of C_{tc}, C_0 and D_c can be assumed based on the exposure condition, materials used, mixture proportions used, etc. Generally, these models are suitable for uncracked concrete only. The cracks that are present in concrete usually increase the rate of transport of deteriorating agents towards the steel thereby reduce the t_i of the structure. A brief discussion about C_{tc} and the evaluation of D_c for the selected concretes is given below.

6.2.1.1. Critical chloride threshold concentration (C_{tc})

As mentioned earlier, the value of C_{tc} depends upon various factors and cannot generally be fixed. These include the microstructure and metallurgical parameters of the rebar, the complex microstructure of the surrounding concrete and transition zone, the pH of the concrete pore solution, binding capacity of cement, the local environmental characteristics, and the test procedures used to evaluate this parameter (Alonso et al., 2000; Pillai and Trejo, 2005; Angst et al., 2009; Angst and Vennesland, 2009). The critical threshold values for different steel reinforcement types have been reported in the literature (Alonso et al., 2000; Trejo and Pillai, 2003; 2004); Table 6.1 presents the C_{tc} values reported by some researchers. A higher threshold would lead to a longer predicted life and vice-versa, provided the other conditions are the same. Therefore, the threshold value should be carefully selected. In the present study, for the estimation of t_i, the C_{tc} value assumed as 0.4% weight of cement, which is the most commonly used value (Austroads, 2000; Broomfield, 2006; ACI 365.1R, 2010; Life-365, 2010).

Table 6.1: Threshold chloride contents reported in literature (Austroads, 2000)

Threshold chloride concentration	Reference
0.1% total chloride by weight of dry concrete	Stoltzner et al. (1997)
0.15% water soluble chloride ion by mass of cement	Holden et al. (1983) and Popovics et al. (1983)
0.17 - 2.5% of chloride by mass of cement	Glass and Buenfeld (1995)
0.4% total chloride by weight of cement	Broomfield (2006)
0.4 - 0.8% total chloride by weight of cement	Locke and Siman (1980)

6.2.1.2. Evaluation of apparent chloride diffusion coefficient (D_c)

Zhang and Gjørv (1994) proposed an accelerated chloride diffusion method, where the steady state rate of chloride penetration is obtained from the slope of the linear part of the increasing chloride content with time (Gjørv, 1994). In order to evaluate the apparent diffusion coefficient, in the present study, the diffusion test has been carried out as per Nordtest Method (NT Build 355, 1997) and the test setup is described in Fig. 1. In this method, two reservoirs are filled with 0.25 N sodium chloride (NaCl) solution and 0.25 N sodium hydroxide (NaOH) solution and are connected by applying a constant voltage of 12 V DC. The chloride ions migrate from the NaCl solution reservoir at the negative side of the specimen to the NaOH solution compartment at the positive side. The chloride flux through the specimen is determined by using the increase in chloride concentration with time in the NaOH solution after steady state is achieved. For this, 50 ml of sample from NaOH reservoir was taken at different intervals for Cl^- content determination. The chloride content in the sample was determined by volumetric titration using the standard test procedure. A curve has been drawn between chloride concentration (mmol/cm^3) and the duration (days). The experiment was stopped when constant and steady state chloride concentration is observed over a period of time (Prabakar et al., 2010c). A typical sample plot showing the relationship between chloride ion concentration (mmol/cm^3) and time (hours) is presented in Figure 6.2 for OPC-0.57 concrete (OPC-0.57, denotes the concrete with OPC binder and w/c of 0.57). For a constant voltage, the chloride concentration of NaOH solution increases gradually and linearly with time. The slope, *dc/dt*, over the linear portion was determined. The value of D_c has been calculated as per the following equation (Zhang and Gjørv, 1994):

$$D_c = \beta_\circ \frac{300kT}{ze_\circ \Delta_\Psi} \frac{LV}{c_\circ A_\circ} \frac{dc}{dt} \cdots (cm^2/s) \tag{6.3}$$

where,

D_c = diffusion coefficient (cm^2/s)

$\beta_\circ$ = correction factor for ionic interaction (1.22 to 1.7 for 0.1 M to 0.5 M of NaCl, for this study, i.e., 0.25M - the β_o value is 1.4)

k = Boltzman's constant (1.38×10^{-16} ergs/K/ion)

T = temperature, °K (273 absolute+32 °C room temp. = 305 °K)

140

L	=	specimen thickness (5 cm)

L = specimen thickness (5 cm)

V = volume of container (250 cm^3)

z = ion valency in the testing chloride salt (1)

e_o = charge of proton (4.8 × 10^{-10} e.s.u.)

∇_ψ = applied electrical potential (12 V)

c_o = initial chloride concentration (2.5×10^{-1} mmol/cm^3, for 0.25 N NaCl)

A_o = area of cross section of specimen (78.50 cm^2)

$\dfrac{dc}{dt}$ = steady state migration rate of chloride ion in mmol/ cm^3.s
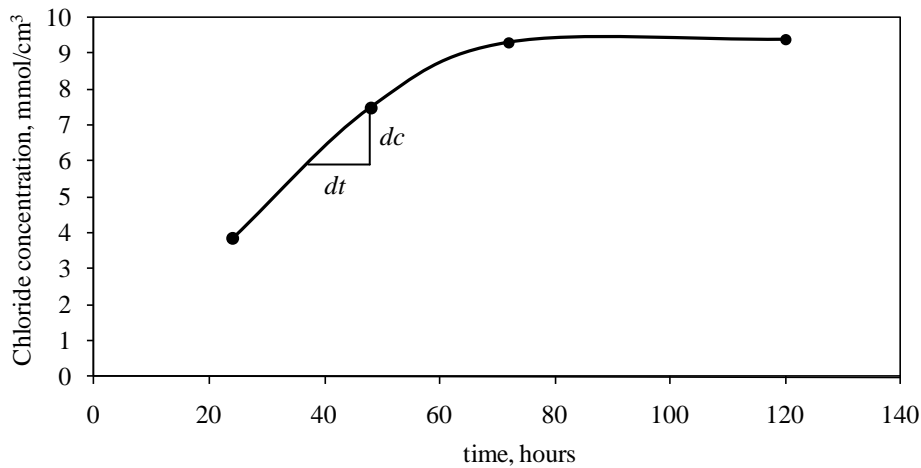
Figure 6.2: Typical plot of relationship between chloride ion concentration and time for OPC-0.57 concrete

It can be stated here that the apparent diffusion coefficient (D_c) obtained experimentally cannot be compared directly with non-steady state diffusion coefficients or those used in service life predictions where chlorides diffuse in a non-steady state manner or are transported by absorption. It is to be noted here that the D_c values are used here to compare the relative corrosion initiation period (t_i) of different concretes.

6.2.2. Stable propagation period (t_{sp})

Researchers have proposed different models for determining the loss in area of reinforcing bar subjected to corrosion (Raupach, 2006). In the present study, t_{sp} has

been computed using the model proposed by Rodriguez et al. (1996). In this model, the loss in rebar diameter, $\phi(t)$ (in mm), at any time t (in years), can be estimated as

$$\phi(t) = \phi(0) - p(t) \tag{6.4}$$

where $\phi(0)$ is the initial diameter of the rebar (in mm), and $p(t)$ is the loss of section (in mm), with time given by,

$$p(t) = 0.0116 \cdot i_{corr}(t_s - t_i) \tag{6.5}$$

where i_{corr} is the average value of corrosion current density (in $\mu A/cm^2$), 0.0116 is a factor which converts $\mu A/cm^2$ to mm/year, t_s is the total time elapsed (in years), t_i is the time for initiation of corrosion (years), and α is a pitting factor (for including the effect of highly localized pitting normally associated with chloride-induced corrosion; for uniform corrosion, $\alpha = 2$; for pitting corrosion, $\alpha = 5$ to 10) (González et al., 1995).

This model is formulated based on Faraday's law, on the assumption that the number of electrons released by the Fe atom during the half cell corrosion reaction is 2, the atomic mass of iron is 55.95 g/mol and the mass density of iron is 7.88 g/cm³ (Vorechovská et al., 2009). Although this model takes into consideration the localized pitting associated with chloride-induced corrosion, the reduction in corrosion current with time is not taken into account. This model gives a conservative estimate for the reduction in bar diameter in the case of pitting corrosion, as the corrosion pits are assumed to be hemispherical in shape (Anoop et al., 2012). Once t_s is estimated, t_{sp} can be computed as:

$$t_{sp} = t_s - t_i \tag{6.6}$$

Compared with the work carried on the initiation period, relatively less research has been reported on the propagation period to deal with the service life prediction of concrete structures. Clear (1989) found a very simple, broad relationship between the corrosion rate and the time required for corrosion development (see Table 6.2).

142

Table 6.2: Measured corrosion rate and time for corrosion development (Clear, 1989)

corrosion rate ($\mu A/cm^2$)	time for corrosion development (year)
0.2 ~ 1	10 ~ 15
1 ~ 10	2 ~ 10
> 10	< 2

6.3. Estimation of Service Life for Selected Concretes

As described in Eq. (6.1), the service life is assumed to be the sum of the initiation and stable propagation periods.

Initiation period

Table 6.1 presents the diffusion coefficient (D_c) values for the selected concretes. The D_c values have been evaluated using the procedure described in Section 6.2.1.2 and the Eq. 6.3. The age of the concrete specimens at the time of diffusion test was about 6 months. It has been observed that the diffusion coefficient value of PPC concrete is nearly double that of the corresponding OPC concrete. Generally, the value of C_0 increases with the time of exposure of the structure. Field data, however, indicate that C_0 tends to reach a 'maximum' value, which generally depends on the concrete porosity and aggressiveness of chloride environment (CSIRO, 2000). In the present study, the surface chloride concentration is assumed to be 1.0% by weight of cement (for marine tidal zone, as in Life-365, 2010). Also, it should be noted that the threshold chloride concentration assumed is same for all concretes, which may not be true and depends on various factors (Richardson, 2002; Trejo and Pillai, 2003). Using the D_c values presented in Table 6.3, corrosion initiation periods have been evaluated with the cover thickness of 20 mm. For computing the initiation period, Eq. (6.2) can be written as:

$$\frac{C(x,t)}{C_0} = \left[1 - erf\left(\frac{x}{2\sqrt{(D_c t_i)}}\right)\right] \tag{6.7}$$

$$\left[1 - \frac{C(x,t)}{C_0}\right] = erf\left(\frac{x}{2\sqrt{(D_c t_i)}}\right) \tag{6.8}$$

$$t_i = \frac{x^2}{4D_c\left[erf^{-1}\left(1 - \frac{C_{tc}}{C_0}\right)\right]^2} \tag{6.9}$$

143

where,

$C(x,t)$ = chloride ion concentration at rebar level or critical threshold value, C_{tc}, assumed as 0.4% weight of cement (or 0.05% in concrete),

C_0 = surface chloride concentration, assumed as 1% by weight of concrete

x = cover thickness, 20 mm

Using the Eq. (6.9) corrosion initiation periods have been computed for the selected concrete mixes, and presented in Table 6.3 (along with D_c values) and Figure 6.3. The solution used for the error function is applicable for a constant surface chloride concentration, C_0 and a constant diffusion coefficient, D_c. However, conditions such as those assumed to solve the differential equation do not exist in reality. In general, Eq. (6.9) can be used to determine t_i for an RC structure provided the chloride concentration in the surrounding environment can considered to be constant over the specified time period. For example, chloride concentration at a concrete surface exposed continuously to sea water could be constant (Pillai, 2010).

Table 6.3: Apparent diffusion coefficient (D_c) and corrosion initiation periods (t_i)

Concrete	Apparent diffusion coefficient, D_c (mm^2/year) ; [m^2/sec]	Corrosion initiation period (t_i), years
OPC-0.57	24.19; [7.67×10^{-13}]	2.1
PPC-0.57	12.36; [3.92×10^{-13}]	4.2
OPC-SP-0.57	21.89; [6.94×10^{-13}]	2.4
OPC-CNI-0.57	22.58; [7.16×10^{-13}]	2.3
OPC-SP-CNI-0.57	20.97; [6.65×10^{-13}]	2.5
PPC-SP-0.57	9.30; [2.95×10^{-13}]	5.6
OPC-SP-0.47	12.05; [3.82×10^{-13}]	4.3
PPC-SP-0.47	3.03; [9.62×10^{-14}]	17.2
PPC-SP-0.37	1.52; [4.81×10^{-14}]	34.2
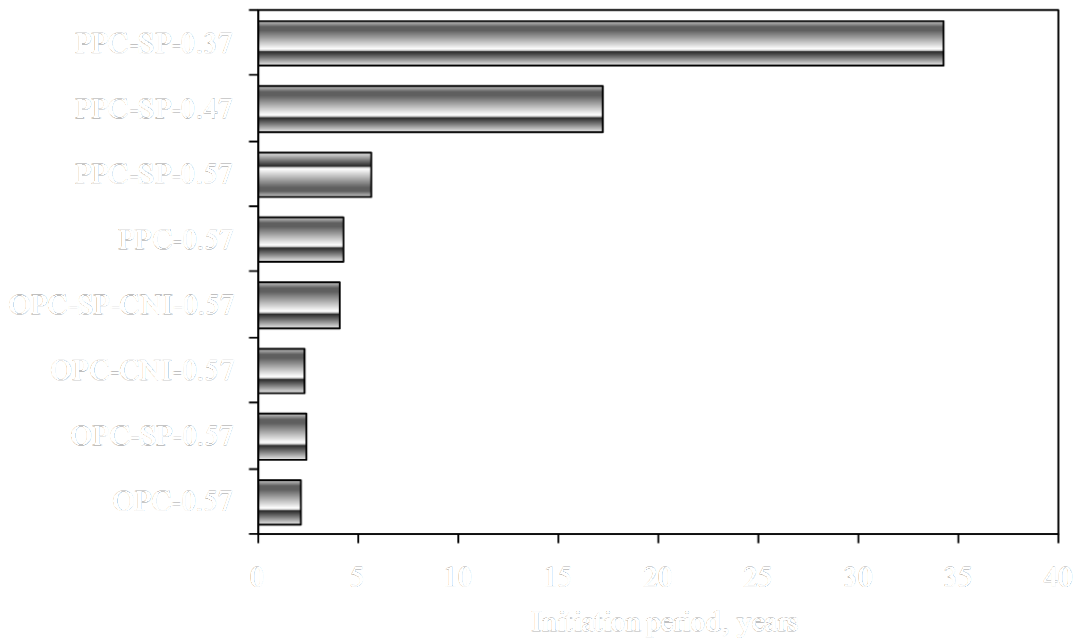
Figure 6.3: Comparison of corrosion initiation period of selected concretes

It can be seen that the corrosion initiation period of PPC-0.57 concrete is nearly double that of the corresponding OPC-0.57 concrete, which is due to the lower diffusion of chlorides in PPC concrete. This can be attributed to the secondary hydration of fly ash with the $Ca(OH)_2$ to form secondary calcium hydrates, causing pore size refinement (Saraswathy and Song, 2007a). The D_c values of OPC, OPC-SP, OPC-CNI and OPC-SP-CNI concretes are, in general, close to one another and hence, the initiation lives are also similar to one another. It can be observed that the corrosion initiation period of concrete with CNI is about 8% more than that of the control concrete (OPC alone). However, any beneficial effect of this has not been seen in the accelerated corrosion test results. In fact, corrosion initiated earlier in the concrete with CNI, possibly due to the highly ionic nature of the pore fluid and lower resistivity of concrete, which have not been taken into account in the estimation of corrosion initiation period. Also, it can be recalled that the charge passed is higher in concretes with CNI, implying that the ionic and/or transport nature of nitrites is more when compared to the chloride diffusion in OPC concrete. The reduction in w/c from 0.57 to 0.37 in PPC-SP concrete reduced the D_c value nearly 6 times. It can also be observed from Figure 6.3 that as w/c decreases, the corrosion initiation period increased since the D_c decreases with a decrease in w/c. This can be expected for

145

other concretes also. However, it is to be noted here that the model for corrosion initiation period is used to compare the relative t_i of different concretes for a specific and initial boundary conditions, and the conclusions cannot be directly extended for all real life validations.

Stable propagation period

Andrade et al. (1990) have given typical ranges of values for corrosion intensity levels (i_{corr}) for different exposure conditions based on measurements made in laboratory specimens, as well as on field data. It is reported that the maximum i_{corr} measured in very aggressive environments is about 100 to 200 $\mu A/cm^2$. It has also been stated that the i_{corr} values vary over a wide range, depending on the chemical composition of the pore fluid surrounding the steel, cover quality and thickness, conductivity of the electrolyte, supply of oxygen, moisture content in concrete, temperature, porosity of concrete, concentration of chlorides, etc. Laboratory gravimetric weight loss measurements have been used here to estimate the equivalent corrosion current density, i_{corr}, for the selected concretes (Ijsseling, 1986; Ahmad, 2009). The computed i_{corr} values for uncracked concrete specimens are presented in Table 6.4 and the details of the computations are provided in the Appendix C.

Table 6.4: Laboratory i_{corr} values for selected uncracked concretes

Concrete	i_{corr} ($\mu A/cm^2$)
OPC-0.57	768
PPC-0.57	289
OPC-SP-0.57	731
OPC-CNI-0.57	1703
OPC-SP-CNI-0.57	1693
PPC-SP-0.57	233
OPC-SP-0.47	507
PPC-SP-0.47	208
PPC-SP-0.37	172

As reported by Andrade et al. (1990) and Austin et al. (2004), the i_{corr} values for extreme chloride induced corrosion conditions are in the range of 100 to 200 $\mu A/cm^2$, and this could be valid for a normal grade of concrete (in the present study, OPC-0.57 concrete is considered to be representative of a normal concrete). Andrade et al. (1990) and González et al. (1995) further reported that values of 1 - 3 $\mu A/cm^2$ are frequent in active corrosion and the values of the order of 10 $\mu A/cm^2$ or higher are seldom observed in the field.

If we consider the laboratory i_{corr} value obtained here for OPC-0.57 concrete, it can be said that there is a large difference between the laboratory i_{corr} value and field i_{corr} values (based on Andrade et al., 1990). Therefore, it is necessary to map the laboratory i_{corr} values to the more realistic field values in order to estimate service life. Hence, for using Eq. (6.5), it is assumed that the i_{corr} value for OPC-0.57 concrete can be taken in the range of the realistic field values. Ausin et al. (1991) attempted to quantify the influence of the corrosion rate on the load bearing capacity of structures and reported that (i) corrosion rates below 1 $\mu A/cm^2$ are unlikely to produce significant reductions on the load bearing capacity, (ii) corrosion rates over 10 $\mu A/cm^2$ can produce important reductions of the nominal resistance of reinforced concrete elements. Hence, for the present study, i_{corr} values equal to 1, 10 and 100 $\mu A/cm^2$ have been taken as possible field values of corrosion rates for OPC-0.57 concrete, representing low, medium and high corrosion rates (i.e., severe/extreme chloride exposures), respectively.

Here, the laboratory i_{corr} value for any other concrete is used to obtain the corresponding field i_{corr} value from the ratio of laboratory i_{corr} values between that particular concrete (say, PPC) and OPC-0.57 concrete as (Morinaga, 1988; Morinaga et al., 1994):

$$\left(\frac{i_{corr,OPC-0.57}}{i_{corr,PPC}} \right)_{Lab} = \left(\frac{i_{corr,OPC-0.57}}{i_{corr,PPC}} \right)_{Field} \tag{6.10}$$

$$\left(i_{corr,PPC} \right)_{Field} = \left(\frac{i_{corr,PPC}}{i_{corr,OPC-0.57}} \right)_{Lab} \times \left(i_{corr,OPC-0.57} \right)_{Field} \tag{6.10a}$$

Now, another important parameter that needs to be set out in order to calculate the stable propagation period (t_{sp}) is the definition of the level or levels of deterioration

147

that may affect the serviceability or the load-carrying capacity of the structure. Table 6.5 presents the levels of deterioration [A, B, C, D and E] classified in the Bulletin No. 162 (CEB, 1983). Andrade et al. (1990) assumed that the levels C and D would require rapid intervention, i.e., the structure would have run out of its residual service life, whereas levels B and A indicate a longer residual service life. Also, among all five damage indicating parameters (colour changes, cracking, spalling, loss of steel section, and deflections), the loss in steel section is considered as the rate-determining parameter.

Hence, in the present study, damage level C or loss in steel section of 10% is assumed as the end of stable propagation period (t_{sp}). Life-365 (2010) takes t_{sp} as 6 years for most commonly used uncoated steels and 20 years for epoxy coated steel.

Table 6.5: Damage levels of reinforced concrete building elements subjected to steel corrosion (CEB 162, 1983; Andrade et al., 1990)

Visual Indications	Damage Levels				
	A	B	C	D	E
Colour changes	Rust stains	As in A	As in A	As in A	As in A
Cracking	Some longitudinal	Several longitudinal Some on stirrups	extensive	As in C	As in C
Spalling	-------	some	extensive	In some areas steel is no more in contact with concrete	As in D
Loss in steel section	---------	~5%	~10%	~25%	Some stirrups broken Main bars buckled
Deflections	---------	--------	---------	possible	apparent

Now, the last step in the estimation of t_{sp} consists of calculating the number of years needed to reach the assumed deterioration level (i.e., 10% loss in steel section from the initiation period). Therefore, the t_{sp} can be estimated as (using Eq. (6.5)):

$$t_{sp} = \frac{\bullet(0) - \bullet(t)}{0.0116 \bullet i_{corr}} \tag{6.11}$$

where,

t_{sp}	=	Stable propagation period (in years)
$\phi(0)$	=	initial diameter of the rebar (in mm)
$\phi(t)$	=	net diameter of the rebar (in mm) after an assumed 10% section loss
i_{corr}	=	average value of corrosion current density ($\mu A/cm^2$)
α	=	pitting factor (for uniform corrosion, $\alpha = 2$; pitting corrosion, $\alpha = 5$ to 10) (Rodriguez et al., 2005)

Knowing the values of t_i and t_{sp}, the total service life (t_s) can be estimated using Eq. (1).

Numerical computation of different cases

Case 1, OPC-0.57 concrete:

Corrosion initiation period = 2.1 years (from Table 6.3); Allowable reduction in rebar cross section = 10% (net diameter = $\sqrt{0.9 \times \text{original diameter}}$) and $\alpha = 6$. Using Eq. (6.11), the service life is estimated as

  (1) 8.1 years when i_{corr}: 1 $\mu A/cm^2$
  (2) 2.7 years when i_{corr}: 10 $\mu A/cm^2$ and
  (3) 2.2 years when i_{corr}: 100 $\mu A/cm^2$

Case 2, PPC-0.57 concrete:

Corrosion initiation period = 4.2 years; Allowable reduction in rebar cross section: 10% (net diameter = $\sqrt{0.9 \times \text{original diameter}}$) and $\alpha = 6$. Using Eq. (6.11), the service is life estimated as

  (1) 20.5 years when i_{corr}: 1 $\mu A/cm^2$
  (2) 5.8 years when i_{corr}: 10 $\mu A/cm^2$ and
  (3) 4.6 years when i_{corr}: 100 $\mu A/cm^2$

The above trends (initiation and propagation period) are in line with the service life predictions made by Andrade et al. (1990). The corrosion initiation, stable propagation and service life of typical selected concretes for 10% loss in section are presented in the following Tables 6.6, 6.7 and 6.8 for different field corrosion rates (i.e., low: 1 $\mu A/cm^2$, medium: 10 $\mu A/cm^2$ and high: 100 $\mu A/cm^2$).

Table 6.6: Service life of concretes when field i_{corr} value of OPC-0.57 concrete is 1 µA/cm^2

Concrete	Corrosion initiation period (t_i), years	Stable propagation period (t_{sp}), years	Service life (t_s), years
OPC-0.57	2.1	6.0	8.1
PPC-0.57	4.2	16.3	20.5
OPC-SP-0.57	2.4	6.3	8.7
PPC-SP-0.57	5.6	20.0	25.6
OPC-CNI-0.57	2.3	2.7	5.0
OPC-CNI-SP-0.57	2.5	2.7	5.2
OPC-SP-0.47	4.3	9.1	13.4
PPC-SP-0.47	17.2	27.4	44.6
PPC-SP-0.37	34.2	27.4	61.6

Table 6.7: Service life of concretes when field i_{corr} value of OPC-0.57 concrete is 10 µA/cm^2

Concrete	Corrosion initiation period (t_i), years	Stable propagation period (t_{sp}), years	Service life (t_s), years
OPC-0.57	2.1	0.6	2.7
PPC-0.57	4.2	1.6	5.8
OPC-SP-0.57	2.4	0.6	3.0
PPC-SP-0.57	5.6	1.9	7.5
OPC-CNI-0.57	2.3	0.2	2.5
OPC-SP-CNI-0.57	2.5	0.2	2.7
OPC-SP-0.47	4.3	0.9	5.2
PPC-SP-0.47	17.2	2.7	19.9
PPC-SP-0.37	34.2	2.7	36.9

Table 6.8: Service life of concretes when field i_{corr} value of OPC-0.57 concrete is 100 µA/cm^2

Concrete	Corrosion initiation period (t_i), years	Stable propagation period (t_{sp}), years	Service life (t_s), years
OPC-0.57	2.1	0.1	2.2
PPC-0.57	4.2	0.2	4.6
OPC-SP-0.57	2.4	0.1	2.3
PPC-SP-0.57	5.6	0.2	5.8
OPC-CNI-0.57	2.3	0.1	2.4
OPC-SP-CNI-0.57	2.5	0.1	2.6
OPC-SP-0.47	4.3	0.1	4.4
PPC-SP-0.47	17.2	0.3	17.5
PPC-SP-0.37	34.2	0.3	34.5

From the above, it can be said that the service life of RC structures subjected to chloride induced corrosion depends largely on the chloride diffusion and aggressiveness of the exposure conditions. Figure 6.4 shows the plot of service life of OPC-0.57 concrete and PPC-0.57 concretes. The service life (t_s) of PPC-0.57 concrete is nearly 2.5 times at the low corrosion rate (of 1 µA/cm^2) and nearly 2 times at the high corrosion rate (of 100 µA/cm^2), when compared to that of OPC-0.57 concrete for similar exposure conditions.

The service life estimations reveal that PPC concrete will have better corrosion resistance than OPC concrete due to the delayed corrosion initiation period and decreased corrosion rate in the propagation period. This can be attributed to the higher resistivity and pore refinement due to secondary hydration in the PPC concrete, as discussed earlier. It can be observed that at the low corrosion rate, the total service life is contributed by both initiation and propagation periods whereas at the high corrosion rates, the total service life is contributed by initiation period only. Similar observations have been made for other w/c of OPC and PPC concretes. Figure 6.5 presents typical plots of service lives of OPC, OPC-SP, OPC-CNI and OPC-SP-CNI concretes for w/c = 0.57. Among all the OPC concretes, the concrete with SP showed better performance; service life is about 10% more than that of control concrete (OPC alone). Similar observations have been made for PPC concretes also; Figure 6.6 gives

the plot of service lives of the PPC-SP concrete for different w/c. It can also be seen that that the service life of PPC-SP-0.37 concrete is nearly 6 times more than that of PPC-SP-0.57 concrete mainly due to the lower diffusion values at lower w/c. Compared to the service life of concrete with OPC-0.57, the service life of OPC-CNI-0.57 is lower at 'low' and 'medium' corrosion rates.
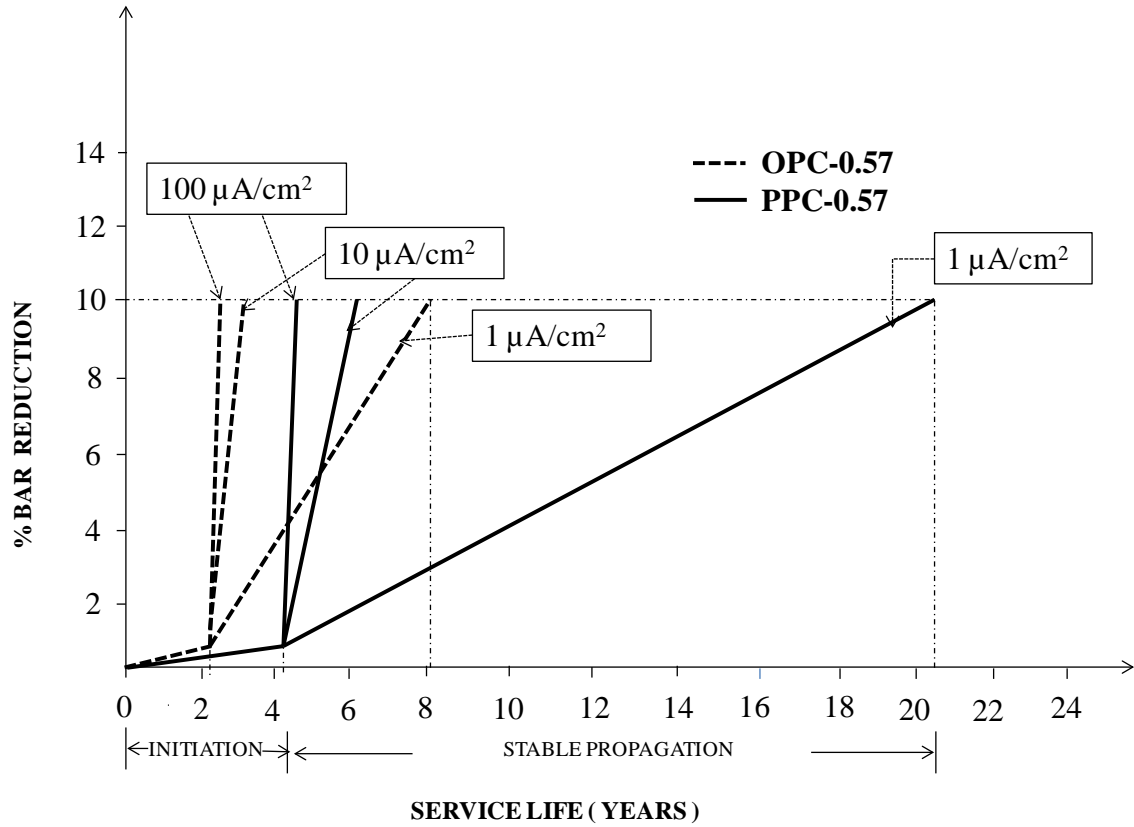
Figure 6.4: Service life of OPC-0.57 and PPC-0.57 concretes for low, medium and high i_{corr} values
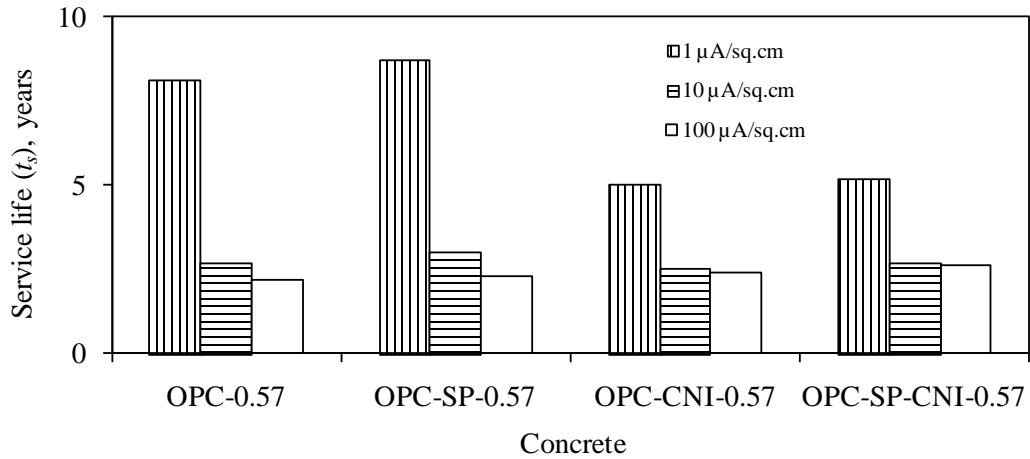
Figure 6.5: Comparison of service lives of different OPC concretes for w/c = 0.57
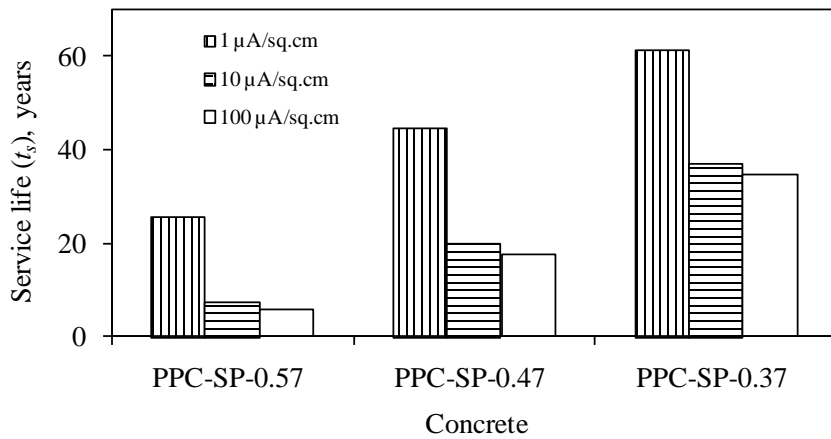
Figure 6.6: Comparison of service lives of PPC-SP concretes for different w/c

6.4. Sensitivity of service life on x, D_c, C_{tc}, C_0

A reliable estimation of service life of RC structures exposed to chloride environment is important for the selection of durable materials for new construction and for the efficient maintenance of existing structures. As described in the previous sections, the service life, in the present study is estimated as the sum of t_i and t_{sp}. The estimation of t_i is based on the Fickian process of diffusion and the governing parameters include x, D_c, C_{tc}, and C_0 assuming the presence of moisture and oxygen for the corrosion to proceed. In the estimation of t_{sp}, i_{corr} is considered as the only variable and that it is indirectly proportional to t_{sp}.

153

Among the variables x, D_c, C_{tc}, and C_0, x is mainly based on specifying a minimum concrete cover as per the design codes. It varies with the severity of the environmental exposure and depends on the quality control and workmanship during construction. There is a considerable level of uncertainty among the other variables. This is due to aging and heterogeneity of concrete, severity of exposure that varies with time and uncertainty in threshold chloride level that depends on type of binder, type of rebar, test methods, etc. Therefore, sensitivity analysis has been carried out on the variables x, D_c, C_{tc}, and C_0 in the estimation of t_i. Figures 6.7 - 6.11 show the plots of t_i vs. D_c for different x values, t_i vs. D_c for different C_{tc} values, t_i vs. D_c for different C_0 values, t_i vs. C_{tc} for different D_c values, and t_i vs. C_0 for different D_c values, respectively.

It can be seen from Figure 6.7 that for the given D_c, as x increases, t_i also increases. Considering 50% variation in x value (in the present study, it is assumed as 20 mm), for the given D_c value equal to 1×10^{-13} mm^2/sec, the maximum variation in t_i is about 125%. From Figure 6.8, it can be seen that as the C_{tc} value increases, the t_i also increases. It can also seen that t_i is more sensitive to D_c up to certain range (i.e., from 5×10^{-14} to 5×10^{-13} mm^2/sec, beyond which t_i is not very sensitive. Considering a 50% variation in C_{tc} value (in the present study, it is assumed as 0.4% weight of cement), for the given D_c value equal to 1×10^{-13} mm^2/sec, the maximum variation in t_i is about 23.5%.

Figure 6.9 shows the plot of t_i vs. D_c with different C_0 values. As observed previously, t_i is more sensitive to D_c for the range of values from 5×10^{-14} to 5×10^{-13} mm^2/sec, beyond which t_i is not very sensitive. For the given D_c value equal to 5×10^{-14} mm^2/sec, when C_0 is equal to 0.1% (i.e., far from marine environment), t_i is about 280 years and when C_0 is equal to 0.5%, t_i is about 47 years. Also, when the C_0 value increases from 0.5% to 2.0%, the decrease in t_i is from 47 to 25 years. That means, for the given value of D_c, t_i is more sensitive when the C_0 is in the range from 0.1% to 0.5%. Beyond 0.5% of C_0, the variation in t_i is very small (see also from Figure 6.10). Considering a 50% variation in C_0 value (in the present study, it is assumed as 1%), for the given D_c value equal to 1×10^{-13} mm^2/sec, the maximum variation in t_i is about *42%*. From Figure 6.11, it can be observed that for the given D_c, t_i is almost linearly proportional to C_{tc}. Assuming D_c value equal to 1.5×10^{-13} mm^2/sec; considering a 50% variation in D_c value, for the given C_{tc} equal to 0.4% weight of cement, the

maximum variation in t_i is about 50%. From the sensitivity analysis, it can be said that the corrosion initiation period is more sensitive to concrete cover depth than D_c and more sensitive to C_0 than C_{tc}. Similar observations have also been reported by Khatri and Sirivivatnanon (2004).
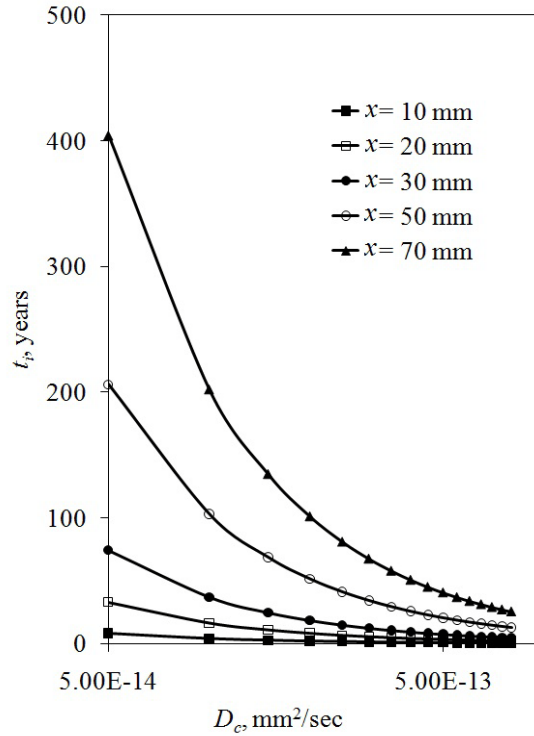
Figure 6.7: Plot of t_i vs. D_c with different x values
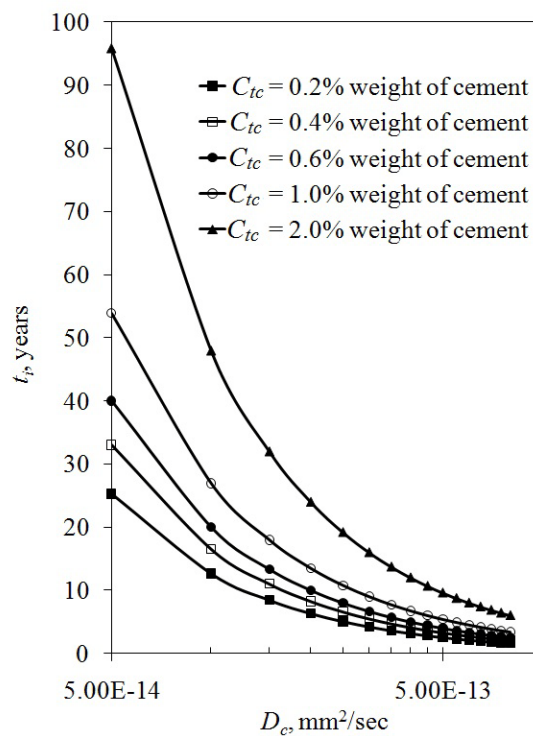
Figure 6.8: Plot of t_i vs. D_c with different C_{tc} values
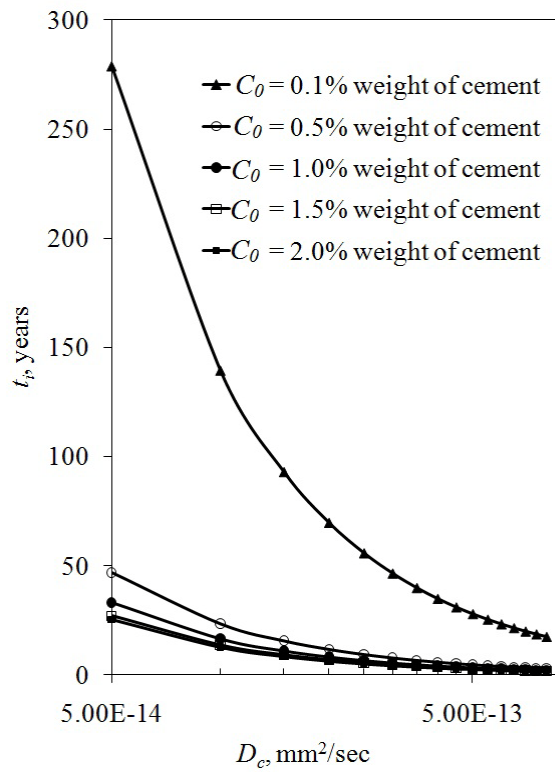
Figure 6.9: Plot of t_i vs. D_c with different C_0 values
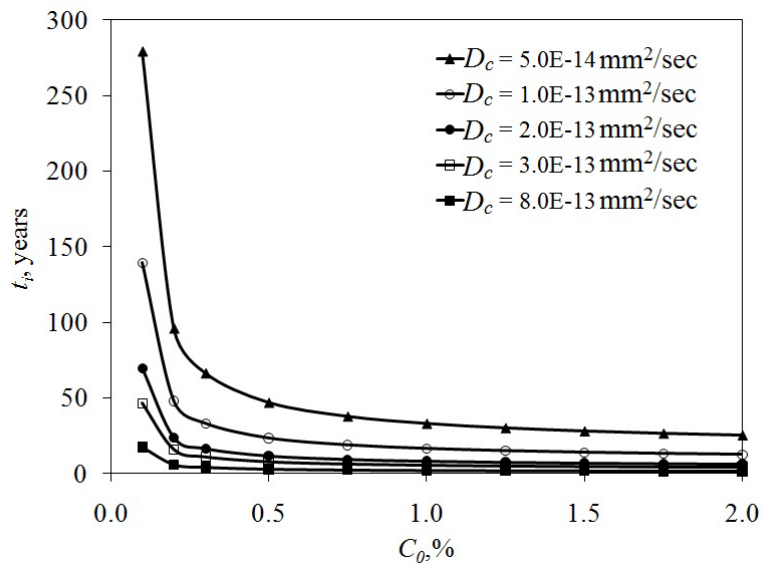
Figure 6.10: Plot of t_i vs. C_0 with different D_c values
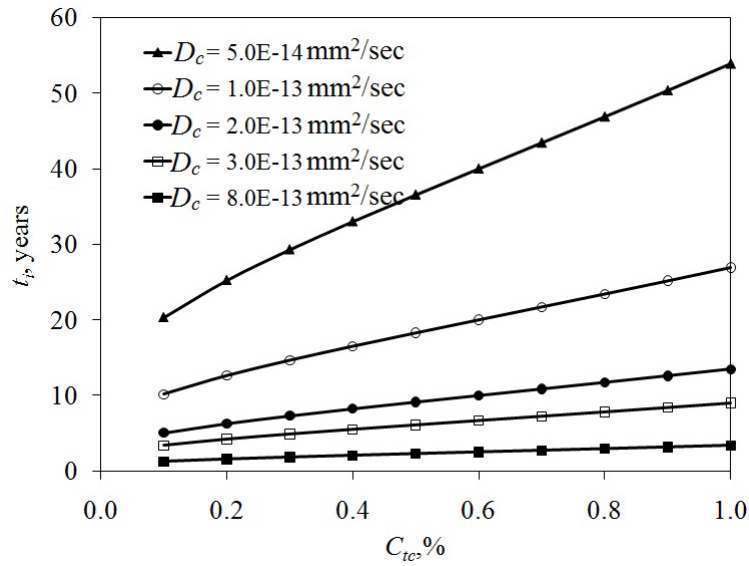
Figure 6.11: Plot of t_i vs. C_{tc} with different D_c values

6.5. Effect of cracking on the service life

The parametric studies carried out in the previous section on service life estimations are for uncracked concretes only. Nevertheless, the proposed methodology can be extended to cracked concrete also, provided the values of the influencing parameters considered, i.e., D_c and i_{corr} of cracked concrete are available. In general, it can be said that the diffusion of chloride ions will be much faster in cracked concrete and hence D_c value of cracked concrete will always be higher (which again depends on the crack geometry, intensity of mechanical loading, exposure conditions, etc.) than that of uncracked concrete. In other words, the t_i will be shorter in the case of cracked concrete. Similarly, the t_{sp} will be shorter, since the gravimetric weight loss, as observed previously is more in cracked concrete.

D_c in cracked concrete - corrosion initiation period (t_i)

Wang et al. (1997) and Aldea et al. (1999a; 1999b) studied the relationship among cracking, water permeability and diffusion. It was reported that concrete permeability as well as diffusion increases with crack width. Wang et al. (1997) stated that a crack opening displacement (COD) smaller than 50 microns under loading had little effect on concrete permeability. However, when COD is increased from 50 microns to 200 microns (0.2 mm) under loading, the permeability increases rapidly. Beyond 200 microns, the rate of increase of water permeability became steady. It appears that

157

there is no quantitative relationship established yet between crack width and diffusion. Many researchers suppose that there is a certain value of crack width known as 'the threshold crack width', below which, the cracks have little influence on transport, mainly because of the self healing effects inside cracks (Jacobsen et al., 1996). According to Wang et al. (1997) and Jang et al. (2011), the threshold crack width for water permeation is around 50 and 80 microns, respectively, beyond which, the increase in crack width increases the diffusion coefficient. Very recently, to evaluate the crack effect on chloride diffusion, Park et al. (2012) performed accelerated migration tests on concrete specimens with various crack widths. The 28-day compressive strength of concrete used was 35 MPa with a D_c value of about 6×10^{-12} m^2/sec. They reported that D_c value increases with an increase in crack width, and that the ratios between the values for cracked and uncracked or sound concrete are 23.5, 38.4, 70.6 and 145.4 for the crack widths of 0.1, 0.2, 0.3 and 0.4 mm, respectively.

In the present study, the D_c values of cracked concretes have not been evaluated and therefore, the above available information is used to estimate the t_i of the cracked OPC-0.57 concrete. The ratios of 38.4 and 145.4 for 0.2 mm and 0.4 mm crack widths are used to get the D_c values for the present cracked OPC-0.57 concrete. Based on this, t_i values are estimated and presented in Table 6.9 (t_i of uncracked concrete was already presented in Table 6.3 and has been repeated here, as needed, for comparison purposes). It can be seen that the corrosion initiation period is almost zero for both 0.2 and 0.4 mm crack widths. In other selected concretes also, similar trends of D_c can be expected between the cracked and uncracked concretes and Table 6.10 shows the t_i values for other selected cracked concretes.

Table 6.9: Approximate t_i values for 0.2 mm and 0.4 mm crack widths in OPC concrete

Concrete	Diffusion coefficient, D_c (mm^2/year) ; [m^2/sec]	Corrosion initiation period (t_i), years
OPC-0.57	24; [7.67×10^{-13}]	2.1
OPC-0.57-0.2	2927; [9.28×10^{-11}]	0.06
OPC-0.57-0.4	11038; [3.5×10^{-10}]	0.01

Table 6.10: t_i values for other selected concretes with crack widths of 0.2 mm and 0.4 mm

Concrete	t_i, years	Concrete	t_i, years
PPC-0.57-0.2	0.11	PPC-SP-0.57-0.2	0.15
PPC-0.57-0.4	0.03	PPC-SP-0.57-0.4	0.04
OPC-SP-0.57-0.2	0.06	OPC-SP-0.47-0.2	0.11
OPC-SP-0.57-0.4	0.02	OPC-SP-0.47-0.4	0.03
OPC-CNI-0.57-0.2	0.06	PPC-SP-0.47-0.2	0.45
OPC-CNI-0.57-0.4	0.02	PPC-SP-0.47-0.4	0.12
OPC-SP-CNI-0.57-0.2	0.06	PPC-SP-0.37-0.2	0.89
OPC-SP-CNI-0.57-0.4	0.02	PPC-SP-0.37-0.4	0.24

i_{corr} in cracked concrete

i_{corr} in cracked concrete

Some researchers argue that crack width has no influence on corrosion rate, whereas the presence of cracks themselves has an influence on it (Beeby, 1983; François and Arliguie, 1999). This may be true for short term corrosion. There is an another view point that for long term corrosion process that there could be healing of cracks due to corrosion products and as the time proceeds, the aggressive species penetrate the concrete in the uncracked zone leading to the same corrosion in the crack zone or uncracked zones. As discussed in previous chapters, it is observed that the presence of crack and crack width affects the corrosion of RC members since the corrosion cracks were first developed in the vicinity of flexural cracks (i.e., prior to corrosion). In a recent study, François et al. (2012) stated that irrespective of crack width (i.e., even with a crack width of 20 microns), chlorides reach the reinforcement. The corrosion cracks generated later gradually minimize the influence of the pre-cracks. However, here again, the magnitude of damage at steel-concrete interface depends on the level of stress transfer between the reinforcement and concrete and also the crack width. Therefore, it can be said that corrosion rate or in this context, the i_{corr} will be higher in cracked concrete, thereby reducing t_{sp} (that again depends on factors such as crack geometry, intensity of mechanical loading, exposure conditions, etc.).

Table 6.11 presents the computed i_{corr} values of selected cracked concrete specimens. The i_{corr} value of OPC-0.57-0.2 concrete is almost twice that of the i_{corr} value of PPC-0.57-0.2. The i_{corr} value of OPC-CNI-0.57-0.2 concrete is nearly 1.5 times that of that of the i_{corr} value of OPC-0.57-0.2. It is generally observed that the increase in the i_{corr} values between the uncracked (refer Table 6.4 for uncracked concretes) to 0.2 mm crack width specimens is observed to be higher than between the 0.2 mm and 0.4 mm crack width specimens. This could be due to the effect of macrocell corrosion. It is further observed that the reduction in diameter of rebar (i.e., due to localized corrosion/pitting) is higher in the case of concretes with higher crack width.

Table 6.11: Laboratory i_{corr} values for the selected pre-cracked concretes

Concrete	i_{corr} ($\mu A/cm^2$)	Concrete	i_{corr} ($\mu A/cm^2$)
OPC-0.57-0.2	1258	OPC-SP-CNI-0.57-0.4	1935
OPC-0.57-0.4	1385	PPC-SP-0.57-0.2	573

PPC-0.57-0.2	631	PPC-SP-0.57-0.4	700
PPC-0.57-0.4	731	OPC-SP-0.47-0.2	854
OPC-SP-0.57-0.2	1205	OPC-SP-0.47-0.4	972
OPC-SP-0.57-0.4	1317	PPC-SP-0.47-0.2	513
OPC-CNI-0.57-0.2	1884	PPC-SP-0.47-0.4	663
OPC-CNI-0.57-0.4	1938	PPC-SP-0.37-0.2	467
OPC-SP-CNI-0.57-0.2	1906	PPC-SP-0.37-0.4	515

Numerical computation for typical 0.2 and 0.4 mm cracked concretes

Case 1, <u>OPC-0.57 concrete with 0.2 mm crack width</u>:

Corrosion initiation period = 0.06 years (from Table 6.9); Allowable reduction in rebar cross section = 10% (net diameter = $\sqrt{0.9 \times \text{original diameter}}$) and • = 8. Using Eq. (6.11), the service life is estimated as

  (4) 4.6 years (1679 days) when i_{corr}: 1 µA/cm^2

  (5) 186 days when i_{corr}: 10 µA/cm^2 and

  (6) 36 days when i_{corr}: 100 µA/cm^2

<u>OPC-0.57 concrete with 0.4 mm crack width</u>:

Corrosion initiation period = 0.01 years (from Table 6.9); Allowable reduction in rebar cross section = 10% (net diameter = $\sqrt{0.9 \times \text{original diameter}}$) and • = 10. Using Eq. (6.11), the service life is estimated as

  (1) 3.6 years (1314 days) when i_{corr}: 1 µA/cm^2

  (2) 135 days when i_{corr}: 10 µA/cm^2 and

  (3) 17 days when i_{corr}: 100 µA/cm^2

Case 2, <u>PPC-0.57 concrete with 0.2 mm crack width</u>:

Corrosion initiation period = 0.11 years (from Table 6.10); Allowable reduction in rebar cross section: 10% (net diameter = $\sqrt{0.9 \times \text{original diameter}}$) and • = 8. Using Eq. (6.11), the service is life estimated as

(4) 12.3 years (4489 days) when i_{corr}: 1 μA/cm^2

(5) 485 days when i_{corr}: 10 μA/cm^2 and

(6) 84 days when i_{corr}: 100 μA/cm^2

PPC-0.57 concrete with 0.4 mm crack width:

Corrosion initiation period = 0.03 years (from Table 6.10); Allowable reduction in rebar cross section: 10% (net diameter = $\sqrt{0.9 \times \text{original diameter}}$) and • = 10. Using Eq. (6.11), the service is life estimated as

(1) 9.8 years (3577 days) when i_{corr}: 1 μA/cm^2

(2) 365 days when i_{corr}: 10 μA/cm^2 and

(3) 47 days when i_{corr}: 100 μA/cm^2

It can be seen from the above calculations, whatever is the crack width and severity of exposure, the PPC concrete performed better in terms of protecting the steel reinforcement subjected to corrosion, even with 0.2 and 0.4 mm crack widths.

6.6. Summary

Based on the review, experimental studies, analysis and interpretation, the following conclusions have been drawn:

- In the present study, the service life is (t_s) assumed as the sum of initiation (t_i) and stable propagation periods (t_{sp}), where, loss in steel section of 10% is taken as the end of stable propagation period (t_{sp}).

- The experimentally evaluated apparent diffusion coefficient (D_c) may not be directly comparable to non-steady state diffusion coefficients or those used in service life predictions where chlorides diffuse in a non-steady manner or are transported by absorption. Nevertheless, the D_c value can be used to estimate the relative t_i of different concretes. t_{sp} is estimated based on the experimentally computed i_{corr} values.

- When the i_{corr} values are low to medium, the service life is contributed by both t_i and t_{sp}. However, at higher i_{corr} values (i.e., severe/extreme chloride exposures), the contribution towards service life is mainly by t_i only.

- For concretes with SP (OPC-SP-0.57 and PPC-SP-0.57), there is an improvement in service life of about 7% to 25% corresponding to the respective control concretes (OPC and PPC concretes).

- The service life of PPC based concrete (PPC-0.57) is nearly twice that of the service life of corresponding OPC based concretes (OPC-0.57). The service life of PPC-SP-0.47 concrete is nearly thrice and PPC-SP-0.37 concrete is nearly 6 times that of the service life of PPC-SP-0.57 concrete.

- From the sensitivity analysis, it is observed that t_i is more sensitive to concrete cover depth than D_c and more sensitive to C_0 than C_{tc}.

- Attempts have been made to reasonably estimate the t_i and t_{sp} values for cracked concretes and observed that whatever is the crack width and severity of exposure, the PPC concrete performed better in terms of protecting the steel reinforcement subjected to corrosion, even with 0.2 and 0.4 mm crack widths.

CHAPTER 7

CONCLUSIONS AND RECOMMENDATIONS FOR FURTHER RESEARCH

7.1. General Conclusions

Overall, the study was able to improve the understanding of the factors that influence the corrosion of steel rebars in concrete, especially in the chloride induced corrosion. The study was also improved the understanding of the influence of cracking on rebar corrosion. The salient conclusions that correspond to the fulfilment of the principal objectives of the present study are given below.

- From the extensive experimental study, it is evident that PPC concretes perform significantly better than OPC concretes not only in uncracked condition but also in pre-cracked conditions, when subjected to a chloride-rich environment. This is mainly due to the lower chloride ion penetrability and higher resistivity of PPC concrete.

- The results obtain also reiterate that better quality concretes (i.e., with lower w/c and better workability) give higher resistance to chloride-induced corrosion than poorer quality concretes, even under cracked conditions.

- The present study confirmed that cracks can cause localised (macrocell) corrosion of rebars within the concrete. The rebar corrosion initiates more rapidly in cracked concrete confirming that cracking influences the corrosion process significantly. The study also confirmed that crack width affects the corrosion behaviour of RC members, and as the crack width increases, localised corrosion is more dominant than uniform corrosion, causing pitting of rebars.

- The rebar corrosion is lower in concrete with lower water to cement ratios, as expected. This is observed both in uncracked and pre-cracked concretes and this is mainly due to the lower permeability and electrical conductivity of concrete.

- Experimental results show that concrete with polycarboxylic ether based superplasticizer (PCE SP) performed marginally better in terms of corrosion

resistance of rebars, when compared to that of control concrete. This is in addition to improving fresh state properties, such as workability. This may be due to better dispersion of cement particles and refinement of pore structure.

- The concretes with calcium nitrite inhibitor (CNI) did not show any corrosion inhibition effect, emphasizing the need for further detailed investigation before arriving at general conclusions. The possible reasons could be due to inadequate/inappropriate dosage, higher conductivity of the pore solution and low concrete resistivity. It could also be that the accelerated corrosion test parameters used here are not appropriate for evaluating the performance of the CNI in concrete.

- The estimated relative service lives of PPC concretes are more than twice that of the service lives of corresponding OPC concretes. This is mainly due to the lower chloride diffusion coefficient and higher resistivity of PPC concrete.

- The simple U-shaped specimen with pre-cracks was found to be useful for the comparative evaluation of corrosion resistance of different concretes.

- In the present study, impressed current has been used to compare the relative corrosion resistance performance of different concretes in the absence and presence of cracks by accelerating the corrosion process. It is, nevertheless, clear that the consequent corrosion processes are different from that under natural environment.

7.2. Specific Conclusions

The specific conclusions derived from the experimental investigations on corrosion resistance performance of concretes with PCE SP and CNI under cracked conditions can be classified under the following

7.2.1. Influence of cement type

- The 28-day compressive strengths of PPC concretes are similar to that of OPC concretes, whereas the split tensile and flexural strengths are higher than those of the corresponding OPC concretes. The 28-day sorptivity values of PPC concretes are lower than that of OPC concretes, possibly because of pore refinement.

- The chloride ion penetrability (through the RCPT test) of PPC is nearly one-third than that of the corresponding OPC concrete indicating better resistance performance in chloride environment.

- Electrochemical measurements, such as half-cell potential and resistivity, indicate a delay in the onset of corrosion in PPC concretes even under cracked conditions compared to that of corresponding OPC concretes. This can be attributed to the higher resistance to the corrosion current and lower penetrability because of pore refinement.

- The overall improvement of gravimetric weight loss in the rebars within PPC concretes with respect to corresponding OPC concretes is in the range of about 2.6 to 2.7 in the case of uncracked concretes and about 1.5 to 2.0, in the case of cracked concretes. The results show that the reduction in rebar diameter (i.e., caused by pitting) is more for OPC concretes compared to that of PPC concretes.

- For the given exposure conditions, the corrosion induced crack widths of PPC concretes are much lower than those of the corresponding OPC concretes. Also, for the given rebar weight loss, the corrosion induced crack width is lower in the case of PPC concrete.

7.2.2. Influence of crack width

- In the pre-cracked specimens, rust stains are first observed at the pre-cracks caused by macrocell corrosion, whereas in the case of uncracked specimens, more uniform corrosion is observed. This shows that rebar corrosion initiates more rapidly in cracked concrete confirming that cracking influences the corrosion process significantly.

- The corrosion induced crack width is generally more in cases of uncracked specimens compared to that of pre-cracked specimens. This is attributed to more egress of corrosion products through crack openings.

- The increase in weight loss is observed to be higher between the uncracked to 0.2 mm crack width specimens than between the 0.2 mm and 0.4 mm crack width specimens. This implies that the presence of the crack influences corrosion more than the crack width itself. Nevertheless, it is observed that the

domination of localized and pitting corrosion as the crack width increases and which is more dangerous compared to uniform corrosion.

7.2.3. Influence of PCE SP and CNI

- The 28 day compressive strengths and RCPT values of concretes with PCE SP are nearly similar to that of respective OPC and PPC concretes. Nevertheless, there is an improvement in durability parameters, such as reduction in water absorption and sorptivity.

- The gravimetric weight loss results show that concrete with PCE SP performed marginally better compared to that of control concrete even under cracked condition. This is in addition to improving fresh state properties such as workability. This may be due to better dispersion of cement particles and refinement of pore structure.

- The concretes with PCE SP are relatively performed better against corrosion resistance when compared to that of the corresponding OPC and PPC concretes alone.

- The 28 day compressive strengths of concretes with CNI are lower; about 20% and 10% compared to that of respective OPC and PPC concretes.

- The chloride ion penetrability (through the RCPT test) of concretes with CNI is higher; 1.6 to 1.8 and 2.5 to 3 times higher than that of the corresponding OPC and PPC concretes. This may be due to high ionic nature of CNI, which causes more negative charge to pass through the concrete.

- The resistivity values of concrete with CNI are significantly lower when compared to that of the respective OPC and PPC concretes. The half-cell potentials of concrete with CNI are initially less negative compared to that of respective concretes without CNI but, however, become more negative in a very short time.

- The corrosion current is more in concretes with CNI compared to that of their respective OPC and PPC concretes. The gravimetric weight loss of rebars in concrete with CNI is higher than that of the concretes without CNI. Visual observation, total charge passed and gravimetric weight loss (% reduction in weight) reveal that concrete with CNI did not show any corrosion inhibition effect. The reason for which has to be investigated with further specific studies.

166

7.2.4. Relative service life estimation

- The total service life (t_s) is assumed as the sum of initiation (t_i) and stable propagation periods (t_{sp}), where, the loss in steel section of 10% is taken as the end of stable propagation period (t_{sp}). The t_i and t_{sp} are estimated based on the experimentally evaluated diffusion coefficient (D_c) and the computed corrosion current density (i_{corr}) values, respectively. When the i_{corr} values are low to medium, the service life is contributed by both t_i and t_{sp}. However, at higher i_{corr} values (i.e., severe/extreme chloride exposures), the contribution towards service life is mainly by the t_i only.

- In uncracked conditions, the service life of PPC based concrete is nearly twice that of the service life of corresponding OPC based concretes. For concretes with SP, there is an improvement in service life of about 7% to 25% corresponding to the respective control concretes (OPC and PPC concretes).

- The service life of PPC-SP-0.47 concrete is nearly 3 times and PPC-SP-0.37 concrete is nearly 6 times that of the service life of PPC-SP-0.57 concrete. The service life OPC-CNI-0.57 is lower compared to that of OPC-0.57 at the assumed 'low' and 'medium' corrosion rates, which needs to be investigated further.

- From the sensitivity analysis, it is observed that t_i is more sensitive to concrete cover depth than D_c and more sensitive to C_0 than C_{tc}.

- Attempts have been made to reasonably estimate the t_i and t_{sp} values for cracked concretes and it is observed that whatever is the crack width and severity of exposure, the PPC concrete performed better in terms of protecting the steel reinforcement subjected to corrosion, even with 0.2 and 0.4 mm crack widths.

7.3. Recommendations for Further Research

From the present study, it is clear that the corrosion resistance performance of RC is affected by many parameters, such as type of binder, water to cement ratio, use of chemical and mineral admixtures, etc. Continued research on the following aspects can give better understanding, and be of more use to researchers and Indian construction industry:

- The present situation of construction industry needs the use of different chemical admixtures for most applications. Influence of these admixtures on corrosion resistance performance needs further attention.

- Also, there is a huge potential of using different inhibitors such as mixed/migrating corrosion inhibitors. Performance of these needs to be investigated for different concretes with and without the presence of cracks.

- The accelerated corrosion studies in chloride environment reveal that concrete with CNI did not show any corrosion inhibition effect. The possible reasons could be due to inadequate/inappropriate dosage. It could also be that the accelerated test parameters used here may not be the most appropriate for evaluating the performance of the CNI in concrete. The present study emphasizes the need for detailed investigation with lower impressed voltages and also by following ASTM G 109 methodology of ponding exposure.

- The basic durability and long term corrosion resistance studies may be extended to concretes with high volumes of fly ash, slag and other wastes in cracked concretes.

- An empirical service life estimation methodology is proposed beyond t_i and attempts have been made to estimate the t_{sp} also. In the t_{sp} estimation, the loss in steel section of 10% is taken as the end of service life. The t_i and t_{sp} are estimated based on the experimentally evaluated D_c and the computed i_{corr} values, respectively. However, the chloride threshold concentration (C_{tc}), the surface chloride concentration (C_0), the rebar type etc. are only assumed, and the actual values may influence the t_i. Therefore, further studies are needed for the reliable estimation of both initiation and propagation periods.

REFERENCES

ACI 201.1R-92 (2010) *Guide for making a condition survey of concrete in service.* ACI Publication, USA.

ACI 201.2R-08 (2010) *Guide to durable concrete.* ACI Publication, USA.

ACI 211.1-91 (2010) *Standard practice for selecting proportions for normal, heavyweight and mass concrete*, ACI Publication, USA.

ACI 222R-01 (2010) *Protection of metals in concrete against corrosion*, ACI Publication, USA.

ACI 224.1R-07 (2010) *Control of cracking in concrete structures.* ACI Publication, USA.

ACI 318-08 (2010) *Building Code Requirements for Structural Concrete and Commentary.* ACI Publication, USA.

ACI 364.1R-07 (2010) *Guide for evaluation of concrete structures before rehabilitation.* ACI Publication, USA.

ACI 365.1R (2010) *Service life prediction – State of the art report*, ACI Publication, USA.

Ahmad, S. (2003) Reinforcement corrosion in concrete structures, its monitoring and service life prediction – a review. *Cement and Concrete Composites*, **25**, 459-471.

Ahmad, S., Bhattacharjee, B., Wason, R. (1997) Experimental service life prediction of rebar corroded reinforced concrete structure. *ACI Materials Journal*, **94 (4)**, 311-316.

Ahmad, S. (2009) Techniques for inducing accelerated corrosion of steel in concrete. *The Arabian Journal for Science and Engineering*, **34(2C)**, 95-104.

Al-Amoudi, O.S.B., Maslehuddin, M., Lashari, A.N., and Almusallam, A.A. (2003) Effectiveness of corrosion inhibitors in contaminated concrete. *Cement and Concrete Composites*, **25**, 439-449.

Aldea, C. M, Shah, S. P., and Karr, A. (1999a) Permeability of cracked concrete. *Materials and Structures,* **32**, 370-376.

Aldea, C. M, Shah, S. P., and Karr, A. (1999b) Effect of cracking on water and chloride permeability on concrete. *Journal of Materials in Civil Engineering, ASCE,* **11 (3)**, 181-187.

Alonso, C., Andrade, C., Rodriguez, J., and Diez, J. M. (1998) Factors controlling cracking of concrete affected by reinforcement corrosion. *Materials and Structures*, **31**, 435-441.

Alonso, C., Andrade, C., Castellote, M., and Castro, P. (2000), Chloride Threshold Values to Depassivate Reinforcing Bars Embedded in a Standardized OPC Mortar. *Cement and Concrete Research,* **30 (7)**, 1047-1055.

Amara, L., Al-Qadi and Diefenderfer, B. K. (2000) Effects of nitrite based corrosion inhibitor on concrete's rapid chloride permeability values and its dielectric properties. *ACI Materials Journal*, **97 (4)**, 465-471.

Amey, S.L., Johnson, D.A., Miltenberger, M.A., and Farzam, H. (1998) Prediction of service life of concrete marine structures: An environmental methodology. *ACI Structural Journal*, **95 (2)**, 205-214.

Andrade, C., Alonso, C., and González, J. A. (1986) Some laboratory experiments on the inhibitor effect of sodium nitrite on reinforcement corrosion. *Cement Concrete and Aggregates*, **8**, 110-116.

Andrade, C., Alonso, M. A. and Gonzalez, J. A. (1990) An initial effort to use the corrosion rate measurements for estimating rebar durability. pp. 29-37. In **Berke, N.S., Chaker, V. and Whiting, D.,** (eds.) *Corrosion rates of steel in concrete*. ASTM STP 1065, Philadelphia, 1990.

Andrade, C. (1993) Calculation of chloride diffusion coefficients in concrete from ionic migration measurements. *Cement and Concrete Research*, **23**, 724-742.

Andrade, C. and Alonso, C. Progress on design and residual life calculation with regard to rebar corrosion of reinforced concrete. pp. 152-164. In **Berke, N. S., Escalante, C., Nmai, C. K., and Whiting, D.,** (eds.) *Techniques to assess the corrosion activity of steel reinforced concrete structures*, , ASTM STP 1276, West Conshohocken, PA, 1996.

Andrade, C. and Martinez, I. Advanced methods of corrosion measurement in real concrete structures. pp. 152-164. In **Helene, P., Figueiredo, E. P., Holland, T. C. and Bittencourt, R.,** (eds.) *Quality of concrete structures and recent advances in concrete materials and testing,* ACI SP 229, American Concrete Institute, Detroit, 2005.

Angst, U., Elsener, B., Larsen, C. K., Vennesland, Ø. (2009) Critical chloride content in reinforced concrete – A review. *Cement and Concrete Research*, **39**, 1122-1138.

Angst, U. and Vennesland, Ø. Critical chloride content in reinforced concrete – State of the art. pp. 311-317. In **Alexander et al. (eds.)** *Concrete repair, rehabilitation and retrofitting II*. Taylor & Francis Group, London, 2009.

Ann, K.Y., Jung H.S., Kim H.S., Kim S.S., and Moon H.Y. (2006) Effect of calcium nitrite-based corrosion inhibitor in preventing corrosion of embedded steel in concrete. *Cement and Concrete Research*, **36**, 530-535.

Ann, K. Y. and Song, H. W. (2007) Chloride threshold level for corrosion of steel in concrete. *Corrosion Science*, **49 (11)**, 4113-4133.

Anoop, M. B., Balaji Rao, K., and Appa Rao, T. V. S. R. (2003) A methodology for durability based service life design of reinforced concrete flexural members. *Magazine of Concrete Research*, 55 (3), 289-303.

Anoop, M. B., Raghuprasad, B. K., and Balaji Rao, K. (2012) A refined methodology for durability based service life estimation of reinforced concrete structural elements considering fuzzy and random uncertainties. *Computer-Aided Civil and Infrastructure Engineering*, 27 (3), 170-186.

Arya, C., and Ofori-Darko, F. K. (1996) Influence of crack frequency on reinforcement corrosion in concrete. *Cement and Concrete Research*, **26 (3)**, 345-353.

Arya, C., and Xu, Y. (1995) Effect of cement type on chloride binding and corrosion of steel in concrete. *Cement and Concrete Research,* **25 (4)**, 893-902.

ASTM C 876-09, (2009) Standard test method for Half-cell potentials of uncoated reinforcing steel in concrete. Annual book of ASTM standards, *American Society of Testing and Materials*, USA.

ASTM C 494-10a (2010) Standard Specification for Chemical Admixtures for Concrete. Annual book of ASTM standards, *American Society of Testing and Materials*, USA.

ASTM C 1202-97 (2009) Standard Test Method for electrical indication of concrete's ability to resist chloride penetration. Annual book of ASTM standards, *American Society of Testing and Materials*, USA.

ASTM E 415-99a (2005) Standard Test Method for Optical emission vacuum spectrometric analysis of carbon and low-alloy steel. Annual book of ASTM standards, *American Society of Testing and Materials*, USA.

ASTM G 1-03 (2009) Standard practice for preparing, cleaning, and evaluating corrosion test specimens. Annual book of ASTM standards, *American Society of Testing and Materials*, USA.

ASTM G 109-07 (2010) Standard test method for determining effects of chemical admixtures on corrosion of embedded steel reinforcement in concrete exposed to chloride environments. Annual book of ASTM standards, *American Society of Testing and Materials*, USA.

Ausin, V., Rodriguez, J., and Ortega, M. (1991) *Measurement of corrosion rates on R.C. Structures: A contribution to the assessment of damaged structures*, Bulletin of the International Association for Shell and spatial structures, **32 (106)**, 87-94.

Austin, S. A., Lyons, R., and Ing, M. J. (2004) Electrochemical behaviour of steel reinforced concrete during accelerated corrosion testing. *Corrosion*, **60 (2)**, 203-212.

Austroads (2000) *Service life prediction of reinforced concrete structures*, Austroads Project No. N.T&E.9813, Austroads Publication No. AP-T07/00, Sydney, Australia.

Bazant, Z. P. (1979) Physical model for steel corrosion in concrete sea structures-theory. *ASCE Journal of the Structural Division*, **105**, pp. 1137-1153.

Baroghel-Bouny, B., Nguyen, T. Q., and Dangla, P. (2009) Assessment and prediction of RC structure service life by means of durability indicators and physical/chemical models. *Cement and Concrete Composites*, **31**, pp. 522-534.

Basheer, P. A. M., and Barbhuiya, S. (2010) Pore structure and transport processes, pp. 14-34, In **Soutsos, M.** (ed.) *Concrete durability: A practical guide to the design of durable concrete structures*, Thomas Telford, London, 2010.

Beeby, A.W. (1978) Corrosion of reinforcing steel in concrete and its relation to cracking. *The Structural Engineer*, **56A (3)**, 77-81.

Beeby, A.W. (1983) Cracking, cover and corrosion of reinforcement. *Concrete International*, **5 (2)**, 35-40.

Bentur, A., Diamond, S., and Berke, S. *Steel Corrosion in Concrete: Fundamentals and Civil Engineering Practice*, E & FN Spon, 1998.

Berke, N. S. (1987) Effect of calcium nitrite and mix design on the corrosion resistance of steel in concrete (part 2 long-term results). Proceedings of *Symposium on Corrosion of Metals in Concrete, Corrosion-87*. National Association of Corrosion Engineers; Houston, p. 134.

Berke, N. S., and Rosenberg, A. Calcium nitrite corrosion inhibitor in concrete. In **Väzquez** (ed.), Proceedings of *International RILEM Symposium on Admixtures for concrete; Improvement of properties*, Barcelona, Spain, 1990.

Berke, N. S., and Sundberg, K.M. The effects of calcium nitrite and microsilica admixtures on corrosion resistance of steel in concrete. pp. 265-280. In **Whiting** (ed.), *Performance of Concrete,* ACI SP-122, Detroit, 1990.

Berke, N. S. (1991) Corrosion inhibitors in concrete. *Concrete International*, 13, 24-27.

Berke, N.S., and Weil, T.G. (1992) World-wide review of corrosion inhibitors in concrete. Proceedings of *Advances in Concrete Technology, Energy, Mines and Services*, Ottawa, Canada MSL 92-6(R), 899-924.

Berke, N. S. and Hicks, M. C. Predicting times to corrosion from field and laboratory chloride data. pp. 41-57. In **Berke, N. S., Escalante, E., Nmai, C. K., and Whiting, D.,** (eds.) *Techniques to assess the corrosion activity of steel reinforced concrete structures,* ASTM, STP 1276, American Society of Testing and Materials, USA, 1996.

Berke, N. S. Hicks, M. C., Malone, J.J., and Rieder, K.A. Holistic approach to corrosion of steel in concrete. pp. 137-155. In **Balaguru, P., Naaman, A., and Weiss, W.** (eds.) *Concrete: Material science to application*, ACI-SP-206, American Concrete Institute, Detroit, 2002.

Berke, N. S. and Hicks, M. C. (2004) Predicting long term durability of steel reinforced concrete with calcium nitrite corrosion inhibitor. *Cement and Concrete Composites*, **26**, 191-198.

Bijen, J. (1996) Benefits of slag and fly ash. *Construction and Building Materials*, **10 (5)**, 309-314.

Bilodeau, A., Sivasundaram, V., Painter, K. E., and Malhotra, V. M. (1994) Durability of concrete incorporating high volumes of fly ash from sources in the U.S. *ACI Materials Journal*, **91 (1)**, 3-12.

Bhaskar, S., Prabakar, J., Srinivasan, P., and Chellappan, A. (2006) Effect of rebar corrosion on the behaviour of bond in reinforced concrete. *The Indian Concrete Journal*, **80 (9)**, 19-26.

Bolzoni, F., Coppola, L., Goidanich, S., Lazzari, L., Ormellese, M., and Pedeferri, M. P. (2004) Corrosion inhibitors in reinforced concrete structures Part I; Preventive technique. *Corrosion Engineering Science and Technology*, **39 (3)**, 219-227.

Broomfield, J. P. *Corrosion of steel in concrete: understanding, investigation and repair,* 2nd Edition, Taylor & Francis Ltd, U.K., 2006.

Broomfield, J. P., Davies, K., Hladky, K., (2002) The use of permanent corrosion monitoring in new and existing reinforced concrete structures. *Cement and Concrete Composites*, **24**, 27-34.

Broomfield, J.P., Rodriguez, J. Ortega, L.M. and Garcia, A.M. (1993) Corrosion rate measurement and life prediction for reinforced concrete structures, In: Proceedings of Structural Faults And Repair-93, Vol.2: pp.155, (Engineering Technical Press, University of Edinburgh).

Browne, R. D. Mechanisms of corrosion of steel in concrete in relation to design, inspection, and repair of offshore and coastal structures. pp. 169-204. In **Malhotra V. M.** (ed.) *Performance of concrete in marine environment*. ACI SP 65, American Concrete Institute, Farmington Hills, Mich, 1980.

BS 8110 (1997) Structural use of concrete - Part 1: Code of practice for design and construction, *British Standards Institution*, London.

Cabrera, J.G. (1996) Deterioration of concrete due to reinforcement steel corrosion. *Cement and Concrete Composites*, **18**, 47-59.

Cady, P. D, and Gannon, E. (1992) Condition evaluation of concrete bridges relative to reinforcement corrosion, SHRP Report No. SHRP-S-330, Strategic Highway Research Program, National Research Council, Washington, DC, pp. 85-105.

Cady, P.D. and Weyers, R.E. (1984) Deterioration rates of concrete bridge decks. *Journal of Transportation Engineering*, **110 (1)**, 35-44.

Callister, Jr., William D. *Materials Science and Engineering: An Introduction*. NY: John Wiley & Sons, Inc., 2000.

CEB (1989) Comité Euro-International du Béton *Durable concrete structures*, Bulletin d'information, No. 182, *Design guide*, (2nd Edition), Paris.

CEB Bulletin No. 162 (1983) Assessment of Concrete structures and design procedures for upgrading, pp. 87-90.

Chamberlin, W.P., and Weyers R.E. Field performance of latex-modified and low-slump dense concrete bridge deck overlays in the United States. pp.1-16. In **Weyers R.E.** (ed.) *Concrete Bridges in Aggressive Environments*, ACI SP 151, American Concrete Institute, Farmington Hills, Mich, 1993.

Chung, D.D.L. (2000) Corrosion control of steel reinforced concrete. *Journal of Materials Engineering and Performance*, **9 (5)**, 585-588.

Clear, K.C. (1989) *Measuring the rate of corrosion of steel in field concrete structures*, Transportation Research Record 1211, Transportation Research Board, National Research Council, Washington DC.

Collepardi, M., Fratesi, R., Moriconi, G., and Biagini, S. (1990a) The use of superplasticizers as steel corrosion reducers in reinforced concrete. In **Väzquez** (ed.), Proceedings of the International RILEM Symposium *on Admixtures for concrete; Improvement of properties*, Barcelona, Spain, 1990.

Collepardi, M., Fratesi, R., Moriconi, G., Coppola, L., and Corradetti, C. (1990b), Use of nitrite salt as corrosion inhibitor admixture in reinforced concrete structures immersed in seawater. In **Väzquez** (Ed.), *Proceedings of the International RILEM Symposium on Admixtures for concrete; Improvement of properties*, Barcelona, Spain, 1990.

Congqi, F., Lundgren, K., Plos, M., and Gylltoft, K. (2006) Bond behaviour of corroded reinforcing steel bars in concrete. *Cement and Concrete Research*, **36 (10)**, 1931-1938.

Coutinho, J.S. (2003) The combined benefits of CPF and RHA in improving the durability of concrete structures. *Cement and Concrete Composites*, **25**, 51-59.

Crane, A. P. *Corrosion of reinforcement in concrete construction,* Society of Chemical Industry, Ellis Horwood Ltd., London, 1983.

CSIRO, Research Report BRE 062, *Guidelines for the use of fly ash concrete in marine environments*, Ash Development Association of Australia, 2000.

Dias, W.P.S. (2004) Influence of drying on concrete Sorptivity. *Magazine Concrete Research*, **56 (9)**, 537-543.

Dinakar, P., Babu, K.G., and Santhanam, M. (2007) Corrosion behaviour of blended cements in low and medium strength concretes. *Cement and Concrete Composites*, **29**, 136-145.

Dhir, R.K., Tham, K. and Dransfield, J. Durability of concrete with superplasticizing admixture. pp. 741-764. In **Scanlon, J.M.,** (ed.), *Concrete durability,* ACI SP 100, American Concrete Institute, Detroit, 1987.

Dillard, J. G., Glanville, J. D., Collins, W. D., Weyers, R.E., and Al-Qadi, I.L. *Concrete bridge protection and rehabilitation: chemical and physical techniques, feasibility studies of new rehabilitation techniques (Report No. SHRP-S-665),* Strategic Highway Research Program, Washington DC, 1993.

DuraCrete. (2000) DuraCrete – Final technical report, Document BE95-1347/R17; www.cur.nl/upload/documents/duracrete/BE1347R17.pdf; . Last accessed in February 2013

Edvardsen, C. (1999) Water permeability and autogenous healing of crack in concrete, *ACI Materials Journal*, **96 (4)** 448–454.

Elsener *Corrosion inhibitors for steel in concrete, State of the Art Report*, European Federation of Corrosion Publications, **35**, Maney Publishing, U.K., 2001.

El-Jazairi, B. and Berke, N. S., The use of calcium nitrite as corrosion inhibiting admixture to steel reinforcement in concrete. pp. 571-585. In **Page, C. L., Treadaway, K. W., and Bamforth, P. B.** (eds.), *Corrosion of reinforcement in concrete*, SCI, Londres, 1990.

Fadayomi, J. (1997) Corrosion inhibitors. *Concrete*, **31 (8)**, 21-23.

FDOT *An accelerated laboratory method for corrosion of reinforced concrete using impressed current*, Manual of Florida sampling and testing methods, Florida Department of Transportation, Tallahassee, FL, 2000, 6 p.

François, R., and Maso, J. C. (1988) Effect of damage in reinforced concrete on carbonation or chloride penetration. *Cement and Concrete Research*, **18**, 961-970.

François, R. and Arliguie, G. (1998) Influence of service cracking on reinforcement steel corrosion. *Journal of Materials in Civil Engineering*, ASCE, **10 (1)**, 14-20.

François, R. and Arliguie, G. (1999) Effect of microcracking and cracking on the development of corrosion in reinforced concrete members. *Magazine of Concrete Research*, **51 (2)**, 143-150.

François, R., Khan, I., Vu, N. A., Mercado, H. and Castel, A. (2012) Study of the impact of localized cracks on the corrosion mechanism. *European Journal of Environmental and Civil Engineering*, **16 (3-4)**, 392-401.

Frank, R., Raoul, J., and Mike, G. *Deteriorated concrete-inspection and physicochemical analysis.* Thomas Telford Limited, London, 2002.

Gagné, R., Boisvert, A., and Pigeon, M. (1996) Effect of superplasticizer dosage on mechanical properties, permeability and freeze-thaw durability of high-strength concretes with and without silica fume. *ACI Materials Journal*, **93 (2)**, 111-120.

Gadve, S. A., Mukherjee, A., and Malhotra, S. N. (2009) Corrosion of steel reinforcements embedded in FRP wrapped concrete. *Construction and Building Materials*, **23**, 153-161.

Gaidis, J.M. (2004) Chemistry of corrosion inhibitors. *Cement and Concrete Composites*, **26**, 181-189.

Gaidis, J.M., and Rosenberg, A. M., (1987). The inhibition of chloride induced corrosion in reinforced concrete by calcium nitrite. *Cement Concrete and Aggregates*, **9**, 30-33.

Gancedo, J.R., C. Alonso, Andrade, C., Gracia, M. (1989). AES study of the passive layer formed on iron in saturated $Ca(OH)_2$ solutions, *Corrosion*, NACE 45 (12), 976-977.

Geiker, M.R., Henriksen, C. and Thaulow, N. (1993) Design for durability: a case story, *Concrete*, 2000, Dhir, R.K. and Jones, M.R. editors. EFN Spon. Vol.1, 64-70.

Gjørv, O. E. Important test methods for evaluation of reinforced concrete durability. Pp. 545-574. In **Mehta, P. K.** (ed.) *Concrete in the 21st century: Past, Present and Future*. ACI SP 144, 1994.

Glass, G. K. and Buenfeld, N. R. Chloride Threshold Levels for Corrosion Induced Deterioration of Steel in Concrete. pp. 429–440. *International Workshop on Chloride Penetration into Concrete*, St Remy-les-Chevreuse, RILEM, October 15–18, 1995.

Gomà, F., Vivar, J., Mauri, J., Costa, J. M., and Vilarrasa, M., Influence of plasticizers on corrosion of reinforcing bars in concrete. pp. 199-208. In **Väzquez** (ed.), *Proceedings of the International RILEM Symposium on Admixtures for concrete; Improvement of properties*, Barcelona, Spain, 1990.

González, J. A., Andrade, C., Alonso, C. and Feliu, S., (1995) Comparison of rates of general corrosion and maximum pitting penetration on concrete embedded steel reinforcement. *Cement and Concrete Research*, **25 (2)**, 257-264.

González, J. A., Ramírez, E., and Bautista, A., (1998) Protection of steel embedded in chloride containing concrete by means of inhibitors. *Cement and Concrete Research*, **28 (4)**, 577-589.

Gu, P. and Beaudoin, J. J. (1998) Estimation of steel corrosion rate in reinforced concrete by means of equivalent circuit fittings of impedance spectra. *Advances in Cement Research*, **10 (2)**, 43-56.

Güneyisi, E., Özturan, T., and Gesolu, M. (2006) Performance of plain and blended cement concretes against corrosion cracking. pp. 189-198. In **Maria S Konsta-Gdoutos** (ed.) Proceedings of *International symposium on Measuring, monitoring and modeling concrete properties-dedicated to S. P. Shah,* Springer, Netherlands.

Hansson, C. M, Mammoliti, L. and Hope, B. B. (1998) Corrosion inhibitors in concrete – Part I: The principles. *Cement and Concrete Research*, **28 (12)**, 1775-1781.

Heiyantuduwa, R., and Alexander, M.G. Performance of an organic inhibitor in concrete affected by both chloride and carbonation induced corrosion. pp. 313-314. In **Alexander** (ed.), *Concrete Repair, Rehabilitation and Retrofitting*, Taylor & Francis group, London, 2006.

Heiyantuduwa, R., Alexander, M.G., and Mackechnie, J.R., (2006) Performance of a Penetrating corrosion inhibitor in concrete affected by carbonation induced corrosion. *Journal of Materials in Civil Engineering, ASCE*, **18 (6)**, 842-850.

Holden W.R., Page C.L., Short M.R. The influence of chlorides and sulphates on durability of reinforced concrete. pp. 143. In **Crane A.P** (ed.), *Corrosion of Reinforcement in concrete construction*, (Ellis Horwood, Hichester), 1983.

Holm, J. (1987) Comparison of the corrosion potential of calcium chloride and a calcium nitrate based non-chloride accelerator- a macro-cell corrosion approach. pp. 35-49. In **Francis W. Gibson** (eds.) *Corrosion, Concrete, and Chlorides-Steel corrosion in concrete: Causes and restraints,* ACI SP 102, American Concrete Institute, USA.

Holm, J. and Geiker, M. (Eds.) *Durability of concrete*, SP-131, ACI, Detroit, USA, 1992.

Hope, B. B., and Ip, A. K. C. (1990) Effect of calcium nitrite and sodium molybdate on corrosion inhibition of steel in simulated concrete environment, In **Väzquez** (ed.), *Proceedings of the International RILEM Symposium on Admixtures for concrete; Improvement of properties*, Barcelona, Spain.

Hover, K. C. (1998) Concrete mixture proportioning with water reducing admixtures to enhance durability: A quantitative model. *Cement Concrete and Composites*, **20**, 113- 119.

Husain, A., Al-Bahar, S., Salam, S.A., and Al-Shamali, O. (2004) Accelerated AC impedance testing for prequalification of marine construction materials. *Desalination*, **165**, 377-384.

Ijsseling, F. P. (1986) Application of electrochemical methods of corrosion rate determination to system involving corrosion product layers. *British Corrosion Journal*, **21 (2)**, 95-101.

IS 383:1970 (2007) Specification for coarse and fine aggregates from natural sources for concrete', *Bureau of Indian Standards (BIS)*, New Delhi.

IS 456:2000 (2005) Code of practice for Plain and Reinforced Concrete, *Bureau of Indian Standards (BIS)*, New Delhi.

IS 516:1959 (2002) Indian standard Methods of tests for strength of concrete, *Bureau of Indian Standards (BIS)*, New Delhi.

IS 1489:1991 (Part I) (2005) Indian standard specification for Portland pozzolana cement (fly ash based), *Bureau of Indian Standards (BIS)*, New Delhi.

IS 1786:2008 (2008) Indian Standard specification for high strength deformed steel bars and wires for concrete reinforcement, *Bureau of Indian Standards (BIS)*, New Delhi.

IS 9103:1999 (2004) Indian Standard, Concrete Admixtures - Specification, *Bureau of Indian Standards (BIS)*, New Delhi.

ISO 8044 (1999) Corrosion of metals and alloys, basic terms and definitions', *International Organization for Standardization*, Geneva.

Issa, M. A., Khalil, A.A., Islam, S. and Krauss, P.D. (2008) Mechanical properties and durability of high performance concrete for bridge decks. *PCI Journal*, **53(4)**, 108-130.

Jacobsen, S., Marchand, J. and Boisbert, L. (1996) Effect of cracking and healing on chloride transport in OPC concrete. *Cement and Concrete Research,* **26 (6)**, 869-881.

Jang, S. Y., Kim, B. S., and Oh, B. H. (2011) Effect of crack width on chloride diffusion coefficients of concrete by steady-state migration tests. *Cement and Concrete Research,* **41**, 9-19.

Jayasree, C., and Gettu, R. (2008) Experimental study of the flow behaviour of superplasticized cement paste. *Materials and Structures*, **41**, 1581-1593.

Jin, S. X., Sagoe, K. K. and Glasser, F. P., (1991) Characteristics of corrosion inhibition admixtures in OPC paste with chloride additions Part 1: Chemistry and electrochemistry. *Magazine of Concrete Research*, 43, 205-213.

Khatri, R. P., and Sirivivatnanon, V. (2004) Characteristic service life for concrete exposed to marine environments. *Cement and Concrete Research*, **34**, 745-752.

Khatib, J.M., and Mangat, P.S. (1999) Influence of superplasticizer and curing on porosity and pore structure of cement. *Cement and Concrete Composites*, **21**, 431-437.

Kondratova, I.L., Montes, P., and Bremner, T.W. (2003) Natural marine exposure results for reinforced concrete slabs with corrosion inhibitors. *Cement and Concrete Composites*, **25**, 483-490.

Kurtis, K. E., and Mehta, K. A critical review of deterioration of concrete due to corrosion of reinforcing steel. pp. 535-554. In **V. M. Malhotra** (ed.), *CANMET/ACI International Conference on Durability of concrete, Admixtures to reduce the permeability of concrete,* ACI SP 170, 1997.

Langford, P., and Broomfield, J. P. (1987) Monitoring the corrosion of reinforcing steel. *Construction repair*, **1 (2)**, 32-36.

Limaye, R.G., Angel, R.D., and Radke, A. S. (2000) Experimental studies on penetrating type corrosion inhibitor in reinforced concrete. *The Indian Concrete Journal*, 22-26.

Li, Z., Peng, J., and Ma, B. (1999) Investigation of chloride diffusion for high performance concrete containing fly ash, microsilica and chemical admixtures. *ACI Materials Journal*, **96 (3)**, 391-396.

Li, Z., Ma, B., Peng, J., and Qi, M. (2000) The microstructure and sulfate resistance mechanism of high-performance concrete containing CNI. *Cement and Concrete Composites*, **22**, 369-377.

Liu, Y. and Weyers, R. E., Time to cracking for chloride induced corrosion in reinforced concrete. pp. 88-107. In Corrosion of reinforcement in concrete construction, (Eds.) **Page, C.L, Bamforth, P.B and Figg, J. W.** (eds.), *The Royal Society of Chemistry*, 1996.

Life-365 S*ervice life prediction model and computer program for predicting the service life and life-cycle cost of reinforced concrete exposed to chlorides*, Version 2.0.1, Life-365 Consortium II, 2010.

Locke, C. E. and Siman, A. Electrochemistry of reinforcing steel in salt-contaminated concrete. pp. 3-16. In **Tonini, D. E. and Gaidis, J. M.** (eds.) *Corrosion of reinforcing steel in concrete*. ASTM STP 713, American Society for Testing Materials, 1980.

Loulizi, A., Al-Qadi I. L., and Diefenderfer, B. K. (2000) Effects of nitrite based corrosion inhibitor on concrete's rapid chloride permeability values and its dielectric properties. *ACI Materials Journal*, **97 (4)**, 465-471.

Luping, T. (2002) *Calibration of the electrochemical methods for the corrosion rate measurement of steel in concrete, NORDTEST Project No. 1531-01*, SP Swedish National Testing and research Institute, Sweden.

Ma, B., Li, Z., Peng, J. (1998) Effect of calcium nitrite on high performance concrete containing fly ash. pp. 113–124. In **Malhotra M.** (ed.) *Six CANMET/ACI International Conference on Fly Ash, Silica Fume, Slag and Natural Pozzolans in Concrete,* Supplementary Papers, Bangkok, Thailand.

Maaddawy, T. A. El, and Soudki, K. A. (2003) Effectiveness of impressed current technique to simulate corrosion of steel reinforcement in concrete. *Journal of Materials in Civil Engineering ASCE*, **15 (1)**, 41-47.

Mackechnie, J. R. and Alexander, M. G. Marine exposure of concrete under selected South African conditions. pp. 205-216. In **Malhotra V. M.** (ed.) *Third ACI/CANMET International Conference on the Performance of Concrete in Marine Environment*, Canada, ACI SP 163, 1996.

Mackechnie, J. R. and Alexander, M. G. *Repair principles for corrosion damaged reinforced concrete structures, Research monograph No. 5*, Department of Civil Engineering, University of Cape Town, S.A., 2001.

Mackechnie, J.R., Alexander, M.G., Heiyantuduwa, R. and Rylands, T. *The effectiveness of organic corrosion inhibitors for reinforced concrete', Research monograph No. 7*, Department of Civil Engineering, University of Cape Town, S.A., 2004.

Maeder, U. (1996), A new class of corrosion inhibitors for reinforced concrete. pp. 215-232. In **Malhotra, V.K.** (ed.) *3rd CANMET/ACI International Conference on Concrete in marine environment,* ACI SP 163, 1996.

Malhotra, V. M. and Mehta, P. K. (2002) *High performance, high volume fly ash concrete: materials, mixture proportioning, properties, construction practice, and case histories*, Marquardt Printing Ltd., Ottawa, Canada.

Malhotra, V. M., and Carino, N.J. *Handbook on Nondestructive testing of concrete*, CRS Press, Washington D.C, 2004.

Mani, K. and Srinivasan, P. (2001) Service life of RC structures in corrosive environment: A comparison of carbon steel and stainless steel bars. *The Indian Concrete Journal*, **75**, 1-12.

Mangat, P. S., and Gurusamy, K. (1987a) Chloride diffusion in steel fibre reinforced concrete containing PFA. *Cement and Concrete Research*, **17**, 640-650.

Mangat, P. S., and Gurusamy, K. (1987b) Chloride diffusion in steel fibre reinforced marine concrete. *Cement and Concrete Research*, **17**, 385-396.

Mangat, P., and Molloy, B. (1991) Factors influencing chloride induced corrosion of reinforcement in concrete. *Material and Structures*, **25 (7)**, 404-411.

Mangat, P., Khatib, J., and Molloy, B. (1994) Microstructure, chloride diffusion and reinforcement corrosion in blended cement paste and concrete. *Cement and Concrete. Composites*, **16 (2)**, 73-81.

Mohammed, T. U.; Otsuki, N.; Hisada, M.; and Shibata, T. (2001) Effect of crack width and bar types on corrosion of steel in concrete. *Journal of Materials in Civil Engineering, ASCE*, **13 (3)** 194-201.

Mohammad, T. U., and Hamada, H. (2001) Discussion of "Chloride Threshold Values to Depassivate Reinforcing Bars Embedded in a Standardized OPC Mortar," by C. Alonso, C. Andrade, M. Castellote, and P. Castro. *Cement and Concrete Research*, V. 31, No. 5, May, pp. 835-838.

Mohammed, T. U., Otsuki, N., and Hamada, H. (2003) Corrosion of steel bars in cracked concrete under marine environment. *Journal of Materials in Civil Engineering, ASCE*, **15 (5)**, 460-469.

Mohammed, H. S. and Knight, S. G.M. (2008) Performance Evaluation of Nitrite Based Corrosion Inhibitor, Proceedings of the *Sixth Structural Convention, SEC–2008*, Chennai, December, 1147–1157.

Montemor, M.F., Simoes, A.M.P., and Ferreira M.G.S. (2003) Chloride-induced corrosion on reinforcing steel: from the fundamentals to the monitoring techniques. *Cement and Concrete Composites*, **25**, 491-502.

Montes, P., Bremner, T.W., and Lister, D. (2004) Influence of calcium nitrite inhibitor and crack width on corrosion of steel in high performance concrete subjected to a simulated marine environment. *Cement and Concrete Composites*, **26**, 243-253.

Montes, P., Bremner, T.W., and Mrawira, D. (2005) Effects of calcium nitrite based corrosion inhibitor and fly ash on compressive strength of high performance concrete. *ACI Materials Journal*, **102 (1)**, 3-8.

Morinaga, S. *Prediction of service lives of reinforced concrete buildings based on rate of corrosion of reinforcing steel*, Special Report of Institute of Technology, Shimizu Corporation, No.23. June 1988.

Morinaga, S., Irino, K., Ohta, T. and Arai, H. Life prediction of existing reinforced concrete structures determined by corrosion, pp.603-618. In **Swamy R. N.** (ed.), *Corrosion and Corrosion Protection of Steel in Concrete*, Sheffield, UK, Sheffield Academic Press, 1994.

NDT James Instruments *Corrosion rate meter for steel in concrete*, Instruction Manual, NDT, USA, 2006.

Neville, A. M. *Properties of concrete*, Addison Wesley Longman Ltd, 1996.

Nmai C. K. and McDonald, D. Long-term effectiveness of corrosion inhibiting admixtures and implications on the design of durable reinforced concrete structures: a laboratory investigation. pp. 1-17. *RILEM International Symposium on The Role of Admixtures in High Performance Concrete*, Monterey, Mexico, 1999.

NT Build 355, Concrete, mortar and cement based repair materials: Chloride diffusion coefficient from migration cell experiments, Nordtest method, 1997.

Ohno, Y., Praparntanatorn, S., and Suzuki, K. Influence of cracking and water cement ratio on macrocell corrosion of steel in concrete, pp. 88-104. In **Page, C.L., Bamforth, P.B., and Figg. J. W.** (eds.) *Corrosion of reinforcement in concrete construction*, Royal Society of Chemistry, London, 1996.

Okaba, S. H., El-Dieb, A. S., and Reda, M. M. (1997) Evaluation of the corrosion resistance of Latex modified concrete (LMC). *Cement and Concrete Research*, **27 (6),** 861-868.

Okada, K., and Miyagawa, T., Chloride corrosion of reinforcing steel in cracked concrete. pp. 237-254. In **Malhotra, V.M (ed.)**, *Performance of concrete in marine environment*, ACI SP 65, American Concrete Institute, 1980.

Ormellese, M., Berra, M., Bolzoni, F., and Pastore, T. (2006) Corrosion inhibitors for chlorides induced corrosion in reinforced concrete structures, *Cement and Concrete Research*, **36**, 536-547.

Otieno, M. B., Alexander, M. G. and Beushausen, H. D. (2010a) Corrosion in cracked and uncracked concrete-influence of crack width, concrete quality and crack re-opening. *Magazine of Concrete Research*, **62**, 393-404.

Otieno M. B, Alexander M. G. and Beushausen H. D. (2010b) Suitability of various measurement techniques for assessing corrosion in cracked concrete. *ACI Materails Journal*, **107(5)**, 481-489.

Otieno, M., Beushausen, H., and Alexander, M., (2011), Prediction of corrosion rate in reinforced concrete structures – a critical review and preliminary results. *Materials and Corrosion*, **62**, pp. 1-14.

Page, C. L. Nature and properties of concrete in relation to reinforcement corrosion, *Corrosion of steel in concrete*, Aachen, February 17-19, 1992.

Page, C. L. and Treadaway, K. W. J. (1982) Aspects of the electrochemistry of steel in concrete. *Nature*, 297, 109-144.

Palsson, R. and Mirza, M. S. (2002) Mechanical response of corroded steel reinforcement of abandoned concrete bridge. *ACI Structural Journal*, **99 (2)**, 157-162.

Palumbo G. Brennestuhl A. M. and Gonzalez F. S. (1994) The importance of subtle materials and chemical considerations in the development of accelerated tests for service performance predictions. pp. 252-267. In **Cragnolino, G and Sridhar, N.** (eds.), *Application of accelerated corrosion tests to service life prediction of materials*, ASTM, STP 1194, West Conshohocken, PA.

Papayianni I. Tsohos G. Oikonomou N. and Mavria P. (2005) Influence of superplasticizer type and mix design parameters on the performance of them in concrete mixtures. *Cement and Concrete Composites,* **27**, 217-222.

Park, S.S., Kwon, S.J., and Jung, S. H. (2012) Analysis technique for chloride penetration in cracked concrete using equivalent diffusion and permeation. *Construction and Building Materials*, **29**, 183-192.

Parrott, L.J. (1990) Damage caused by carbonation of reinforced concrete. *Materials and Structures*, **23 (3)**, 230-234.

Pettersson K. Jørgensen O. and Fidjestøl P. The effects of the cracks on reinforcement corrosion in high performance concrete in a marine environment. pp. 185-200. In **Malhotra V.M.** (ed.) *Third CANMET/ACI International conference on performance in marine environment,* ACI SP 163, 1996.

Pillai, R. G., and Trejo, D. (2005) Surface condition effects on critical chloride threshold of steel reinforcement. *ACI Materials Journal*, **102 (2)**, 103-109.

Pillai, R. G. Corrosion and service life prediction of reinforced concrete structures. pp.29-37. In **Pillai, R. G.** (ed.), *Deterioration and rehabilitation of concrete structures (ACECON 2010)*, IIT Madras, 2010.

Polder, R., Rooij, M. r. and Breugel, K. van. Validation of models for service life prediction-Experiences from the practice. pp.292-301. In **Kovler, K.** (ed.), *Concrete durability and service life planning (ConcreteLife'06)*, RILEM Publications, 2006.

Popovics S., Simeonov Y., Boshinov G., Barovsky N. Durability of reinforced concrete in sea water. pp.19. In **Crane,A.P.** (ed.), *Corrosion of Reinforcement in concrete construction*, (Ellis Horwood, Chichester), 1983.

Poursaee, A., and Hansson, C. M. (2008) The influence of longitudinal cracks on the corrosion protection afforded reinforcing steel in high performance concrete. *Cement and Concrete Research*, **38**, 1098-1105.

Poursaee, A., and Hansson, C. M. (2009) Potential pitfalls in assessing chloride-induced corrosion of steel in concrete. *Cement and Concrete Research*, **39**, 391-400.

Prabakar, J., Manoharan, P. D. and Neelamegam, M. (2010a) Influence of sodium nitrate in concrete as corrosion inhibitor in chloride environment. *Indian Concrete Institute Journal*, **July-September**, 7-12.

Prabakar, J., Manoharan, P. D., Neelamegam, M., and Nagesh R. Iyer. (2010b) Estimation of depassivation period of steel in concrete based on chloride diffusion tests, *Journal of Structural Engineering,* CSIR-SERC, **37 (1)**, 8-16.

Prabakar, J., Manoharan, P. D., and Chellappan, A. (2010c) Diffusion characteristics of OPC concrete of various grades under accelerated test conditions. *Construction and Building Materials*, **24 (3)**, 346-352.

Prabakar, J., Manoharan, P. D. and Neelamegam, M. (2011) Effect of fly ash on durability and performance of concrete. *The Indian Concrete Journal*, **November**, 9-15.

Pradhan, B., and Bhattacharjee. B. (2007) Role of steel and cement type on chloride induced corrosion in concrete. *ACI Materials Journal*, **104 (6)**, 612-619.

Pradhan, B., and Bhattacharjee. B. (2009) Performance evaluation of rebar in chloride contaminated concrete by corrosion rate. *Construction and Building Materials*, **23 (6)**, 2346-2356.

Prezzi, M., Geyskens, P., and Monteiro, J. M. P. (1996) Reliability approach to service life prediction of concrete exposed to marine environment. *ACI Materials Journal*, **93 (6)**, 544-551.

Purvis, R.L., Graber, D.R., Clear, K.C., and Markow, M.J. (1992) *A Literature Review of Time-Deterioration Prediction Techniques*. SHRP-C/UFR-92-613, National Research Council, Washington, D.C., U.S.A.

Purvis, R.L., Babaei, K., Clear, K.C. and Markow, M.J. (1994) Life - cycle cost analysis for protection and rehabilitation of concrete bridges relative to reinforcement corrosion, SHRP-S-377, National Research Council, Washington, D.C., U.S.A.

Rajamane N.P., Chellappan A., Neelamegam M., Annie Peter J., Dattatreya J.K., Prabakar J., Srinivasan P., Bhaskar S., Sabita, D., Ambily, P.S., and Harish, K.V. *Studies on evaluation of durability of cracked RC members using fly ash concrete subjected to accelerated corrosion and carbonation*, GAP-02541, SERC, Chennai (Internal report), 2008.

Rathishkumar, P., ManojKumar, P., Rajashekar, B., and Nageswar, G., (2002) Sorptivity characteristics of High Performance Mortars. *Journal of The Institution of Engineers (India)* **83**, 153-159.

Raupach, M. (2006) Models for the propagation phase of reinforcement corrosion: an overview. *Materials and Corrosion*, **57 (8)**, 605-613.

Richardson, M. *Fundamentals of durable reinforced concrete*, Londres e Nova Iorque, Spon press, London, 2002.

Rixom, R. and Mailvaganam, N. *Chemical admixtures for concrete*, Third edition, E &FN SPON, Ltd. London, 1999.

Ramachandran, V.S. (Ed.), *Concrete Admixtures Handbook: Properties, Science and Technology*, Second Edition, NOYES Publications, 1995.

Rodriguez, P., Ramirez and Bonzalez, E J. A. (1994) Methods for studying corrosion in reinforced concrete. *Magazine of Concrete Research*, **46 (167)**, 81-90.

Rodriguez, J., Ortega, L. M., Casal, J., and Diez, J. M. Assessing structural conditions of concrete structures with corroded reinforcement. pp. 65-78. In **Dhir R K and Jones M. R.** (eds.), *Concrete repair, rehabilitation and protection*, E & FN Spon, London, 1996.

Rodriguez, J., Ortega, L. M., Aragoncillo, J., Izquierdo, D. and Andrade, C. Methodology for the structural assessment of concrete affected by reinforcement corrosion, pp. 305-318. In **Helene et al.** (eds.), *Quality of Concrete Structures and Recent Advances in Concrete Materials and Testing*, ACI SP 229, Michigan, USA, 2005.

Roy, S. K. and Northwood, D. O. Admixtures to reduce the permeability of concrete. pp. 267-284. In **Malhotra V. M.** (ed.), Fourth *CANMET/ACI Conference on Durability of concrete*, ACI SP 170, Formington Hills, MI, 1997.

Sahmaran, M., Victor, C. Li, and Andrade, C. (2008) Corrosion resistance performance of steel-reinforced engineered cementitious composite beams. *ACI Materials Journal*, **105 (3)**, 243-250.

Sakumoto, Y., Nakazato, T., and Matsuzaki, A. (1996) Properties of stainless steel for building structures. *ASCE Journal of Structural Engineering*, **122**, 1-6.

Sakr, K. (2005) Effect of cement type on the corrosion of reinforcing steel bars exposed to acidic media using electrochemical techniques. *Cement and Concrete Research*, **35**, 1820-26.

Saraswathy, V. and Song, H. W. (2007a) Evaluation of corrosion resistance of Portland pozzolana cement and fly ash blended cements in pre-cracked reinforced concrete slabs under accelerated testing conditions. *Materials Chemistry and Physics*, **104**, 356-361.

Saraswathy, V. and Song, H. W. (2007b) Improving the durability of concrete by using inhibitors. *Building environment*, **42**, 464-72.

Saraswathy, V., and Song, H. W. (2008) Evaluation of cementitious repair mortars for corrosion resistance. *Portugaliae Electrochimica Acta*, **26/5**, 417-432.

Saricimen, H., Maslehuddin, M., AI-Tayyib, A.J., AI-Mana, A.I., (1995) Permeability and durability *of* blended *cement* concrete *cured in the* field and laboratory conditions. *ACI Materials Journal*, **9 (2)**, 111-116.

Scott, A. C., LaFave, J.M., Trybulski, J., Lovett, D., Lima, J., Pfeifer, D.W., (2005) Effectiveness of corrosion inhibiting admixture combinations in structural concrete. *Cement & Concrete Composites*, **27**, 688-703.

Scott, A., and Alexander, M.G. (2007) The influence of binder type, cracking and cover on corrosion rates of steel in chloride contaminated concrete. *Magazine of Concrete Research,* **59 (7)**, 495-505.

Schiessl P. Influence of the composition of concrete on the corrosion protection of the reinforcement. pp. 1633-1645. In **Scanlon, J.M.,** (ed.), *Concrete durability,* ACI SP 100, American Concrete Institute, Detroit, 1987.

Schiessl, P., and Mörsch, N. (2000) Effectiveness and harmlessness of calcium nitrite as a corrosion inhibitor. In **Cabrera, J. G. and Rivera, R.,** (eds.) *Proceedings of International Conference on The Role of Admixtures in High Performance Concrete,* Monterey, Mexico, RILEM Publications, 2000.

Schießl, P., and Raupach, M. (1997) Laboratory studies and calculations on the influence of crack width on chloride induced corrosion of steel in concrete, *ACI Materials Journal*, **94 (1)**, 56-62.

Selim, I. Z. (1998) Corrosion behaviour and chloride attack of reinforcing steel in presence of concrete admixtures. *Journal of Material Science and Technology,* 1**4**, 339-343.

Sharp, J. V., Figg, J. W., and Leeming, M. B. The assessment of corrosion of reinforcement in marine concrete by electrochemical and other methods. pp. 105-125. In **Malhotra, V. M.** (ed.) *Proceedings of Second International Conference Concrete in marine environment*, ACI SP 109,1988.

Shetty, M.S*Concrete technology*, Theory and practice, S. Chand & Co Ltd., 2005.

Silverman, D. C and Carrico, J. E. (1988) Electrochemical impedance technique – A practical tool for corrosion prediction. *Corrosion*, **44 (5)**, 280-287.

Sivasundaram, V., Carette, G. G. and Malhotra, V. M. (1989) Properties of concrete incorporating low quantity of cement and high volumes of low calcium fly ash, Fly Ash, Silica Fume, Slag, and Natural Pozzolans in Concrete. pp. 45-71. In **Malhotra, V.M.** (ed.) *ACI SP 114*, 1989.

Soleymani, H. R, and Ismail, M. E. (2004) Comparing corrosion measurement methods to access the corrosion activity of laboratory OPC and HPC concrete specimens. *Cement and Concrete Research*, **34**, 2037-2044.

Stoltzner, E., Knudsen, A., and Buhr, B. Durability of marine structures in Denmark. pp.59-68. In **Blankvoll, A. (ed.)**, *Proceedings of International Conference-Repair of concrete structures, From theory to practice In a marine environment*, Norway, 1997.

Song, H. W. and Saraswathy V. (2007) Corrosion monitoring of reinforced concrete structures – A review. *International Journal of Electrochemical Science*, **2**, 1-28.

Song, H. W., Saraswathy, V., Muralidharan, S., Lee, C. H., and Thangavel, K. (2009) Corrosion performance of steel in composite concrete system admixed with chloride and various alkaline nitrites. *Corrosion Engineering Science and Technology*, **44 (6)**, 408-415.

Stern, M. and Geary, A. L. (1957) Electrochemical polarization I: theoretical analysis of shape of polarization curves, *Journal of Electrochemistry Society*, (104), pp. 56-63, cited by Luping, T., (2002), Calibration of the electrochemical methods for the corrosion rate measurement of steel in concrete, NORDTEST Project No. 1531-01, SP Swedish National Testing and Research Institute.

Srinivasan P., Mani K., and Chellappan A. (2008) Use of corrosion inhibitors in enhancing the life of reinforced concrete structure against chloride induced corrosion, Proceedings of the Sixth Structural Convention, SEC – 2008, Dec. 18-20, Chennai, India, 1063-1068.

Suzuki, K., Ohno, Y., Praparntanatorn, S., and Tamura, H. Mechanism of steel corrosion in cracked concrete in Corrosion of reinforcement in concrete. pp. 19-28. In Page, C., **Treadaway, K., and Bamforth, P.** (eds.) *Society of Chemical Industry*, 1990.

Swamy, R. N. Superplasticizers and concrete durability, pp. 361-382. In **V. Malhotra** (ed.) *Superplasticizers and other chemical admixtures in concrete*, ACI SP 119, 1989.

Tamizhselvi, V., and Knight, S. G. M. (2007) Electrochemical investigations to evaluate the performance of inhibitors to control rebar corrosion. *Indian Concrete Institute Journal*, **8 (1)**, 7-13.

Taylor, P. C., Nagi, M. A., and Whiting, D. A. (1999) Threshold chloride content for corrosion of steel in concrete: A literature review, PCA R&D Sl. No. 2169, Illinois.

Thangavel, K., Muralidharan, S., and Saraswathy, V. (2009) Migrating *VS* admixed corrosion inhibitors for steel in Portland, Pozzolana and Slag cement concretes under macrocell condition. *The Arabian Journal of Science and Engineering.* **34 (2C)**, 81-93.

Thompson, N. G. and Lankard, D. R. (1997) Improved concretes for corrosion resistance (Report No. FHWA-RD-96-207), Federal Highway Administration, Washington, DC, 176 pp.

Trépanier, S. M., Hope, B. B., and Hansson, C. M. (2001) Corrosion inhibitors in concrete Part III. Effect on time to chloride induced corrosion initiation and subsequent corrosion rates of steel in mortar. *Cement and Concrete Research*, **31**, 713-718.

Trejo, D., and Pillai, R. G. (2003) Accelerated chloride threshold testing: Part I – ASTM A 615 and A 706 Reinforcement. *ACI Materials Journal*, 100 (6), 519-527.

Trejo, D., and Pillai, R. G. (2004) Accelerated chloride threshold testing: Part II – Corrosion resistant Reinforcement. *ACI Materials Journal*, 101 (1), 57-64.

Tuutti, K. (1980) Service life of structures with regard to corrosion of embedded steel, in Performance of concrete in marine environment. pp. 223-236. In **Malhotra V. M.** (ed.), *ACI SP 65*, 1980.

Tuutti, K., (1982) *Corrosion of Steel in Concrete*, CBI, research report 4, 1982, Stockholm.

USDT-Publication No. 00-081 *Materials and methods for corrosion control of reinforced and prestressed concrete structures in new construction*, U. S. Department of Transportation, 2000.

Vedalakshmi, R., Renugha Devi, R., Emmanual, B., and Palaniswamy, N. (2008) Determination of diffusion coefficient of chloride in concrete: an electrochemical impedance spectroscopic approach. *Materials and Structures*, **41 (7)**, 1315-1326.

Visser, J. H. M. and Polder R. B. Concrete binder performance evaluation in service life design. pp.330-340. In **Kovler, K.** (ed.), *Concrete durability and service life planning (ConcreteLife'06)*, RILEM Publications, 2006.

Vorechovská, D., Chromá, M., Podroužek, J., Rovnaníková, P. & Teplý, B. (2009) Modelling of chloride concentration effect on reinforcement corrosion. C*omputer-Aided Civil and Infrastructure Engineering*, **24(6)**, 446-58.

Wang, K., Jansen, D. C., and Shah, S. P. (1997) Permeability study of cracked concrete. *Cement and Concrete Research,* **27**, 381-393.

Weyers, P.E. (1998) Service life model for concrete structures in chloride laden environments. *ACI Materials Journal*, **95 (4)**, 445-453.

Weyers, R.E., Fitch, M.G., Larsen, E.P., Al-Qadi, I.L., Chamberlin, W.P. and Hofman, P.C. *Concrete bridge protection and rehabilitation: Chemical and physical techniques – Service life estimates, Strategic Research Program*, SHRP-S-668, National Research Council, Washington, D.C., 1994.

Winnefeld, F., Becker, S., Pakuschi, J., and Götz, T. (2007) Effects of the molecular architecture of comb shaped superplasticizers on their performance in cementitious systems. *Cement and Concrete Composites,* **29**, 251-262.

Yuan, Y., Ji, Y., and Shah, S. P. (2007) Comparison of two accelerated corrosion techniques for concrete structures. *ACI Structural Journal*, **104 (3)**, 344-347.

Yu, C. W., and Bull, J. W. (2006) *Durability of materials and structures in building and civil engineering*, CRC Press, USA.

Zhang, T. and Gjørv, O. E. (1994) An electrochemical method for accelerated testing of chloride diffusivity in concrete. *Cement and Concrete Research*, **24 (8)**, 1534-1548.

Chennai Mettex Lab Private Limited, Guindy, Chennai.

www.concreteconstruction.net, Last accessed in July 2010.

www.corrosionsource.com/corrosioneering/journal/Jun02_Miksic, Last accessed in March 2010.

www.cortecvci.com/Publications/Papers/Cortec%202020-2.pdf, Last accessed in March 2012.

This page is intentionally left blank

PUBLICATIONS BASED ON THE THESIS WORK

I. REFEREED JOURNALS

1. **Bhaskar, S., Gettu, R., Bharatkumar, B.H., and Neelamegam, M.** Chloride-Induced Corrosion of Steel in Cracked OPC and PPC Concretes: Experimental Study. *Journal of Materials in Civil Engineering, ASCE,* **23 (7)**, pp. 1057-1066, 2011.

2. **Bhaskar, S., Gettu, R., Bharatkumar, B.H., and Neelamegam, M.** Studies on chloride induced corrosion of reinforcement steel in cracked concrete. *International Journal of Structural Durability & Health Monitoring, Tech Science Press, USA,* **7 (4)**, pp. 231-252, 2011.

3. **Bhaskar, S., Gettu, R., and Bharatkumar, B.H.** Corrosion of rebars in reinforced concrete-A review of the corrosion mechanisms, assessment techniques and control measures. *ICI Journal,* Oct-Dec. pp. 35-54, 2011.

4. **Bhaskar, S., Bharatkumar, B.H., Gettu, R., and Neelamegam, M.** Effect of corrosion on the bond behaviour of OPC and PPC concretes. (Special Issue on Sustainable built environment), *Journal of Structural Engineering, SERC*, **37 (1)**, 37-42, 2010.

5. **Bhaskar, S., Gettu, R., and Bharatkumar, B.H.** Accelerated corrosion test on cracked reinforced concrete with and without PCE superplasticizer, *International Journal of 3R's, Dr. Fixit Publications,* **3 (1),** 358-367, Jan-Mar. 2012, pp. 358-367.

6. **Bhaskar, S., Bharatkumar, B.H., Gettu, R., and Neelamegam, M.** Strength, bond and durability related properties of concretes with mineral admixtures, *The Indian Concrete Journal*, **86 (2)**, 9-16, 2012.

II. PRESENTATIONS IN CONFERENCES

1. **Bhaskar, S., Gettu, R., and Bharatkumar, B.H.** Influence of chemical admixtures on the corrosion of rebars in cracked concrete. *Proceedings of the 2nd International Conference on Microstructure related durability of cementitious composites*, *Microdurability 2012*, Amsterdam, The Netherlands, April 2012 (CD form).

2. **Bhaskar, S., Gettu, R., Bharatkumar, B.H. and Neelamegam**, **M.** Benefits of portland pozzolana cement in chloride induced corrosion protection in concrete. *Proceedings of the 3rd Asian Conference on Ecstasy in Concrete, ACECON 2010*, Chennai, December, 2010, 363-372.

3. **Bhaskar, S., Bharatkumar, B.H., Gettu, R. and Neelamegam, M.**, Influence of water to cement ratio on corrosion of steel in OPC concretes. *International Conference & Expo on Corrosion, CORCON-2010,* Goa, September, 2010 (CD form).

4. **Bhaskar, S., Gettu, R., Bharatkumar, B.H. and Neelamegam, M.**, Comparison of corrosion in reinforced pre-cracked members of OPC and PPC

concretes. *National Seminar on Advances in construction engineering practice (ACEP-2010)*, Annamalai Nagar, February, 2010, 71-78.

5. **Bhaskar, S., Gettu, R.,, Bharatkumar, B.H., Ramanjaneyulu, K. and Nagesh R. Iyer.** Effect of cracking on chloride induced corrosion of reinforcement bars in concrete. *International Conference on Advances in Building Sciences and Rehabilitation and Restoration of Structures*, Chennai, February 2013, 555-562.

CURRICULAM - VITAE

1. **NAME**   : Sangoju Bhaskar

2. **DATE OF BIRTH**   : 10-10-1969

3. **EDUCATIONAL QUALIFICATIONS**

   Bachelor of Engineering (B. E)

   Specialization   : Civil Engineering

   University   : Osmania University, Hyderabad

   Master of Technology (M. Tech.)

   Specialization   : Structural Engineering

   University   : J.N.T. University, Hyderabad

   Doctor of Philosophy (Ph.D)

   Institution   : Indian Institute of Technology Madras

   Registration   : 20-07-2007

DOCTORAL COMMITTEE

CHAIR PERSON   :   Dr. S. R. Gandhi
Professor and Head,
Department of Civil Engineering

GUIDE(S)   :   Dr. Ravindra Gettu
Professor,
Department of Civil Engineering

                                 Dr. B. H. Bharatkumar
Senior Principal Scientist,
CSIR-Structural Engineering Research
Centre, Chennai

MEMBERS   :   Dr. K. Ramamurthy
Professor,
Department of Civil Engineering

                     :   Dr. K. Ganesh Babu
Professor,
Department of Ocean Engineering

                     :   Dr. K. Ramanjaneyulu
Chief Scientist,
CSIR-Structural Engineering Research
Centre, Chennai

                     :   Dr. Manu Santhanam
Associate Professor,
Department of Civil Engineering